Climate change projections for west of Wellington's Tararua and Remutaka Ranges

Prepared for Greater Wellington Regional Council

September 2022

Climate, Freshwater & Ocean Science

Prepared by:
Gregor Macara
John-Mark Woolley
Abha Sood (Regional Climate Modelling)
Stephen Stuart (Regional Climate Modelling)

For any information regarding this report please contact:

Gregor Macara
Climate Scientist
Climate Data and Applications
+64-4-386 0509
gregor.macara@niwa.co.nz

National Institute of Water & Atmospheric Research Ltd (NIWA)
301 Evans Bay Parade, Hataitai, Wellington 6021
Private Bag 14901, Kilbirnie, Wellington 6241

Phone +64 4 386 0300

NIWA CLIENT REPORT No:	2022069WN
Report date:	September 2022
NIWA Project:	WRC22301

Quality Assurance Statement		
	Reviewed by:	Petra Pearce Manager – Climate, Atmosphere and Hazards NIWA Auckland
	Formatting checked by:	Jess Moffat
	Approved for release by:	Alison MacDiarmid

Cover Image: Pukerua Bay – [Credit: Gregor Macara]

Contents

Executive summary 8

1 Introduction 9

2 Condensed Methodology and limitations 11

2.1 Representative Concentration Pathways 11

2.2 Maps and tabulated climate projections 12

2.3 Limitations 13

3 Observed climate change west of Wellington's ranges 14

3.1 Mean temperature changes already observed 14

3.1.1 Comparison to projections 14

3.2 Changes already observed in temperature extremes 17

3.3 Changes already observed in extreme rainfall events 22

3.4 Climate change signal emergence for extremes 25

4 Future climate west of Wellington's ranges 27

4.1 Temperature 27

4.1.1 Maximum temperature 27

4.1.2 Minimum temperature 38

4.1.3 Growing degree days 49

4.1.4 Hot days 52

4.1.5 Extreme hot days 55

4.1.6 Heatwave days 58

4.1.7 Warm nights 61

4.1.8 Frost days 64

4.1.9 Cold days 68

4.2 Rainfall 71

4.2.1 Rainfall totals 71

4.2.2 Wet days 82

4.2.3 99th percentile of daily rainfall, and rare extreme rainfall events 93

4.2.4 Dry spells 102

4.3 Other climate variables 105

4.3.1 Potential evapotranspiration deficit 105

4.3.2 Windy days 108

5 Summary and conclusions 110

5.1 Recommendations for future work 111

6 Acknowledgements ... 113

7 Glossary of abbreviations and terms ... 114

8 References ... 115

Appendix A Global and New Zealand climate change ... 120

Appendix B Year to year climate variability and climate change ... 122

The effect of El Niño and La Niña ... 122

The effect of the Interdecadal Pacific Oscillation ... 123

The effect of the Southern Annular Mode ... 124

The influence of natural variability on climate change projections ... 124

Appendix C Methodology ... 126

Observed climate change west of Wellington's ranges ... 126

Climate modelling ... 126

Representative Concentration Pathways ... 128

Appendix D CMIP6 climate modelling and latest IPCC Assessment ... 130

Appendix E Climate projection panels ... 131

Tables

Table 3-1: Site information and adjustments applied to the Wellington daily temperature record. 18

Table 3-2: Site information and adjustments applied to the Masterton daily temperature record. 18

Table 3-3: Trends in daily maximum temperature extremes over 1912-2018 at Wellington (Kelburn) and Masterton. Trends are in "days per decade", and are shown only where statistically significant at the 5% level. 19

Table 3-4: Trends in daily minimum temperature extremes over 1912-2018 at Wellington (Kelburn) and Masterton. Trends are in "days per decade", and are shown only where statistically significant at the 5% level. 19

Table 8-1: Projected changes in seasonal and annual mean temperature (in °C) between 1986-2005 and 2031-2050, for the Wellington region, as derived from statistical downscaling. 126

Table 8-2: Projected change in global mean surface air temperature for the mid- and late- 21st century relative to the reference period of 1986-2005 for different RCPs. 129

Figures

Figure 1-1: District boundaries of the area west of Wellington's ranges. 10

Figure 2-1:	Example maps before (left) and after (right) nearest neighbour interpolation.	12
Figure 3-1:	Mean annual temperature for Wellington (Kelburn).	14
Figure 3-2:	Observed temperature change for Wellington (Kelburn) compared to projected (RCP4.5) change.	16
Figure 3-3:	Observed temperature change for New Zealand compared to projected (RCP4.5) temperature change.	17
Figure 3-4:	Annual-average (in days/year), for each decade from 1910-1919 to 2010-2018 of extremes for maximum temperature.	20
Figure 3-5:	Annual-average (in days/year), for each decade from 1910-1919 to 2010-2018 of extremes for minimum temperature.	21
Figure 3-6:	Annual maxima rainfall time series from Kelburn (Wellington) for a range of event durations.	23
Figure 3-7:	Annual maxima rainfall time series from Wellington Airport for a range of event durations.	24
Figure 3-8:	Annual maxima rainfall time series from Paraparaumu for a range of event durations.	25
Figure 4-1:	Modelled annual mean maximum temperature, average over 1986-2005.	29
Figure 4-2:	Modelled seasonal mean maximum temperature, average over 1986-2005.	30
Figure 4-3:	Projected annual mean maximum temperature changes by 2040 and 2090 under RCP2.6, RCP4.5 and RCP8.5.	31
Figure 4-4:	Projected seasonal mean maximum temperature changes by 2040 under RCP2.6.	32
Figure 4-5:	Projected seasonal mean maximum temperature changes by 2090 under RCP2.6.	33
Figure 4-6:	Projected seasonal mean maximum temperature changes by 2040 under RCP4.5.	34
Figure 4-7:	Projected seasonal mean maximum temperature changes by 2090 under RCP4.5.	35
Figure 4-8:	Projected seasonal mean maximum temperature changes by 2040 under RCP8.5.	36
Figure 4-9:	Projected seasonal mean maximum temperature changes by 2090 under RCP8.5.	37
Figure 4-10:	Modelled annual mean minimum temperature, average over 1986-2005.	40
Figure 4-11:	Modelled seasonal mean minimum temperature, average over 1986-2005.	41
Figure 4-12:	Projected annual mean minimum temperature changes by 2040 and 2090 under RCP2.6, RCP4.5 and RCP8.5.	42
Figure 4-13:	Projected seasonal mean minimum temperature changes by 2040 under RCP2.6.	43
Figure 4-14:	Projected seasonal mean minimum temperature changes by 2090 under RCP2.6.	44
Figure 4-15:	Projected seasonal mean minimum temperature changes by 2040 under RCP4.5.	45
Figure 4-16:	Projected seasonal mean minimum temperature changes by 2090 under RCP4.5.	46
Figure 4-17:	Projected seasonal mean minimum temperature changes by 2040 under RCP8.5.	47

Figure 4-18:	Projected seasonal mean minimum temperature changes by 2090 under RCP8.5.	48
Figure 4-19:	Median annual Growing Degree-Days (GDD) base 10°C.	50
Figure 4-20:	Projected increase in number of growing degree days per year (base 10°C) at 2040 (2031-2050) and 2090 (2081-2100) for RCP2.6 (top panels), RCP4.5 (middle panels) and RCP8.5 (bottom panels).	51
Figure 4-21:	Modelled annual number of hot days (days with maximum temperature ≥25°C), average over 1986-2005.	53
Figure 4-22:	Projected annual hot day (days with maximum temperature ≥25°C) changes by 2040 and 2090, under RCP2.6, RCP4.5 and RCP8.5.	54
Figure 4-23:	Modelled annual number of extreme hot days (days with maximum temperature >30°C), average over 1986-2005.	56
Figure 4-24:	Projected annual extreme hot day (days with maximum temperature >30°C) changes by 2040 and 2090, under RCP2.6, RCP4.5 and RCP8.5.	57
Figure 4-25:	Modelled annual number of heatwave days (≥ three consecutive days with maximum temperatures > 25°C), average over 1986-2005.	59
Figure 4-26:	Projected annual heatwave day (≥ three consecutive days with maximum temperatures > 25°C) changes by 2040 and 2090, under RCP2.6, RCP4.5 and RCP8.5.	60
Figure 4-27:	Modelled annual number of warm nights (daily minimum temperature >15°C), average over 1986-2005.	62
Figure 4-28:	Projected annual warm night (daily minimum temperature >15°C) changes by 2040 and 2090, under RCP2.6, RCP4.5 and RCP8.5.	63
Figure 4-29:	Modelled annual number of frost days (daily minimum temperature ≤0°C), average over 1986-2005.	66
Figure 4-30:	Projected annual number of frost day (daily minimum temperature ≤0°C) changes by 2040 and 2090 under RCP2.6, RCP4.5 and RCP8.5.	67
Figure 4-31:	Modelled annual number of cold days (days with maximum temperature <10°C), average over 1986-2005.	69
Figure 4-32:	Projected annual cold day (days with maximum temperature <10°C) changes by 2040 and 2090, under RCP2.6, RCP4.5 and RCP8.5.	70
Figure 4-33:	Modelled annual rainfall (mm), average over 1986-2005.	73
Figure 4-34:	Modelled seasonal rainfall (mm), average over 1986-2005.	74
Figure 4-35:	Projected annual rainfall changes (%).	75
Figure 4-36:	Projected seasonal rainfall changes (%) by 2040 for RCP2.6.	76
Figure 4-37:	Projected seasonal rainfall changes (%) by 2090 for RCP2.6.	77
Figure 4-38:	Projected seasonal rainfall changes (%) by 2040 for RCP4.5.	78
Figure 4-39:	Projected seasonal rainfall changes (%) by 2090 for RCP4.5.	79
Figure 4-40:	Projected seasonal rainfall changes (%) by 2040 for RCP8.5.	80
Figure 4-41:	Projected seasonal rainfall changes (%) by 2090 for RCP8.5.	81
Figure 4-42:	Modelled annual wet days (daily rainfall ≥1 mm), average over 1986-2005.	84
Figure 4-43:	Modelled seasonal wet days (daily rainfall ≥1 mm), average over 1986-2005.	85
Figure 4-44:	Projected annual wet day (daily rainfall ≥1 mm) changes.	86
Figure 4-45:	Projected seasonal wet day (daily rainfall ≥1 mm) changes by 2040 for RCP2.6.	87

Figure 4-46: Projected seasonal wet day (daily rainfall ≥1 mm) changes by 2090 for RCP2.6. 88
Figure 4-47: Projected seasonal wet day (daily rainfall ≥1 mm) changes by 2040 for RCP4.5. 89
Figure 4-48: Projected seasonal wet day (daily rainfall ≥1 mm) changes by 2090 for RCP4.5. 90
Figure 4-49: Projected seasonal wet day (daily rainfall ≥1 mm) changes by 2040 for RCP8.5. 91
Figure 4-50: Projected seasonal wet day (daily rainfall ≥1 mm) changes by 2090 for RCP8.5. 92
Figure 4-51: Modelled annual 99th percentile daily rainfall average over 1986-2005. 94
Figure 4-52: Projected annual 99th percentile daily rainfall changes by 2040 and 2090, under RCP2.6, RCP4.5 and RCP8.5. 95
Figure 4-53: The change in rainfall exceedances with climate change for Kelburn. 97
Figure 4-54: The change in rainfall exceedances with climate change for Wellington Aero. 98
Figure 4-55: The change in rainfall exceedances with climate change for Paraparaumu. 99
Figure 4-56: Historic (1853-2016) 10-minute duration, 100-year magnitude rainfall depths for the area west of Wellington's ranges. 100
Figure 4-57: Projected changes to 10-minute duration, 100-year magnitude rainfall depths by 2040 and 2090, under RCP2.6, RCP4.5 and RCP8.5. 101
Figure 4-58: Modelled annual number of dry spell days (≥ ten consecutive days with daily rainfall < 1 mm), average over 1986-2005. 103
Figure 4-59: Projected annual dry spell day (≥ ten consecutive days with daily rainfall < 1 mm) changes by 2040 and 2090, under RCP2.6, RCP4.5 and RCP8.5. 104
Figure 4-60: Modelled annual potential evapotranspiration deficit accumulation (mm), average over 1986-2005. 106
Figure 4-61: Projected annual potential evapotranspiration deficit accumulation (mm) changes by 2040 and 2090 under RCP2.6, RCP4.5 and RCP8.5. 107
Figure 4-62: Projected change in the annual number of windy days (>10 m/s) by 2040 and 2090, under RCP2.6, RCP4.5 and RCP8.5. 109
Figure 8-1: New Zealand national temperature series, 1909-2021. 121
Figure 8-2: Average summer percentage of normal rainfall during La Niña (left) and El Niño (right). 123
Figure 8-3: New Zealand air temperature - historical (black) and future projections for four RCPs and six downscaled climate models, illustrating future year-to-year variability. 125
Figure 8-4: Schematic diagram showing the dynamical downscaling approach. 127
Figure 8-5: CMIP5 multi-model simulated time series from 1950-2100 for change in global annual mean surface temperature relative to 1986-2005. 129

Executive summary

The climate west of Wellington's Tararua and Remutaka Ranges is already changing, and these changes will continue for the foreseeable future. It is internationally accepted that human greenhouse gas emissions are the dominant cause of recent global climate change, and that further changes will result from increasing concentrations of greenhouse gases in the atmosphere.

Downscaled results of selected global climate models based on three Representative Concentration Pathway (RCP) scenarios (RCP2.6, RCP4.5 and RCP8.5) of how human greenhouse gas emissions might change in future are presented in this report. The rationale for choosing these three scenarios is to present a broad spectrum of scenarios ranging from a 'high end' scenario if atmospheric greenhouse gas concentrations continue to rise at high rates (RCP8.5), to a 'low end' scenario if very stringent global actions are taken to mitigate greenhouse gas emissions (RCP2.6).

Changes to the future climate of west of the ranges are likely to be considerable, but typically less pronounced than east of these ranges i.e. the Wairarapa. The following bullet points outline some key findings of this report:

- Heavy rainfall events (as indicated by the 99th-percentile of daily rainfall totals) are generally projected to become more severe in the future. By 2040, the magnitude of heavy rainfall events is projected to change by -1% to +12% (RCP8.5). By 2090, heavy rainfall event magnitude is projected to increase by 1-12% (RCP2.6) or 2-30% (RCP8.5).

- Rarer extreme rainfall events such as one-in-one-hundred year events are also expected to increase in both frequency (between two-fold and three fold increases for various durations) and magnitude (up to 40% increase).

- Drought potential is projected to increase across the area, with annual accumulated Potential Evapotranspiration Deficit (PED) totals increasing with time and greenhouse gas concentrations. By 2040, PED totals are projected to increase by 10-120 mm (RCP8.5). By 2090, PED totals are projected to increase by 10-80 mm (RCP2.6) or 10-135 mm (RCP8.5).

- Annual average growing degree days (GDD) are projected to increase by 150-300 GDD by 2040 under RCP8.5. By 2090, growing degree days are projected to increase by 85-200 GDD (RCP2.6) or 500-850 GDD (RCP8.5). These upper-range increases would see areas west of Wellington's ranges observing GDD totals comparable to those observed historically (1981-2010) in Auckland and low elevations of Northland.

- Increasing maximum temperatures will result in more hot days (daily maximum temperature ≥25°C), although extreme hot days (daily maximum temperature >30°C) are expected to remain uncommon for many parts of the area. By 2040, up to 10 more annual hot days are projected (all RCPs), with up to 10 (RCP2.6) or 5-50 (RCP8.5) more annual hot days by 2090.

- The average number of frost days are expected to decrease with time, as greenhouse gas concentrations increase. The largest numerical decreases are projected for high elevation and inland locations. Overall, up to 10 fewer frost days are projected by 2040 (RCP8.5), with up to 10 (RCP2.6) or up to 30 (RCP8.5) fewer frost days by 2090. Smaller decreases are generally projected for coastal locations because fewer frosts currently occur in these locations.

1 Introduction

Climate change is already affecting New Zealand, including west of the Tararua and Remutaka Ranges, with impacts on our natural environment, the economy, and communities. Climate change is highly likely to increasingly pose challenges to New Zealanders' way of life. Greenhouse gas emission reductions are required globally to avoid the greatest projected climate changes.

Greater Wellington Regional Council (GWRC) commissioned the National Institute of Water and Atmospheric Research (NIWA) to undertake a review of climate change projections for west of Wellington's ranges (regional extent shown in Figure 1-1). This work is based on earlier reports examining the climate change projections and impacts for the Greater Wellington Region (Pearce *et al.*, 2017; 2019, Woolley *et al.*, 2020); GWRC requested an additional report for the area west of Wellington's ranges, focussing solely on the climate change projections of this area.

This work follows the publication of the Intergovernmental Panel on Climate Change (IPCC) Fifth Assessment Report in 2013 and 2014, and the New Zealand climate change projections report published by the Ministry for the Environment (Ministry for the Environment, 2018). The contents of this technical report include analysis of climate projections for this area in greater detail than the national-scale analysis. Regional-scale climate projection maps have been provided for 15 different climate variables and indices. Although the IPCC Sixth Assessment Report was released in 2021 and 2022, the national downscaling required to produce detailed projections for New Zealand won't be available until around 2024 (see Appendix D).

This technical report describes changes which are likely to occur over the 21st century to the climate west of Wellington's ranges. Consideration about future change incorporates knowledge of both natural variations in the climate, and changes that may result from increasing global concentrations of greenhouse gases and decreasing stratospheric ozone destruction that are contributed to by human activities. Climatic variables discussed in this report include temperature, rainfall and potential evapotranspiration deficit (a measure of drought potential). Commentary on climate change impacts and implications for some of the different environments and sectors of the area are not provided, as these are discussed in the earlier report produced for the Greater Wellington Region. Readers are referred to that report (Pearce *et al.*, 2017) for a discussion of the anticipated climate change impacts for this area.

Some of the information that underpins portions of this report resulted from academic studies based on the Fifth Assessment Report of the Intergovernmental Panel on Climate Change (IPCC, 2013; 2014a; 2014b; 2014c). Details specific to the area were based on scenarios for New Zealand that were generated by NIWA from downscaling of global climate model simulations. This effort utilised several IPCC representative concentration pathways for the future, and this was achieved through NIWA's core-funded Regional Modelling Programme. The climate change information presented in this report is consistent with recently-updated national-scale climate change guidance produced for the Ministry for the Environment (2018).

A brief introduction to global and New Zealand climate change, based on the IPCC Sixth Assessment Report, is provided in Appendix A. Components of interannual climate variability are described in Appendix B.

Figure 1-1: District boundaries of the area west of Wellington's ranges.

2 Condensed Methodology and limitations

A detailed methodology explaining the modelling approach for the climate change projections presented in this report is provided in Appendix C. This section provides a brief introduction to representative concentration pathways (RCPs) (Section 2.1), how the maps and tabulated climate projections are derived (Section 2.2), and limitations on the results and use of data presented in this report (Section 2.3). A video highlighting the key findings of this report (complementary to the Wairarapa video published by GWRC in 2021) will be developed by NIWA for GWRC.

2.1 Representative Concentration Pathways

In this report, the downscaled results of the selected global climate models based on three RCP scenarios (RCP2.6, RCP4.5 and RCP8.5) are presented. The RCPs are scenarios of how greenhouse gas concentrations and other atmosphere pollutants might change during the 21st century. The rationale for choosing these three scenarios was to present a broad spectrum of scenarios ranging from a 'high end' scenario if atmospheric greenhouse gas concentrations continue to rise at high rates (RCP8.5), to a 'low end' scenario if very stringent global actions are taken to mitigate greenhouse gas emissions (RCP2.6). RCP2.6 may include carbon positive[1] management strategies, and is representative of a scenario that aims to keep global warming *likely* below 2°C above pre-industrial temperatures. RCP4.5 could be realistic if moderate global action is taken soon towards mitigating greenhouse gas emissions.

RCP8.5 is described as a high emissions scenario, with greenhouse gas concentrations continuing to increase at the current or an accelerated rate. Whilst global emissions are unlikely to continue increasing at current rates to the end of the 21st century (Hausfather & Peters, 2020), the RCP8.5 projections serve the purpose of defining the upper envelop of likely futures required for high risk impacts. Additional unaccounted risks resulting from other mechanisms (e.g. positive feedback loops) may result in impacts similar to those projected in the RCP8.5 scenario, even if the emissions scenario doesn't play out as projected. Examples of positive feedback loops include the melting of permafrost in Arctic regions, melting ice (e.g. Arctic sea ice) and clouds. Notably, RCP8.5 most closely resembles the total cumulative carbon dioxide emissions from 2005-2020, thus remaining RCPs assume a level of mitigation during the 2005-2020 period that did not occur (Schwalm *et al.*, 2020).

The RCPs inform projections which provide plausible futures under climate change. However, climate change over the remainder of the 21^{st} century and beyond is uncertain. This is due to:

- It is unknown how greenhouse gas concentrations will actually change over this period. Emissions may be significantly reduced, or they may continue to increase, or they may plateau. The three RCPs represent three representative choices among a wide range of possible options.
- Limitations in understanding of climate processes and how they are represented in the climate models used to predict how the climate will change. There is considerable complexity and inherent uncertainty in climate modelling (e.g. the response of the Antarctic ice sheet to increasing temperatures resulting in increased sea level rise).
- Uncertainty in natural climate variability.

[1] A "carbon positive" management strategy includes actions that support the reduction of atmospheric carbon, such as the cultivation and growing of grasses and forests, and the recycling of carbon into soil nutrients from organic materials and food waste (McDonough, 2016).

This inherent uncertainty is the basis for why projected climate changes (for the globe and for New Zealand) are modelled based on a suite of RCPs. For risk assessments, it is best practice (e.g. as was done for the National Climate Change Risk Assessment; Ministry for the Environment, 2020) to consider climate change projections based on a range of RCPs, including a high concentration pathway. The RCP8.5 projections serve the purpose of defining the upper envelope of likely futures required for high risk impacts.

2.2 Maps and tabulated climate projections

The climate projections presented in this report are based on the same underlying model data that were presented in previous reports commissioned by GWRC (Pearce *et al.*, 2017; 2019, Woolley *et al.*, 2020). This report differs from the previous reports by focussing on the area west of Wellington's ranges, with climate projection maps generated in a way which improves the illustration of projections for this part of the region. GIS datasets for climate projections of all four RCPs were previously provided to GWRC, and are used to inform their climate mapping tool (https://mapping1.gw.govt.nz/gw/ClimateChange/).

Downscaled climate projection data is presented as 5 km x 5 km square pixels over New Zealand. Data were downscaled only where low-resolution cells in the climate model consisted of land coverage and where they overlapped high-resolution cells on land. For display purposes, NIWA has undertaken interpolation to continue the climate projections to the coast for the climate change and historic climate maps presented in Section 4. The nearest neighbour interpolation method was used to do this, where the value of the empty coastal cell was estimated using the value of the nearest neighbouring cells (Figure 2-1). Because the values at these locations are estimates generated simply for presentation purposes (i.e. not a direct output of the climate change model), mapped climate change values at these coastal locations should be interpreted based on the general large-scale pattern projected for the adjacent land.

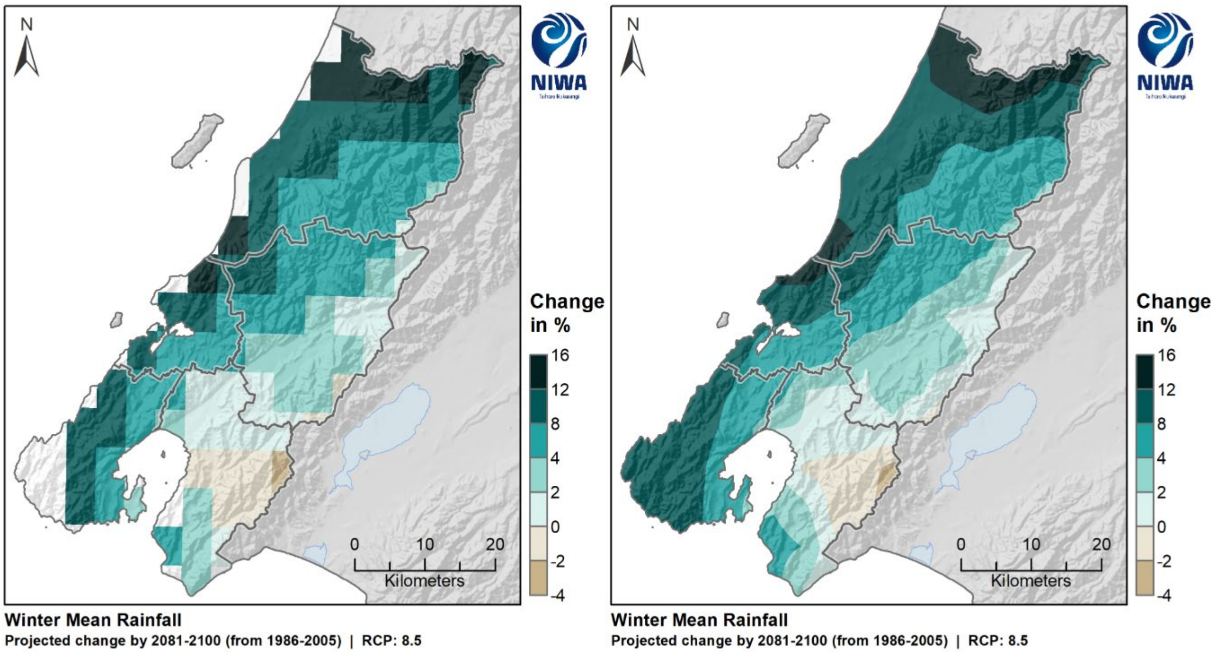

Figure 2-1: Example maps before (left) and after (right) nearest neighbour interpolation.

At the start of each subsection in Section 4.1.1 to Section 4.3.2, summary tables present an overview of the projected changes across the area. Note, these changes are relative to the 1986-2005 (1995) baseline. These span the entire range of projections illustrated in the associated maps. As such, only isolated portions of the area may observe projected changes at the lower and upper limits of the range presented in the summary tables. The reader is referred to the maps for detailed projections, and also referred to the limitations (Section 2.3) associated with the interpretation of these maps.

Note, the legend increments for many of the maps presented in this report are not linear. This is necessary to encapsulate the observed spatial variability in the area. The historic map is not provided for mean wind speed as these data have not been bias-corrected, and therefore do not provide a reliable representation of the observed magnitude of this variable.

2.3 Limitations

As with any modelling exercise, there are limitations on the results and use of the data. This section outlines some of these limitations and caveats that should be considered when using this report.

- Though only a small number of model simulations (six) were possible due to the large computing resources required for running climate model simulations, they were very carefully selected to cover a wide range of climate model projections.
- The average of six models is used in this report, however data from individual models is available for further assessment if required in the future. The six models chosen represented historic climate conditions in New Zealand well, and span a range of future outcomes. The climate signal is better represented by ensemble averages since the uncertainty due to climate models and internal variability is much reduced.
- The time periods chosen for historic and future projection span 20-year periods. This is seen as a relatively short timeframe to understand average conditions in the historic period and in the future, as there is likely an influence of underlying low frequency climate variability (e.g. decadal signals from climate drivers like the Interdecadal Pacific Oscillation etc.). However, as climate data is subject to significant trends, a short period is more homogenous and representative. Moreover, the IPCC uses 20-year periods, so we have followed that approach for consistency.
- Care needs to be taken when interpreting grid-point-scale projections such as those available in the GIS layers provided to GWRC. The data have been bias-corrected, downscaled and interpolated from the 30 km regional climate model grid to the 5 km grid across New Zealand using physically based models and interpolation. The regional climate model and bias correction may not accurately reproduce the role of the Tararua and Remutaka Ranges in blocking rainfall from the Tasman Sea, or the maritime influence of the sea on temperature indices, for example. Therefore, the data from these grid points does not correspond to on-the-ground observations. It is more appropriate to consider relative patterns rather than absolute values, e.g. the magnitude of change at different time periods and scenarios.

Although there are some limitations and caveats in the approach used here, considerable effort has been made to generate physically consistent climate change projections for this area at unprecedented temporal and spatial resolutions. A considerable research effort has also been dedicated to validating simulated climate variables, and thus the projections provide a good basis for risk assessments and adaptation plans.

3 Observed climate change west of Wellington's ranges

3.1 Mean temperature changes already observed

New Zealand's seven-station temperature series comprises a homogenised temperature record derived from seven locations[2] (Mullan *et al.*, 2010). One of these locations is Wellington (Kelburn), which provides an opportunity to examine how temperatures have changed for a location representative of coastal, low-elevation areas of the area.

Figure 3-1 shows Wellington's (Kelburn) mean annual temperature from 1909-2021. There is considerable interannual variability, which is due to a combination of natural causes, such as the El Niño Southern Oscillation, together with other random year-to-year fluctuations ("climate noise"), as well as anthropogenic influences (e.g. greenhouse gas emissions). According to these data, Wellington's (Kelburn) coldest year occurred in 1930 (11.38°C), and the warmest year occurred in 2018 (13.85°C). Overall, a trend of +0.1°C per decade is observed, which is significant at the 5% level ($p < 0.05$)[3].

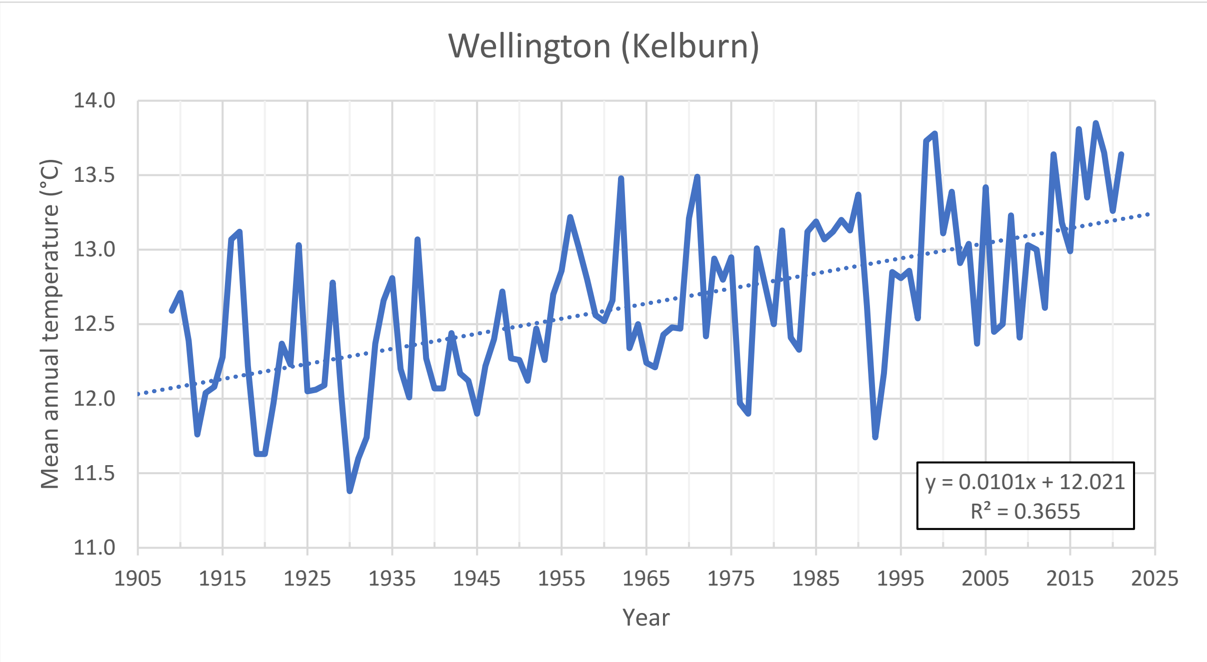

Figure 3-1: Mean annual temperature for Wellington (Kelburn). This site is part of New Zealand's seven-station series, so data homogenisation has been carried out. Trend (dotted line) is approximately +0.1°C/decade, which is significant at $p < 0.05$.

3.1.1 Comparison to projections

The purpose of this section is to provide context for contemporary temperature observations (in this case from 1986-2021), and to help illustrate that due to ongoing observed warming, a portion of the projected temperature changes have already materialised. Specifically, projected temperature changes presented in this report are relative to 1995 (1986-2005). Given we are now at 2022 (at the time of writing), a portion of the projected temperature changes will have already occurred. This section should not be used to assess the accuracy of the projected temperature data because natural

[2] For further details on New Zealand's seven-station temperature series: https://niwa.co.nz/seven-stations

[3] $P < 0.05$ is a measure of statistical significance, indicating a 5% chance of rejecting the null hypothesis when it is true. In this instance, the null hypothesis - that there has been no trend observed in Wellington's (Kelburn) temperature - is rejected.

random climate variability will be large compared to the human-induced climate change over this short time period.

Wellington (Kelburn) and New Zealand temperature data (using the homogenised seven-station temperature series) were compared with projected temperature data to assess contemporary temperature changes. For Wellington (Kelburn) and New Zealand, three timeseries are presented for the period 1986-2021, respectively:

1. *Tmean*: The homogenised annual average temperature;
2. *Tmean (20-yr avg)*: The 20-year moving average annual temperature. The series begins in 1995 and ends in 2011, i.e. the 1995 Tmean (20-yr avg) is the average annual temperature from 1986-2005, whilst the 2011 Tmean (20-yr avg) is the average annual temperature from 2002-2021;
3. *RCP4.5*: Projected temperature change from 1995 (1986-2005) to 2040 (2031-2050) under RCP4.5. Data were obtained from Table 5 of Ministry for the Environment (2018) and calculated as follows:

    3.1 *Wellington*: Using Wellington's regionally averaged projected annual temperature change of 0.9°C (5th percentile to 95th percentile = 0.5-1.2°C. See Table 8-1 in Appendix C for further details). Averaged over the 45-year period from 1995-2040, this equals an average increase of 0.020°C per year. This average increase was applied iteratively to Wellington's (Kelburn) 1995 *Tmean (20-yr avg)* (13.0°C) to generate the *RCP4.5* timeseries.

    3.2 *New Zealand*: Projected annual temperature change of 0.8°C (5th percentile to 95th percentile = 0.4-1.3°C). Averaged over the 45-year period from 1995-2040, this equals an average increase of 0.018°C per year. This average increase was applied iteratively to New Zealand's 1995 *Tmean (20-yr avg)* (12.6°C) to generate the *RCP4.5* timeseries.

    3.3 Note, the rates of change calculated above are only relevant to 2040. Under the RCP4.5 scenario, future greenhouse gas concentrations are such that the average annual rate of change by 2090 (2081-2100) is lower than by 2040. For Wellington and New Zealand the average annual rate of change by 2090 under RCP4.5 is +0.015°C.

    3.4 Note, by calculating average annual projected temperature increases from 1995 to 2040, the interannual variability of projected temperature data is removed. Interannual variability is present in modelled temperature projections, and it will remain a feature of New Zealand's future climate.

Figure 3-2 shows observed and projected temperatures for Wellington (Kelburn). In the 16-year period from 1995-2011, Wellington's (Kelburn) 20-year moving average annual temperature increased 0.16°C, from 12.96°C to 13.12°C. Based on these data, approximately 18% of Wellington's (Kelburn) projected warming by 2040 under RCP4.5 has materialised. These findings are similar to those of Masterton (Macara *et al.*, 2021), where approximately 22% of the town's projected warming by 2040 has occurred during the 15-year period from 1995-2010. Note, the rate of projected change for the Wellington region under RCP4.5 (Figure 3-2; dashed line) is +0.2°C per decade, which is double Wellington's observed rate of change illustrated in Figure 3-1.

Figure 3-3 shows observed and projected temperatures for New Zealand. Notable features illustrating interannual climate variability include i) relatively low temperatures in the early 1990's, associated with suppressed global temperatures as a result of the 1991 Mount Pinatubo eruption, and ii) relatively high temperatures in the late 1990's, associated with enhanced global temperatures as a result of an exceptionally strong El Niño event from 1997-98. In the 16-year period from 1995-2011, New Zealand's 20-year moving average annual temperature increased 0.29°C, from 12.62°C to 12.91°C. Based on these data, approximately 36% of New Zealand's projected warming by 2040 under RCP4.5 has materialised.

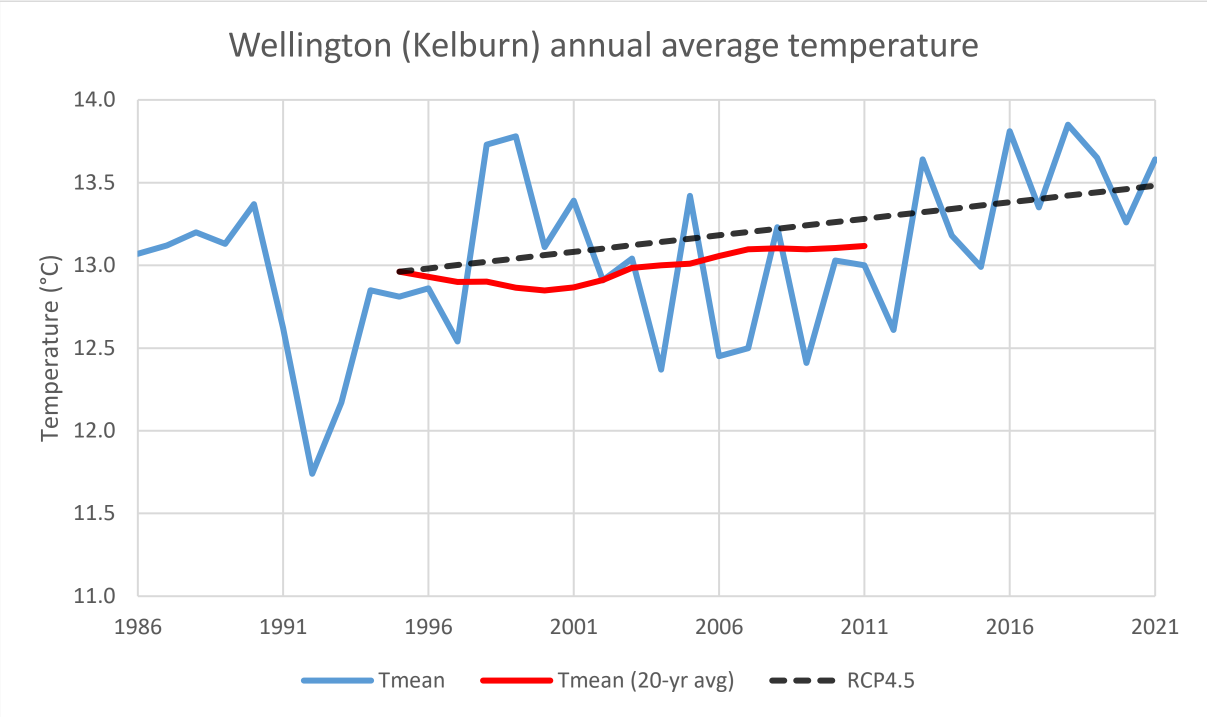

Figure 3-2: Observed temperature change for Wellington (Kelburn) compared to projected (RCP4.5) change. See text above for a description of how these timeseries were generated.

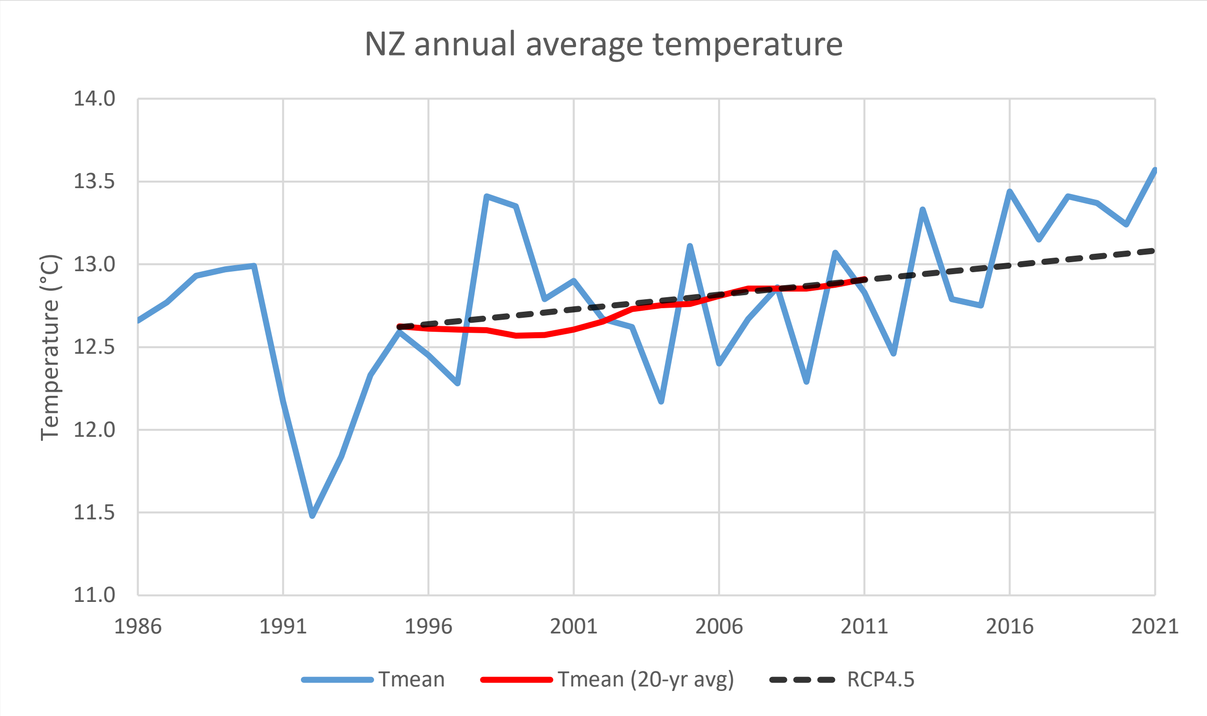

Figure 3-3: Observed temperature change for New Zealand compared to projected (RCP4.5) temperature change. See text above for a description of how these timeseries were generated.

3.2 Changes already observed in temperature extremes

Wellington (Kelburn) temperature data were examined to see how temperature extremes have changed. Another location included in New Zealand's seven-station temperature series is Masterton, and these data have been included here to enable a comparison of observed changes for two areas of the Greater Wellington Region that have a distinct climate. Note, this information has been obtained directly from a previous GWRC-commissioned NIWA report (Pearce *et al.*, 2019), and the reader is referred to that report for further methodology details. The analysis makes use of recent digitisation of early historical temperature data not yet available on NIWA's Climate Database. Time series of daily maximum and minimum temperatures were appended in the same way as noted in the seven-station report for monthly mean temperatures (Mullan *et al.*, 2010). A simple first-order homogenisation was applied by using the same adjustments as Mullan *et al.* (2010) calculated for the monthly temperatures. Note that these recently digitised data have not been quality controlled beyond simple outlier assessment.

Table 3-1 and Table 3-2 show the periods and adjustments applied to build up the homogeneous records at Wellington (Kelburn) and Masterton. Note that adjustments are different for maximum and minimum temperatures. An important caveat is that the daily data have only been adjusted by the average monthly offsets. An improved (second-order) homogenisation would consider changes in the width of the normal distribution about the means which could be important when considering extremes, but this was outside the scope of this work. A further improvement, which might be investigated in future, is to consider how the distribution of daily temperatures varies with weather types (i.e. typical synoptic weather situations that New Zealand experiences, after Kidson (2000)).

Table 3-1: Site information and adjustments applied to the Wellington daily temperature record. The Kelburn (Wellington Botanic Gardens) site is the 'reference' site, and therefore has zero adjustment.

Site Name (Agent Number)	Period	Maximum temperature Adjustment (°C)	Minimum temperature Adjustment (°C)
Buckle St, Mount Cook (3431)	Jan 1909 to Jun 1912	-0.4	-1.1
Thorndon Esplanade (3391)	Jul 1912 to Dec 1927	-1.1	-0.7
Kelburn (3385)	Jan 1928 to Aug 2005	0.0	0.0
Kelburn AWS (25354)	Sep 2005 to Present	0.0	-0.1

Table 3-2: Site information and adjustments applied to the Masterton daily temperature record. The East Taratahi site is the 'reference' site, and therefore has zero adjustment.

Site Name (Agent Number)	Period	Maximum temperature Adjustment (°C)	Minimum temperature Adjustment (°C)
Workshop Road, Masterton (2473)	Feb 1912 to May 1920	-1.0	-0.1
Essex Street, Masterton (2473)	Jun 1920 to Nov 1942	-0.2	-0.4
Waingawa substation (2473)	Dec 1942 to Dec 1990	+0.2	-0.3
East Taratahi AWS (2612)	Jan 1991 to Oct 2009	0.0	0.0
Martinborough EWS (21938)	Nov 2009 to Present	+0.2	-0.8

Subject to this caveat, Figure 3-4 and Figure 3-5 show the time series of extremes for selected thresholds, as follows:

- Maximum temperature: Cold days < 10°C, Hot days > 25°C, Hot days > 30°C;
- Minimum temperature: Warm nights > 15°C, Cold nights < 5°C, Frosts (< 0°C)

The time series were calculated by first counting the extremes for each calendar year (pro-rating if there were significant blocks of missing data in the summer or winter months), and then averaging the annual count over each decade from the 1910s to 2010s. The first decade (1910s) has only eight years (1912-1919) for Masterton, and the last decade (2010s) has only nine years (2010-2018).

There is a significant difference between the Kelburn and Masterton sites in terms of the average number of extremes: Masterton experiences both hotter days and colder nights than Kelburn, a distinguishing feature found in many parts of New Zealand between inland and west coast sites. Whilst decadal variability is apparent in the data, some trends have emerged.

For maximum temperature (Figure 3-4):

- Cold days < 10°C: a decrease in the number of cold days at both sites since the 1930s.
- Hot days > 25°C: not much of a trend.
- Hot days > 30°C: a lot of variability from decade to decade at Masterton, and very few occurrences of extreme hot days above 30°C recorded at Kelburn.

For minimum temperature (Figure 3-5):

- Warm nights > 15°C: an increase in the number of warm nights at both sites since the 1930s and 1940s.
- Cold nights < 5°C: a decrease in the number of cold nights, with the trend more evident at Kelburn.
- Frosts (< 0°C): a general decline in frost occurrence over time at Masterton, with very low occurrences at Kelburn.

Table 3-3 and Table 3-4 show significant trends in the annual counts displayed graphically by decade in Figure 3-4 and Figure 3-5. For maximum temperature, the reduction in cold days (maximum below 10°C) is statistically significant at the 5% level, but the hot day trends are not significant. For minimum temperature, trends in all three statistics are significant: warm nights > 15°C are increasing, cold nights < 5°C are decreasing, and frosts are decreasing. The sign of all trends is consistent with an overall warming of the climate.

Table 3-3: Trends in daily maximum temperature extremes over 1912-2018 at Wellington (Kelburn) and Masterton. Trends are in "days per decade", and are shown only where statistically significant at the 5% level. Trends are calculated from 1912, since Masterton has no data for 1909-1912. Years with 30 days or more missing are not included. Time series of these indices are shown in Figure 3-4.

	Cold Days < 10°C		Hot Days > 25°C		Hot Days > 30°C	
	Wellington	Masterton	Wellington	Masterton	Wellington	Masterton
Trend (days/decade)	-1.3	-2.0	x	x	x	x

Table 3-4: Trends in daily minimum temperature extremes over 1912-2018 at Wellington (Kelburn) and Masterton. Trends are in "days per decade", and are shown only where statistically significant at the 5% level. Trends are calculated from 1912, since Masterton has no data for 1909-1912. Years with 30 days or more missing are not included. Time series of these indices are shown in Figure 3-5.

	Warm Nights > 15°C		Cold Nights < 5°C		Frosts < 0°C	
	Wellington	Masterton	Wellington	Masterton	Wellington	Masterton
Trend (days/decade)	+1.4	+0.9	-3.3	-2.2	-0.4	-1.6

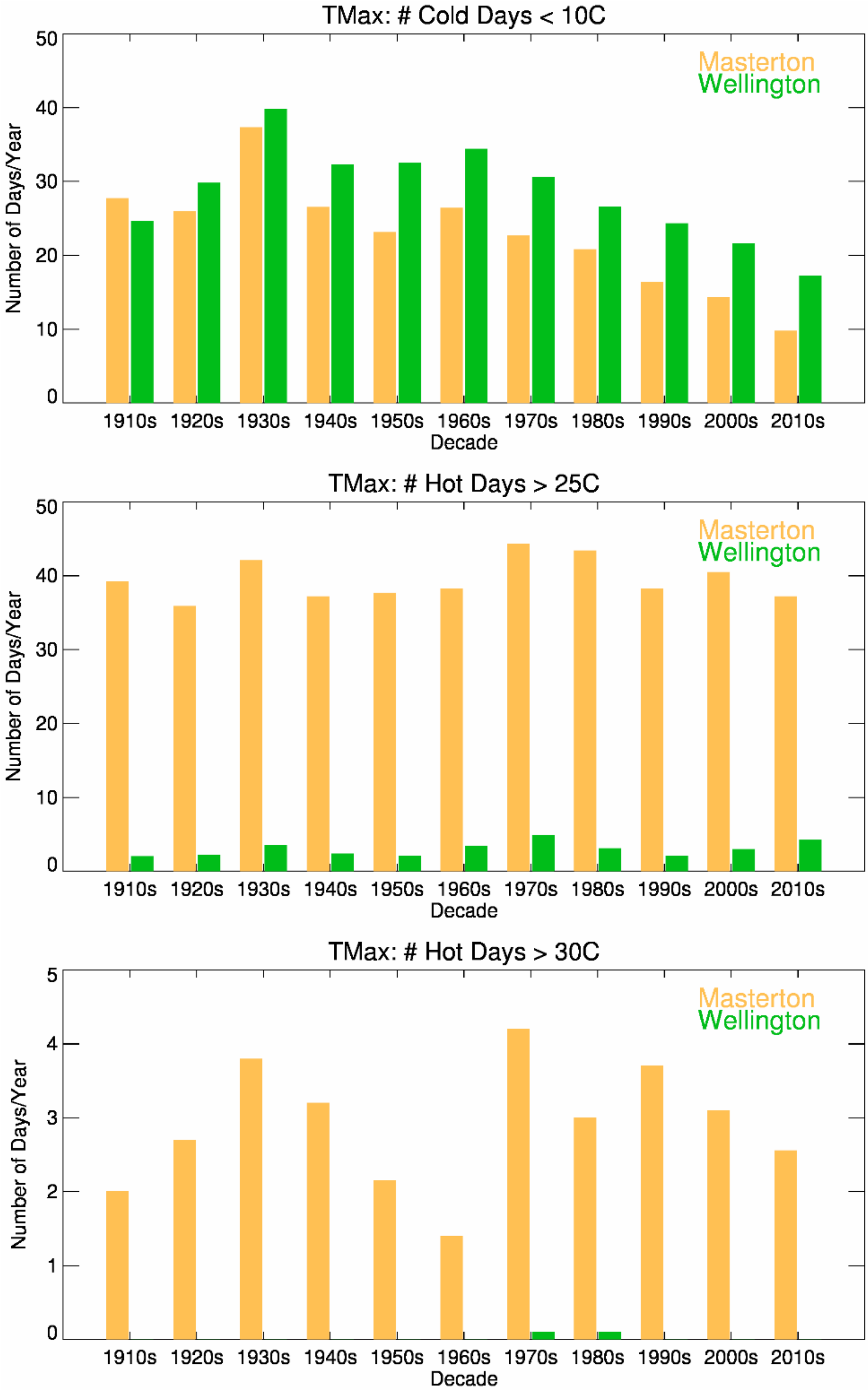

Figure 3-4: Annual-average (in days/year), for each decade from 1910-1919 to 2010-2018 of extremes for maximum temperature.

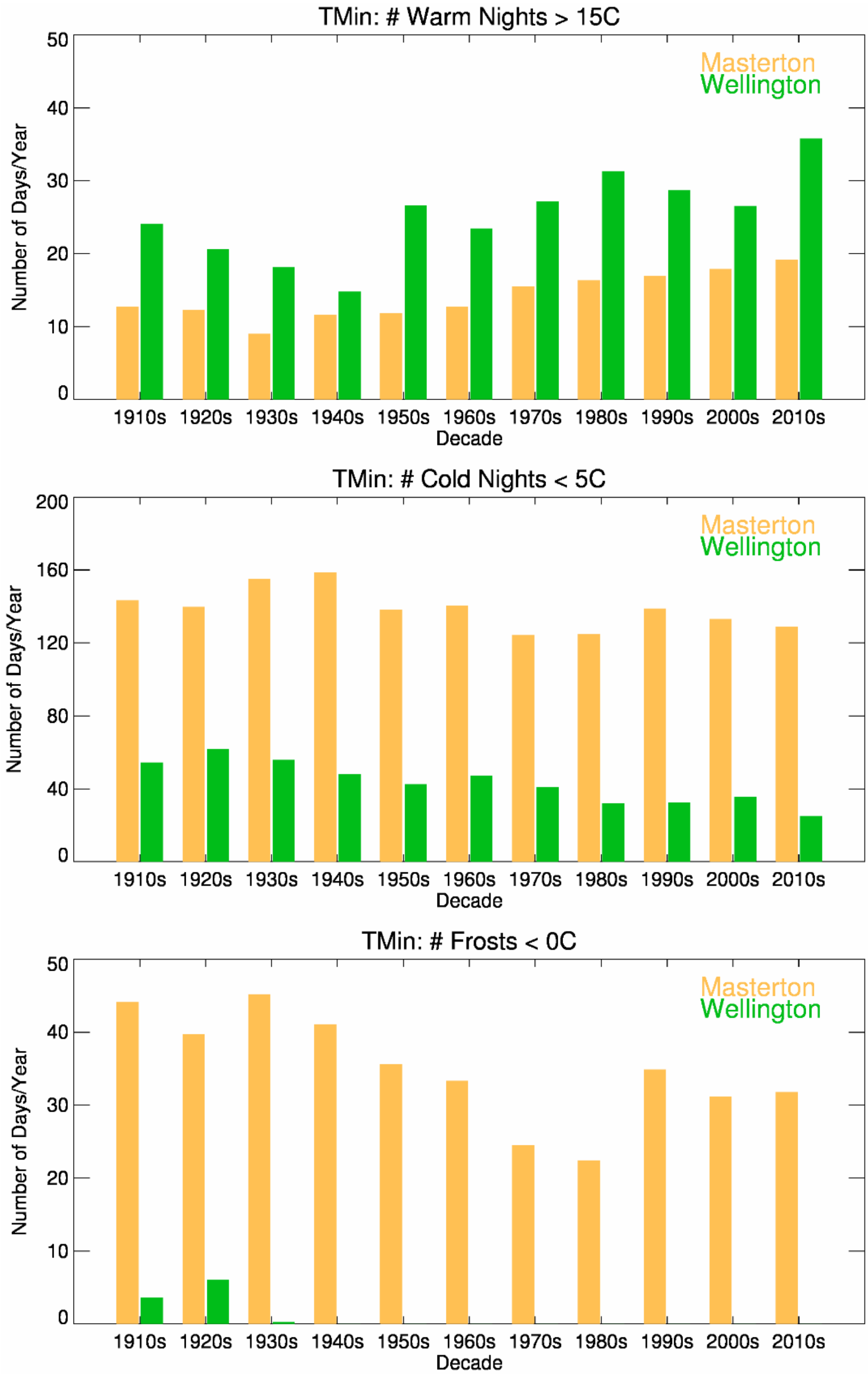

Figure 3-5: Annual-average (in days/year), for each decade from 1910-1919 to 2010-2018 of extremes for minimum temperature.

3.3 Changes already observed in extreme rainfall events

Figure 3-6 to Figure 3-8 contain annual precipitation maxima series for gauges located at Kelburn (Wellington), Wellington Airport and Paraparaumu, respectively. These stations were chosen as they have a long and contiguous record relative to other gauges in the area. These analyses were first presented in Pearce *et al.* (2019), but the figures below have been updated to include additional contemporary data (i.e. up to and including the year 2021). The nine panels in each figure contain the maxima series for different event durations ranging from 10 minutes to 5 days (120 hours). Linear trends have been fitted to all these time-series. To assess the robustness of the trends in the presence of sporadic very large extremes, trends have also been fitted after removing the largest and smallest outliers.

Note, with a warmer atmosphere, an increase in extreme rainfall is expected (see Section 4.2.3), even though it takes time for a change signal to be discernible from natural variability for a highly variable parameter such as rainfall (see Section 3.4 for further details on climate change signal emergence).

For Kelburn (Wellington) (Figure 3-6), this is mainly to test whether the two large short-duration events around the year 2000 are the main contributor to the positive trends for 10-min, 30-min and 1-hr duration events. As can be seen, while the magnitude of the trend reduces when these events are removed, the trends are still significant even when the most extreme 10% of points are removed. After removal of the most extreme points, the 1-hour duration trend comes to approximately 5 ± 2 mm/century. Expressed relative to the mean 1-hour annual maxima this equates to a 25% ± 10% increase per century.

This result needs to be treated with some scepticism as significant positive trends are not observed in other long-term records in this area. The record for Wellington Airport (Figure 3-7) actually shows a significant negative trend for the shortest durations and no significant trends for longer durations. However, there does appear to be some discontinuity in the available sub-hourly records for Wellington Airport, as they show a step decrease for the last twenty years of the record which may be due to an instrument change in 1995, and is likely to be distorting any real trend.

For Paraparaumu (Figure 3-8), no statistically significant trends (at the 5% level) are found for any event duration.

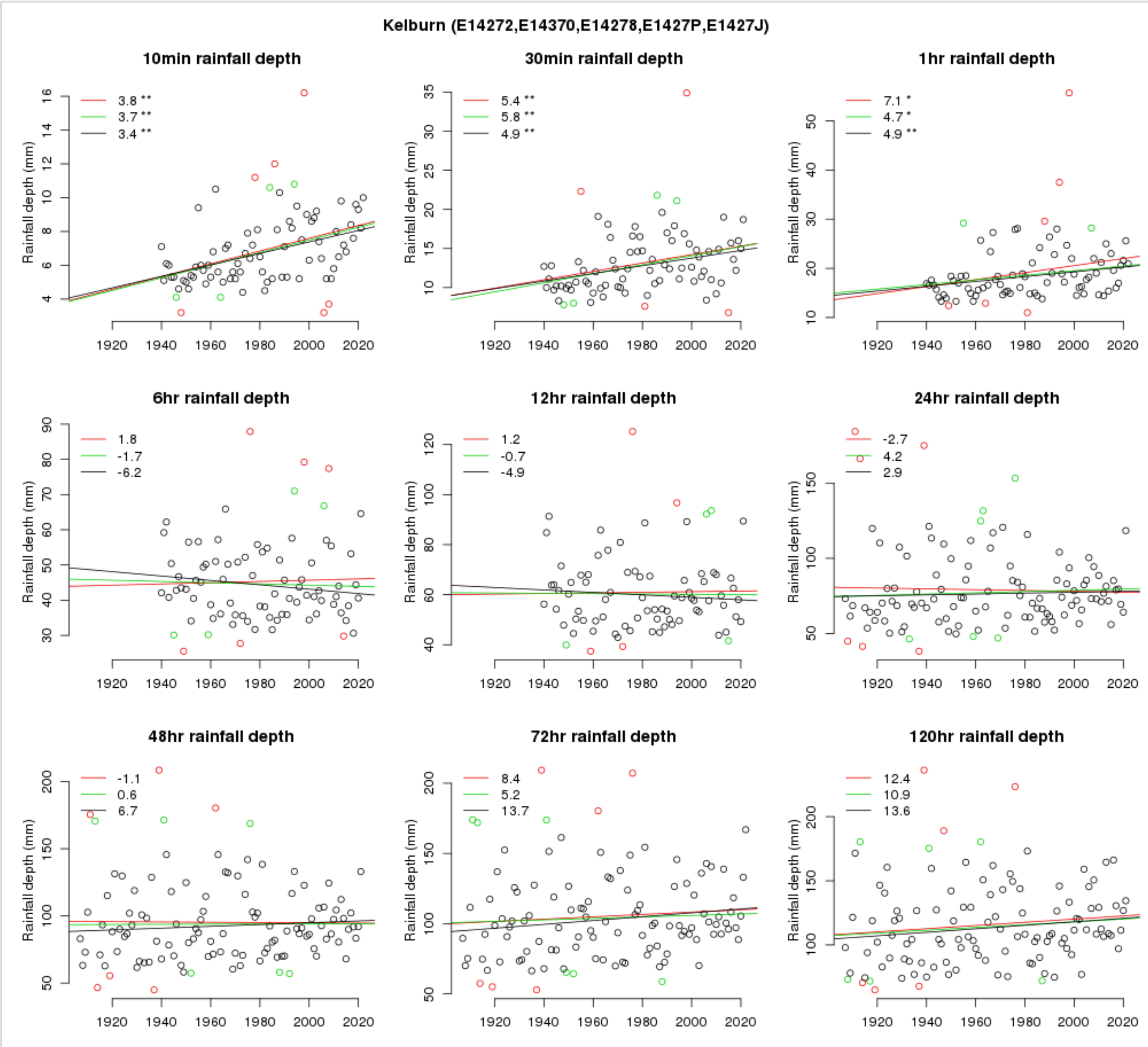

Figure 3-6: Annual maxima rainfall time series from Kelburn (Wellington) for a range of event durations. For each duration, trends have also been estimated with the trend magnitudes (in mm/century) shown in the figure legends. A '*' or '**' indicates significance at the 5% or 1% level, respectively. The red lines are trends fitted to all points in the series. The green lines are fitted after the most extreme 5% of points are removed; i.e. excluding the red points which are the top and bottom 2.5%. The black lines are fitted after both green and red points are removed (the top and bottom 5% of data points). For Kelburn (Wellington), the sub-daily record spans 1940-2021 and the daily record spans 1907-2021, although there is missing data between 1906 and 1927.

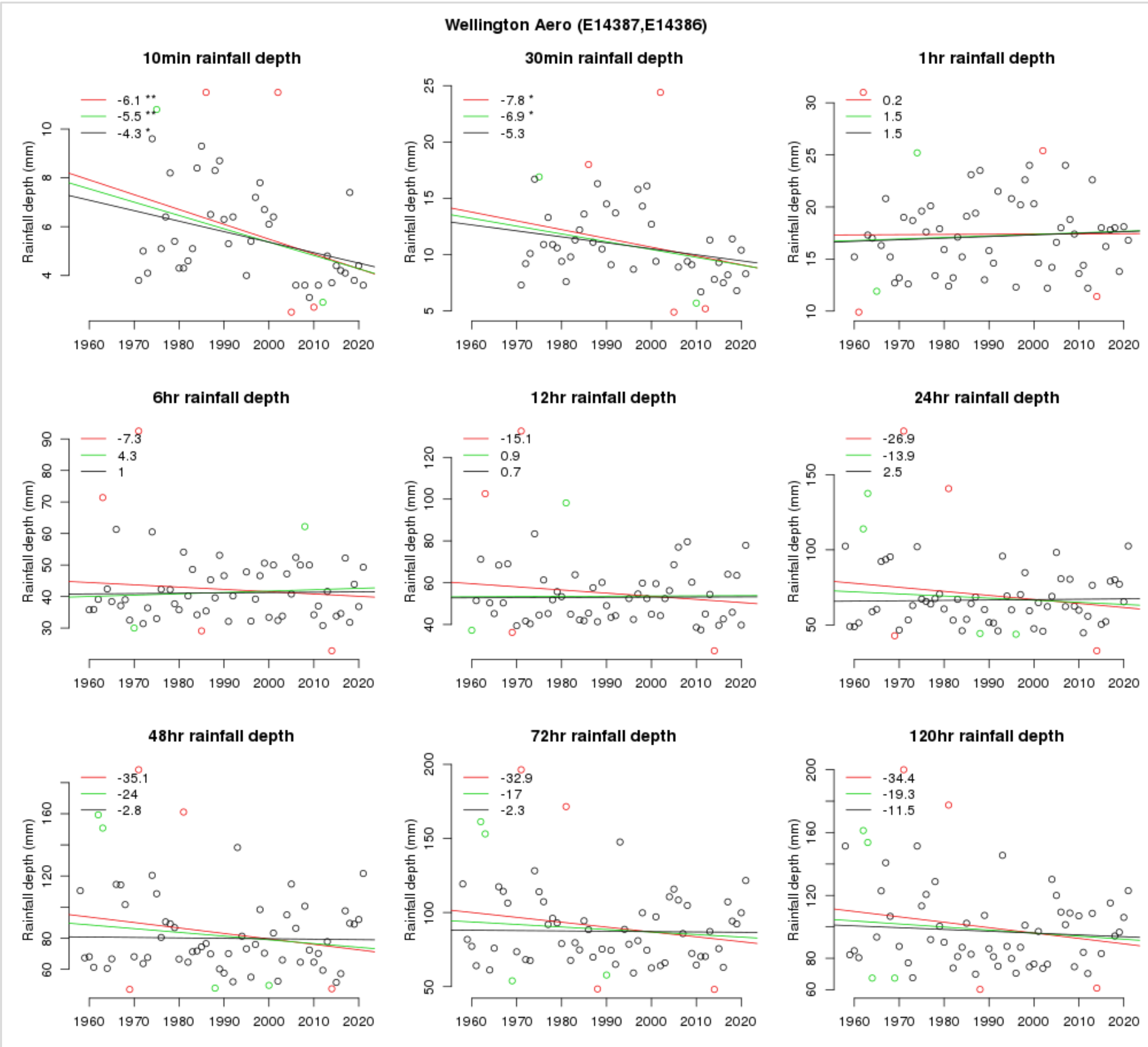

Figure 3-7: Annual maxima rainfall time series from Wellington Airport for a range of event durations. For each duration, trends have also been estimated with the trend magnitudes (in mm/century) shown in the figure legends. A '*' indicates significance at the 5% level. The red lines are trends fitted to all points in the series. The green lines are fitted after the most extreme 5% of points are removed; i.e. excluding the red points which are the top and bottom 2.5%. The black lines are fitted after both green and red points are removed (the top and bottom 5% of data points). For Wellington Airport, the sub-daily record spans 1960-2021 and the daily record spans 1958-2021.

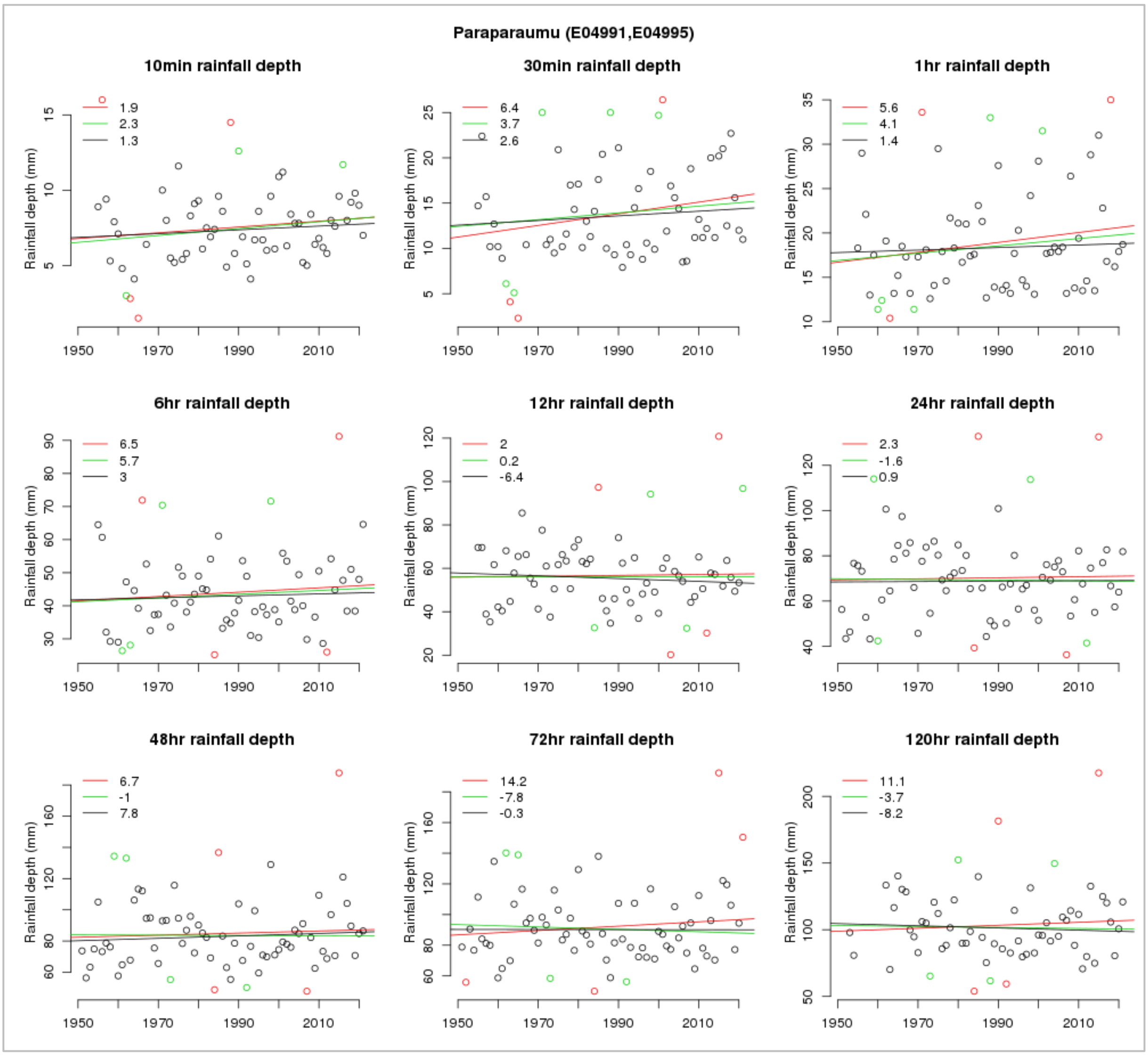

Figure 3-8: Annual maxima rainfall time series from Paraparaumu for a range of event durations. For each duration, trends have also been estimated with the trend magnitudes (in mm/century) shown in the figure legends. The trend magnitudes are not significant at the 5% level. The red lines are trends fitted to all points in the series. The green lines are fitted after the most extreme 5% of points are removed; i.e. excluding the red points which are the top and bottom 2.5%. The black lines are fitted after both green and red points are removed (the top and bottom 5% of data points). For Paraparaumu, the sub-daily record spans 1956-2021 and the daily record spans 1951-2021.

3.4 Climate change signal emergence for extremes

Wellington’s (Kelburn) mean temperature has increased at a rate of approximately 0.1°C per decade from 1909-2021 (Section 3.1), with a corresponding positive trend in warm nights, and negative trend in cold days, cold nights and frosts (Section 3.2). However, no statistically significant trend in hot days (both > 25°C, and > 30°C) is observed. In addition, no statistically significant trend in extreme rainfall is observed at Paraparaumu (Section 3.3). Considering this, it is important to note that it may be some time before statistically significant trends emerge in various climate and weather extremes, due to the noise (i.e. variability) of weather data and rarity of these extremes. This concept is termed the Time of Emergence (ToE), defined by Hawkins and Sutton (2012) as the time at which the signal of climate change emerges from the noise of natural variability.

ToE is widely acknowledged as a useful metric, but Frame *et al.* (2017) suggest a more useful metric for understanding climate change may be the *ratio* of climate signal to noise (S/N), which the authors define as a measure of the amplitude of change expressed in terms of units of existing variability. In other words, how much has the climate shifted relative to the background variability at a given location. As noted by Hawkins *et al.* (2020), S/N is important for climate impacts, as large changes outside past experience could be particularly harmful for ecosystems that have a limited ability to adapt. Impacts could additionally be anticipated for the primary sector and civil infrastructure, as societies are often adapted for the range of local climate experienced (Hawkins *et al.*, 2020).

The concept of emergence highlights a challenge with both observations and projections of future extreme weather. Because extreme weather is rare, a very long record is needed before a climate change signal becomes detectable in the number of events: for instance, a period much longer than 50 years would be needed before the shift of 1-in-50-year events to 1-in-30-year events became evident. While risks associated with some extreme events might have changed substantially because those events have become more or less likely, it might still be too early to be able to discern those changes in the observational record. Similarly, it is entirely possible that fewer extreme events might occur over the next decade even while the risk of those events increases, due to the aforementioned factors of noise and rarity. Farther in the future though, the number of extreme events should gradually match expectations.

At present, no studies have addressed ToE or S/N for the area. However, this shouldn't preclude climate change mitigation and adaptation efforts. Indeed, such efforts should be viewed as prudent given 1) contemporary extreme rainfall events in New Zealand were exacerbated (Dean *et al.*, 2013) and more likely (Rosier *et al.*, 2015) as a result of anthropogenic climate change, and 2) future climate changes projected for the area (Section 4). A large Beca consortium commissioned by GWRC and the Territorial Authorities of the Wellington Region is currently looking into localised climate change impacts for the region.

4 Future climate west of Wellington’s ranges

4.1 Temperature

4.1.1 Maximum temperature

Projected maximum temperature changes (°C, relative to 1986-2005)

Annual:

Period	RCP2.6	RCP4.5	RCP8.5
2040	+0.50-1.00	+0.75-1.00	+0.75-1.25
2090	+0.50-1.00	+1.25-1.75	+2.50-3.25

Seasonal:

	RCP2.6		RCP4.5		RCP8.5	
	2040	2090	2040	2090	2040	2090
Summer	+0.50-1.00	+0.50-1.00	+0.75-1.25	+1.00-1.75	+0.75-1.25	+2.25-3.50
Autumn	+0.50-1.00	+0.75-1.00	+0.75-1.25	+1.25-1.75	+1.00-1.50	+3.00-3.75
Winter	+0.50-1.00	+0.50-1.00	+0.50-1.00	+1.00-1.75	+0.50-1.25	+2.25-3.50
Spring	+0.50-0.75	+0.25-0.75	+0.50-1.00	+1.00-1.50	+0.50-1.00	+2.00-3.00

Maximum temperatures are generally recorded in the afternoon hours of the day, and therefore are known as day-time temperatures. Historic (average over 1986-2005) and future (average over 2031-2050 and 2081-2100) maps for mean maximum temperature are shown in this section. The historic maps show annual and seasonal mean maximum temperature in units of degrees Celsius (°C) and the future projection maps show the change in mean maximum temperature compared with the historic period. Note that the historic maps are on a different colour scale to the future projection maps. To aid comparison between the range of projections of annual and seasonal maximum temperature, a 30-panel figure of all projection maps is included in Appendix E.

For the historic period, annual mean maximum temperatures range between 15-18°C for much of the area (Figure 4-1). Highest annual mean maximum temperatures of 17-18°C are observed around Ōtaki, with lower ranges of 12-15°C for eastern and higher elevation areas. For most populated locations of the area, summer mean maximum temperature range between 20-22°C, while winter mean maximum temperatures range between 10-14°C (Figure 4-2). Autumn mean maximum temperatures are typically higher than the corresponding temperatures in spring. Interannual variability of temperatures (not shown in the maps) is a feature of the area. For the historic period 1986-2005, Kelburn’s annual mean daily maximum temperature ranged from a high of 16.7°C in 1998 and 1999, to a low of 14.4°C in 1992.

Representative concentration pathway (RCP) 2.6

By 2040, annual mean maximum temperatures are projected to increase by 0.50-1.00°C under RCP2.6 (Figure 4-3). At the seasonal scale, summer, autumn and spring maximum temperatures are projected to increase by 0.50-0.75°C for most of the area, while increases for winter range between 0.75-1.00°C for a greater proportion of the area (Figure 4-4).

By 2090, projected changes to annual mean maximum temperatures show a similar spatial pattern as 2040, with increases of 0.50-1.00°C for the area (Figure 4-3). Autumn maximum temperatures are projected to increase by 0.75-1.00°C throughout the area (Figure 4-5). Spring is projected to have maximum temperature increases ranging between 0.25-0.50°C for southernmost parts of the area.

Representative concentration pathway (RCP) 4.5

By 2040, annual mean maximum temperatures are projected to increase by 0.75-1.00°C under RCP4.5 (Figure 4-3). At the seasonal scale, summer and autumn maximum temperatures are projected to increase by 0.75-1.25°C, while increases for spring predominantly range between 0.50-0.75°C (Figure 4-6).

By 2090, projected changes to annual mean maximum temperatures are higher than 2040, with increases of 1.25-1.75°C for the area (Figure 4-3). Autumn and winter maximum temperatures are projected to increase by 1.25-1.75°C for most of the area, with highest autumn increases of 1.50-1.75°C predominantly north of Tawa and Lower Hutt (Figure 4-7). Lowest increases to seasonal maximum temperatures of 1.00-1.25°C are projected in spring for most of the area, and coastal areas north of Porirua in summer.

Representative concentration pathway (RCP) 8.5

By 2040, annual mean maximum temperatures are projected to increase by 0.75-1.25°C under RCP8.5 (Figure 4-3). At the seasonal scale, projected increases are greatest in autumn, ranging between 1.00-1.50°C throughout the area (Figure 4-8). The projected increases in summer and winter are alike, mostly ranging between 0.75-1.00°C, although a small portion about Ōtaki sees increases of 0.50-0.75°C. Spring is projected to have maximum temperature increases ranging from 0.50-1.00°C.

By 2090, projected increases to maximum temperatures are considerable, with annual increases of 2.50-3.25°C projected for the area (Figure 4-3). At the seasonal scale, autumn maximum temperatures are projected to increase by the most across the area, with increases of 3.00-3.75°C (Figure 4-9). Given the historic (1986-2005) mean maximum temperature in autumn is 16-18°C for much of the area, such increases could mean the autumn maximum temperatures for these parts range from approximately 19-24°C by 2090 under RCP8.5. Under this scenario, autumn maximum temperatures would be about equal or even slightly higher than historic (1986-2005) summer maximum temperatures. Spring is projected to experience the smallest increases, although they are still considerable, ranging from 2.00-3.00°C.

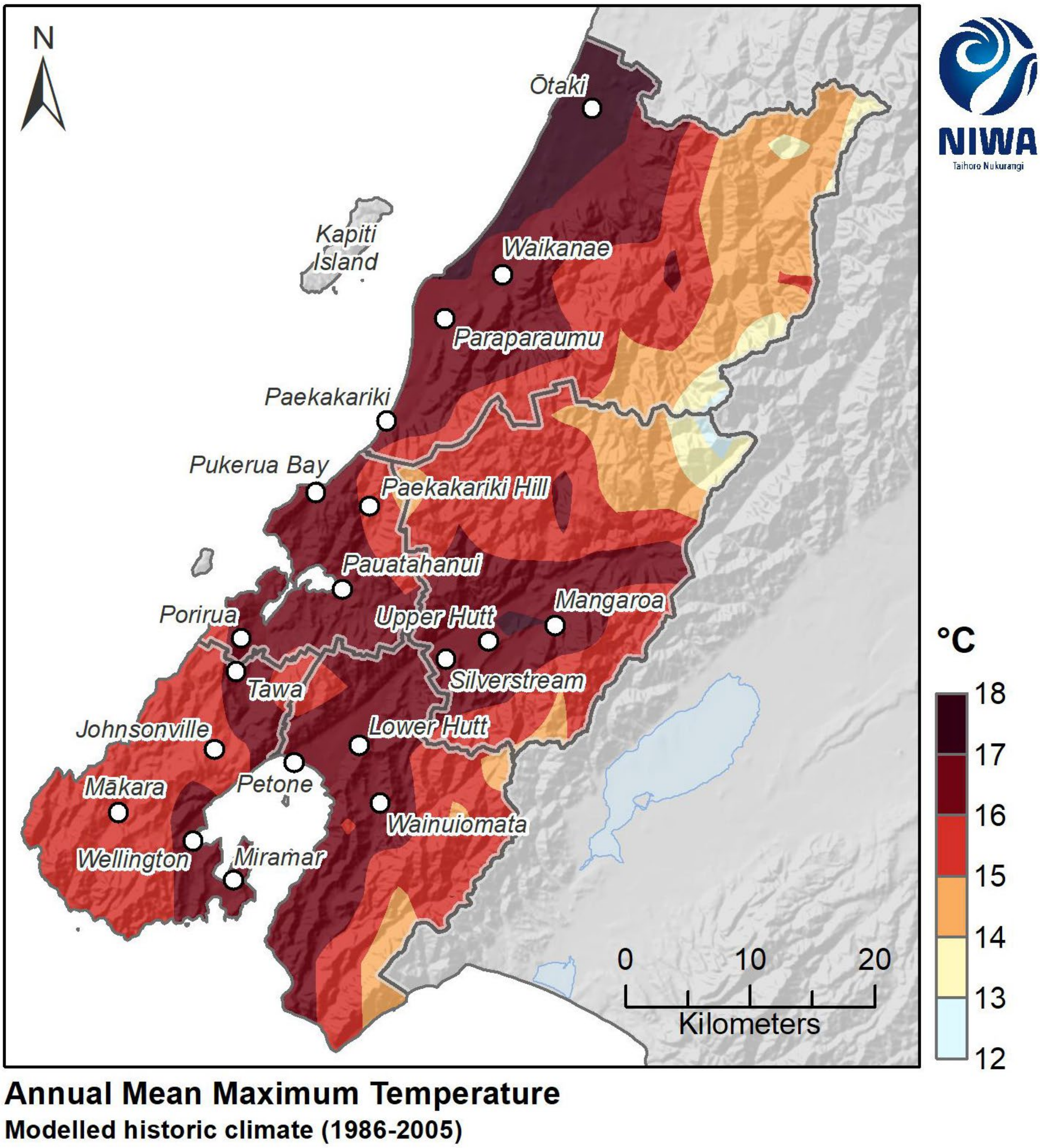

Figure 4-1: Modelled annual mean maximum temperature, average over 1986-2005. Results are based on dynamical downscaled projections using NIWA's Regional Climate Model. Resolution of projection is 5km x 5km.

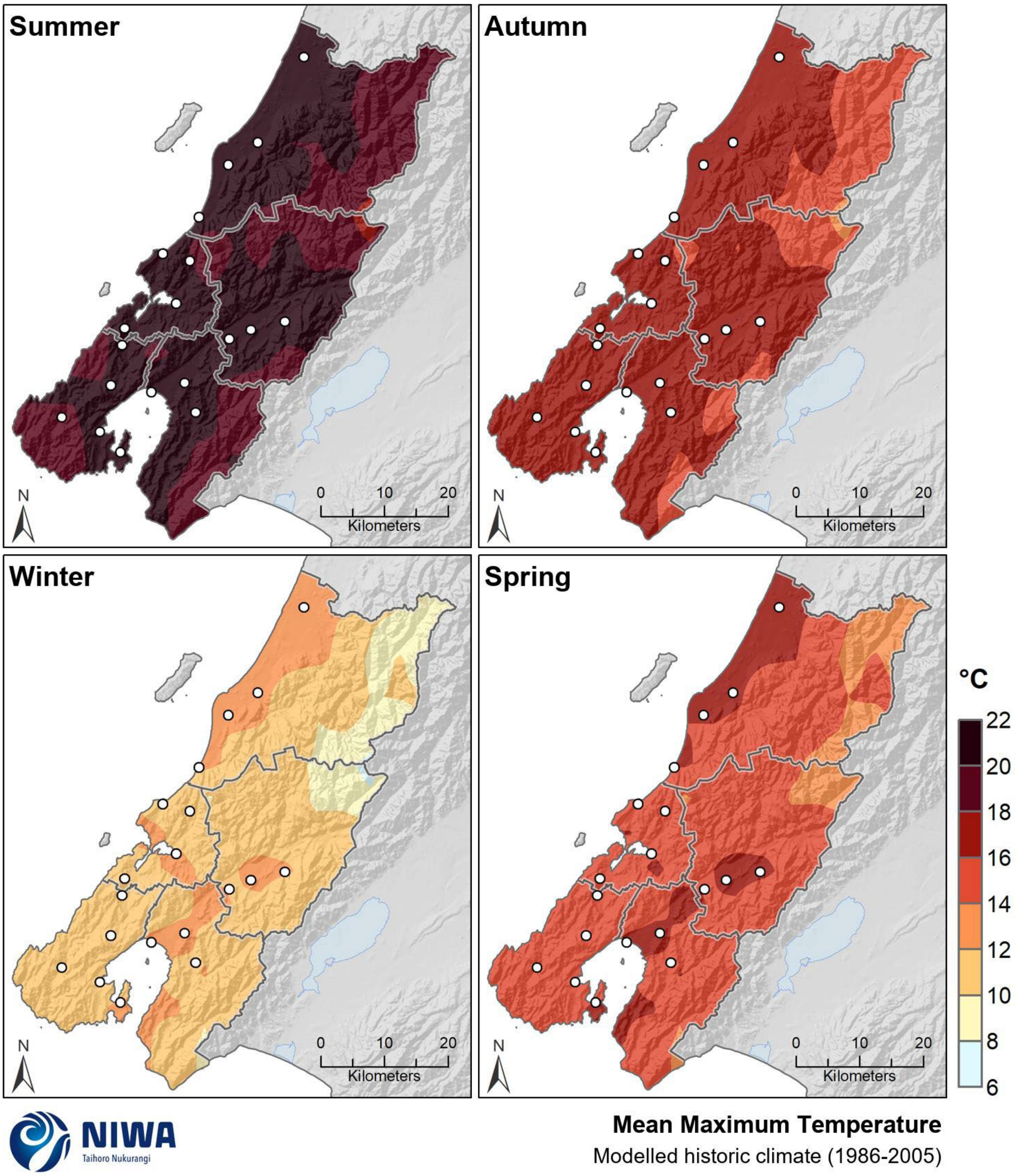

Figure 4-2: Modelled seasonal mean maximum temperature, average over 1986-2005. Results are based on dynamical downscaled projections using NIWA's Regional Climate Model. Resolution of projection is 5km x 5km.

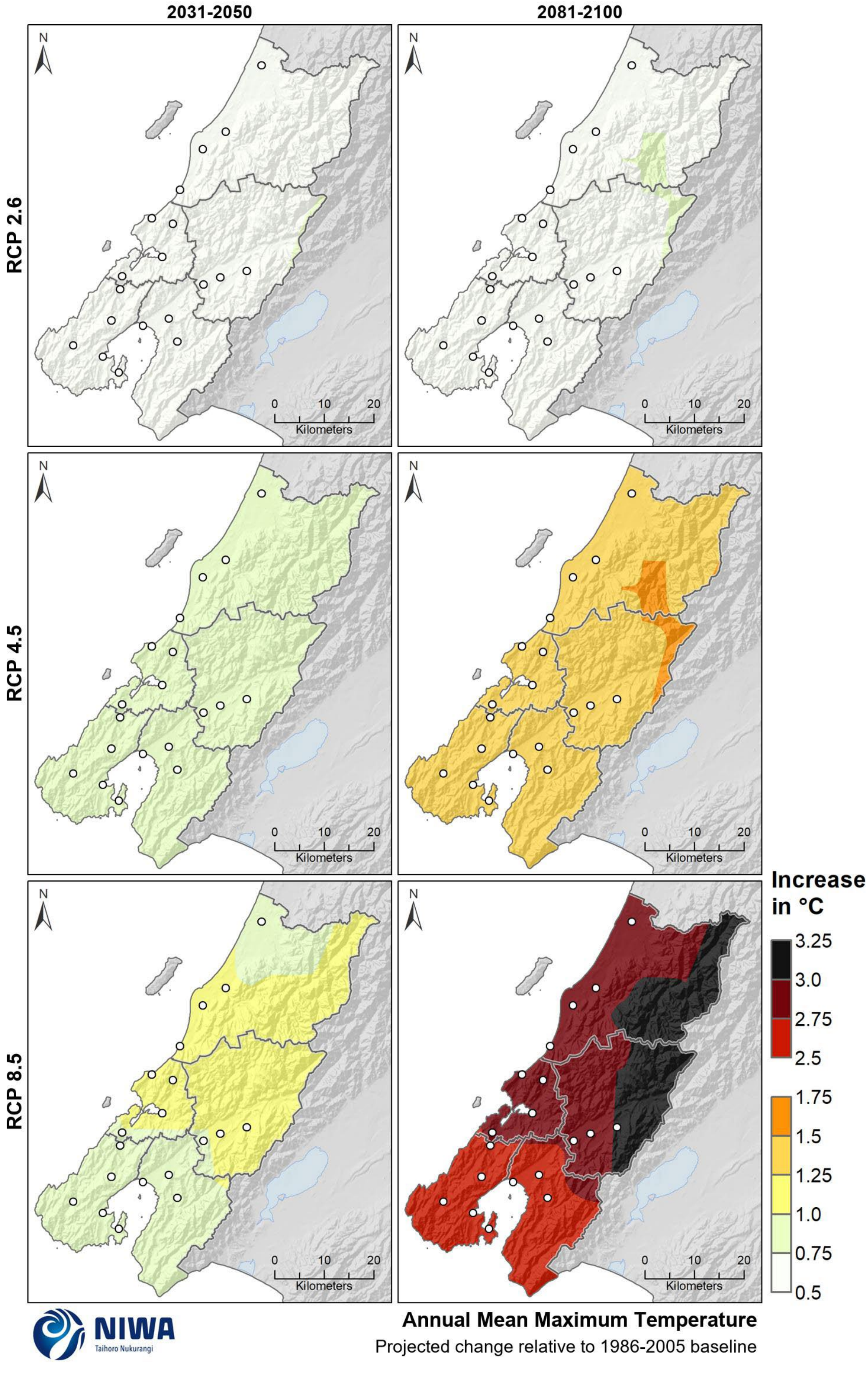

Figure 4-3: Projected annual mean maximum temperature changes by 2040 and 2090 under RCP2.6, RCP4.5 and RCP8.5. Relative to 1986-2005 average, based on the average of six global climate models. Results are based on dynamical downscaled projections using NIWA's Regional Climate Model. Resolution of projection is 5km x 5km. Note, a scale break is required to encapsulate the considerable difference in projected temperature change by 2090 under RCP2.6 compared to RCP8.5.

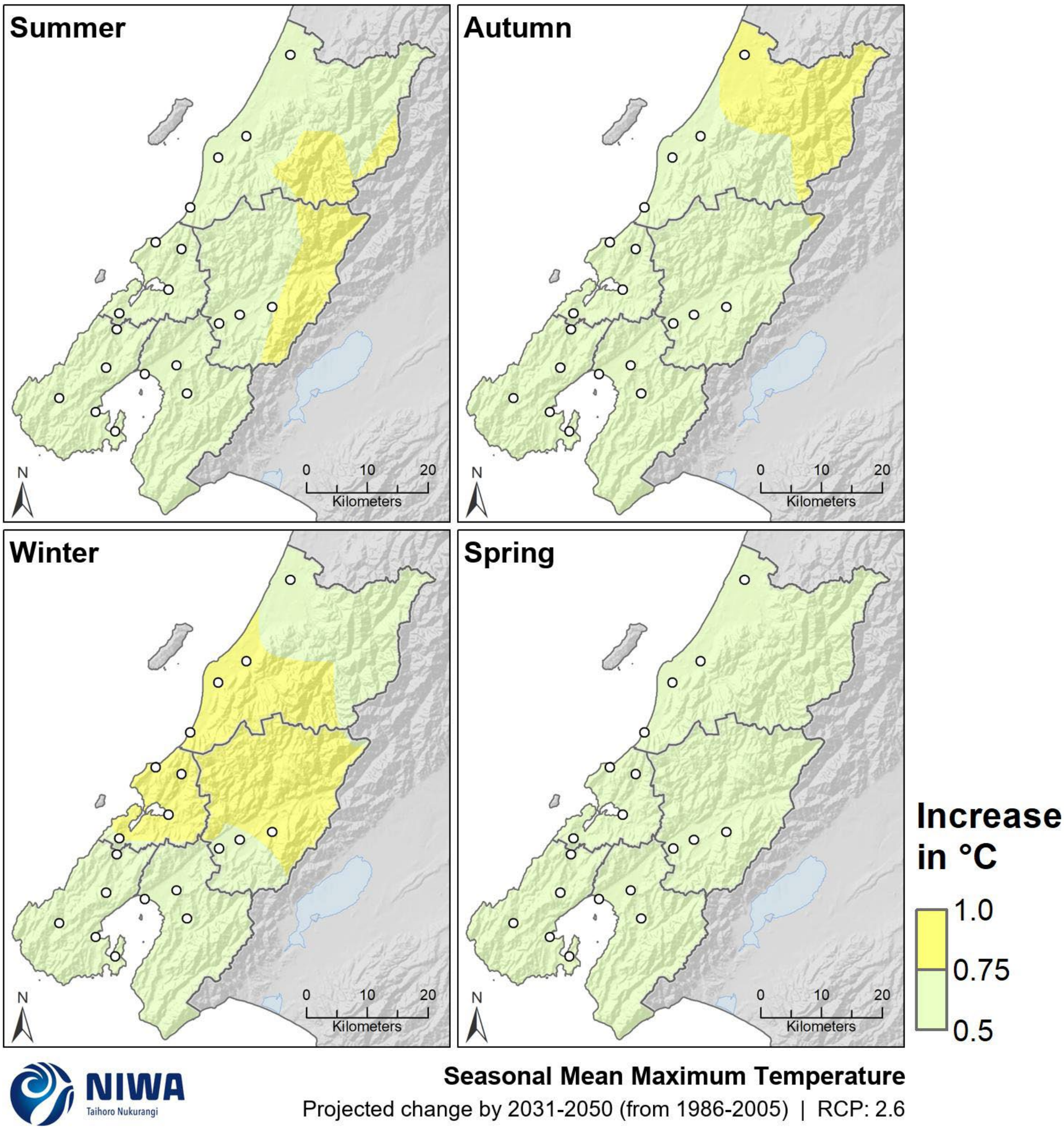

Figure 4-4: Projected seasonal mean maximum temperature changes by 2040 under RCP2.6. Relative to 1986-2005 average, based on the average of six global climate models. Results are based on dynamical downscaled projections using NIWA's Regional Climate Model. Resolution of projection is 5km x 5km.

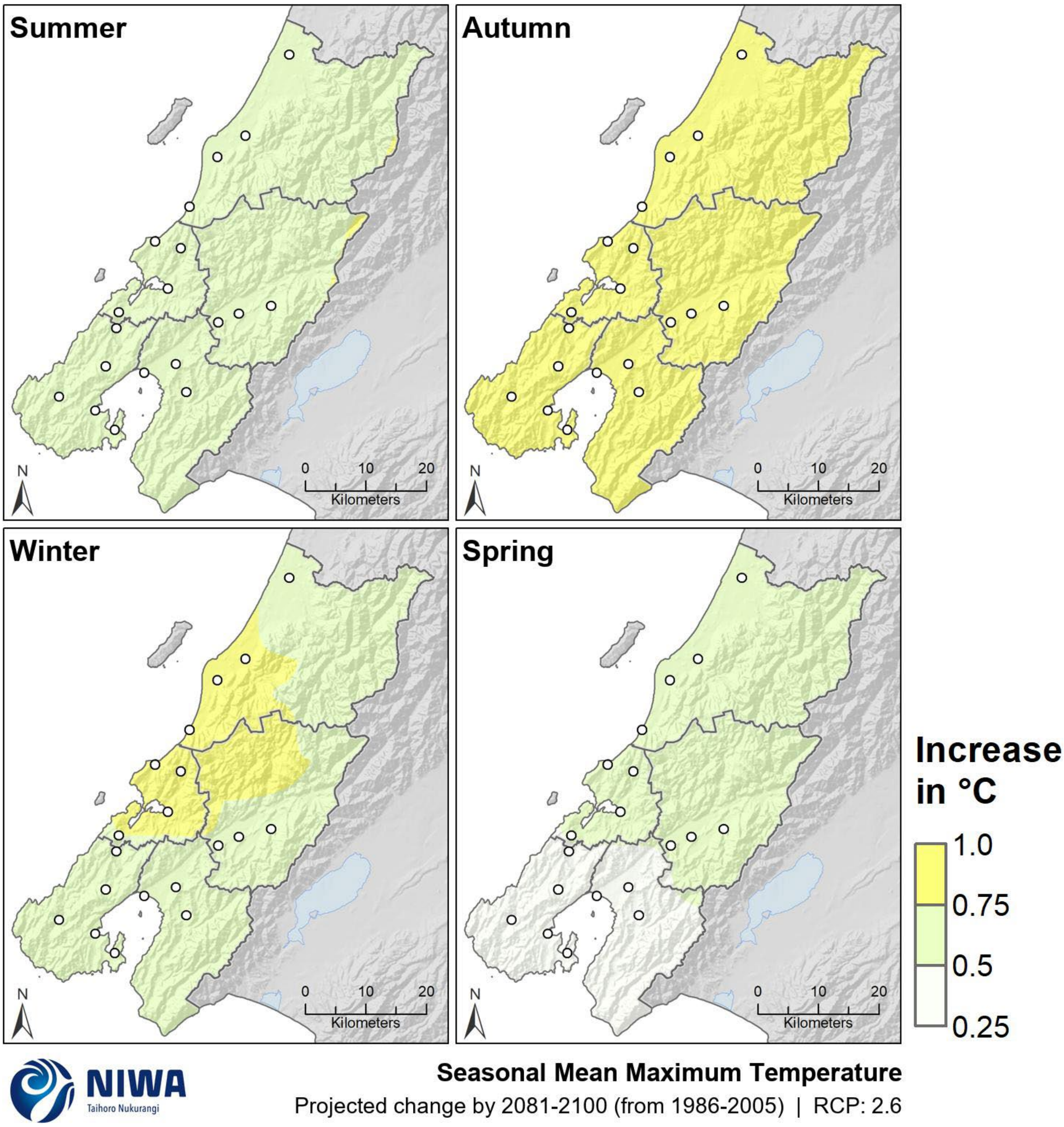

Figure 4-5: Projected seasonal mean maximum temperature changes by 2090 under RCP2.6. Relative to 1986-2005 average, based on the average of six global climate models. Results are based on dynamical downscaled projections using NIWA's Regional Climate Model. Resolution of projection is 5km x 5km.

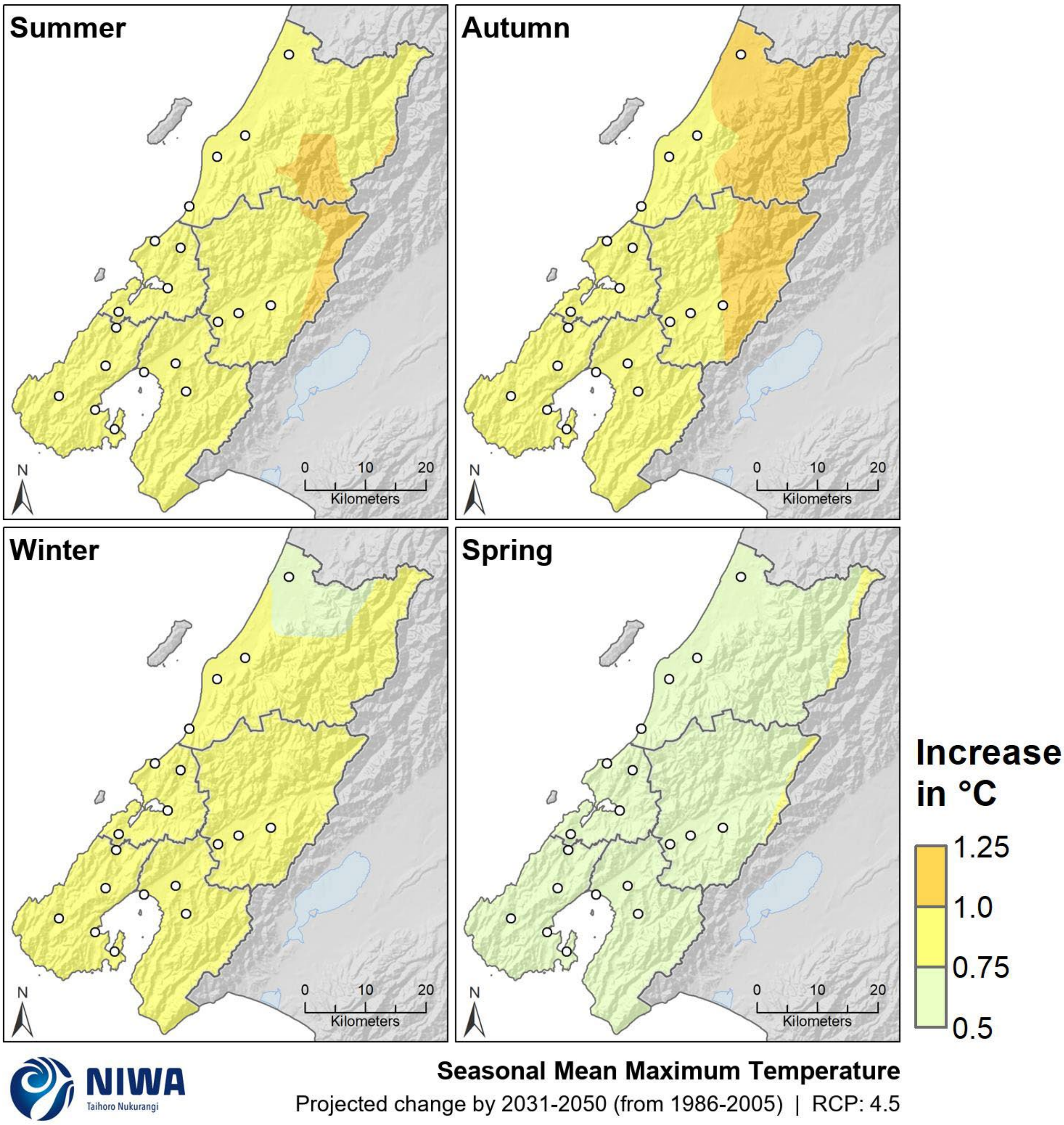

Figure 4-6: Projected seasonal mean maximum temperature changes by 2040 under RCP4.5. Relative to 1986-2005 average, based on the average of six global climate models. Results are based on dynamical downscaled projections using NIWA's Regional Climate Model. Resolution of projection is 5km x 5km.

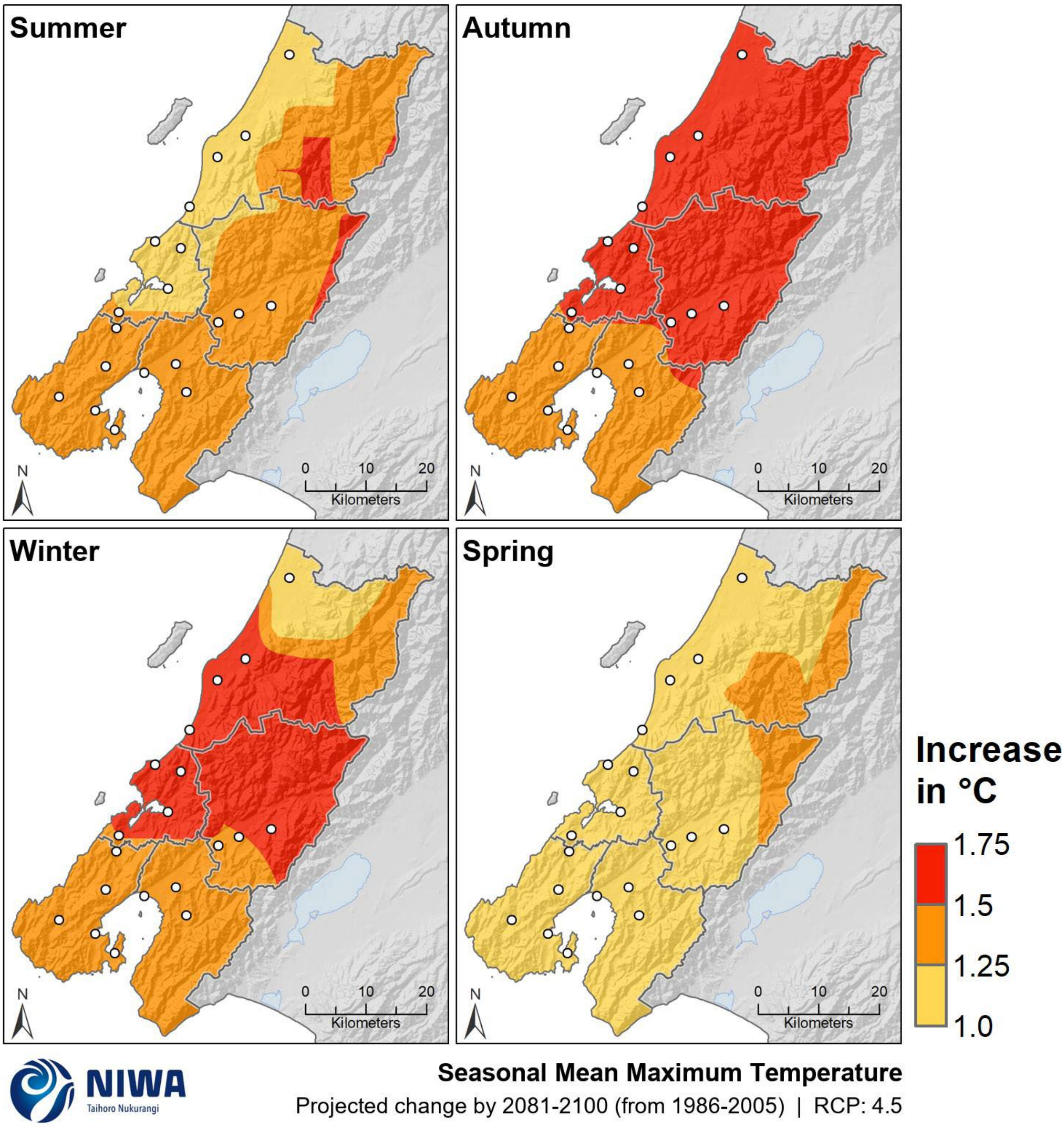

Figure 4-7: Projected seasonal mean maximum temperature changes by 2090 under RCP4.5. Relative to 1986-2005 average, based on the average of six global climate models. Results are based on dynamical downscaled projections using NIWA's Regional Climate Model. Resolution of projection is 5km x 5km.

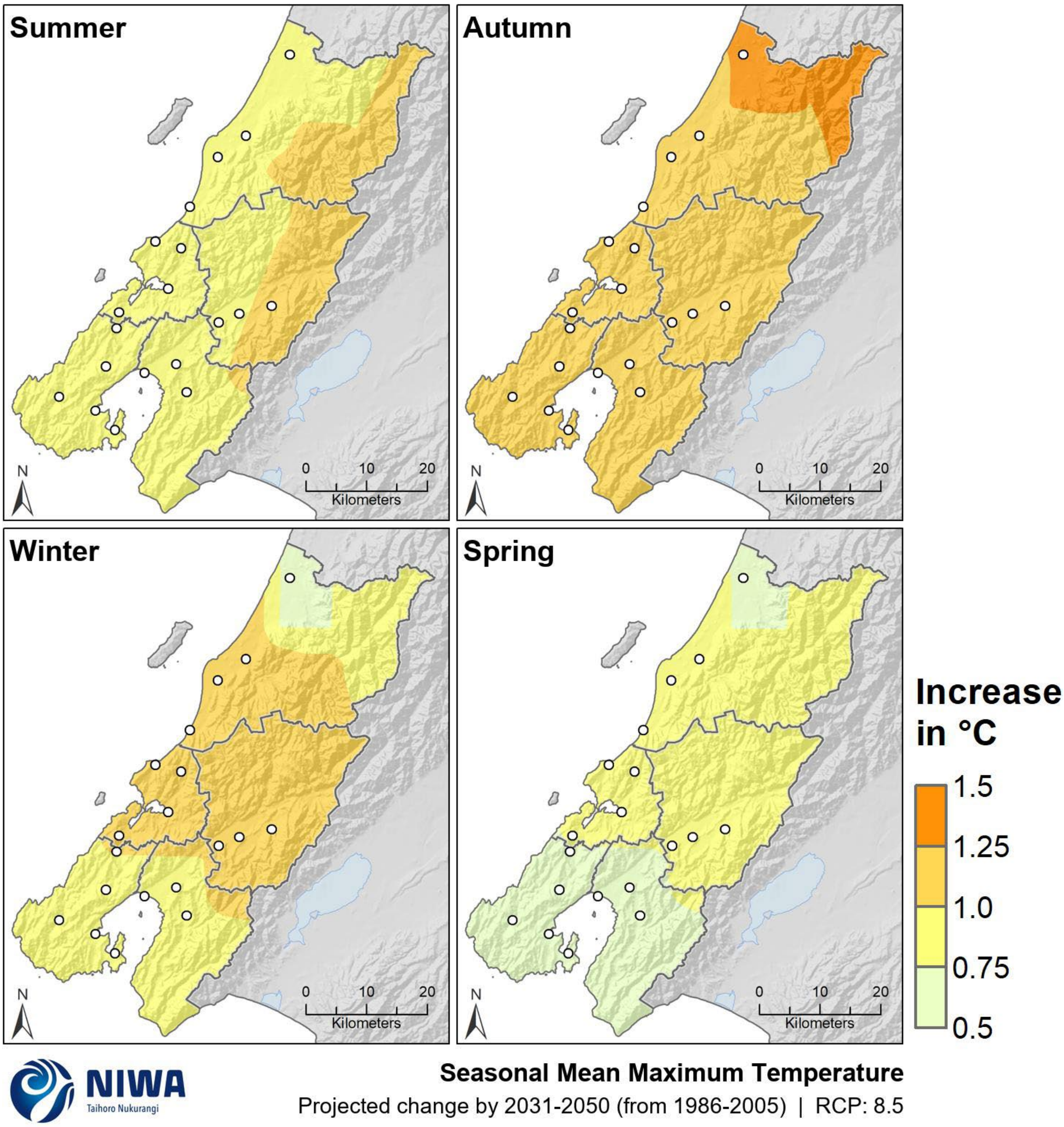

Figure 4-8: Projected seasonal mean maximum temperature changes by 2040 under RCP8.5. Relative to 1986-2005 average, based on the average of six global climate models. Results are based on dynamical downscaled projections using NIWA's Regional Climate Model. Resolution of projection is 5km x 5km.

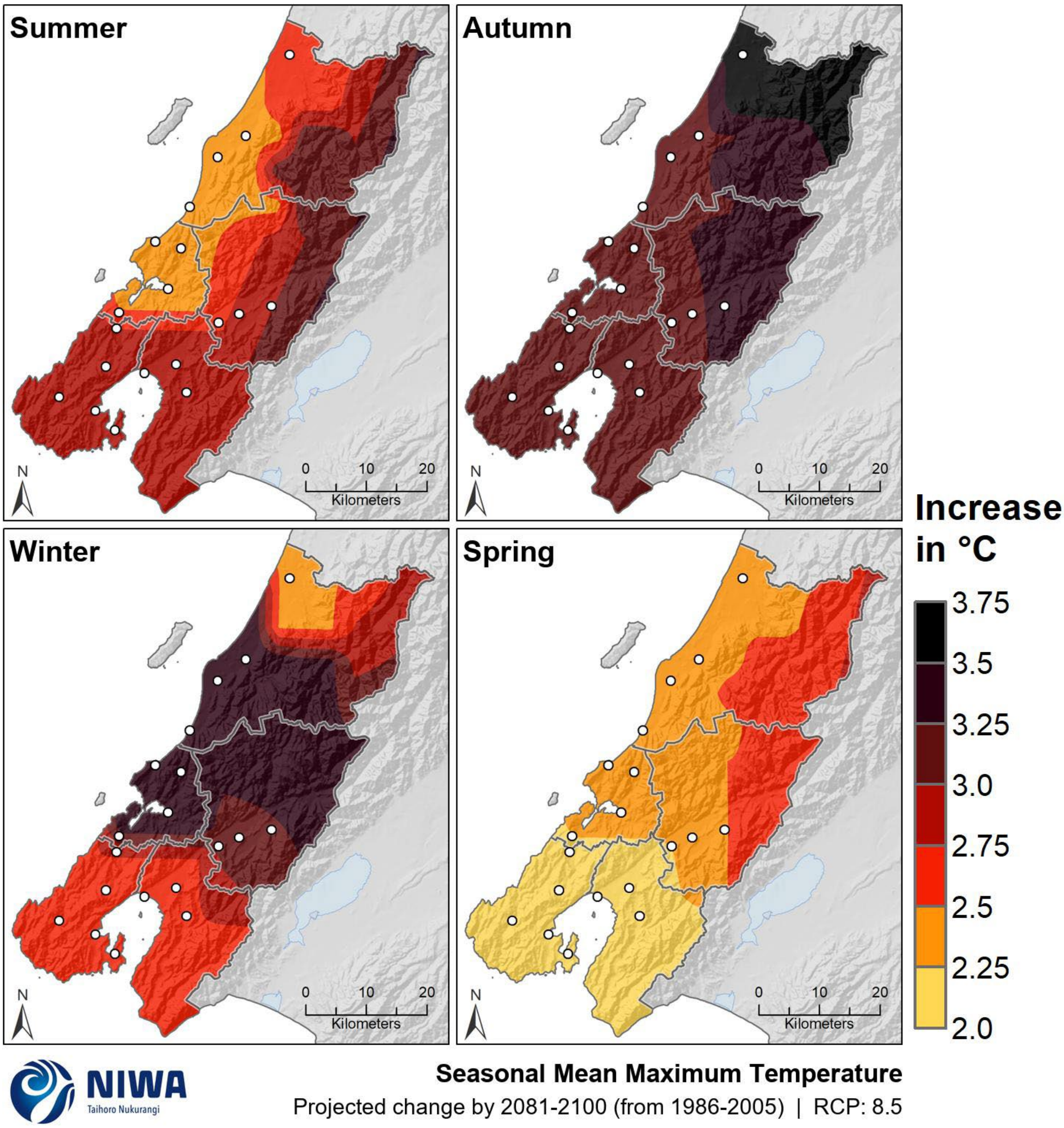

Figure 4-9: Projected seasonal mean maximum temperature changes by 2090 under RCP8.5. Relative to 1986-2005 average, based on the average of six global climate models. Results are based on dynamical downscaled projections using NIWA's Regional Climate Model. Resolution of projection is 5km x 5km.

4.1.2 Minimum temperature

Projected minimum temperature changes (°C, relative to 1986-2005)

Annual:

Period	RCP2.6	RCP4.5	RCP8.5
2040	+0.25-0.75	+0.50-0.75	+0.50-0.75
2090	+0.25-0.75	+0.75-1.25	+1.75-2.50

Seasonal:

	RCP2.6		RCP4.5		RCP8.5	
	2040	2090	2040	2090	2040	2090
Summer	+0.25-0.75	+0.25-0.75	+0.25-0.75	+0.75-1.25	+0.50-0.75	+1.75-2.25
Autumn	+0.25-0.75	+0.50-0.75	+0.50-1.00	+1.00-1.25	+0.75-1.00	+2.00-2.75
Winter	+0.25-0.75	+0.25-0.50	+0.25-0.75	+0.50-1.00	+0.25-0.75	+1.50-2.25
Spring	+0.25-0.75	+0.25-0.50	+0.50-0.75	+0.75-1.25	+0.50-0.75	+2.00-2.25

Minimum temperatures are generally recorded in the early hours of the morning, and therefore are known as night-time temperatures. Historic (average over 1986-2005) and future (average over 2031-2050 and 2081-2100) maps for mean minimum temperature are shown in this section. The historic maps show annual and seasonal mean minimum temperature in units of degrees Celsius (°C) and the future projection maps show the change in mean minimum temperature compared with the historic period, in units of °C. Note that the historic maps are on a different colour scale to the future projection maps. To aid comparison between the range of projections of annual and seasonal minimum temperature, a 30-panel figure of all projection maps is included in Appendix E.

For the historic period, coastal and southern portions of the area have the highest annual mean minimum temperatures ranging from 9-11°C (Figure 4-10). Annual mean minimum temperatures range between 7-9°C for many inland and higher elevation areas. Lowest annual mean minimum temperatures of 4-6°C are observed in the Tararua Range in the northeast of the the area area. Winter mean minimum temperatures between 0-2°C are observed for the highest elevations, and between 4-6°C for most low elevation areas (Figure 4-11). Highest seasonal mean minimum temperatures of 12-14°C are observed in summer for coastal and low elevation parts of the area.

Representative concentration pathway (RCP) 2.6

By 2040, annual mean minimum temperatures are projected to increase by 0.25-0.75°C under RCP2.6 (Figure 4-12). Projected increases to seasonal minimum temperatures range between 0.25-0.75°C (Figure 4-13).

By 2090, increases to annual mean minimum temperatures of 0.25-0.75°C are projected (Figure 4-12). Summer, winter and spring minimum temperatures are projected to increase by 0.25-0.50°C for most of the area, while autumn is projected to have minimum temperature increases ranging from 0.50-0.75°C (Figure 4-14).

Representative concentration pathway (RCP) 4.5

By 2040, annual mean minimum temperatures are projected to increase by 0.50-0.75°C under RCP4.5 (Figure 4-12). Projected increases to seasonal minimum temperatures in the area mostly range between 0.25-0.75°C (Figure 4-15). The exception is in autumn for northern parts of the area, where increases of 0.75-1.00°C are projected.

By 2090, increases to annual mean minimum temperatures of 0.75-1.25°C are projected for the area (Figure 4-12). Summer and spring minimum temperatures are also projected to increase by 0.75-1.25°C, while autumn is projected to have minimum temperature increases ranging between 1.00-1.25°C throughout the area (Figure 4-16). Winter minimum temperatures are projected to increase by 0.50-1.00°C.

Representative concentration pathway (RCP) 8.5

By 2040, annual mean minimum temperatures are projected to increase by 0.50-0.75°C under RCP8.5 in the area (Figure 4-12). At the seasonal scale, summer and spring minimum temperatures are projected to increase by 0.50-0.75°C throughout the area (Figure 4-17). Autumn minimum temperatures are projected to increase by 0.75-1.00°C throughout the area, while winter minimum temperature increases of 0.25-0.75°C are projected for the area.

By 2090, projected increases to minimum temperatures are greater than under RCP2.6 and RCP4.5, with annual increases of 1.75-2.50°C projected for the area (Figure 4-12). At the seasonal scale, autumn minimum temperatures are projected to increase the most compared with the other seasons (+2.00-2.75°C; Figure 4-18). Increases of 2.00-2.25°C are projected for spring, and increases of 1.50-2.25°C are projected for winter.

Notably, the projected increases in maximum temperature are greater than the projected increases for minimum temperature in the area. This would result in an enhanced diurnal temperature range (i.e., the difference between the daily maximum and minimum air temperature). The projected changes to diurnal temperature range are largest in winter, with much of the area projected to experience an increase in annual diurnal temperature range of 0.50-1.00°C by 2090 under RCP8.5. See Pearce et al. (2017) for further details.

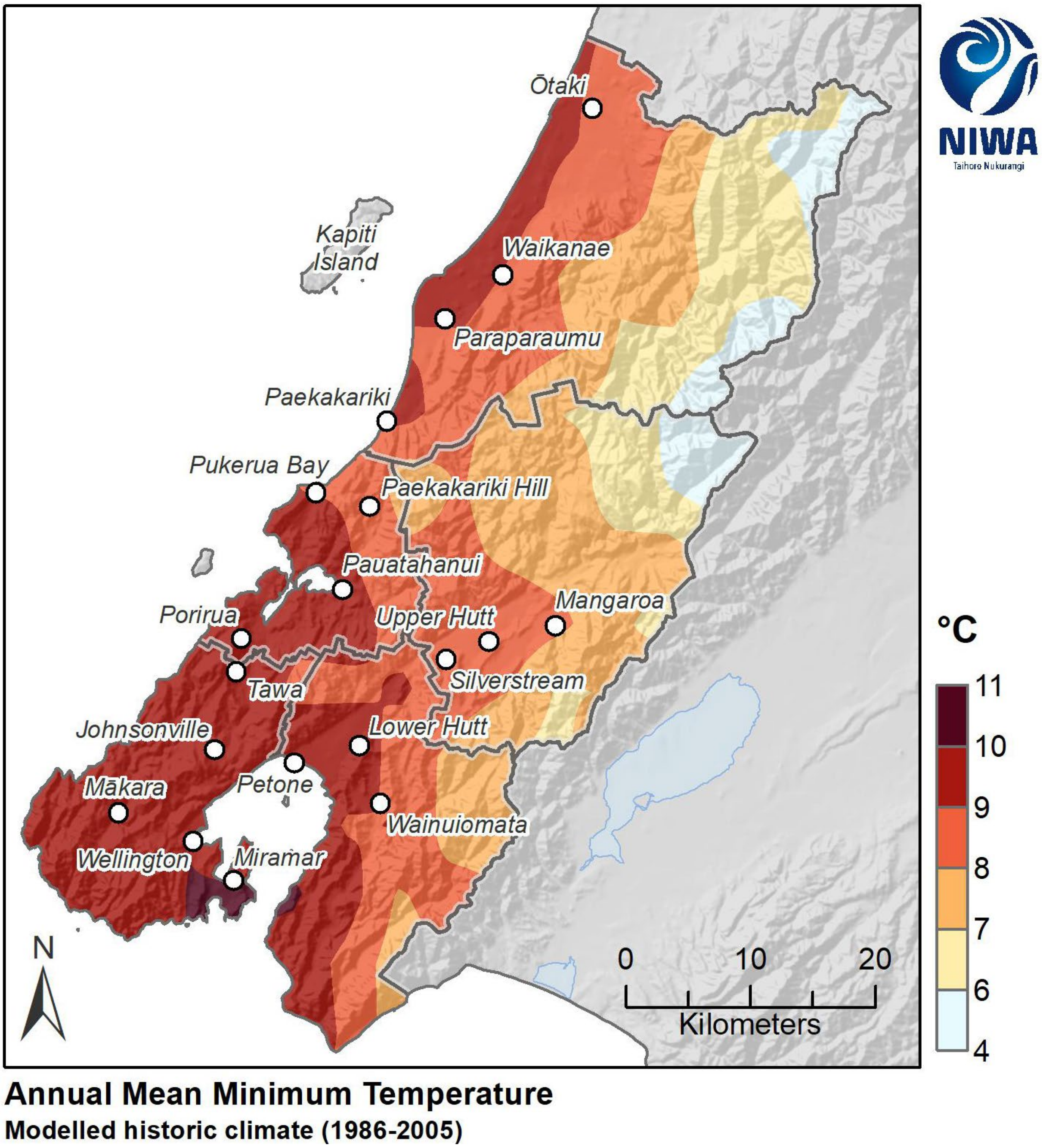

Figure 4-10: Modelled annual mean minimum temperature, average over 1986-2005. Results are based on dynamical downscaled projections using NIWA's Regional Climate Model. Resolution of projection is 5km x 5km.

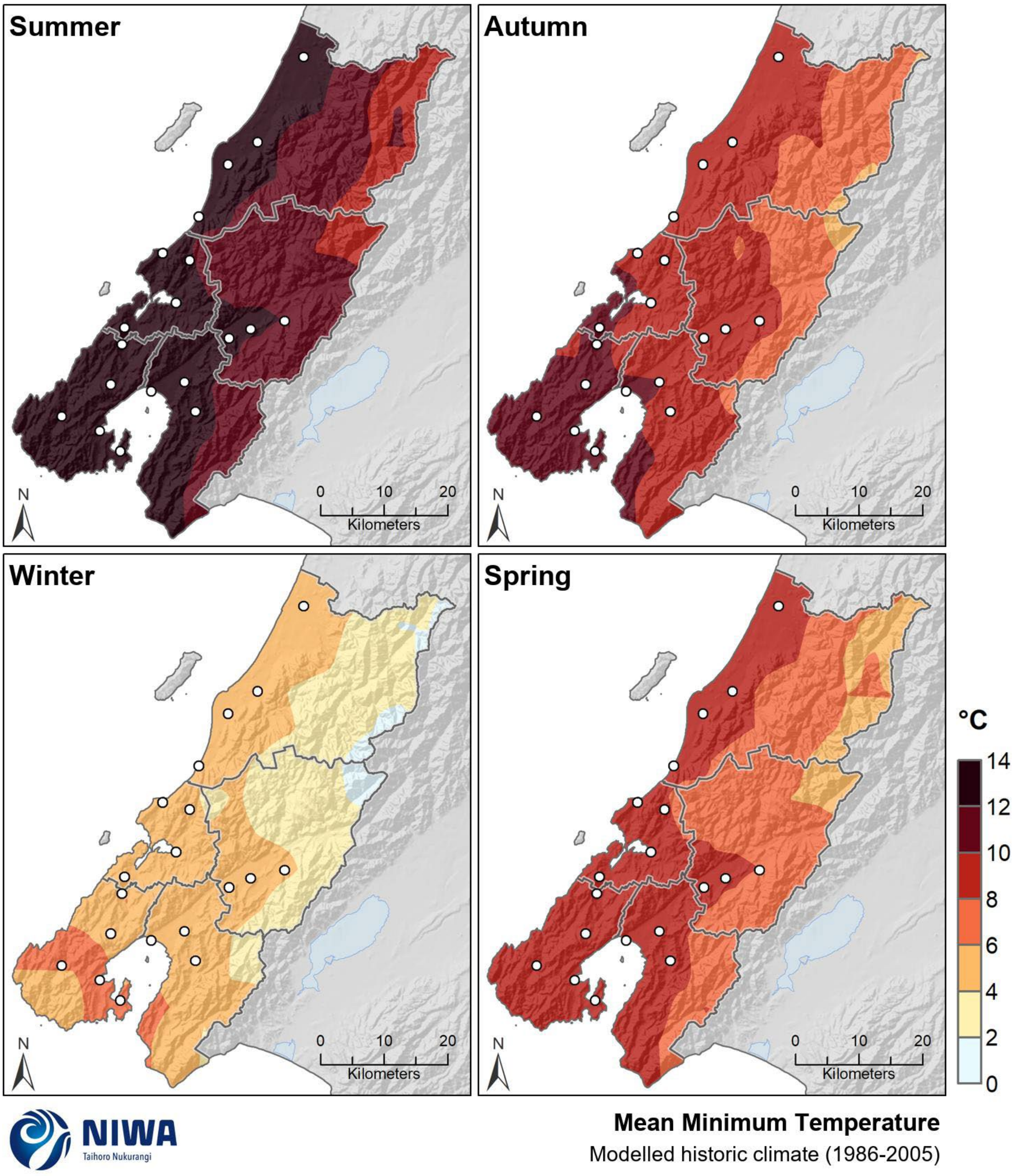

Figure 4-11: Modelled seasonal mean minimum temperature, average over 1986-2005. Results are based on dynamical downscaled projections using NIWA's Regional Climate Model. Resolution of projection is 5km x 5km.

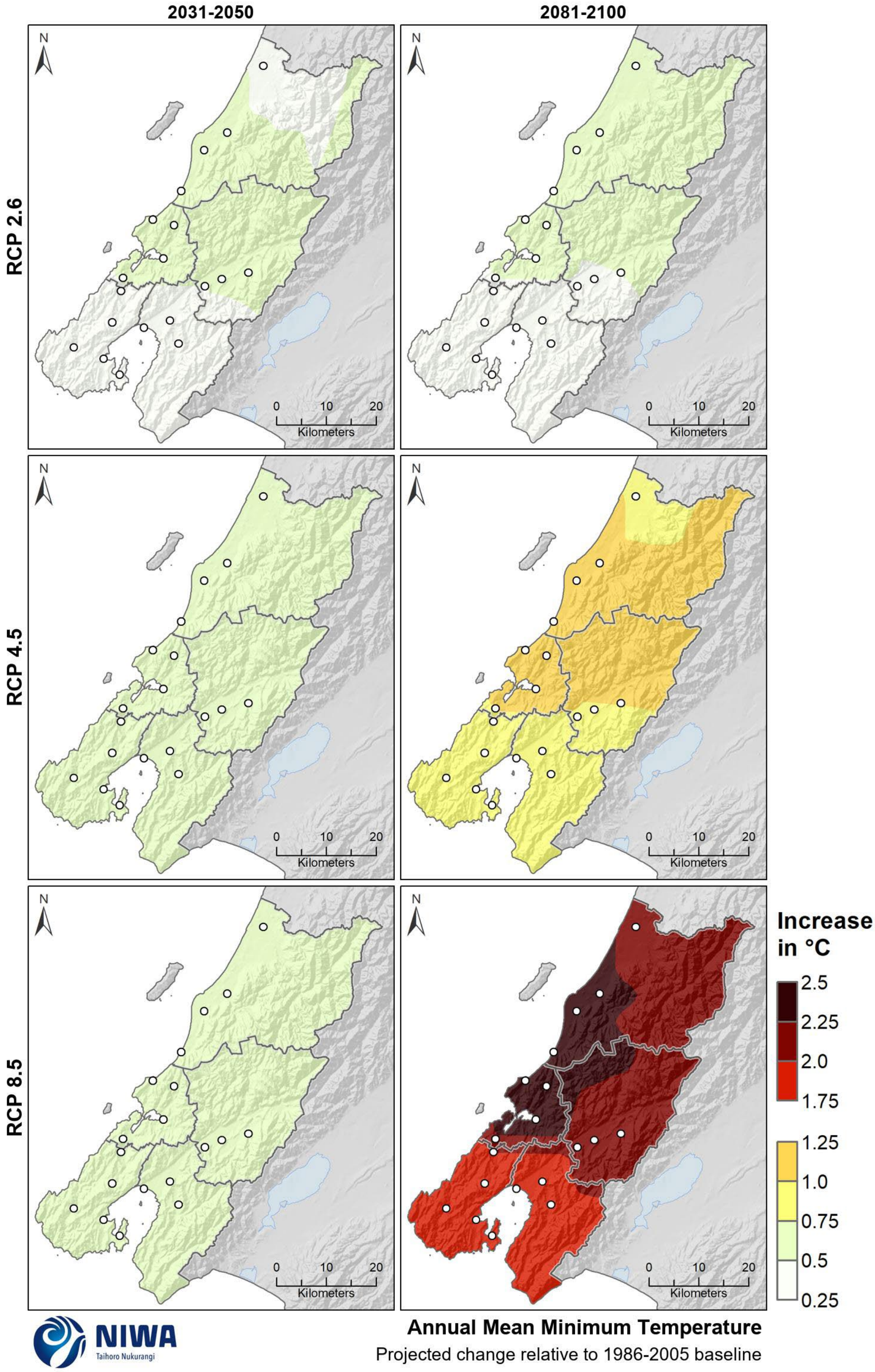

Figure 4-12: Projected annual mean minimum temperature changes by 2040 and 2090 under RCP2.6, RCP4.5 and RCP8.5. Relative to 1986-2005 average, based on the average of six global climate models. Results are based on dynamical downscaled projections using NIWA's Regional Climate Model. Resolution of projection is 5km x 5km. Note, a scale break is required to encapsulate the considerable difference in projected temperature change by 2090 under RCP2.6 compared to RCP8.5.

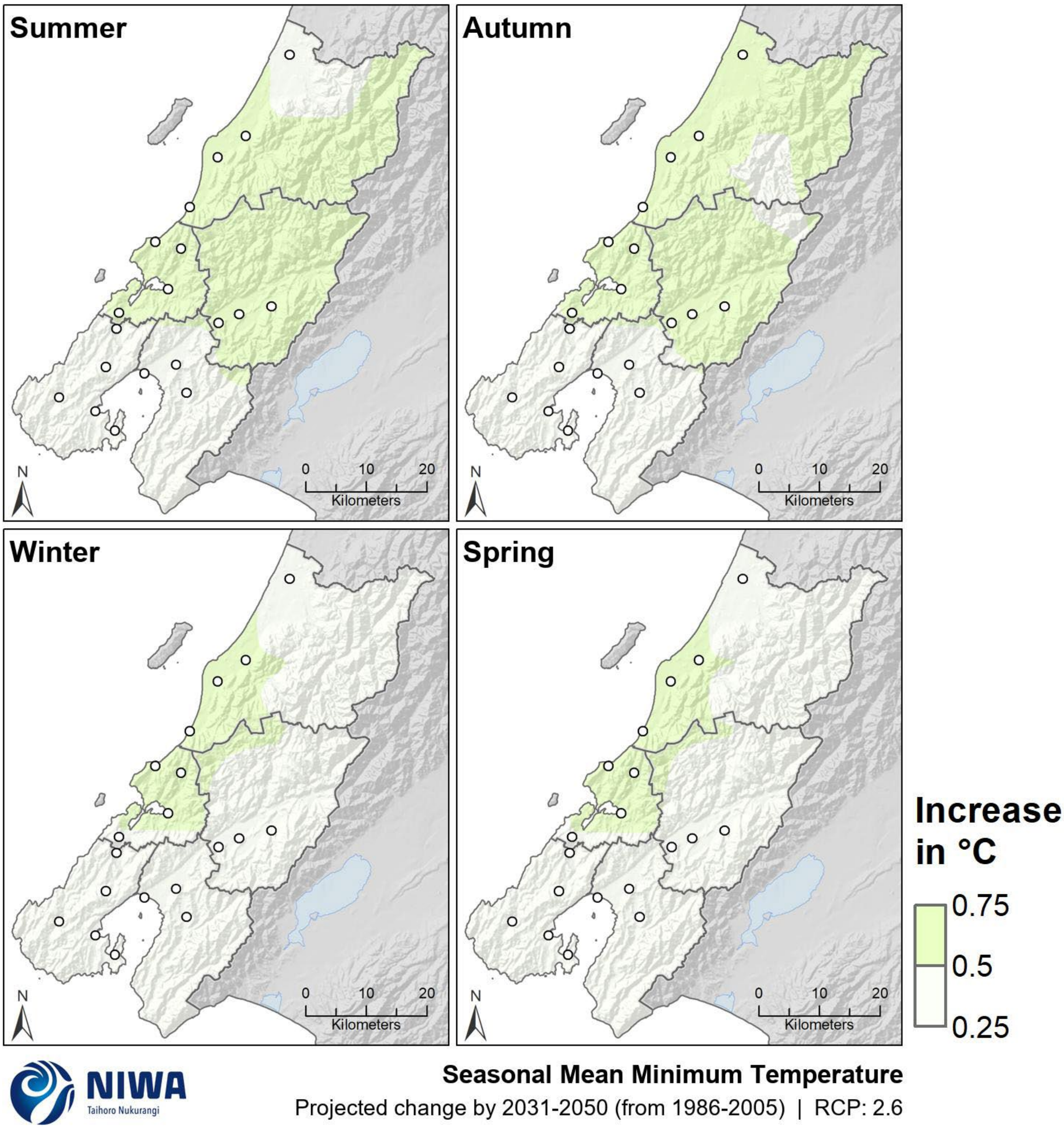

Figure 4-13: Projected seasonal mean minimum temperature changes by 2040 under RCP2.6. Relative to 1986-2005 average, based on the average of six global climate models. Results are based on dynamical downscaled projections using NIWA's Regional Climate Model. Resolution of projection is 5km x 5km.

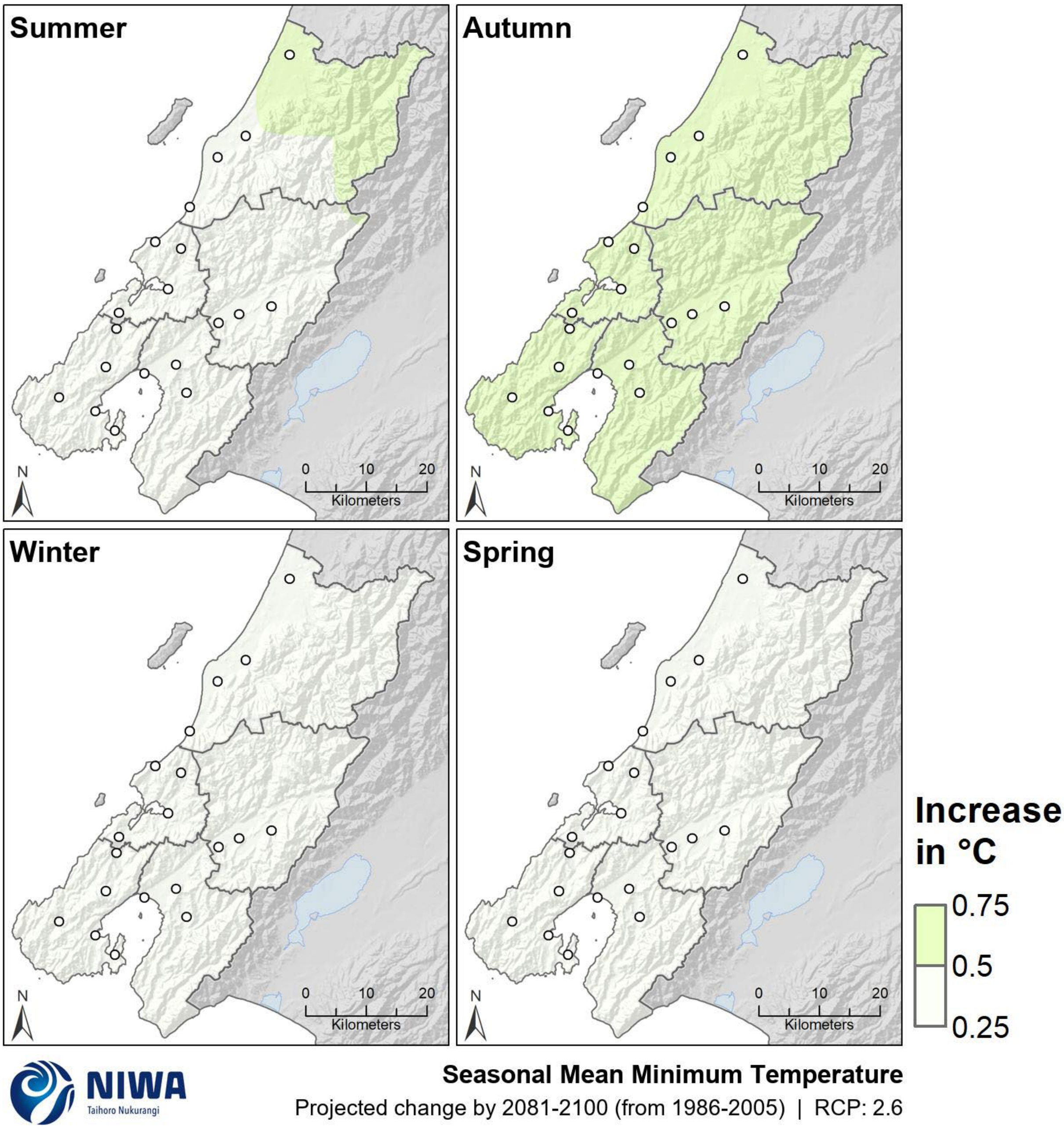

Figure 4-14: Projected seasonal mean minimum temperature changes by 2090 under RCP2.6. Relative to 1986-2005 average, based on the average of six global climate models. Results are based on dynamical downscaled projections using NIWA's Regional Climate Model. Resolution of projection is 5km x 5km.

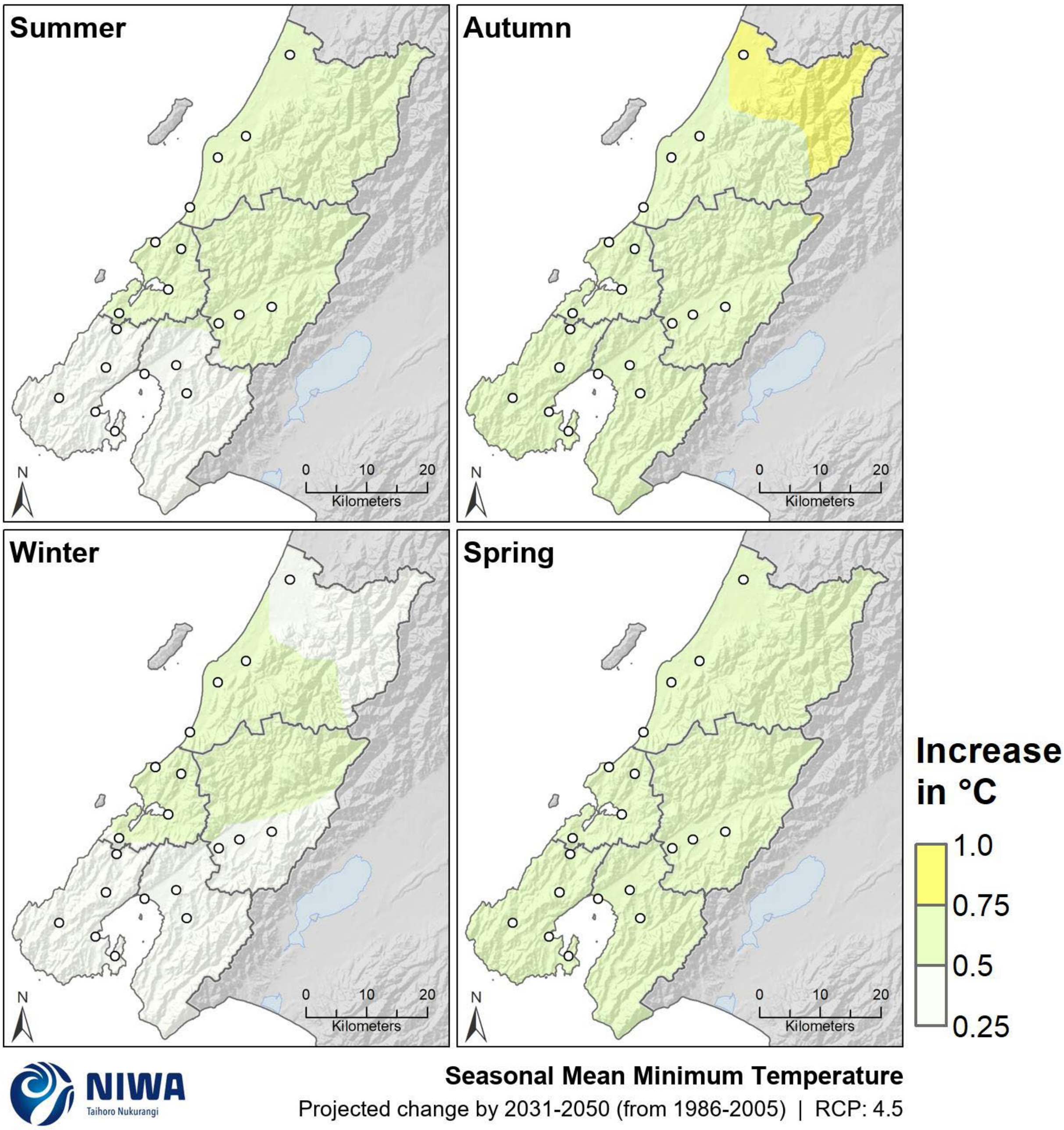

Figure 4-15: Projected seasonal mean minimum temperature changes by 2040 under RCP4.5. Relative to 1986-2005 average, based on the average of six global climate models. Results are based on dynamical downscaled projections using NIWA's Regional Climate Model. Resolution of projection is 5km x 5km.

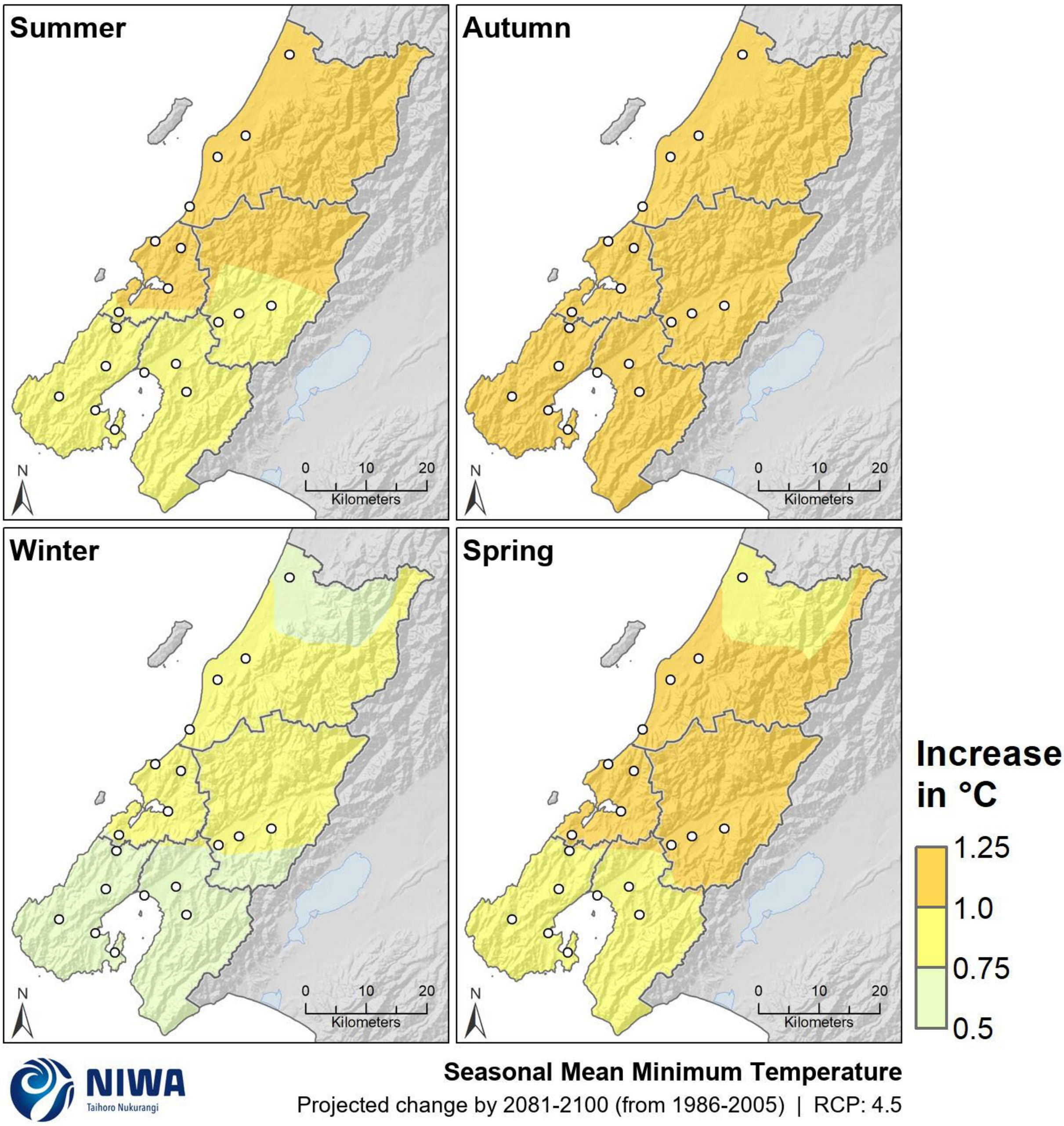

Figure 4-16: Projected seasonal mean minimum temperature changes by 2090 under RCP4.5. Relative to 1986-2005 average, based on the average of six global climate models. Results are based on dynamical downscaled projections using NIWA's Regional Climate Model. Resolution of projection is 5km x 5km.

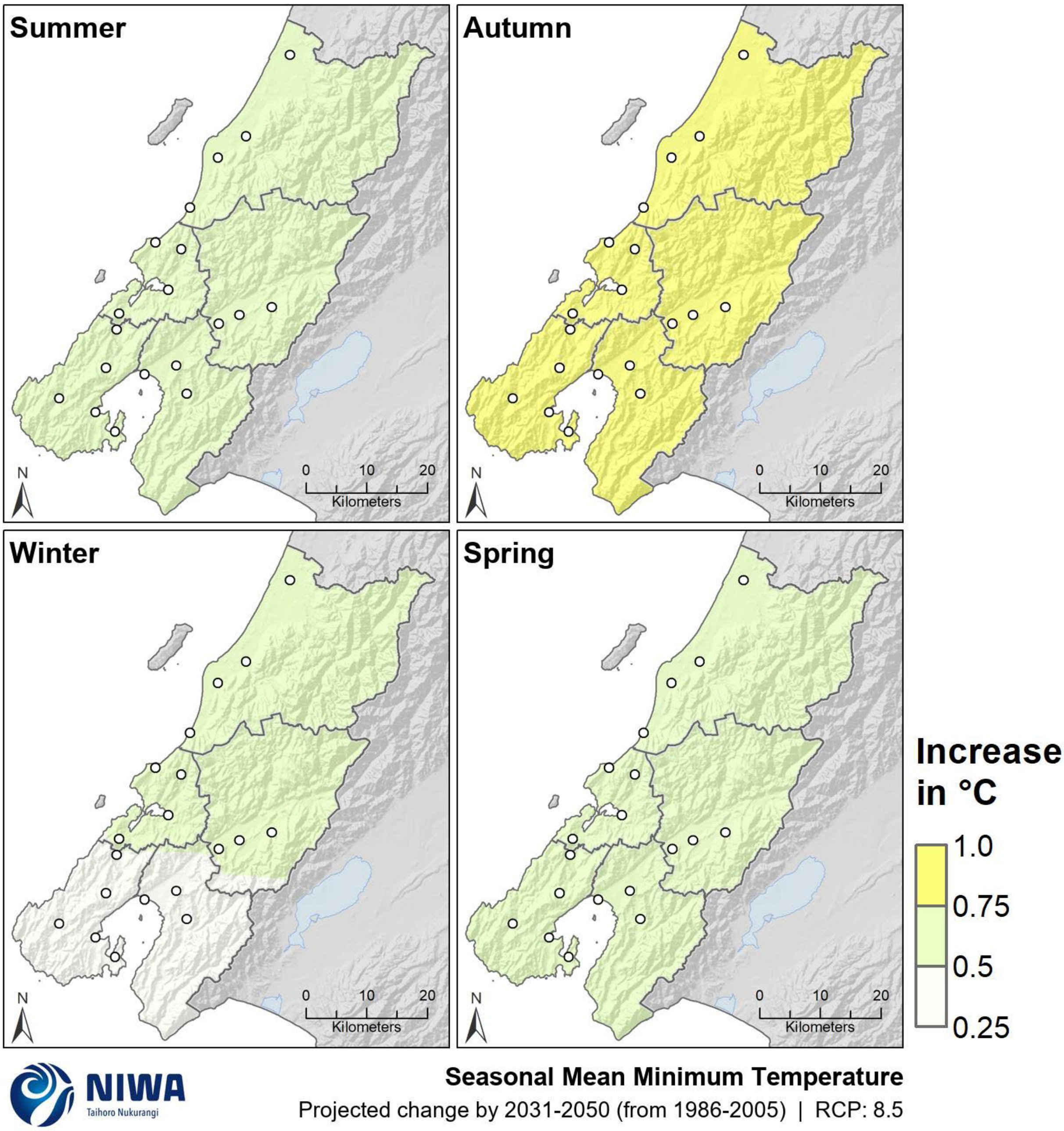

Figure 4-17: Projected seasonal mean minimum temperature changes by 2040 under RCP8.5. Relative to 1986-2005 average, based on the average of six global climate models. Results are based on dynamical downscaled projections using NIWA's Regional Climate Model. Resolution of projection is 5km x 5km.

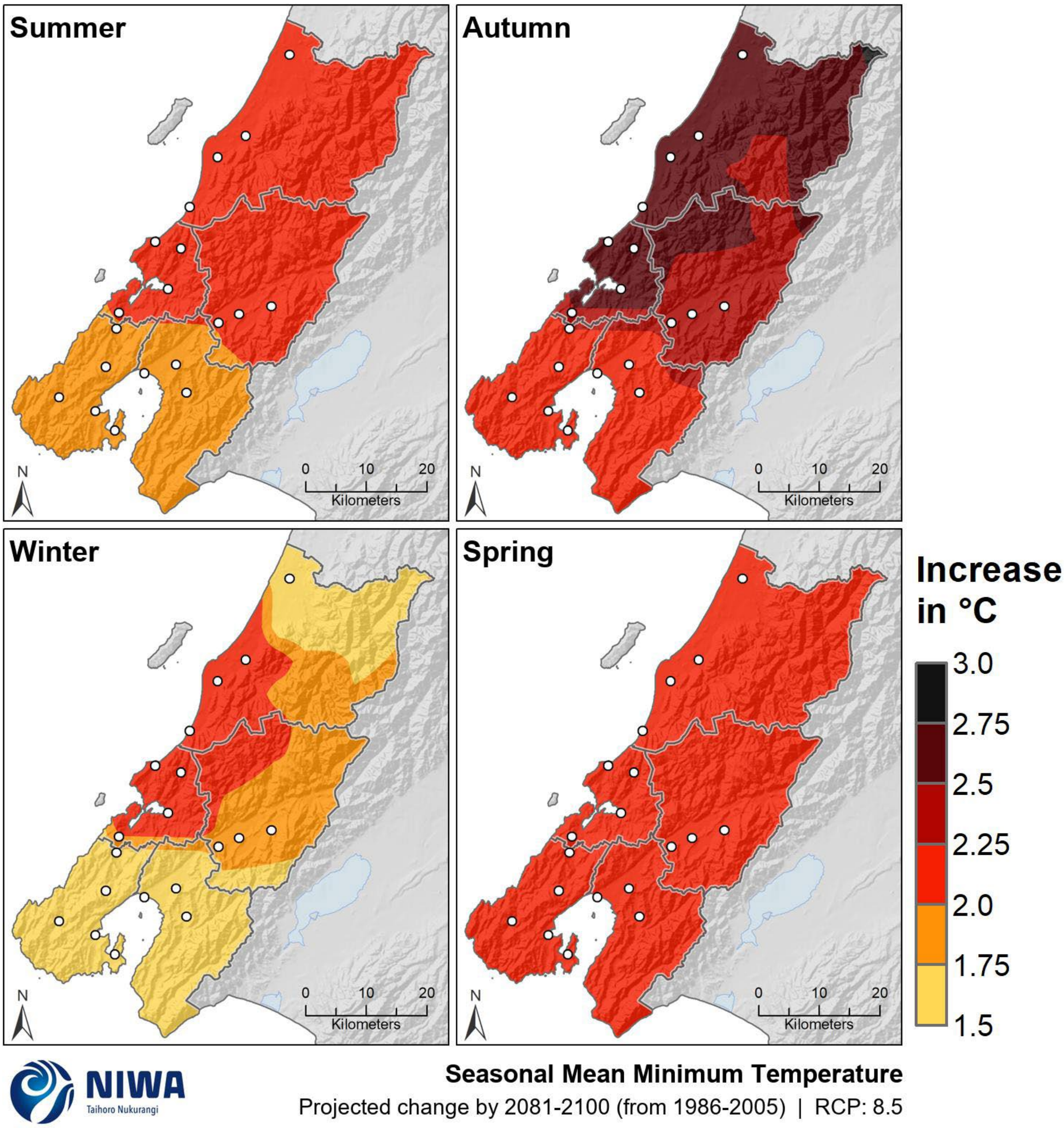

Figure 4-18: Projected seasonal mean minimum temperature changes by 2090 under RCP8.5. Relative to 1986-2005 average, based on the average of six global climate models. Results are based on dynamical downscaled projections using NIWA's Regional Climate Model. Resolution of projection is 5km x 5km.

4.1.3 Growing degree days

Projected growing degree day (base 10°C) changes (relative to 1986-2005)

Annual:

Period	RCP2.6	RCP4.5	RCP8.5
2040	+85-200	+85-250	+150-300
2090	+85-200	+200-400	+500-850

Growing degree-days (GDD) express the sum of daily temperatures above a selected base temperature (e.g. 10˚C) that represent a threshold for plant growth. The average amount of growing degree-days in a location may influence the choice of crops to grow, as different species have different temperature thresholds for survival. The daily GDD total is the amount the daily average temperature exceeds the threshold value (e.g. 10°C) per day. For example, a daily average temperature of 18°C would have a GDD base 10°C value of 8. The daily GDD values are accumulated over the period 1 July to 30 June to calculate an annual GDD value.

Historic (average over 1986-2005) and future (average over 2031-2050 and 2081-2100) maps for GDD are shown in this section. The historic maps show annual average GDD and the future projection maps show the change in GDD compared with the historic average. Note that the historic maps are on a different colour scale to the future projection maps.

Historic growing degree-days range between 1000-1400 GDD for most populated parts of the area (Figure 4-19). The highest elevation terrain in the Tararua Range and Remutaka Range observes 300-800 GDD annually.

Representative concentration pathway (RCP) 2.6

By 2040 and 2090, increases of 85-200 GDD are projected throughout the area (Figure 4-20), with increases of 150-200 GDD for most populated areas. This is a notable increase relative to the historic period, showing that considerable changes are predicted even for this low-range scenario.

Representative concentration pathway (RCP) 4.5

By 2040, increases to GDD are projected (Figure 4-20), with increases of 200-250 GDD projected for coastal areas north of Tawa, and a small inland portion about Upper Hutt.

By 2090, increases of 300-350 GDD are projected for most low elevation and coastal parts of the area, with increases of 350-400 GDD projected about Pauatahanui, Paekakariki, Paraparaumu and Waikanae (Figure 4-20). Such increases would see low elevation areas observing GDD totals comparable to those observed historically (1981-2010) in low elevations of Hawke’s Bay (Macara, 2018).

Representative concentration pathway (RCP) 8.5

By 2040, increases of 200-250 GDD are projected for most low elevation and coastal parts, with increases of 150-200 GDD projected for eastern areas (Figure 4-20).

By 2090, considerable increases of 500-850 GDD are projected (Figure 4-20). The smallest increases of 500-600 GDD are projected for the highest elevations of the Tararua Range, whereas increases of

700-850 GDD are projected for most low elevation, populated parts of the area. Such increases would see low elevation areas observing GDD totals comparable to those observed historically (1981-2010) in Auckland and low elevations of Northland (Macara, 2018).

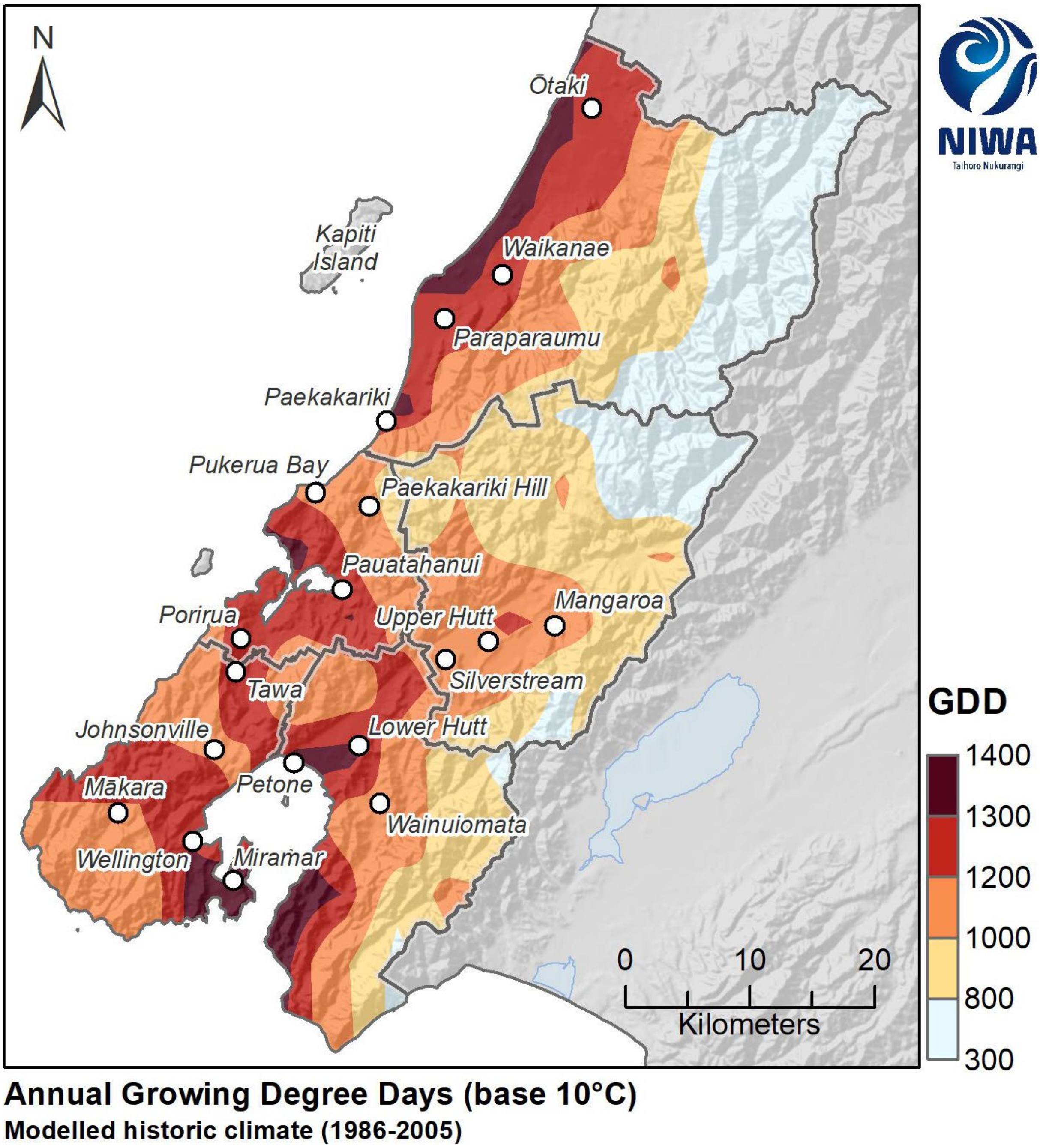

Figure 4-19: Median annual Growing Degree-Days (GDD) base 10°C. Results are based on dynamical downscaled projections using NIWA's Regional Climate Model. Resolution of projection is 5km x 5km.

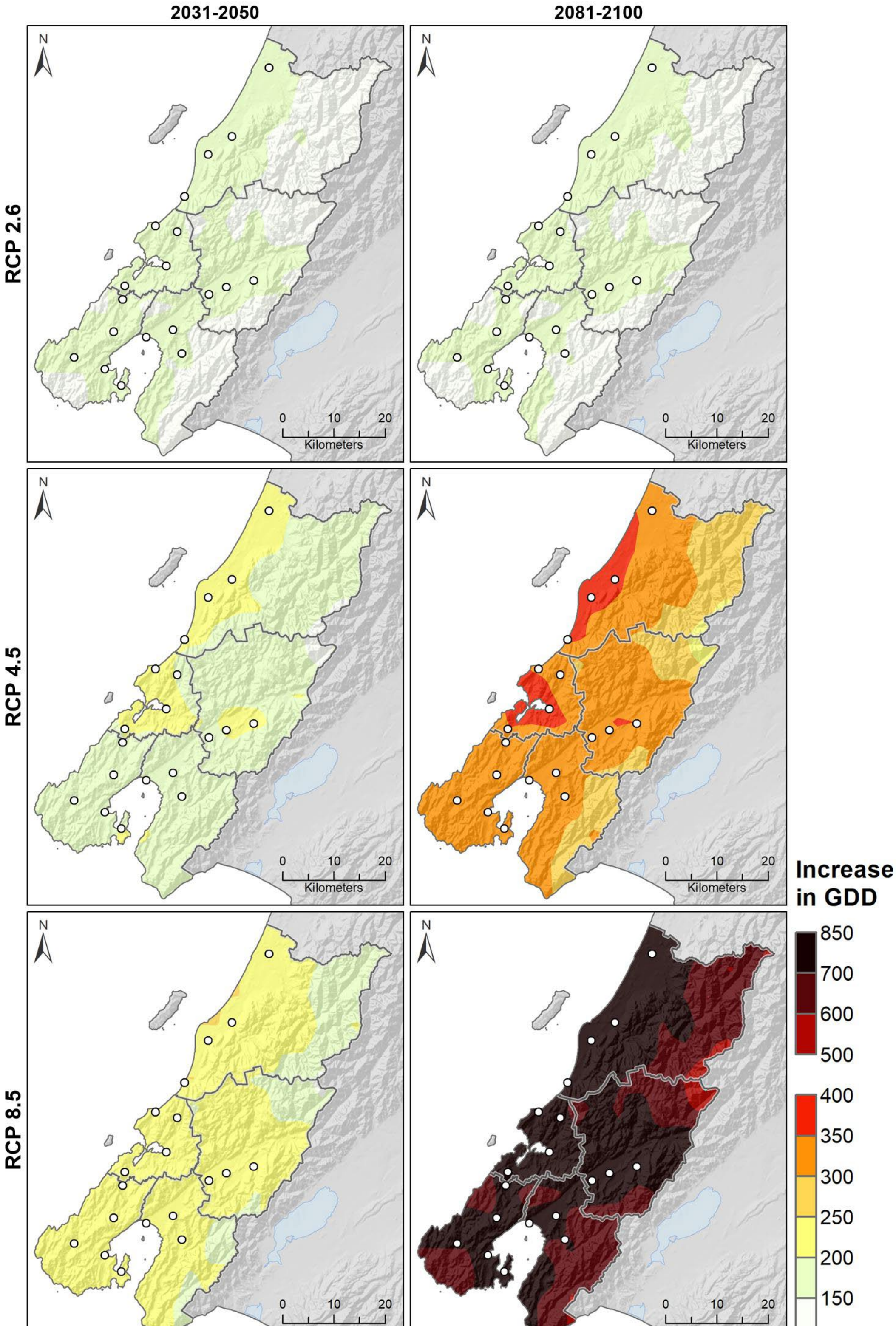

Figure 4-20: Projected increase in number of growing degree days per year (base 10°C) at 2040 (2031-2050) and 2090 (2081-2100) for RCP2.6 (top panels), RCP4.5 (middle panels) and RCP8.5 (bottom panels). Projected change is relative to 1986-2005. Results are based on dynamically downscaled projections and show the average of six global climate models. Resolution of projection is 5km x 5km.

4.1.4 Hot days

Projected hot day changes (relative to 1986-2005)

Annual:

Period	RCP2.6	RCP4.5	RCP8.5
2040	Up to +10	Up to +10	Up to +10
2090	Up to +10	+1-20	+5-50

In this report, a hot day is considered to occur when the maximum temperature reaches 25°C or higher. Historic (average over 1986-2005) and future (average over 2031-2050 and 2081-2100) maps for hot days are shown in this section. The historic maps show annual average number of hot days and the future projection maps show the change in the number of hot days compared with the historic average. Note that the historic maps are on a different colour scale to the future projection maps.

For the historic period, hot days occur most regularly around Ōtaki. Here, the annual number of hot days averages 10-13 days per year (Figure 4-21). Other coastal and low elevation areas typically observe 5-10 hot days per year. Hot days are uncommon in high elevation terrain toward the northeast of the area.

Representative concentration pathway (RCP) 2.6

By 2040 and 2090, increases of up to 10 hot days are projected for most of the area (Figure 4-22). Greatest increases of 5-10 days are projected about Ōtaki, parts of the Hutt Valley, and some areas near Wellington Harbour.

Representative concentration pathway (RCP) 4.5

By 2040, projected increases to hot days are similar to those by the corresponding time under RCP2.6 (Figure 4-22), with increases of up to 10 hot days projected.

By 2090, increases of 5-15 hot days are projected for most of the area. Highest increases of 15-20 hot days are projected northern parts near Ōtaki (Figure 4-22).

Representative concentration pathway (RCP) 8.5

By 2040, an increase of up to 10 hot days is projected (Figure 4-22). The largest increases of 5-10 days are projected for most low elevation populated areas.

By 2090, considerable increases of 5-50 hot days are projected (Figure 4-22). Largest increases of 40-50 hot days are projected about Ōtaki and Upper Hutt. This is the equivalent of approximately 6-7 additional weeks of hot days compared to the historic climate.

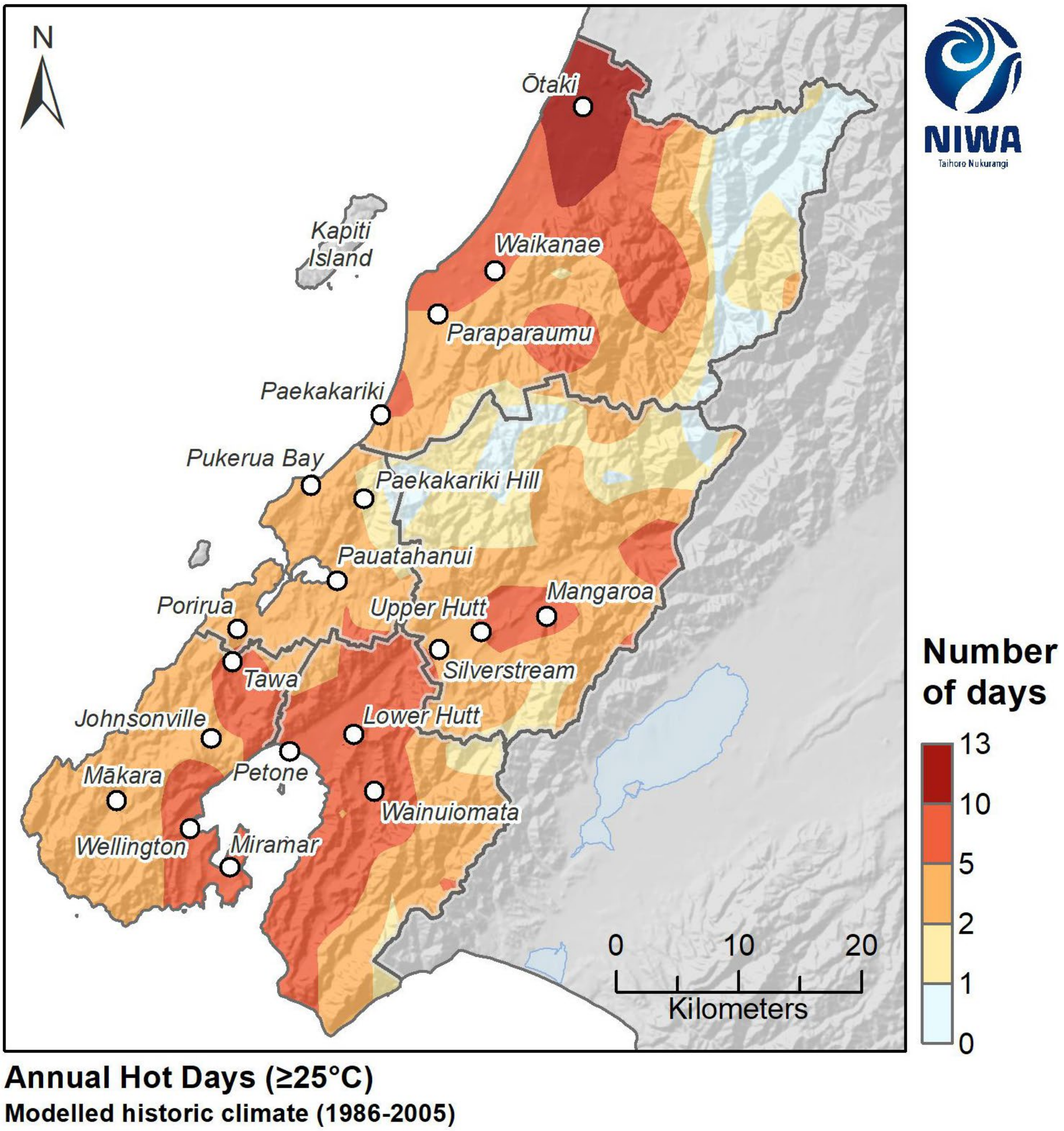

Figure 4-21: Modelled annual number of hot days (days with maximum temperature ≥25°C), average over 1986-2005. Results are based on dynamical downscaled projections using NIWA's Regional Climate Model. Resolution of projection is 5km x 5km.

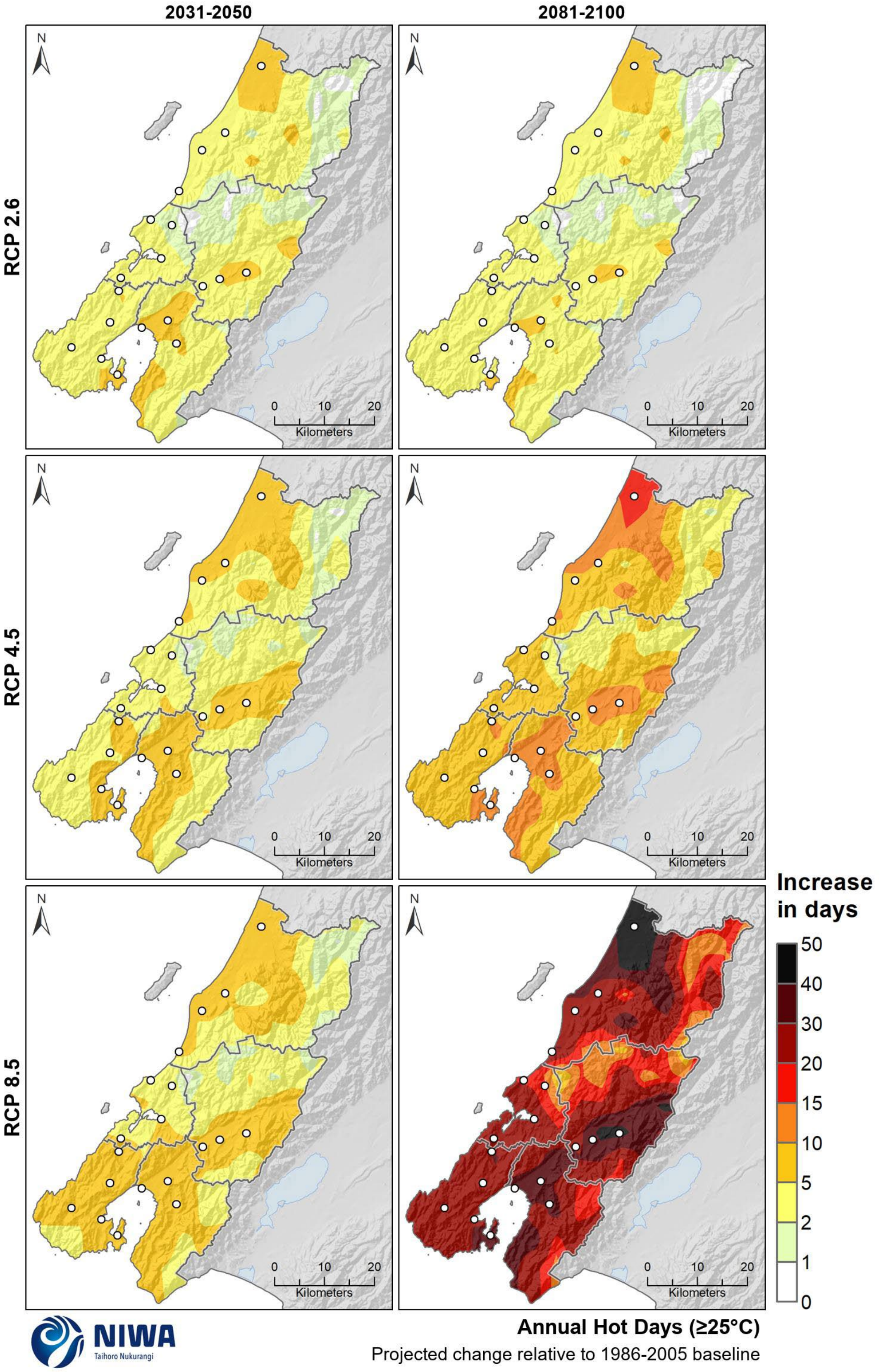

Figure 4-22: Projected annual hot day (days with maximum temperature ≥25°C) changes by 2040 and 2090, under RCP2.6, RCP4.5 and RCP8.5. Changes relative to 1986-2005 average, based on the average of six global climate models. Results are based on dynamical downscaled projections using NIWA's Regional Climate Model. Resolution of projection is 5km x 5km.

4.1.5 Extreme hot days

Projected extreme hot day changes (relative to 1986-2005)

Annual:

Period	RCP2.6	RCP4.5	RCP8.5
2040	Up to +0.5	Up to +0.5	Up to +1
2090	Up to +0.5	Up to +1.5	Up to +5

In this report, an extreme hot day is considered to occur when the maximum temperature is above 30°C. Historic (average over 1986-2005) and future (average over 2031-2050 and 2081-2100) maps for extreme hot days are shown in this section. The historic maps show annual average numbers of extreme hot days and the future projection maps show the change in the annual number of extreme hot days compared with the historic period. Note that the historic maps are on a different colour scale to the future projection maps.

For the historic period, extreme hot days are a rare occurrence anywhere west of Wellington's ranges. The annual number of extreme hot days averages no higher than 0.25, or no more than one extreme hot day every four years (Figure 4-23). This is largely due to the area's exposure to airflows arriving directly off the sea, which has a moderating influence on the daily maximum temperatures observed during summer.

Representative concentration pathway (RCP) 2.6

By 2040 and 2090, little change in extreme hot days is expected, with increases of up to 0.5 extreme hot days projected (Figure 4-24).

Representative concentration pathway (RCP) 4.5

By 2040, little change in extreme hot days is expected, with increases of up to 0.5 extreme hot days projected (Figure 4-24).

By 2090, increases of up to 1 extreme hot day are projected for low elevation areas near Wellington Harbour, including Lower Hutt, Petone, Wainuiomata, Wellington City and Miramar (Figure 4-24).

Representative concentration pathway (RCP) 8.5

By 2040, the pattern of change under RCP8.5 is similar to that projected for the same time period under RCP4.5. The main difference is a higher projected increase of 1 extreme hot day about Lower Hutt and Petone (Figure 4-24).

By 2090, notable increases of up to 5 extreme hot days are projected for the area (Figure 4-24). Largest increases of 2-5 days are projected about southern parts of the area south of Porirua and Silverstream. Smaller increases of up to 2 extreme hot days are projected near Ōtaki, while little change is projected for the highest elevation terrain and coastal areas from Pauatahanui to Waikanae (up to +0.5 extreme hot days).

It is worth noting that the spatial resolution of the climate models is not precise enough to account for the local-scale topographic and meteorological features that contribute to extreme hot days. Therefore, the projected increases may be underestimated in some locations.

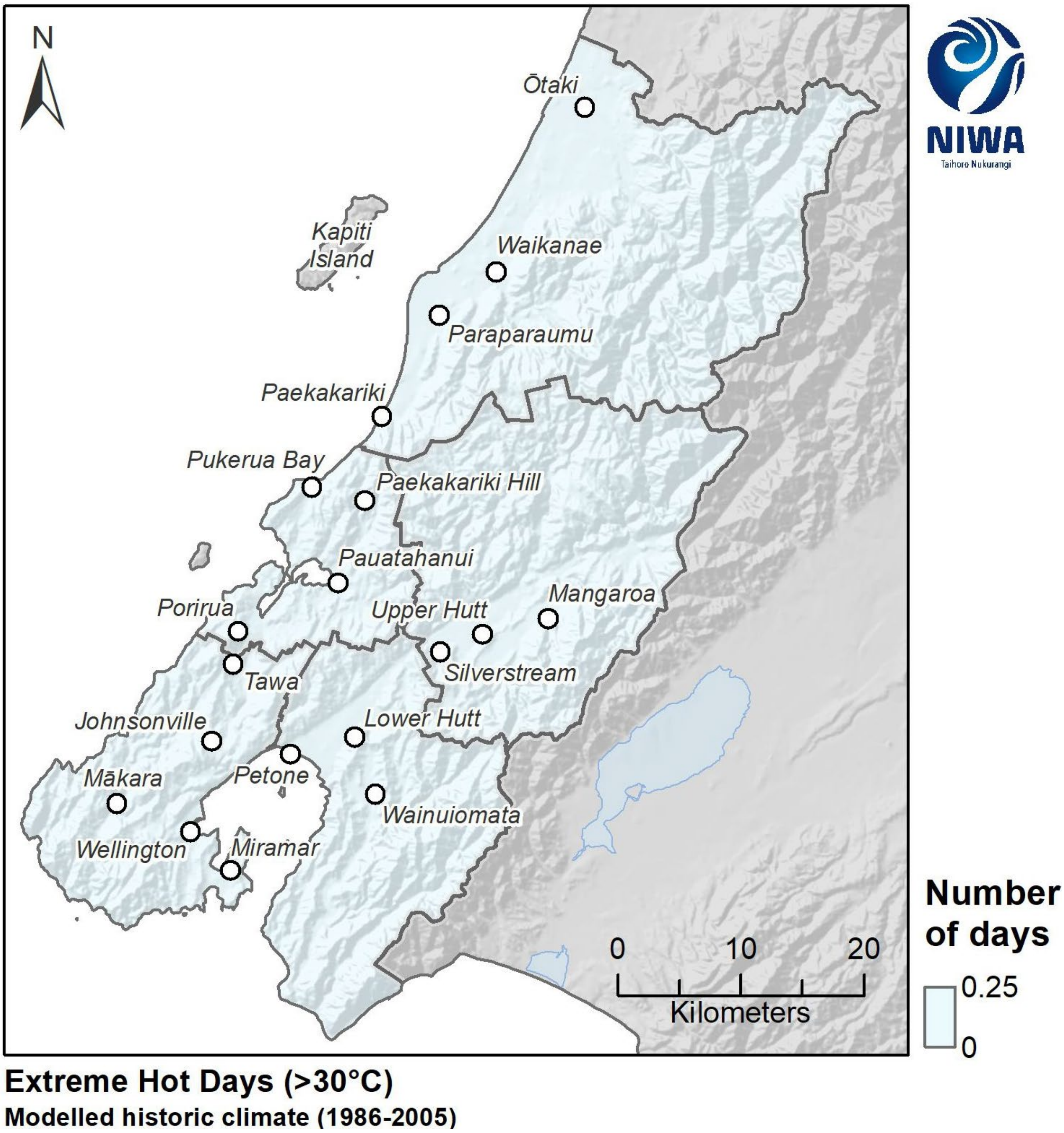

Figure 4-23: Modelled annual number of extreme hot days (days with maximum temperature >30°C), average over 1986-2005. Results are based on dynamical downscaled projections using NIWA's Regional Climate Model. Resolution of projection is 5km x 5km.

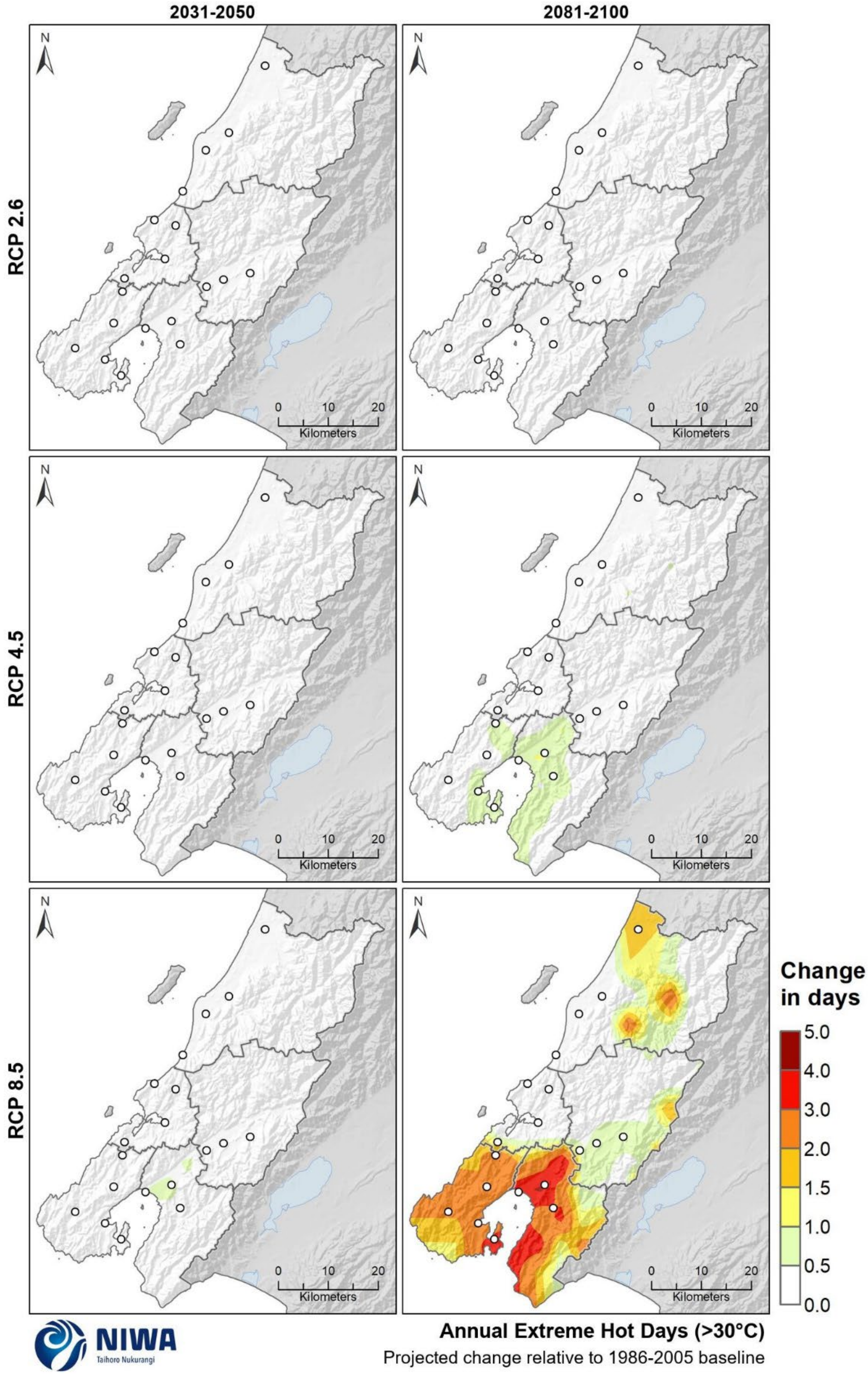

Figure 4-24: Projected annual extreme hot day (days with maximum temperature >30°C) changes by 2040 and 2090, under RCP2.6, RCP4.5 and RCP8.5. Changes relative to 1986-2005 average, based on the average of six global climate models. Results are based on dynamical downscaled projections using NIWA's Regional Climate Model. Resolution of projection is 5km x 5km.

4.1.6 Heatwave days

Projected heatwave day changes (relative to 1986-2005)

Annual:

Period	RCP2.6	RCP4.5	RCP8.5
2040	Up to +5	Up to +5	Up to +10
2090	Up to +5	Up to +10	Up to +35

The definition of a heatwave as considered here is a period of three or more consecutive days where the maximum daily temperature exceeds 25°C. This calculation is an aggregation of all days per year that are included in a heatwave (i.e., ≥ three consecutive days with maximum temperature > 25°C), no matter the length of the heatwave. Thus, a 3-day heatwave contributes 3 days, and a 5-day heatwave contributes 5 days, and a single 3-day and a single 5-day heatwave add up to 8 days for a year, etc. The annual heatwave days are then averaged over the 20-year period of interest (e.g., 2031-2050), and the six global models, to determine the ensemble-average annual heatwave-day climatology (past) and future projections.

Historic (average over 1986-2005) and future (average over 2031-2050 and 2081-2100) maps for heatwave days are shown in this section. The historic maps show annual average numbers of heatwave days and the future projection maps show the change in the annual number of heatwave-days compared with the historic period. Note that the historic maps are on a different colour scale to the future projection maps.

For the historic period, the annual number of heatwave days is highest for northern areas near Ōtaki (Figure 4-25), with 2-3 heatwave days per year (i.e. approximately one heatwave per year). Areas around Lower Hutt, Petone and Wainuiomata on average experience 1-2 heatwave days per year (i.e. less than one heatwave per year). Remaining areas of the area experience an average of less than one heatwave day per year, i.e., on average less than one heatwave event every three years.

Representative concentration pathway (RCP) 2.6

By 2040 and 2090, increases of up to 5 heatwave days are projected (Figure 4-26), with highest increases of 2-5 heatwave days projected for areas near Ōtaki, the Hutt Valley and Miramar. For some locations that don't historically observe heatwaves, e.g. Lower Hutt and Miramar, these projected increases will result in an average of approximately 1-2 heatwaves per year. This demonstrates that notable changes are projected for some areas regardless of the future emissions scenario.

Representative concentration pathway (RCP) 4.5

By 2040, increases of up to 5 heatwave days are projected (Figure 4-26), with highest increases of 2-5 heatwave days projected for areas near Ōtaki, the Hutt Valley, Miramar and Wainuiomata.

By 2090, increases of up to 10 heatwave days are projected (Figure 4-26), with highest increases of 5-10 heatwave days projected for northern areas near Ōtaki, and parts of the Hutt Valley. Increases of 2-5 heatwave days are projected for Waikanae, Paraparaumu, Porirua, Tawa and areas near Wellington city including Johnsonville and Mākara.

Representative concentration pathway (RCP) 8.5

By 2040, increases of up to 10 heatwave days are projected (Figure 4-26). Projected increases of 2-5 heatwave days are typical for the Hutt Valley and Ōtaki.

By 2090, large increases of up to 35 heatwave days are projected (Figure 4-26). Largest increases of 30-35 heatwave days are projected for areas near Mangaroa and Ōtaki. This is the equivalent of approximately 4-5 additional weeks of heatwave days compared to the historic climate. For other locations in the area, projected increases of 10-20 heatwave days are common, with higher increases expected about the Hutt Valley, Wainuiomata and Miramar. Increases of 5-10 heatwave days are projected for Porirua, Pauatahanui and Pukerua Bay.

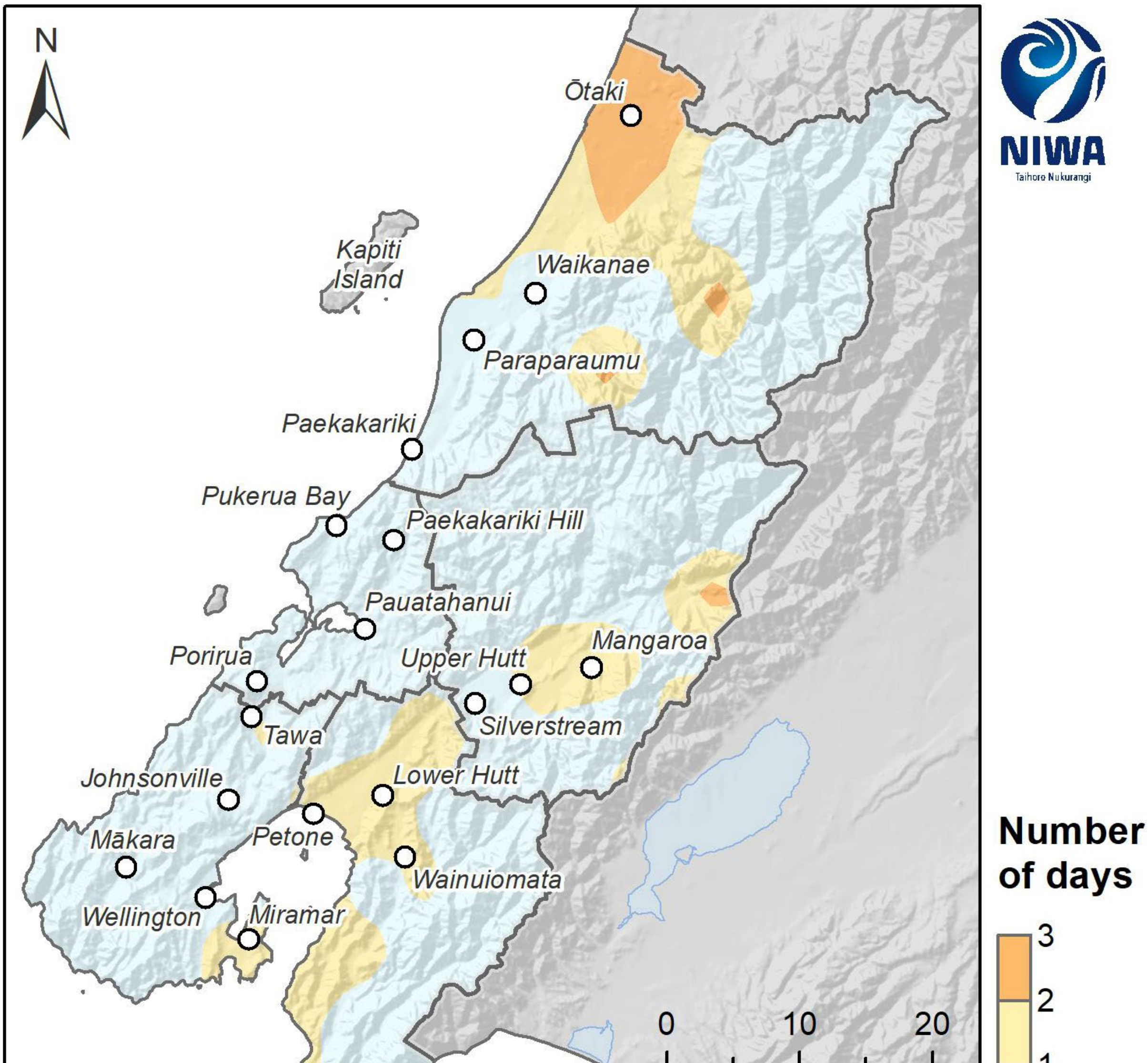

Figure 4-25: Modelled annual number of heatwave days (≥ three consecutive days with maximum temperatures > 25°C), average over 1986-2005. Results are based on dynamical downscaled projections using NIWA's Regional Climate Model. Resolution of projection is 5km x 5km.

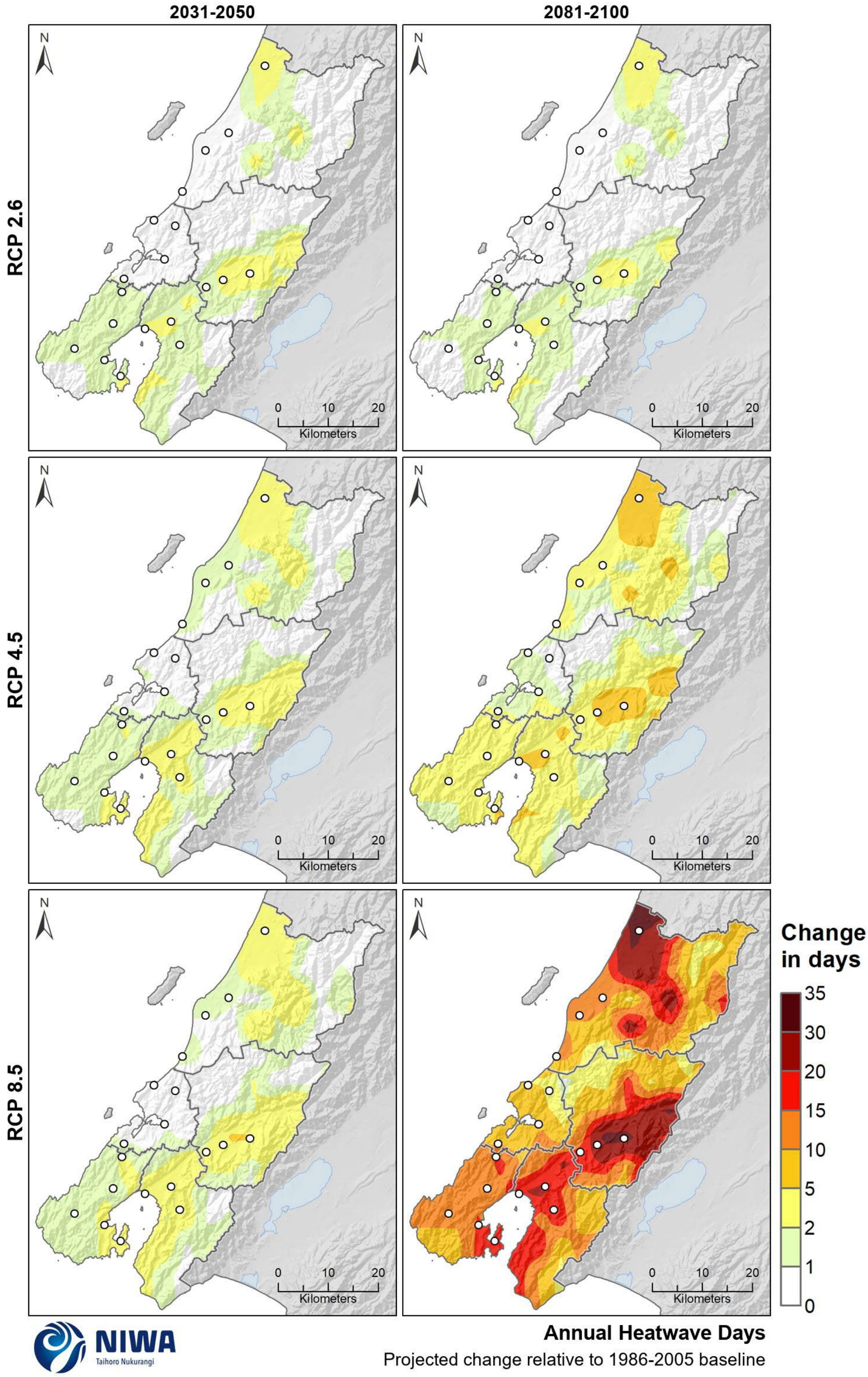

Figure 4-26: Projected annual heatwave day (≥ three consecutive days with maximum temperatures > 25°C) changes by 2040 and 2090, under RCP2.6, RCP4.5 and RCP8.5. Changes relative to 1986-2005 average, based on the average of six global climate models. Results are based on dynamical downscaled projections using NIWA's Regional Climate Model. Resolution of projection is 5km x 5km.

4.1.7 Warm nights

Projected warm night changes (relative to 1986-2005)

Annual:

Period	RCP2.6	RCP4.5	RCP8.5
2040	Up to +15	Up to +15	Up to +15
2090	Up to +15	1-30 more	1-55 more

In this report, a warm night is considered to occur when the daily minimum temperature is higher than 15°C. Historic (average over 1986-2005) and future (average over 2031-2050 and 2081-2100) maps for warm nights are shown in this section. The historic maps show annual average number of warm nights and the future projection maps show the change in the number of warm nights compared with the historic average. Note that the historic maps are on a different colour scale to the future projection maps.

For the historic period, warm nights occur most regularly in southern and coastal parts of the area. Here, the annual number of warm nights averages 30-50 per year (Figure 4-27), with highest annual warm nights of 40-50 per year about Wellington City and Porirua. Warm nights are less prevalent for remaining areas. Silverstream and Upper Hutt average 10-20 warm nights per year, while higher elevations to the east of the area average less than 5 warm nights per year.

Representative concentration pathway (RCP) 2.6

By 2040 and 2090, increases of up to 15 warm nights are projected (Figure 4-28), with increases of 5-10 warm nights projected for most populated parts of the area. Increases of up to 5 warm nights are projected for higher elevation eastern parts of the area. Increases of 10-15 warm nights are projected for areas near Porirua, which is a considerable change compared to the historic climate.

Representative concentration pathway (RCP) 4.5

By 2040, increases of up to 15 warm nights are projected (Figure 4-28), with highest increases of 10-15 warm nights projected about Wellington Harbour, and coastal parts of the area from Tawa north to Ōtaki. Increases of 5-10 warm nights are projected for much of Hutt Valley.

By 2090, increases of up 1-30 warm nights are projected. Largest increases of 20-30 warm nights are projected for areas about Wellington city, Porirua and Pauatahanui (Figure 4-28). Most remaining parts of the area observe a projected increase of 5-20 warm nights.

Representative concentration pathway (RCP) 8.5

By 2040, the projected pattern of change under RCP8.5 is similar to that projected for the same time period under RCP4.5. The main difference is projected increases of 10-15 warm nights for more extensive parts of the area, including Lower Hutt and Wainuiomata (Figure 4-28).

By 2090, considerable increases of 1-55 warm nights are projected (Figure 4-28). Largest increases of 40-55 warm nights are projected for areas relatively close to the sea. This is the equivalent of approximately 6-8 additional weeks of warm nights compared to the historic climate.

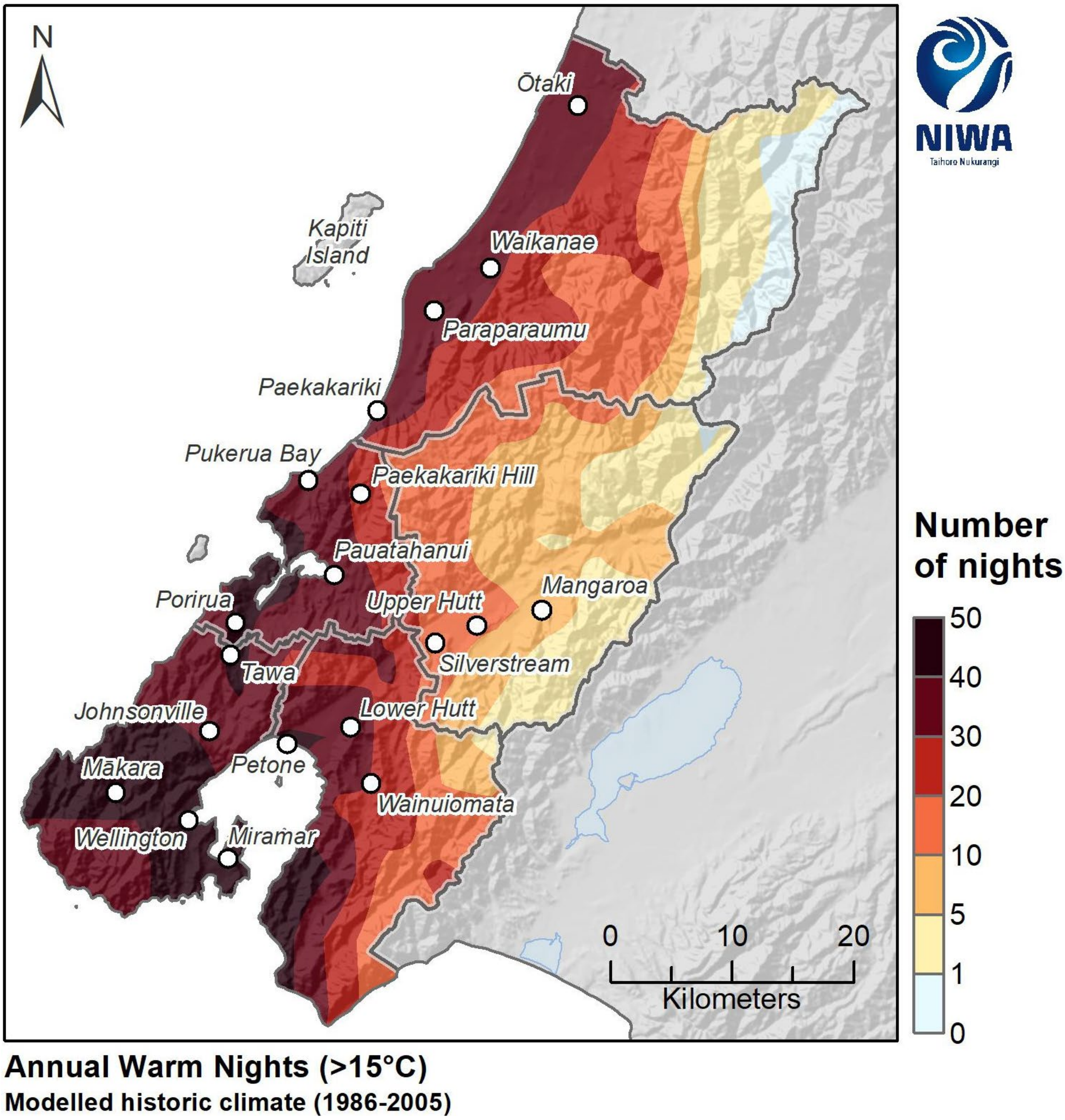

Figure 4-27: Modelled annual number of warm nights (daily minimum temperature >15°C), average over 1986-2005. Results are based on dynamical downscaled projections using NIWA's Regional Climate Model. Resolution of projection is 5km x 5km.

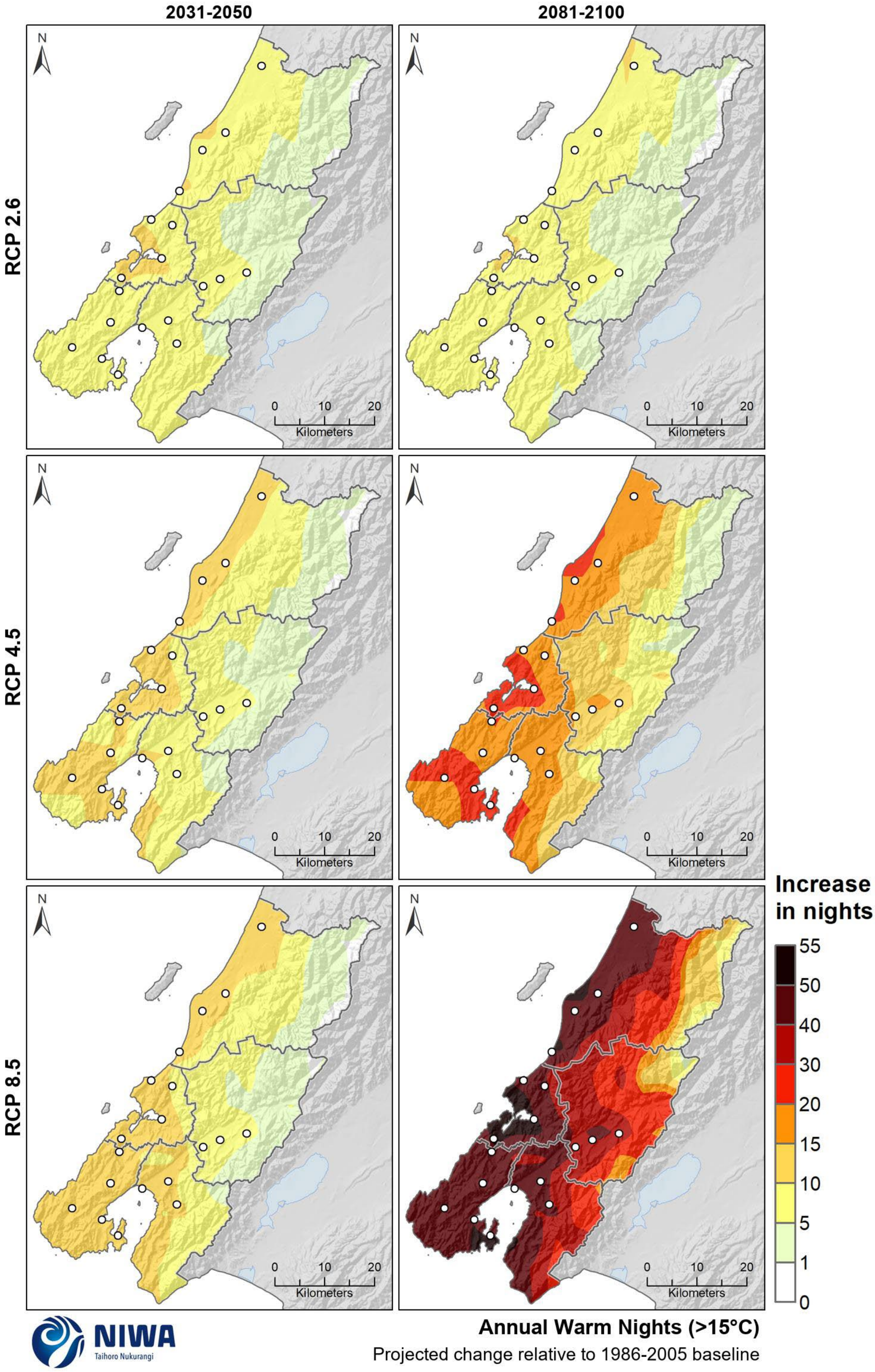

Figure 4-28: Projected annual warm night (daily minimum temperature >15°C) changes by 2040 and 2090, under RCP2.6, RCP4.5 and RCP8.5. Changes relative to 1986-2005 average, based on the average of six global climate models. Results are based on dynamical downscaled projections using NIWA's Regional Climate Model. Resolution of projection is 5km x 5km.

4.1.8 Frost days

Projected frost day changes (relative to 1986-2005)

Annual:

Period	RCP2.6	RCP4.5	RCP8.5
2040	Up to 10 fewer	Up to 15 fewer	Up to 10 fewer
2090	Up to 10 fewer	Up to 20 fewer	Up to 30 fewer

A frost day is defined in this report when the modelled daily minimum air temperature is equal to or lower than 0°C (also known as a cold night). This is purely a temperature-derived metric for assessing the potential for frosts over the 5 km x 5 km climate model grid. Frost conditions are influenced at the local scale (i.e. finer scale than 5 km x 5 km) by temperature, topography, wind, and humidity, so the results presented in this section can be considered as the large-scale temperature conditions conducive to frosts. Historic (average over 1986-2005) and future (average over 2031-2050 and 2081-2100) maps for frost days are shown in this section. The historic maps show annual average numbers of frost days and the future projection maps show the change in the annual number of frost days compared with the historic period. Note that the historic maps are on a different colour scale to the future projection maps.

For the modelled historic period, southwestern portions of the area about Petone, Johnsonville, Mākara, Wellington city and Miramar have the lowest number of frost days (Figure 4-29). This is partly due to the influence of the sea, which moderates daily extreme temperatures compared to inland locations. In addition, it is because these locations near Cook Strait are typically windier than the remainder of the area, and frost usually only occurs during calm or very light wind conditions. Inland and coastal parts of the area north of Tawa generally observe 1-10 frost days per year, with 20-70 frost days for northeastern parts about the Tararua Range.

Note, we expect to observe discrepancies when comparing the modelled historic period with the observed historic period. The modelled data are of a spatial resolution that is not precise enough to account for the local-scale topographic and meteorological features that contribute to the occurrence of frost days. This is relevant for low elevation inland locations like Upper Hutt, where the conditions conducive to frost (clear skies and light winds) enable rapid radiative losses and subsequent cooling of the near-surface air temperature, as well as cold-air pooling (a process where cold air drains into low elevation basins and valleys due to its relatively high density). This results in marked temperature differences over short vertical and horizontal distances, which are characterised by *inversions* (where temperature increases with altitude). In spite of this, the projected change to frost days (Figure 4-30) remain a useful indicator of the broad changes anticipated in the area, noting these changes are calculated relative to the modelled historic period.

Representative concentration pathway (RCP) 2.6

By 2040 and 2090, up to 10 fewer frost days are projected (Figure 4-30), with highest decreases of 5-10 frost days projected in the Tararua Range. Decreases of 1-2 frost days are projected for coastal areas north of Pauatahanui.

Representative concentration pathway (RCP) 4.5

By 2040, up to 15 fewer frost days are projected (Figure 4-30), with highest decreases of 5-15 days projected towards the northeast of the area. Decreases of 1-5 days are projected for many remaining areas north of Porirua.

By 2090, up to 20 fewer frost days are projected. Decreases of 2-5 days are projected for western parts from Ōtaki south to Pauatahanui (Figure 4-30).

Representative concentration pathway (RCP) 8.5

By 2040, the projected pattern of change under RCP8.5 is very similar to that projected for the same time period under RCP4.5 (Figure 4-30).

By 2090, up to 30 fewer frost days are projected (Figure 4-30). Decreases of 2-10 days are projected for many western parts of the area to the north of Tawa, with highest deceases of 15-30 days to the northeast in the Tararua Range.

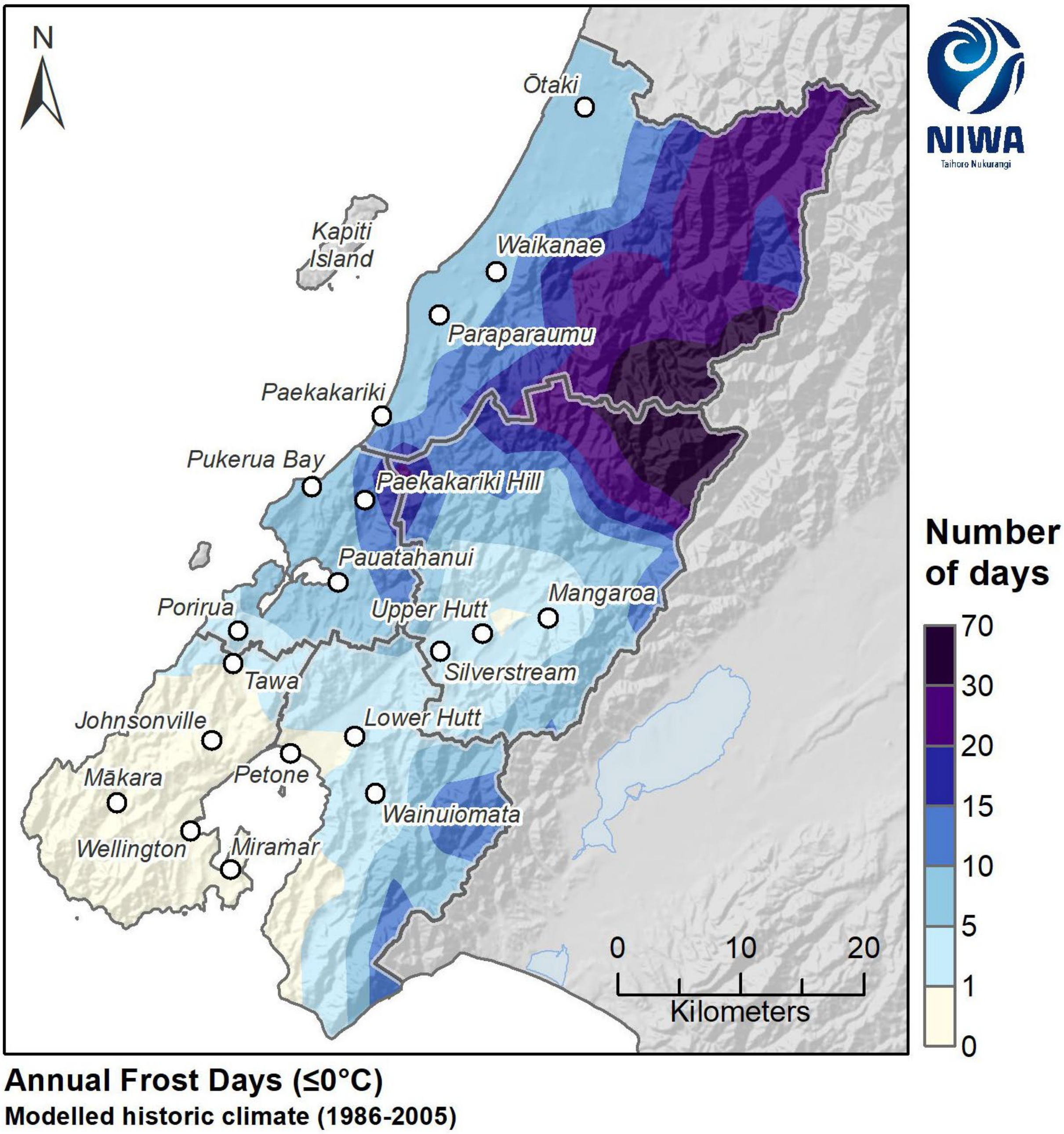

Figure 4-29: Modelled annual number of frost days (daily minimum temperature ≤0°C), average over 1986-2005. Results are based on dynamical downscaled projections using NIWA's Regional Climate Model. Resolution of projection is 5km x 5km.

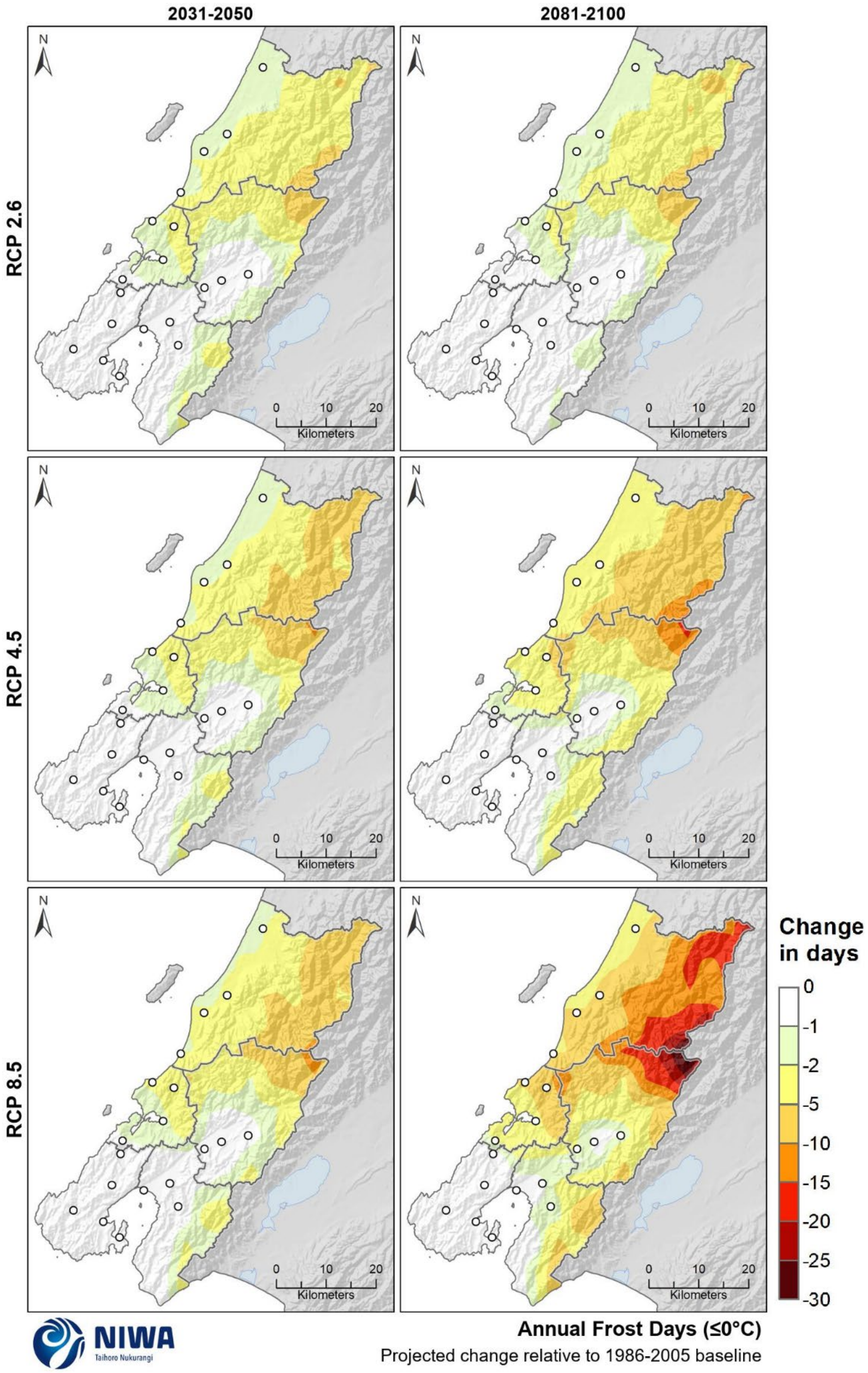

Figure 4-30: Projected annual number of frost day (daily minimum temperature ≤0°C) changes by 2040 and 2090 under RCP2.6, RCP4.5 and RCP8.5. Relative to 1986-2005 average, based on the average of six global climate models. Results are based on dynamical downscaled projections using NIWA's Regional Climate Model. Resolution of projection is 5km x 5km.

4.1.9 Cold days

Projected cold day changes (relative to 1986-2005)

Annual:

Period	RCP2.6	RCP4.5	RCP8.5
2040	2-20 fewer	2-30 fewer	2-30 fewer
2090	2-20 fewer	2-40 fewer	5-85 fewer

In this report, a cold day is considered to occur when the daily maximum air temperature is less than 10°C. Historic (average over 1986-2005) and future (average over 2031-2050 and 2081-2100) maps for cold days are shown in this section. The historic maps show annual average number of cold days and the future projection maps show the change in the number of cold days compared with the historic average. Note that the historic maps are on a different colour scale to the future projection maps.

For the historic period, cold days occur most regularly in the high elevation terrain among the Tararua and Remutaka Ranges. Here, the annual number of cold days averages 40-130 days (Figure 4-31). Cold days occur less frequently about Ōtaki, where the average annual number of cold days is 5-10 days.

Representative concentration pathway (RCP) 2.6

By 2040 and 2090, decreases to cold days are projected throughout the area (Figure 4-32), with highest decreases of 15-20 cold days projected for high elevation parts of the Tararua Range. Most of the area observes a projected decrease of 5-10 cold days.

Representative concentration pathway (RCP) 4.5

By 2040, decreases of 2-30 cold days are projected throughout the area (Figure 4-32), with highest decreases of 15-30 cold days projected for higher elevation eastern parts of the area.

By 2090, decreases of 2-40 cold days are projected. Decreases of 5-20 cold days are projected for many parts of the area, with higher decreases of 20-40 days projected in the Tararua and Remutaka Ranges (Figure 4-32).

Representative concentration pathway (RCP) 8.5

By 2040, the projected pattern of change under RCP8.5 is similar to that projected for the same time period under RCP4.5. Overall, 2-30 fewer cold days are projected for the area (Figure 4-32).

By 2090, considerable decreases of 5-85 cold days are projected (Figure 4-32). Largest decreases of 40-85 days are projected about the Tararua Range. Projected changes of 10-30 fewer cold days are common for the remainder of the area. It is anticipated this will have impacts and implications for biodiversity and pest control: these are discussed in an earlier report produced for the Greater Wellington Region (Pearce *et al.*, 2017).

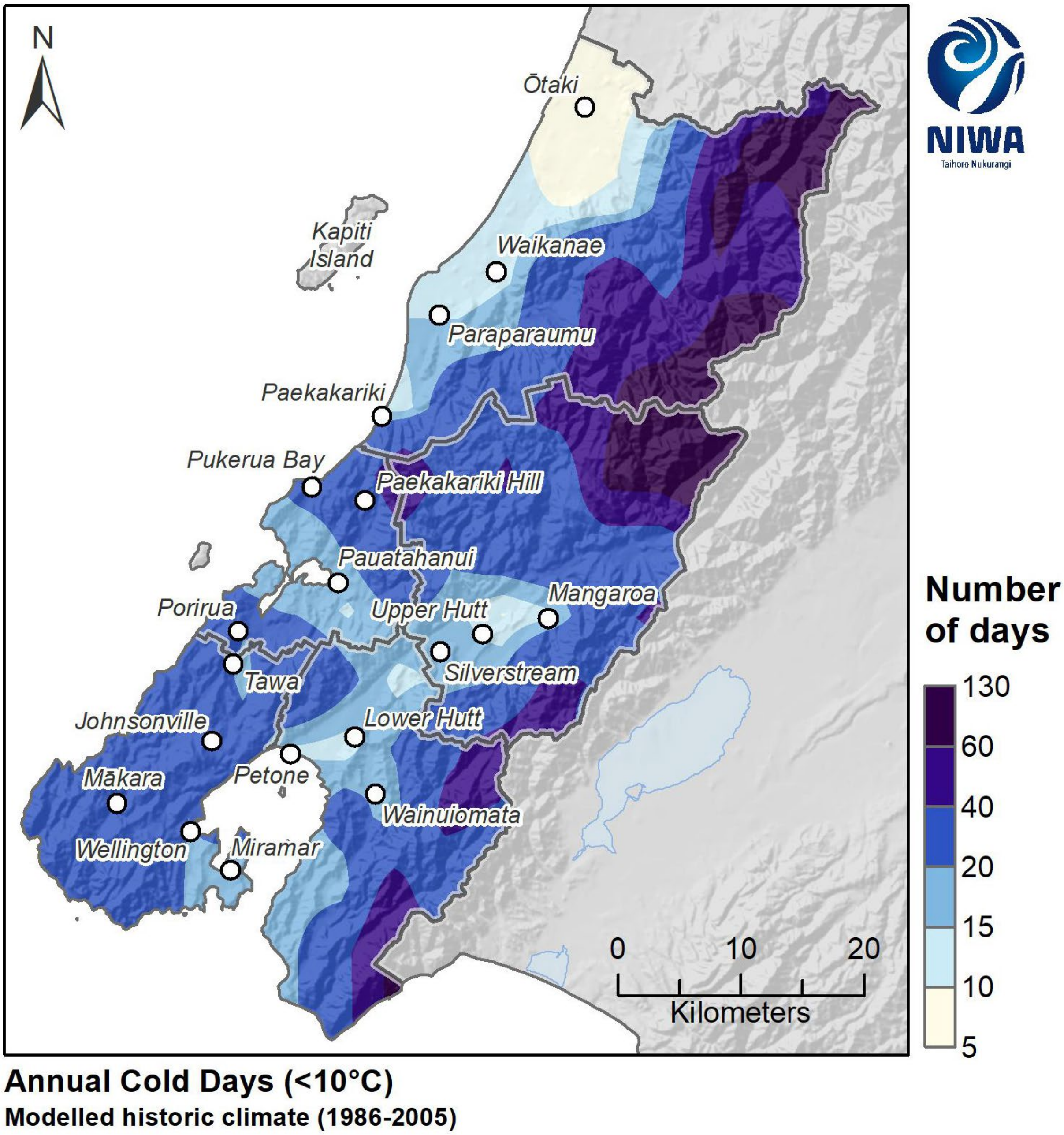

Figure 4-31: Modelled annual number of cold days (days with maximum temperature <10°C), average over 1986-2005. Results are based on dynamical downscaled projections using NIWA's Regional Climate Model. Resolution of projection is 5km x 5km.

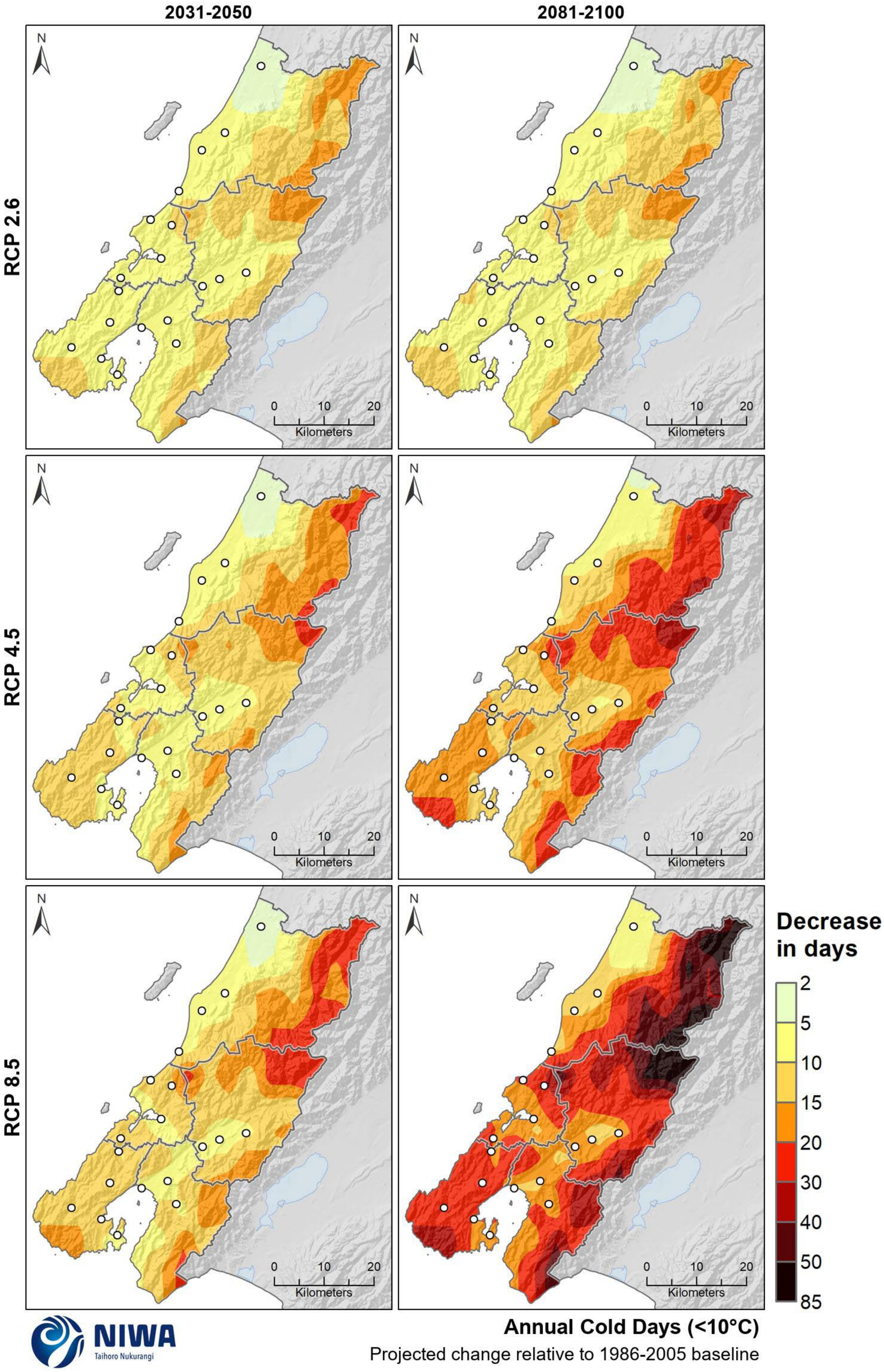

Figure 4-32: Projected annual cold day (days with maximum temperature <10°C) changes by 2040 and 2090, under RCP2.6, RCP4.5 and RCP8.5. Changes relative to 1986-2005 average, based on the average of six global climate models. Results are based on dynamical downscaled projections using NIWA's Regional Climate Model. Resolution of projection is 5km x 5km.

4.2 Rainfall

4.2.1 Rainfall totals

Projected rainfall total changes (%, relative to 1986-2005)

Annual:

Period	RCP2.6	RCP4.5	RCP8.5
2040	Up to +8%	-2% to +8%	-2% to +4%
2090	Up to +4%	-2% to +8%	-8% to +12%

Seasonal:

	RCP2.6		RCP4.5		RCP8.5	
	2040	2090	2040	2090	2040	2090
Summer	Up to +8%	Up to +8%	-4% to +8%	-2% to +8%	-8% to +4%	-8% to +12%
Autumn	Up to +8%	-2% to +4%	-4% to +12%	-4% to +8%	+2-12%	-8% to +12%
Winter	-2% to +8%	-2% to +4%	Up to +12%	-4% to +8%	-4% to +8%	-4% to +16%
Spring	-2% to +8%	+2-12%	+2-8%	-2% to +4%	-2% to +4%	-4% to +12%

This section contains maps showing historic total rainfall and the future projected change in total rainfall. Historic rainfall maps are in units of mm per year or season (average over 1986-2005) and future (average over 2031-2050 and 2081-2100) maps show the percentage change in rainfall compared with the historic total. To aid comparison between the range of projections of annual and seasonal rainfall totals, a 30-panel figure of all projection maps is included in Appendix E.

For the modelled historic period, the highest annual rainfall totals are recorded in the high elevations and around the east of the area, with 2000-6500 mm/year or more (Figure 4-33). The lowest annual rainfall totals are recorded in low elevation areas around Miramar, Porirua and Ōtaki (1000-1100 mm). The entire area receives regular rainfall throughout the year, although summer is typically the driest season (Figure 4-34).

Representative concentration pathway (RCP) 2.6

By 2040, annual rainfall is projected to increase by up to 8% (Figure 4-35). Increases of 4-8% are projected for southwestern parts of the area in summer and autumn (Figure 4-36). Increases of up to 4% are common for most populated parts in winter and spring, with small decreases of up to 2% projected for isolated eastern parts.

By 2090, annual rainfall is projected to increase by up to 4% (Figure 4-35). The greatest annual changes are projected for areas near the coast (2-4%), whereas inland areas observe a small projected increase of up to 2%. Projected seasonal rainfall changes are varied, ranging from a decrease of up to 2% through to an increase of up to 12% (Figure 4-37). Increases of 2-12% are projected throughout the area in spring.

Representative concentration pathway (RCP) 4.5

By 2040, projected change in annual rainfall ranges from -2% to +8% throughout the area (Figure 4-35). Greater changes are projected seasonally, with summer and autumn decreases of up to 4% projected for some eastern parts, increases of 8-12% projected for southwestern parts about Mākara in autumn and winter (Figure 4-38).

By 2090, annual rainfall changes of -2% to +8% are projected (Figure 4-35). Increases of 2-8% are projected for many western and southwestern parts in autumn and winter (Figure 4-39), whilst small decreases of up to 2% are projected about Upper Hutt in summer and winter.

Representative concentration pathway (RCP) 8.5

By 2040, projected change to annual rainfall ranges from -2% to +4% throughout the area (Figure 4-35). Rainfall decreases of 2-8% are projected from Paraparaumu south to Wainuiomata in summer, with increases of 4-8% projected for most of the area in autumn (Figure 4-40). Winter and spring changes of ±4% are projected for many parts.

By 2090, a stronger pattern of change is evident, with a more prominent decrease in projected rainfall for eastern parts, and increase in projected rainfall for western parts, compared to other RCP scenarios. At the annual timeframe, projected rainfall changes of -8% to +12% are projected (Figure 4-35). A summer and autumn rainfall reduction of 4-8% is projected for the Tararua Range (Figure 4-41). Winter increases of up to 16% are projected, with greatest increases of 8-16% along the western coastline and to the north about Ōtaki.

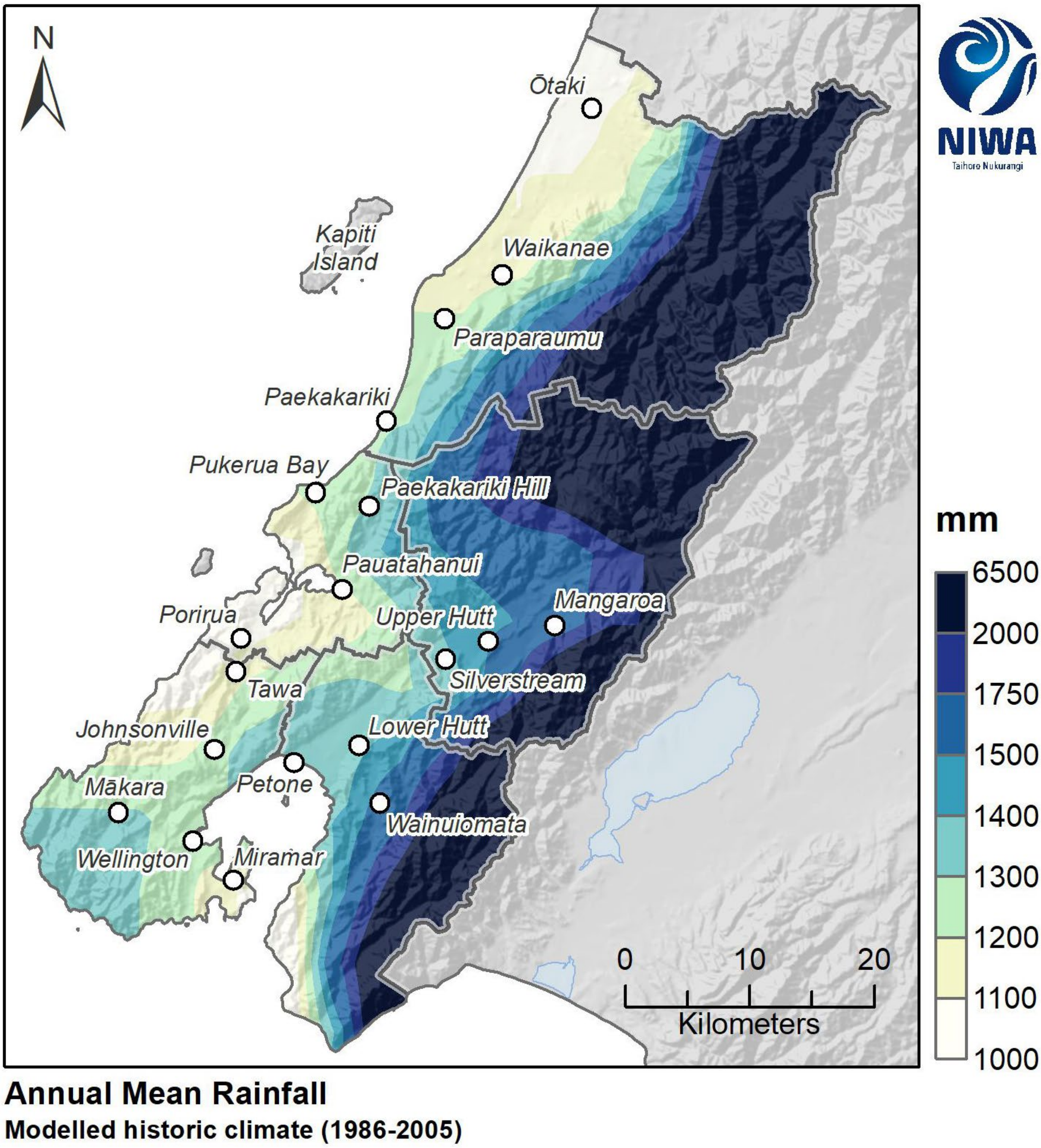

Figure 4-33: Modelled annual rainfall (mm), average over 1986-2005. Results are based on dynamical downscaled projections using NIWA's Regional Climate Model. Resolution of projection is 5km x 5km.

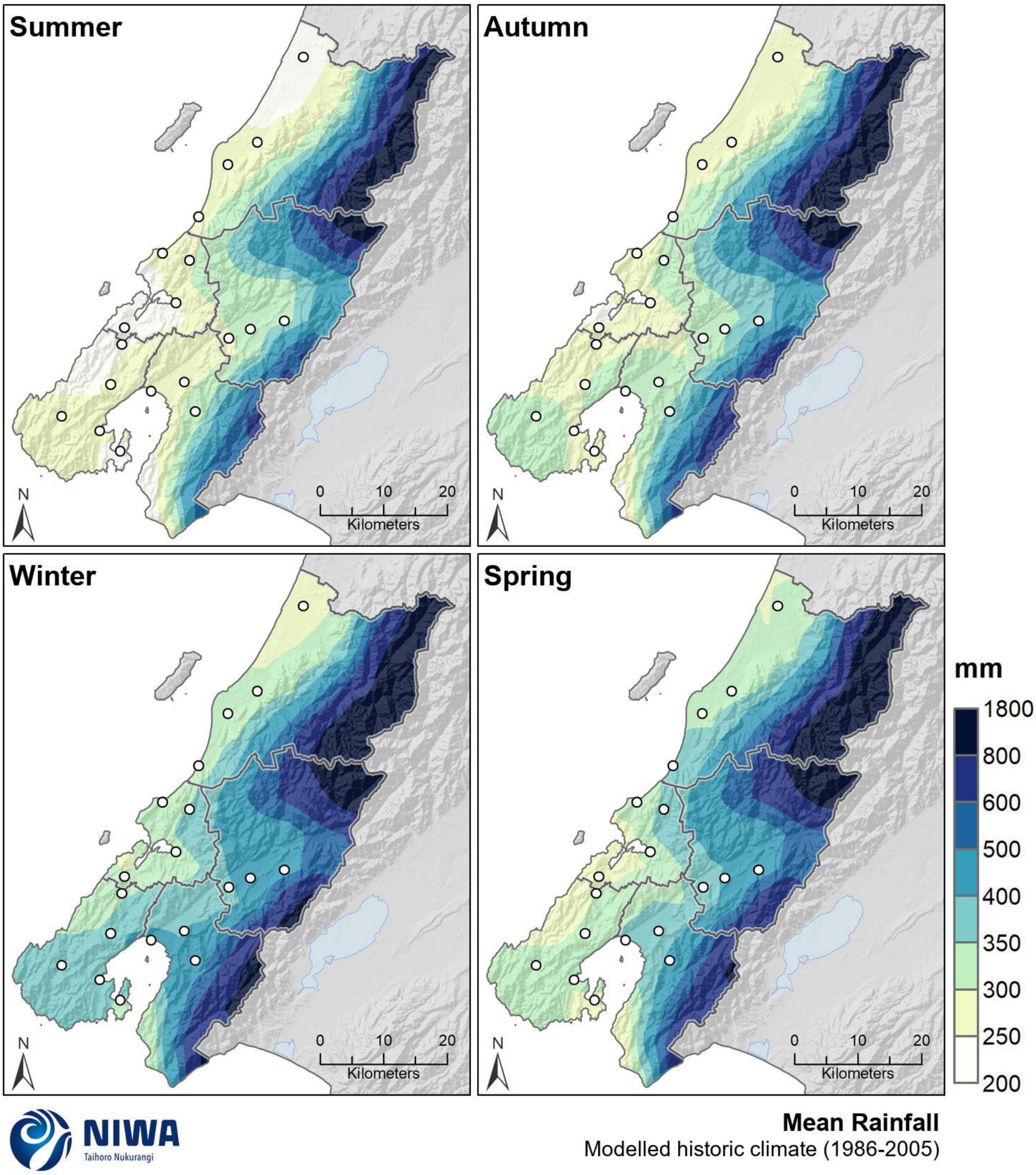

Figure 4-34: Modelled seasonal rainfall (mm), average over 1986-2005. Results are based on dynamical downscaled projections using NIWA's Regional Climate Model. Resolution of projection is 5km x 5km.

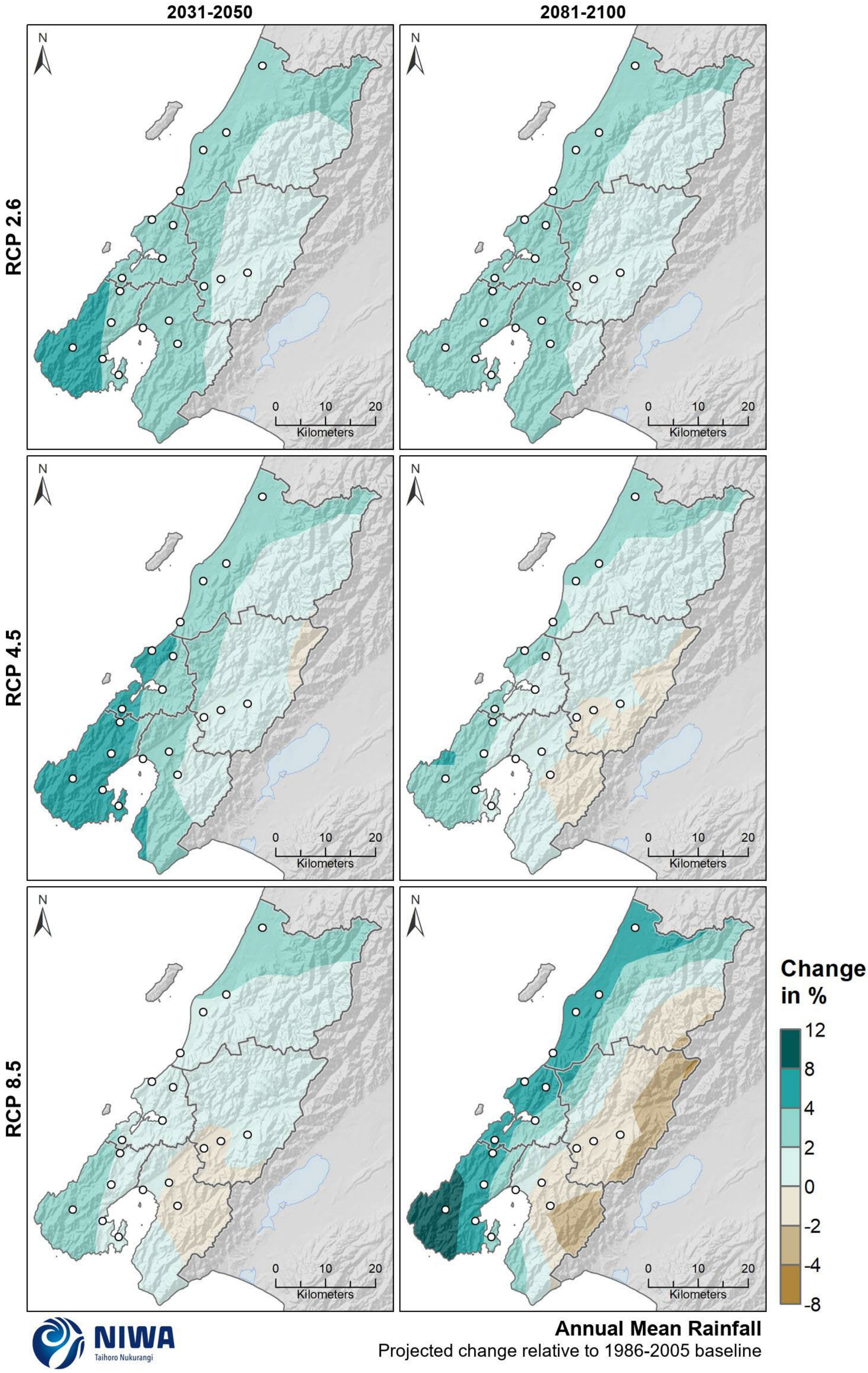

Figure 4-35: Projected annual rainfall changes (%). Relative to 1986-2005 average, based on the average of six global climate models. Results are based on dynamical downscaled projections using NIWA's Regional Climate Model. Resolution of projection is 5km x 5km.

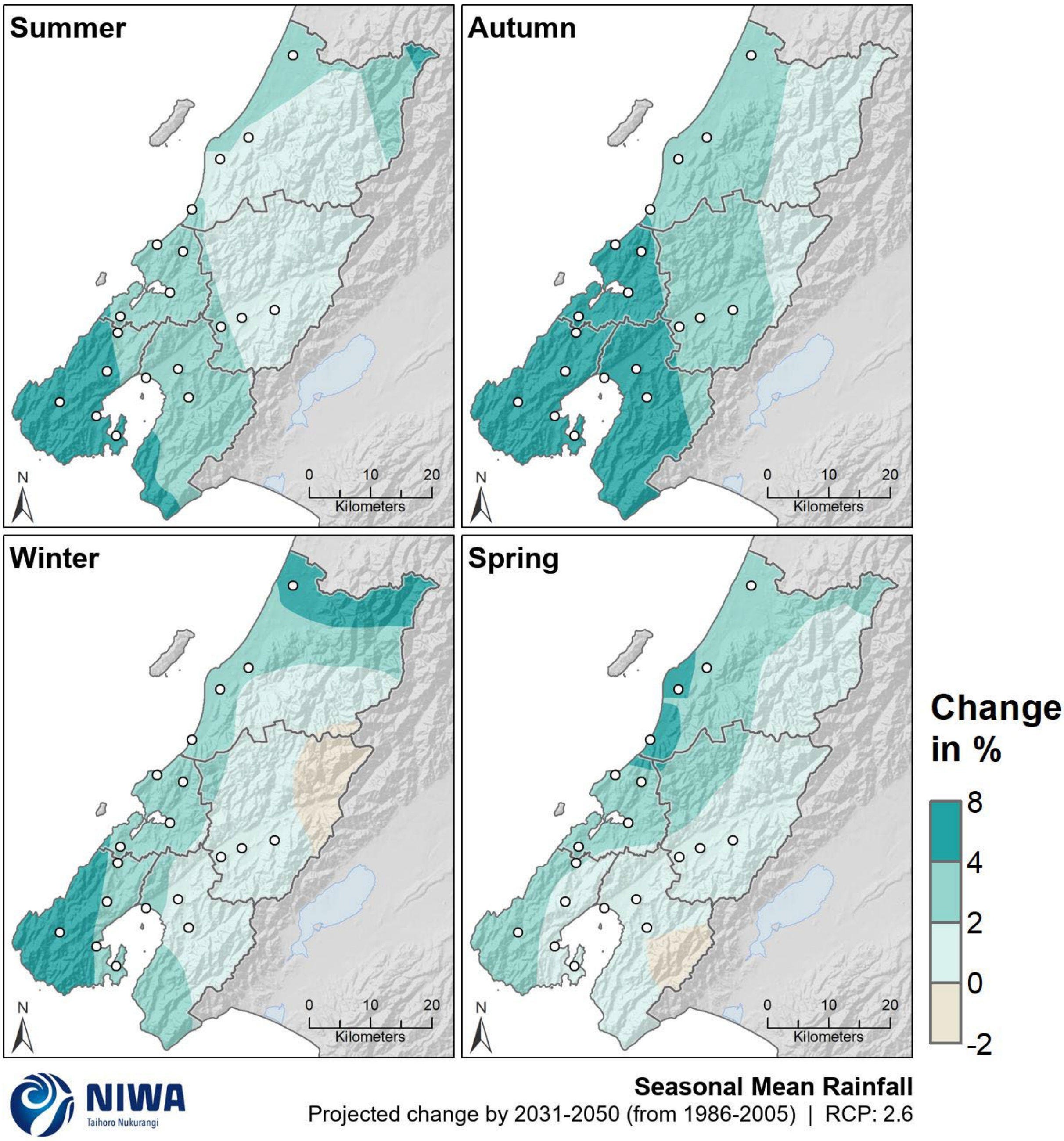

Figure 4-36: Projected seasonal rainfall changes (%) by 2040 for RCP2.6. Relative to 1986-2005 average, based on the average of six global climate models. Results are based on dynamical downscaled projections using NIWA's Regional Climate Model. Resolution of projection is 5km x 5km.

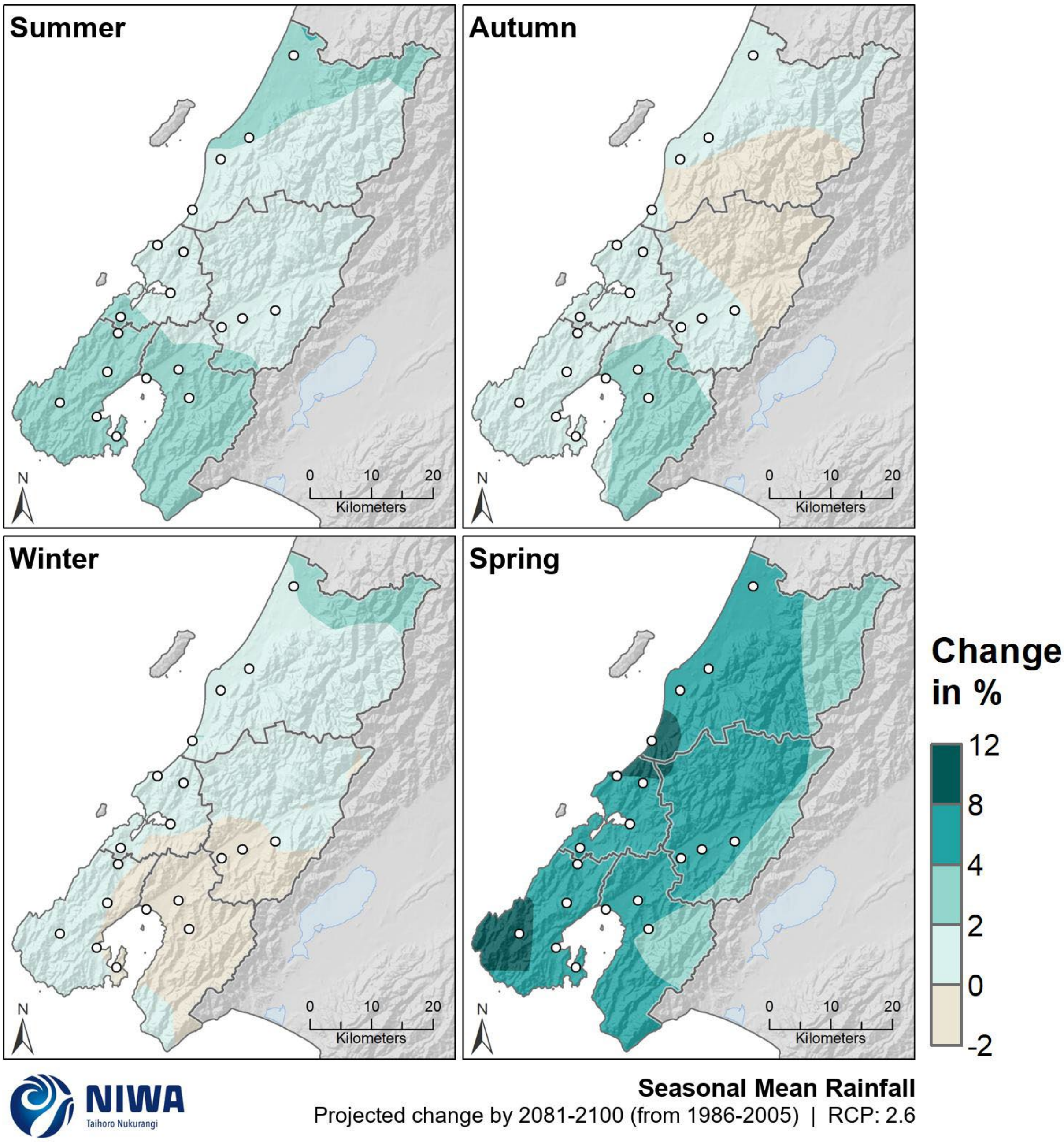

Figure 4-37: Projected seasonal rainfall changes (%) by 2090 for RCP2.6. Relative to 1986-2005 average, based on the average of six global climate models. Results are based on dynamical downscaled projections using NIWA's Regional Climate Model. Resolution of projection is 5km x 5km.

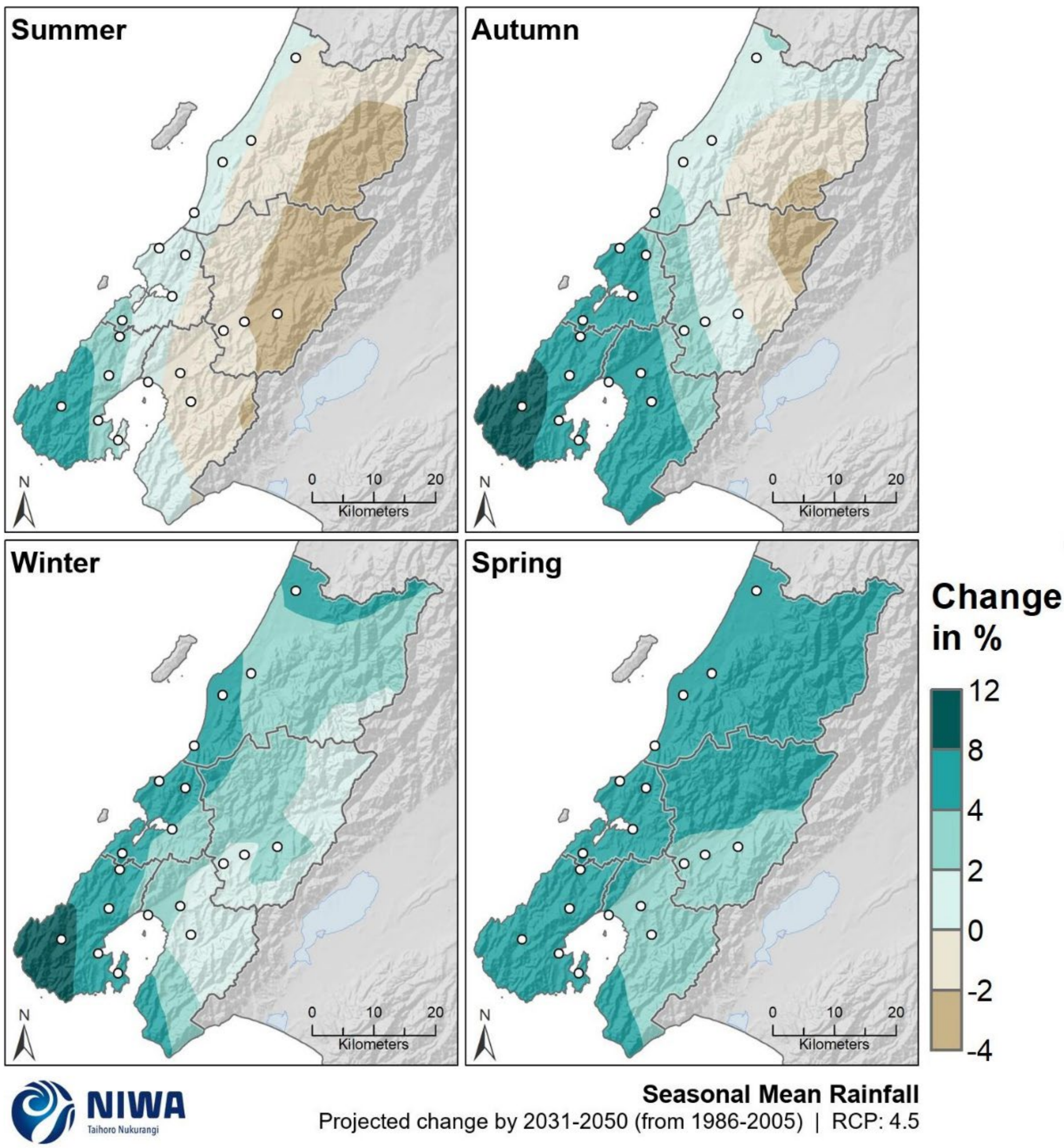

Figure 4-38: Projected seasonal rainfall changes (%) by 2040 for RCP4.5. Relative to 1986-2005 average, based on the average of six global climate models. Results are based on dynamical downscaled projections using NIWA's Regional Climate Model. Resolution of projection is 5km x 5km.

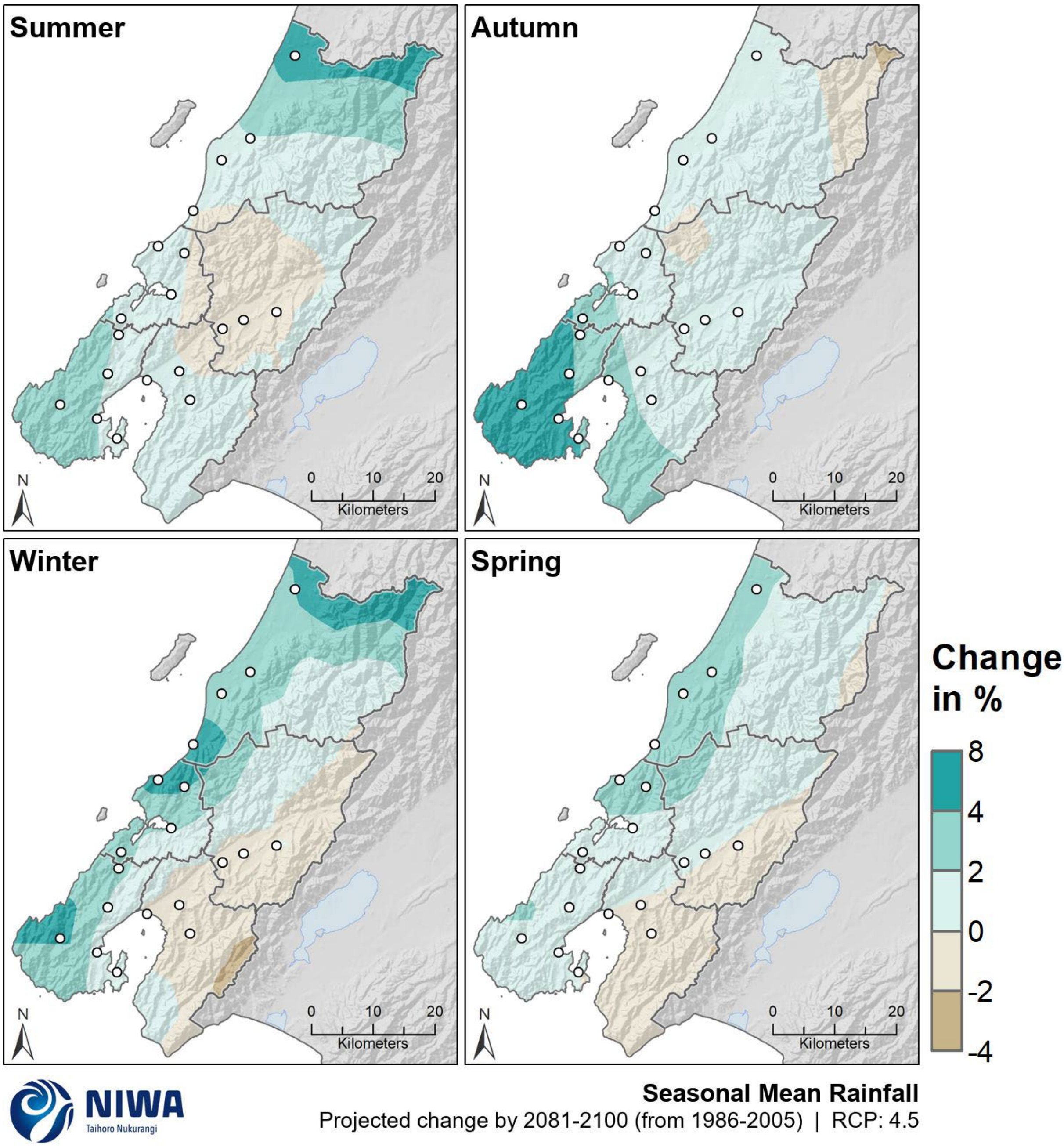

Figure 4-39: Projected seasonal rainfall changes (%) by 2090 for RCP4.5. Relative to 1986-2005 average, based on the average of six global climate models. Results are based on dynamical downscaled projections using NIWA's Regional Climate Model. Resolution of projection is 5km x 5km.

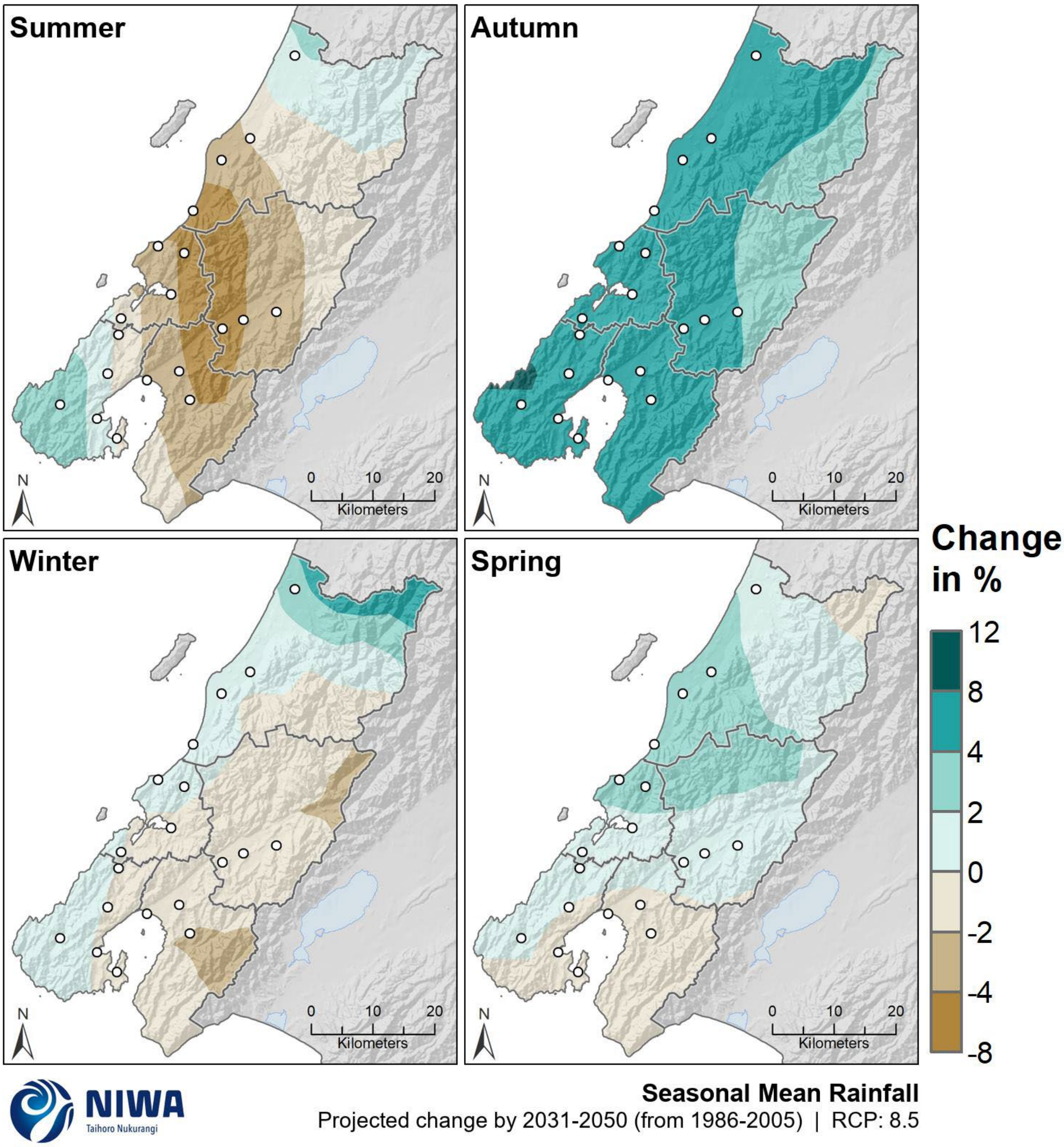

Figure 4-40: Projected seasonal rainfall changes (%) by 2040 for RCP8.5. Relative to 1986-2005 average, based on the average of six global climate models. Results are based on dynamical downscaled projections using NIWA's Regional Climate Model. Resolution of projection is 5km x 5km.

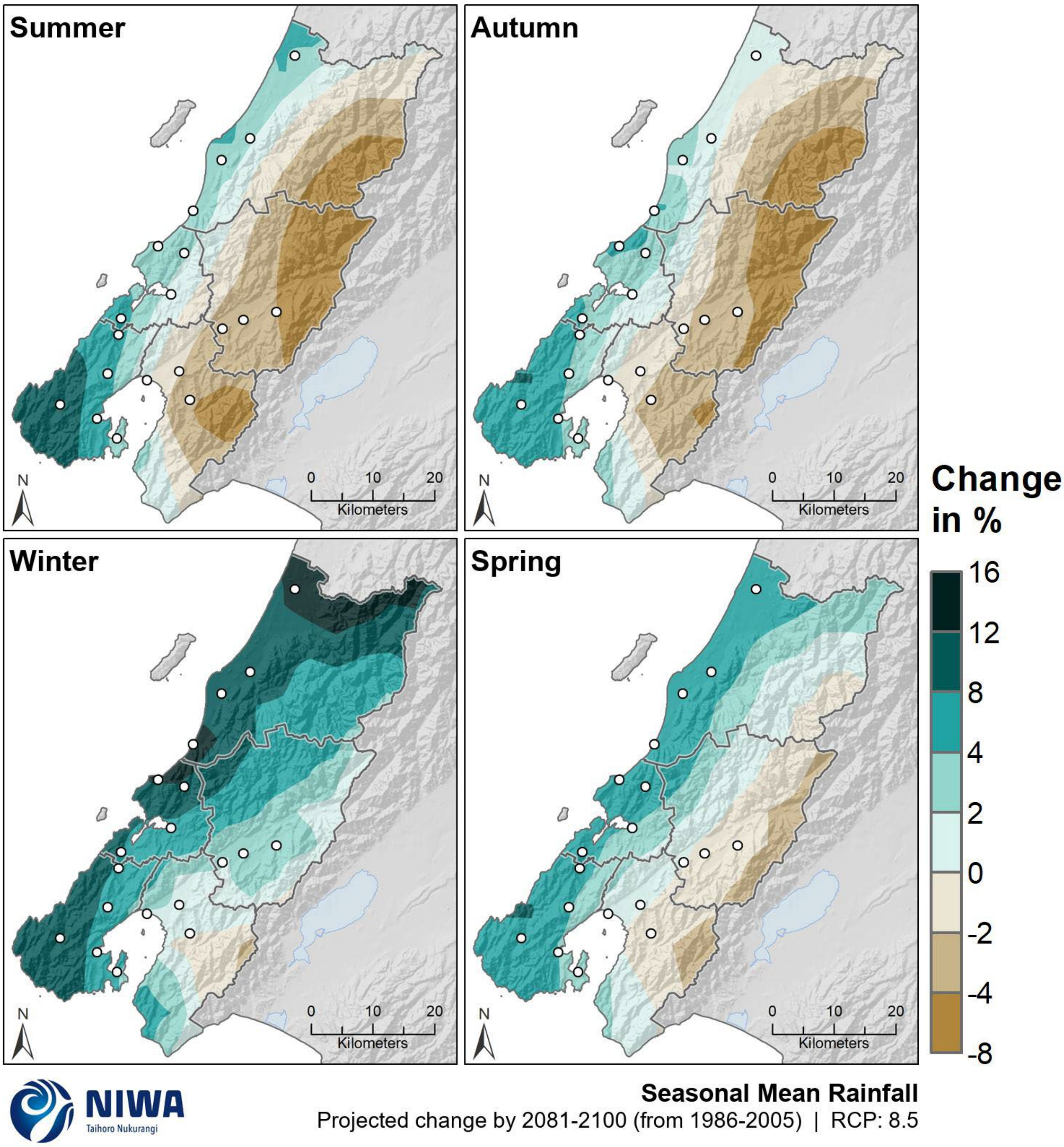

Figure 4-41: Projected seasonal rainfall changes (%) by 2090 for RCP8.5. Relative to 1986-2005 average, based on the average of six global climate models. Results are based on dynamical downscaled projections using NIWA's Regional Climate Model. Resolution of projection is 5km x 5km.

4.2.2 Wet days

Projected wet day changes (relative to 1986-2005)

Annual:

Period	RCP2.6	RCP4.5	RCP8.5
2040	-6 to +2	-6 to +1	-8 to +1
2090	-4 to +1	-12 to +1	2-21 fewer

Seasonal:

	RCP2.6		RCP4.5		RCP8.5	
	2040	2090	2040	2090	2040	2090
Summer	± 1	-2 to +1	-4 to +1	-2 to +1	-4 to +1	1-6 fewer
Autumn	-2 to +1	-2 to +1	-2 to +1	-4 to +1	-2 to +1	-4 to +1
Winter	± 2	-2 to +1	-2 to +1	-4 to +1	-4 to +1	-8 to +2
Spring	-2 to +1	-2 to +1	-1 to +2	-4 to +1	-2 to +1	-6 to +1

In this report, 'wet days' are days when at least 1 mm of rainfall is recorded. Historic (average over 1986-2005) and future (average over 2031-2050 and 2081-2100) maps for wet days are shown in this section. The historic maps show annual and seasonal average numbers of wet days and the future projection maps show the change in the number of wet days compared with the historic period. Note that the historic maps are on a different colour scale to the future projection maps. To aid comparison between the range of projections of annual and seasonal wet days, a 30-panel figure of all projection maps is included in Appendix E.

For the modelled historic period, the most wet days are recorded to the east of the area about the Tararua Range, with 180-240 wet days annually (Figure 4-42). The lowest annual wet day totals are recorded near Mākara, where 120-130 wet days are observed annually. Seasonally, the highest number of wet days are observed in winter (35-65 wet days), with 25-55 wet days observed in summer and autumn (Figure 4-43).

Representative concentration pathway (RCP) 2.6

By 2040, projected change to annual wet days ranges from -6 to +2 days throughout the area (Figure 4-44). Seasonally, decreases of 1-2 wet days are projected for southeastern parts in autumn, winter and spring (Figure 4-45). For the remainder of the area, a projected change of ±1 wet day is typical for all seasons.

By 2090, projected change to annual wet days ranges from -4 to +1 wet days throughout the area (Figure 4-44). For each season, projected changes range from -2 to +1 wet days (Figure 4-46).

Representative concentration pathway (RCP) 4.5

By 2040, projected change to annual wet days ranges from -6 to +1 days (Figure 4-44). Seasonally, the most widespread decreases are projected in summer, with 1-4 fewer wet days for most of the area (Figure 4-47). Increases of 1-2 wet days are projected in spring for coastal parts for Paekakariki north to Ōtaki.

By 2090, projected change to annual wet days ranges from -12 to +1 days throughout the area (Figure 4-44). Greatest decreases of 8-12 wet days are projected for southeastern parts about the Remutaka Range. In winter, much of the southern half of the area observe a projected decrease of 2-4 wet days. Autumn decreases of 1-2 wet days are projected for most of the area.

Representative concentration pathway (RCP) 8.5

By 2040, projected change to annual wet days ranges from -8 to +1 days throughout the area (Figure 4-44). Decreases of 1-4 wet days are projected for most of the area in summer (Figure 4-49). Projected changes in autumn and spring range from -2 to +1 wet days.

By 2090, 2-21 fewer annual wet days are projected (Figure 4-44). Decreases of 2-8 wet days are projected for much of the area in winter (Figure 4-50). Projected decreases of 1-4 wet days are typical for most of the area in the remaining three seasons.

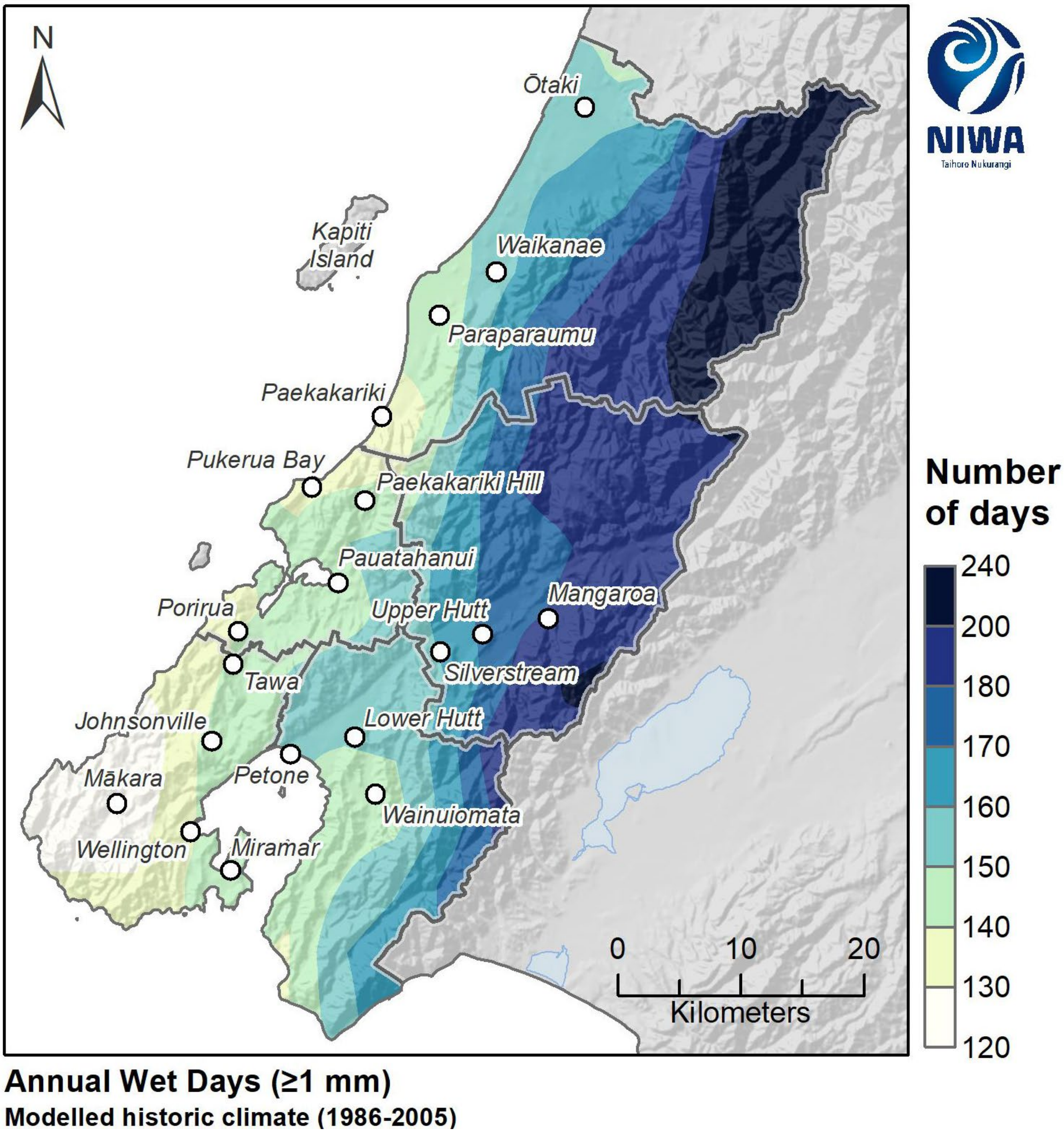

Figure 4-42: Modelled annual wet days (daily rainfall ≥1 mm), average over 1986-2005. Results are based on dynamical downscaled projections using NIWA's Regional Climate Model. Resolution of projection is 5km x 5km.

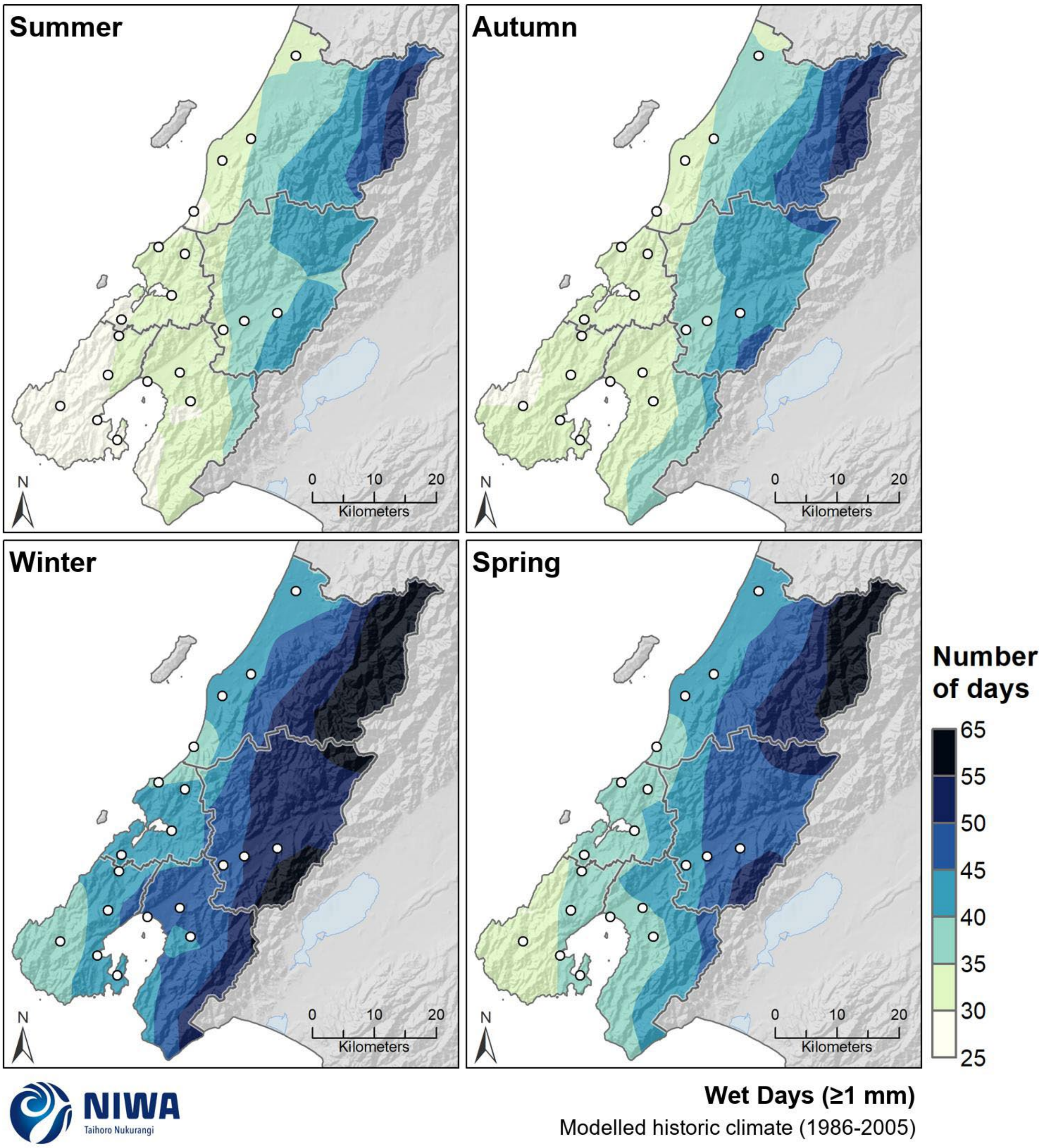

Figure 4-43: Modelled seasonal wet days (daily rainfall ≥1 mm), average over 1986-2005. Results are based on dynamical downscaled projections using NIWA's Regional Climate Model. Resolution of projection is 5km x 5km.

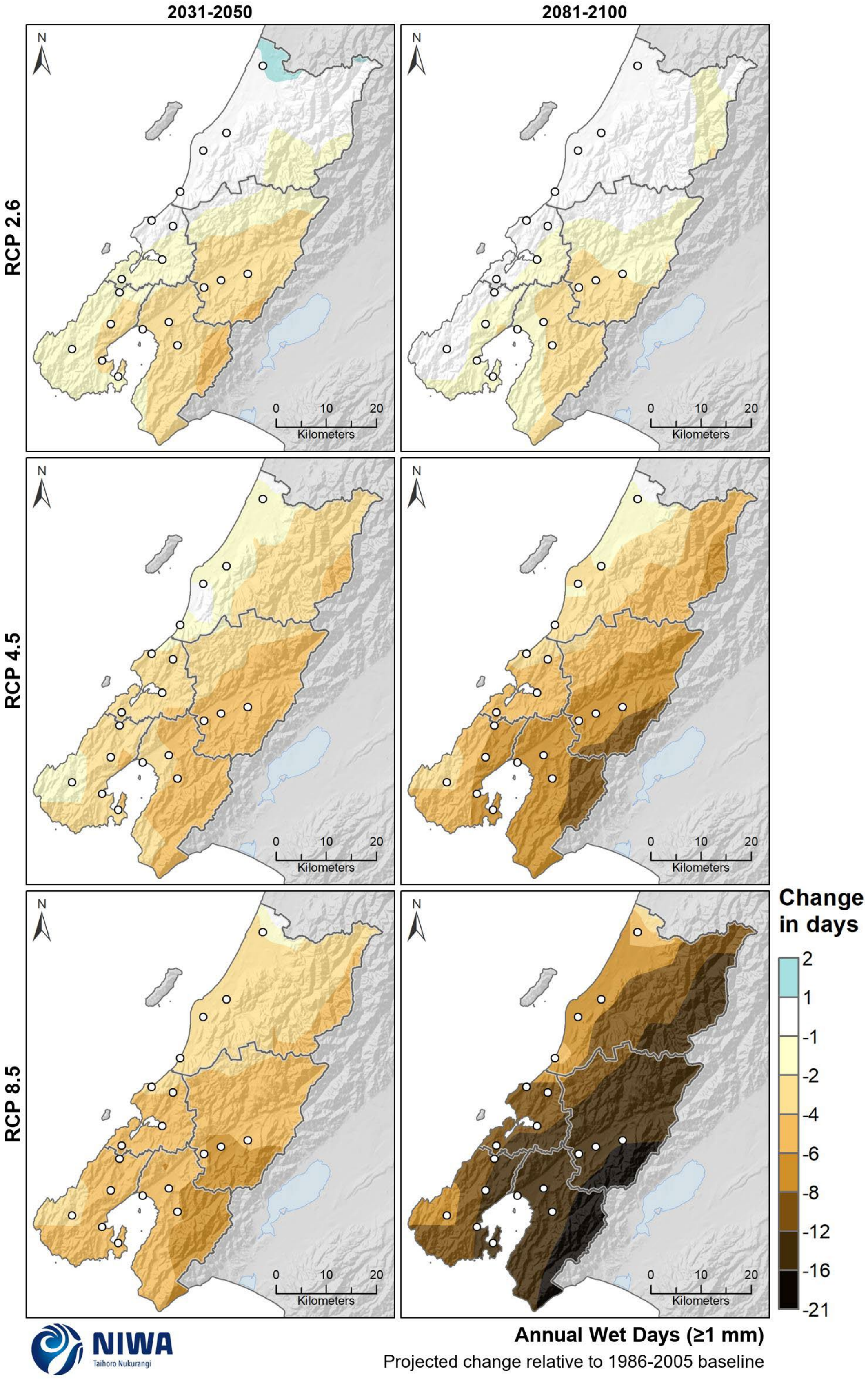

Figure 4-44: Projected annual wet day (daily rainfall ≥1 mm) changes. Relative to 1986-2005 average, based on the average of six global climate models. Results are based on dynamical downscaled projections using NIWA's Regional Climate Model. Resolution of projection is 5km x 5km.

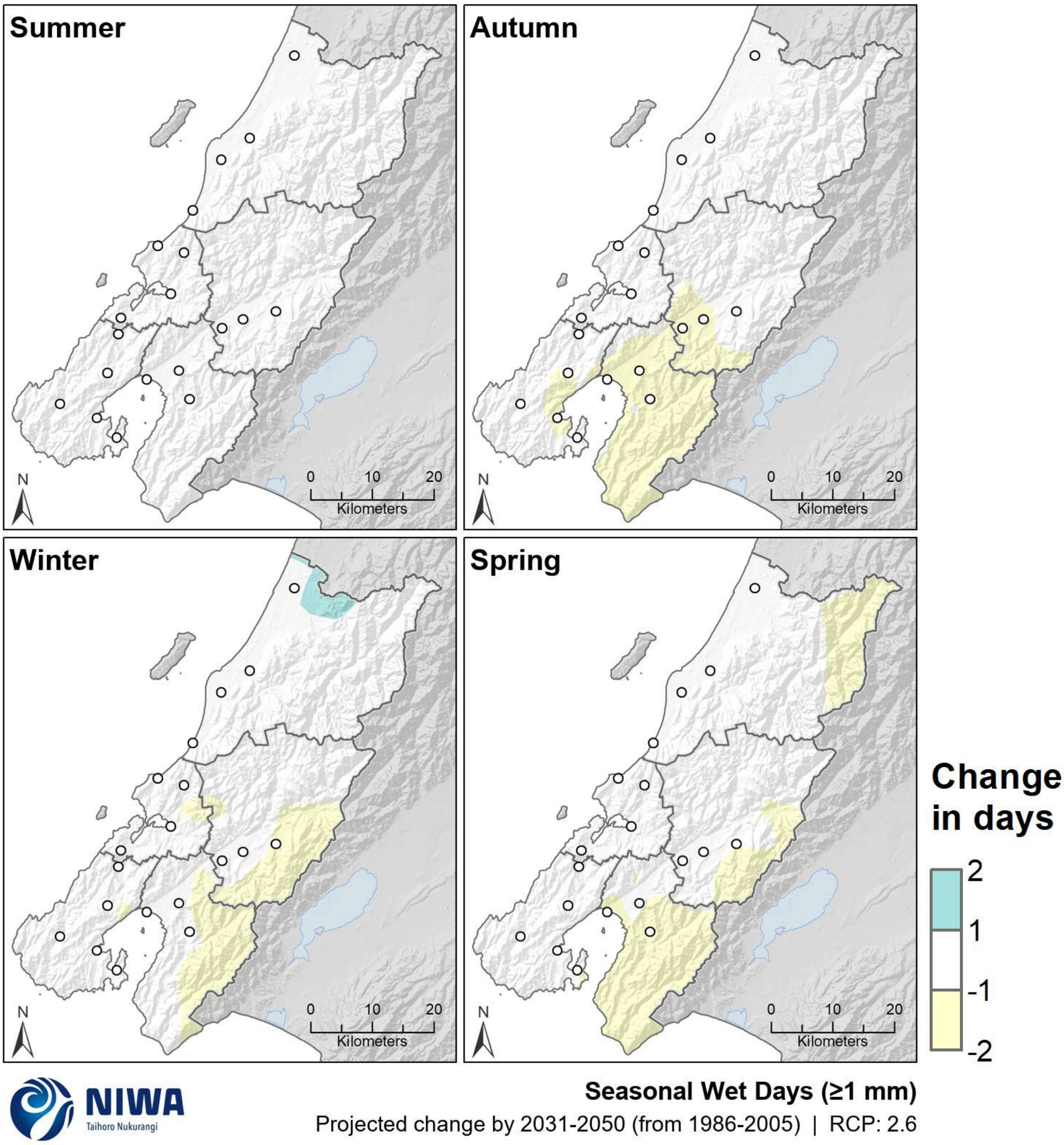

Figure 4-45: Projected seasonal wet day (daily rainfall ≥1 mm) changes by 2040 for RCP2.6. Relative to 1986-2005 average, based on the average of six global climate models. Results are based on dynamical downscaled projections using NIWA's Regional Climate Model. Resolution of projection is 5km x 5km.

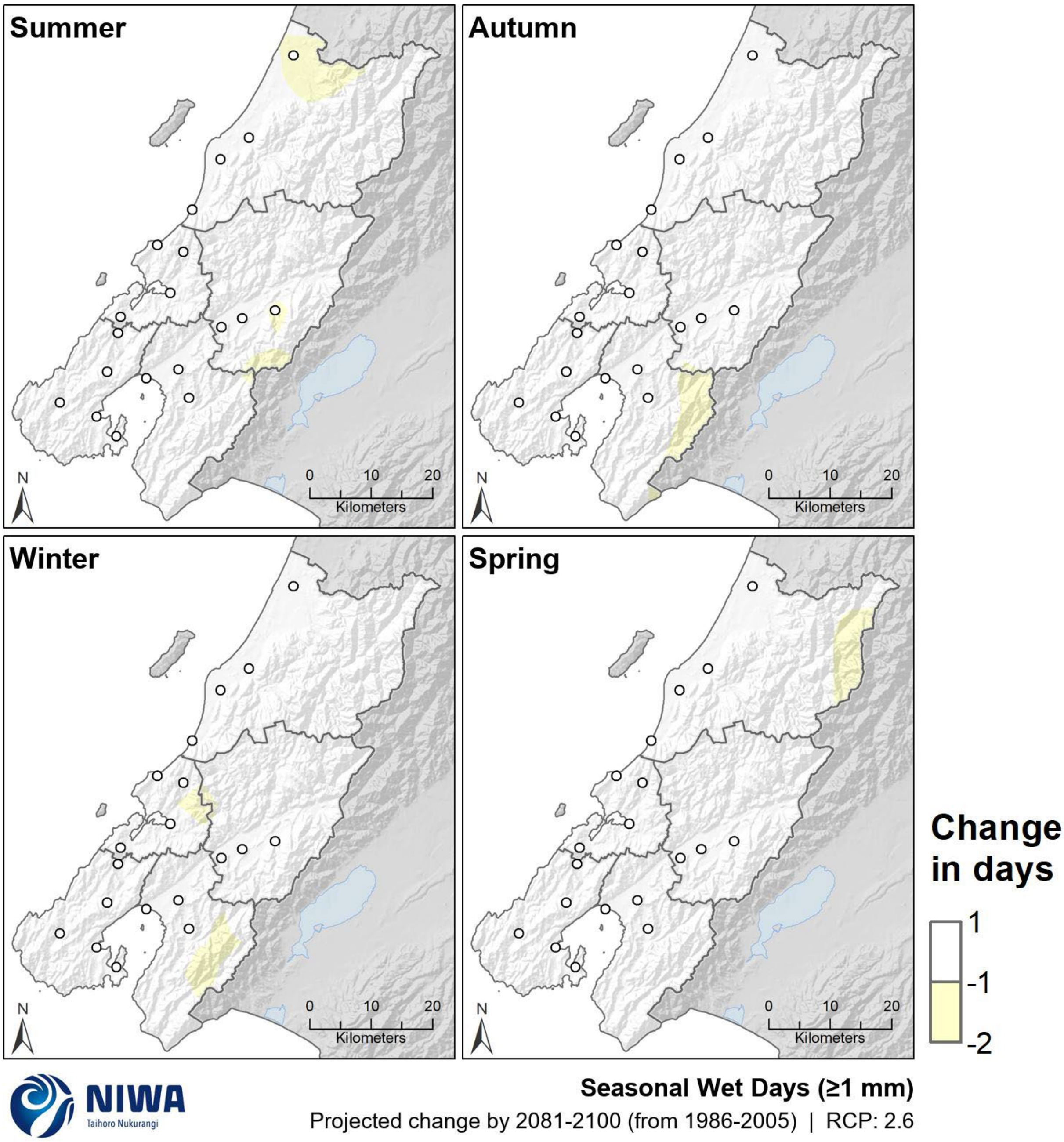

Figure 4-46: Projected seasonal wet day (daily rainfall ≥1 mm) changes by 2090 for RCP2.6. Relative to 1986-2005 average, based on the average of six global climate models. Results are based on dynamical downscaled projections using NIWA's Regional Climate Model. Resolution of projection is 5km x 5km.

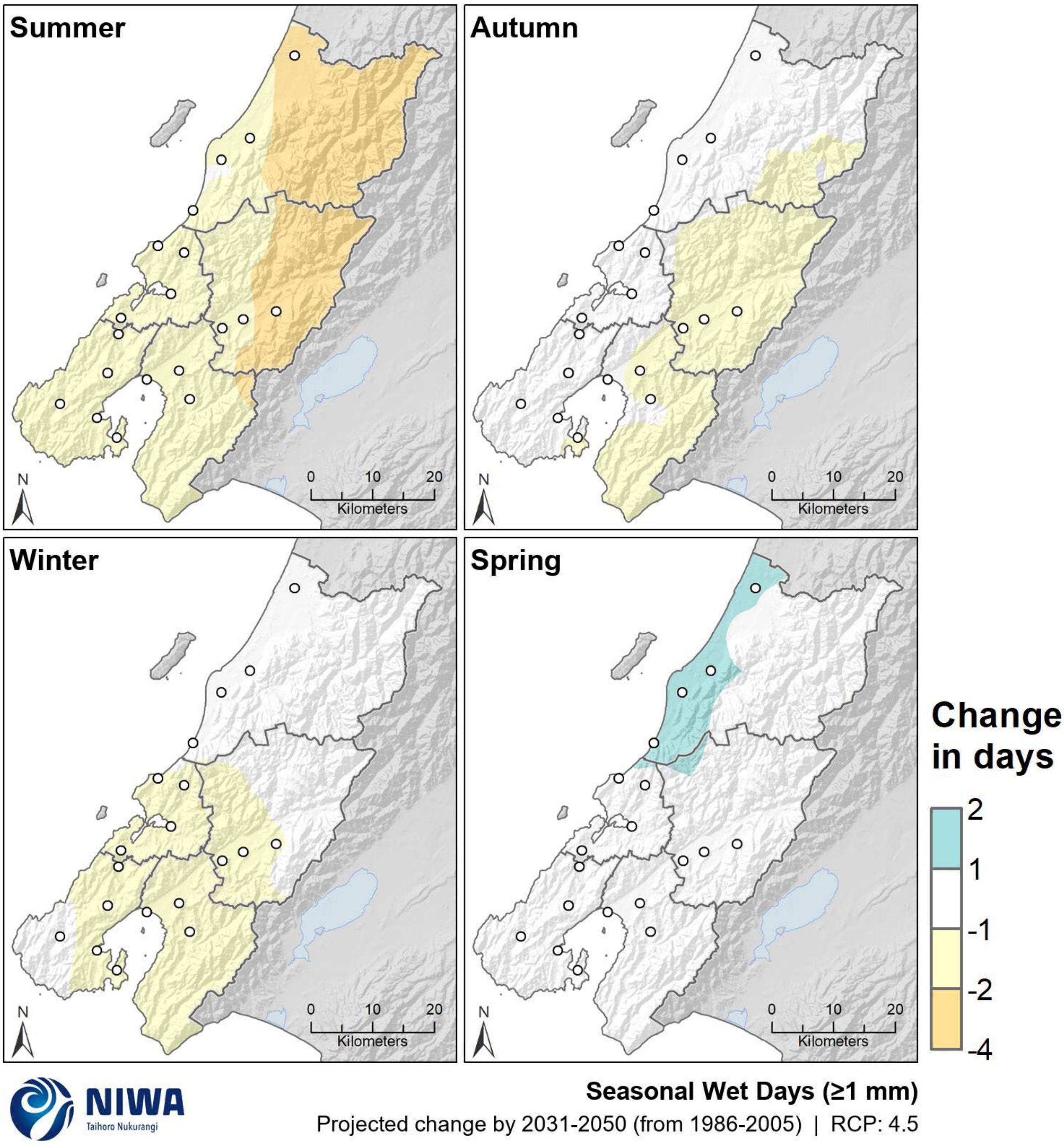

Figure 4-47: Projected seasonal wet day (daily rainfall ≥1 mm) changes by 2040 for RCP4.5. Relative to 1986-2005 average, based on the average of six global climate models. Results are based on dynamical downscaled projections using NIWA's Regional Climate Model. Resolution of projection is 5km x 5km.

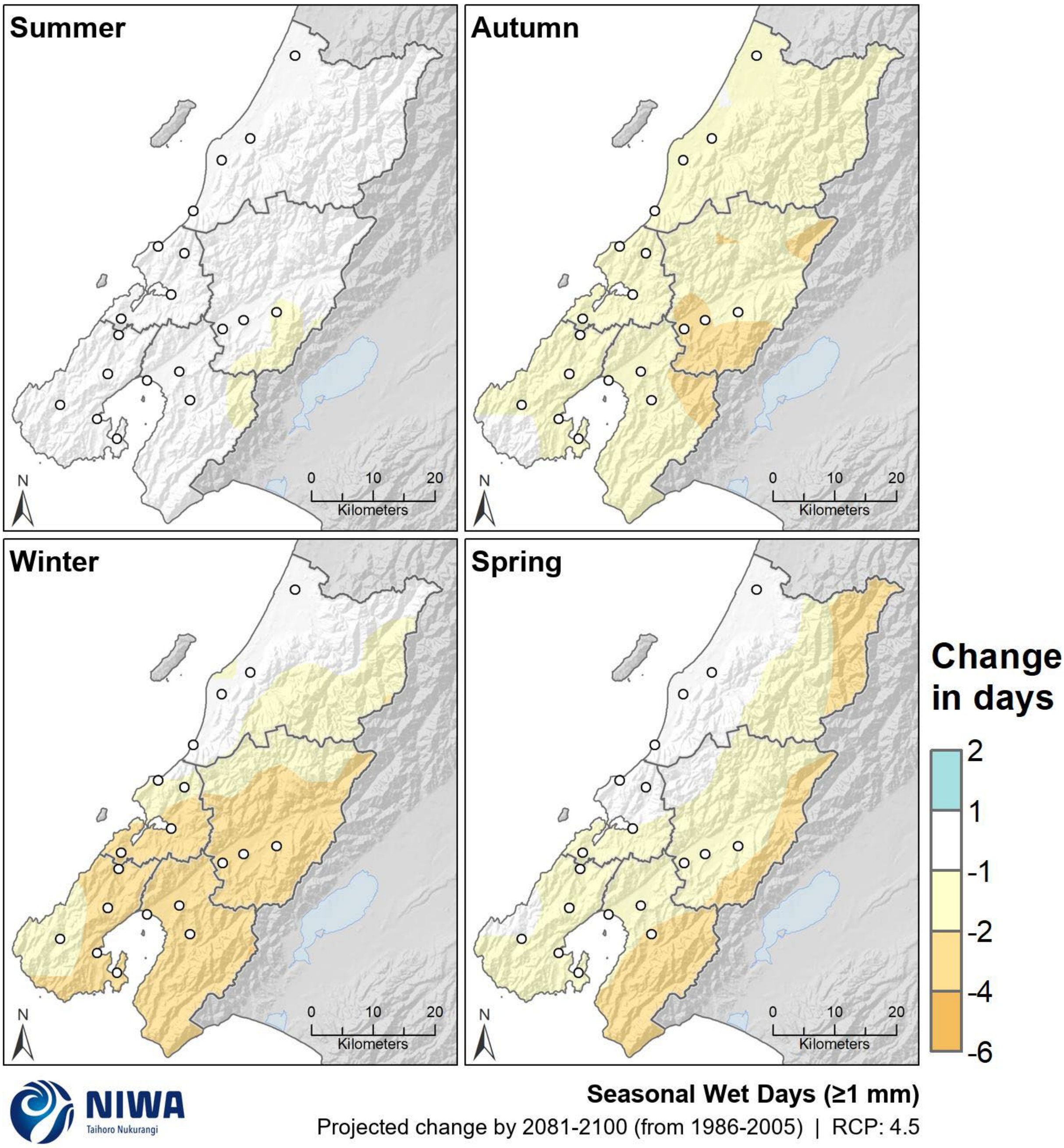

Figure 4-48: Projected seasonal wet day (daily rainfall ≥1 mm) changes by 2090 for RCP4.5. Relative to 1986-2005 average, based on the average of six global climate models. Results are based on dynamical downscaled projections using NIWA's Regional Climate Model. Resolution of projection is 5km x 5km.

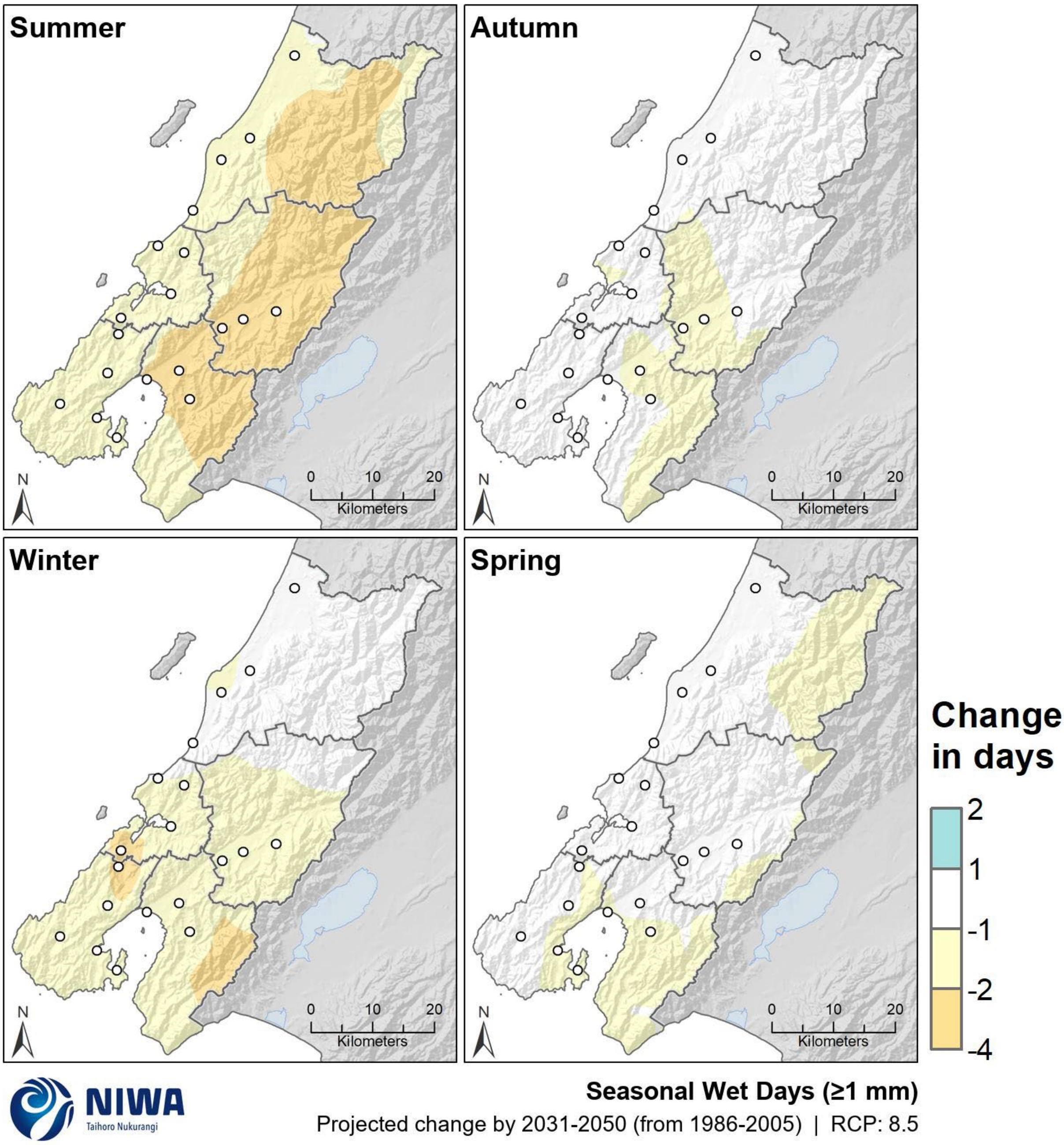

Figure 4-49: Projected seasonal wet day (daily rainfall ≥1 mm) changes by 2040 for RCP8.5. Relative to 1986-2005 average, based on the average of six global climate models. Results are based on dynamical downscaled projections using NIWA's Regional Climate Model. Resolution of projection is 5km x 5km.

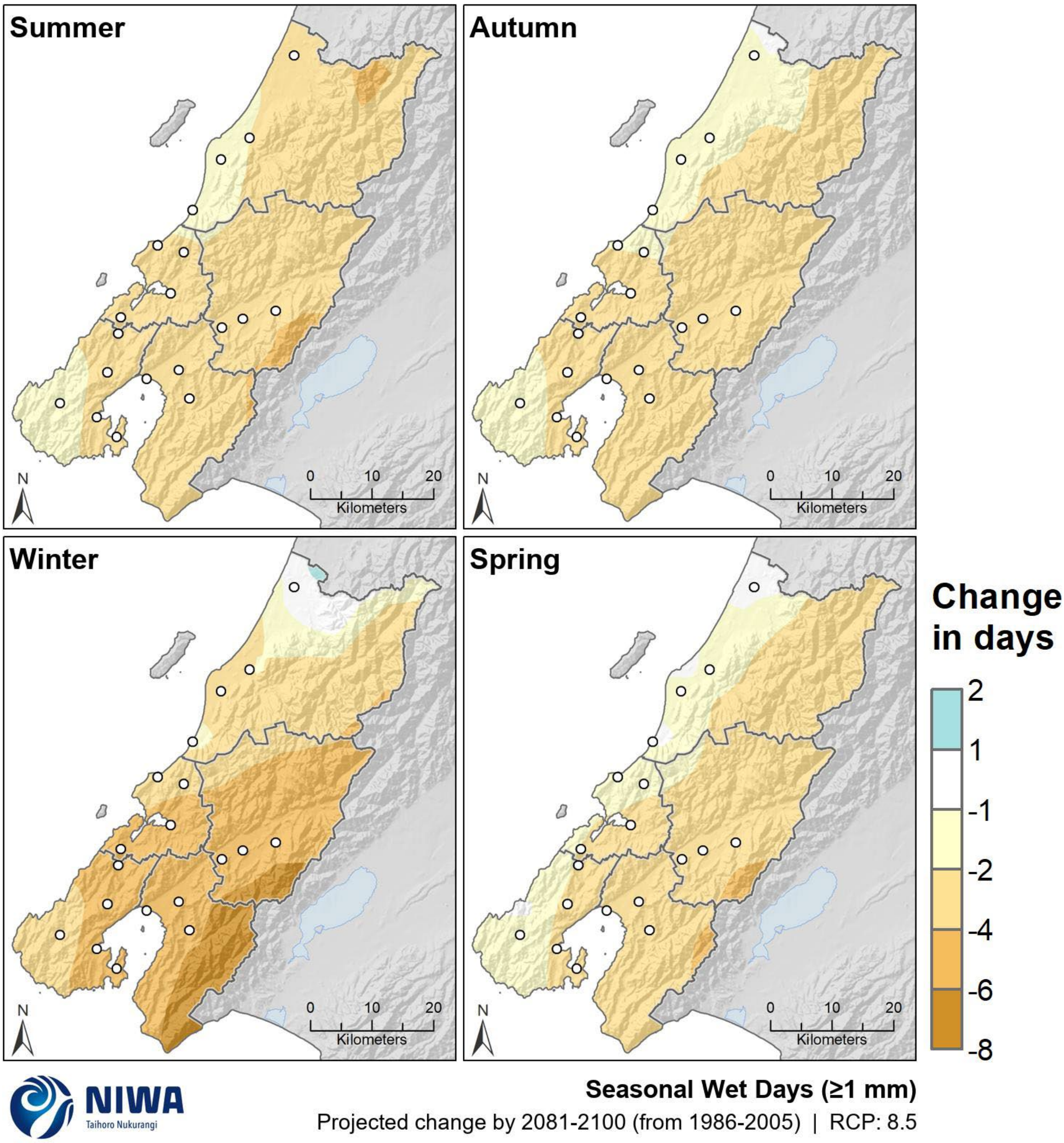

Figure 4-50: Projected seasonal wet day (daily rainfall ≥1 mm) changes by 2090 for RCP8.5. Relative to 1986-2005 average, based on the average of six global climate models. Results are based on dynamical downscaled projections using NIWA's Regional Climate Model. Resolution of projection is 5km x 5km.

4.2.3 99th percentile of daily rainfall, and rare extreme rainfall events

Projected 99th percentile of daily rainfall changes (relative to 1986-2005)

Annual:

Period	RCP2.6	RCP4.5	RCP8.5
2040	-2% to +12%	-1% to +16%	-1% to +12%
2090	+1-12%	+2-16%	+2-30%

The 99th percentile of daily rainfall refers to the amount of rainfall exceeded by the top 1% of wet days (≥1 mm of rainfall). This measure allows us to interpret what changes are expected for the very wettest days each year. As shown in Figure 4-42 (Section 4.2.2), the area west of Wellington's ranges historically observes between 120-240 wet days per year, depending on location. Therefore, the top 1% of annual wet days ranges from 1.2-2.4 days, and the 99th percentile of daily rainfall is the rainfall total exceeded on these 1.2-2.4 days.

Note that the 99th percentile is a relatively low threshold for engineering purposes (Ministry for the Environment, 2008). Projections of rare and extreme rainfall events are an important consideration for the area west of Wellington's ranges, and can be accessed via NIWA's High Intensity Rainfall Design System (HIRDS version 4; Carey-Smith *et al.*, 2018). Additionally, future projections for extreme rainfall in the Greater Wellington Region (including this area) are presented in Pearce *et al.* (2019) and Woolley *et al.* (2020); these are available from GWRC. A short presentation of some of the high intensity rare events is reproduced here in Figure 4-53 to Figure 4-57.

For the historic period, the highest annual average 99th percentile daily rainfall total is recorded in the Tararua Range, with 100-180 mm observed there (Figure 4-51). The lowest total is for areas about Ōtaki, Waikanae, Pauatahanui and Porirua, with 30-40 mm observed in these parts. Totals of 40-60 mm are prevalent for most remaining parts of the area.

Representative concentration pathway (RCP) 2.6

By 2040 and 2090, the magnitude of the annual 99th percentile daily rainfall is projected to increase by up to 12% for most of the area (Figure 4-52). The exception is northeastern parts about the Tararua Range in 2040, with small decreases of up to 2% projected.

Representative concentration pathway (RCP) 4.5

By 2040, projected changes range from -1% to +16% in the area. An increase of 8-16% is projected for coastal parts about and south of Pukerua Bay (Figure 4-52).

By 2090, the magnitude of the annual 99th percentile daily rainfall is projected to increase by 2-16% in the area (Figure 4-52). The largest projected increases of 12-16% occur about Wellington city and Miramar.

Representative concentration pathway (RCP) 8.5

By 2040, projected changes range from -1% to +12% in the area (Figure 4-52). The range of projected changes encompassing both increases and decreases illustrate that rainfall indicators do not necessarily respond linearly to different RCP scenarios, and highlight the greater uncertainty associated with the rainfall signal, compared to temperature.

By 2090, increases of 2-30% are projected for the area (Figure 4-52). Largest increases of 20-30% days are projected for the southwest of the area, as far north as Porirua.

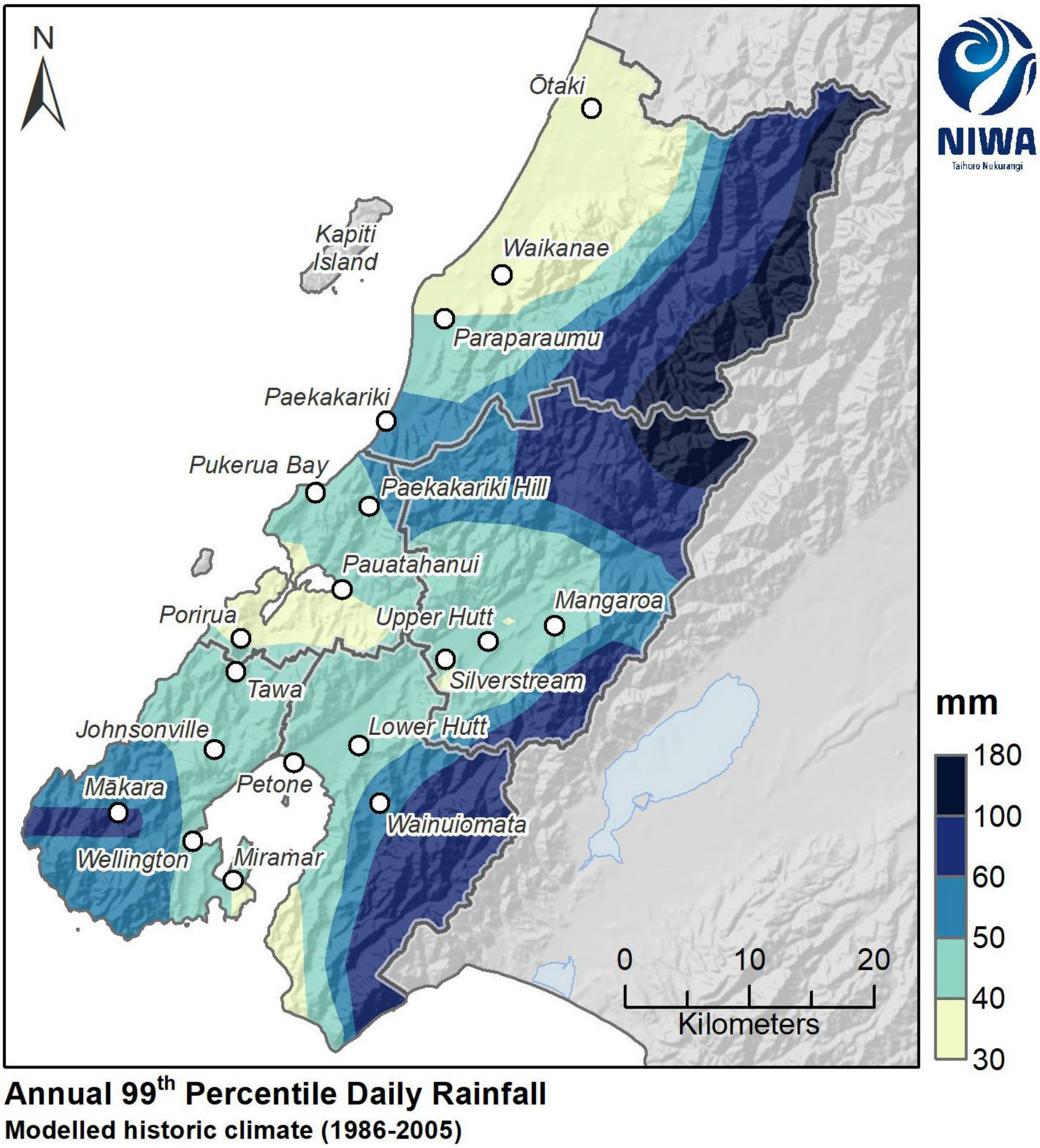

Figure 4-51: Modelled annual 99th percentile daily rainfall average over 1986-2005. Results are based on dynamical downscaled projections using NIWA's Regional Climate Model. Resolution of projection is 5km x 5km.

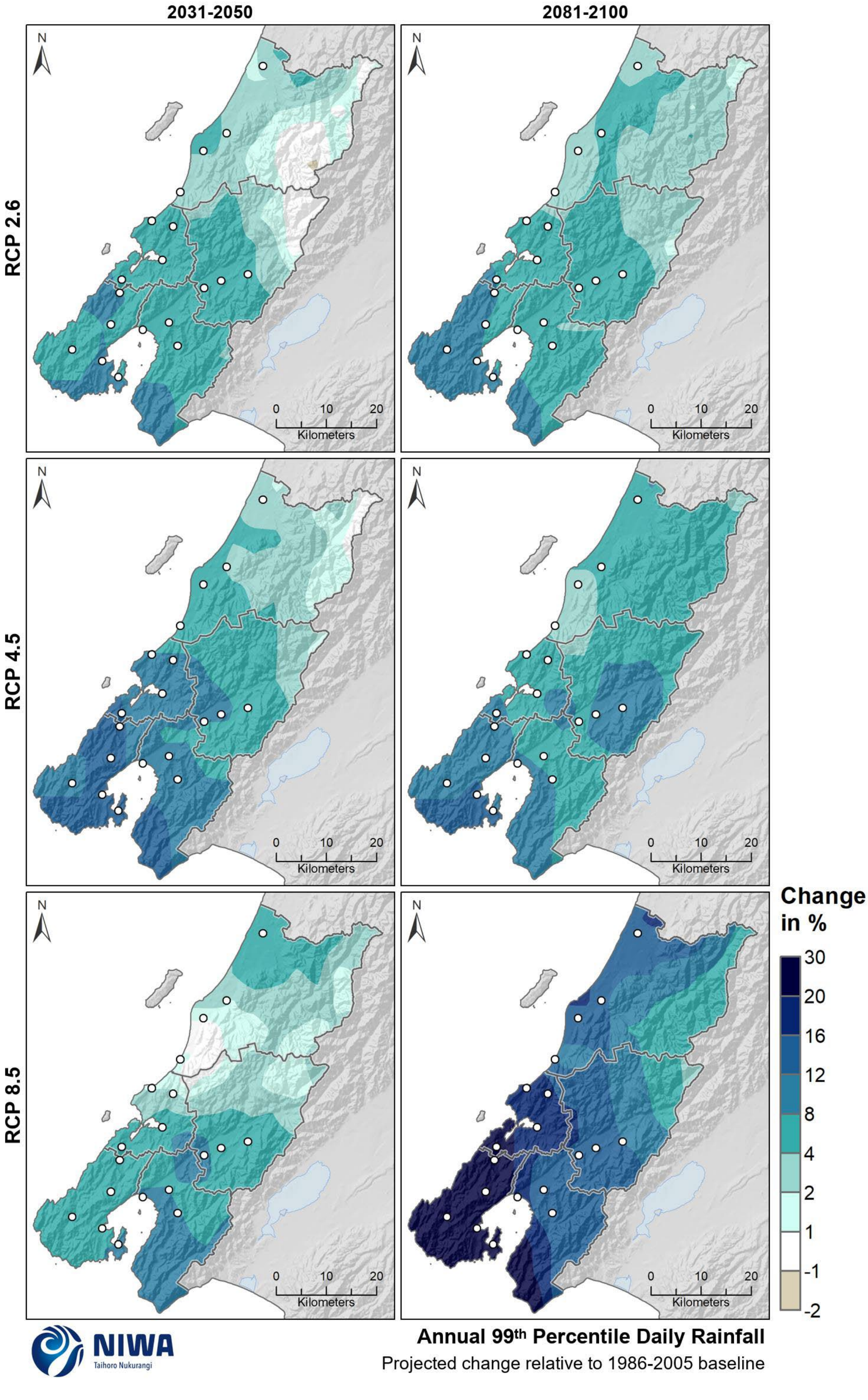

Figure 4-52: Projected annual 99th percentile daily rainfall changes by 2040 and 2090, under RCP2.6, RCP4.5 and RCP8.5. Changes relative to 1986-2005 average, based on the average of six global climate models. Results are based on dynamical downscaled projections using NIWA's Regional Climate Model. Resolution of projection is 5km x 5km.

To complement the projections of changes to the daily rainfall shown in this section up to now, figures illustrating future changes to rainfall events more extreme than the 99th percentile are reproduced below. Figure 4-53 to Figure 4-55 show changes in rainfall threshold exceedances (originally presented in Woolley *et al.*, 2020) for Kelburn, Wellington Airport and Paraparaumu, respectively. Figure 4-56 and Figure 4-57 show the 1-in-100-year rainfall depth for a 10-minute duration event (originally presented in Pearce *et al.*, 2019). The purpose of reproducing and adapting these figures is to emphasise that extreme rainfall events are projected to become more frequent and more severe for various duration thresholds and magnitudes. Readers should consult Woolley *et al.* (2020) for details of the methodology used to generate Figure 4-53 to Figure 4-55, and Pearce *et al.* (2019) for methodology details associated with Figure 4-56 and Figure 4-57. Note, previous NIWA reports focussing on extreme events for the Wellington Region are available from the GWRC's webpage.

Figure 4-53 to Figure 4-55 illustrate significant frequency increases for mid-century (green) and late-century (blue) above the climatological (red) lines, with increases typically between two-fold and three-fold for late-century (shaded area).

Figure 4-56 and Figure 4-57 illustrate increases of up to 8 mm for 10-min (short duration) rainfall events. This implies an additional 48 mm/h rate within ten minutes, on top of already high rates for the Kāpiti Coast, with considerable potential to increase flash flooding.

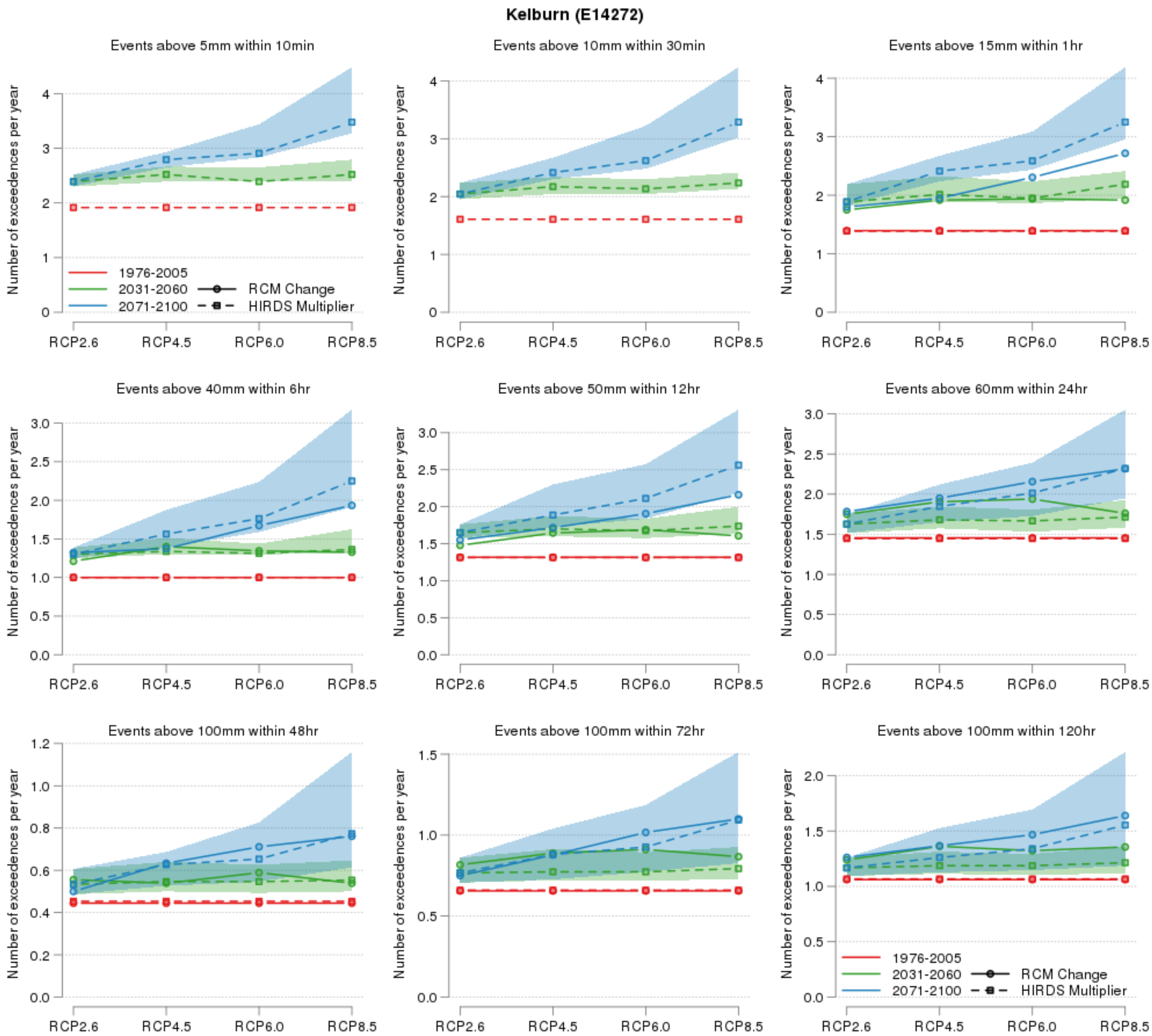

Figure 4-53: The change in rainfall exceedances with climate change for Kelburn. The results from the first (HIRDS-based) analysis are shown by the dashed lines, where the red lines are for the current climate. The shading shows the range produced when using climate change factors. The solid lines show results from direct RCM analysis, where the red line is the number of exceedances above a threshold adjusted to closely match the observed number of exceedances. For both methods, the green line is the mid-century time slice and the blue line is for the end of century period. Sourced from Woolley *et al.* (2020).

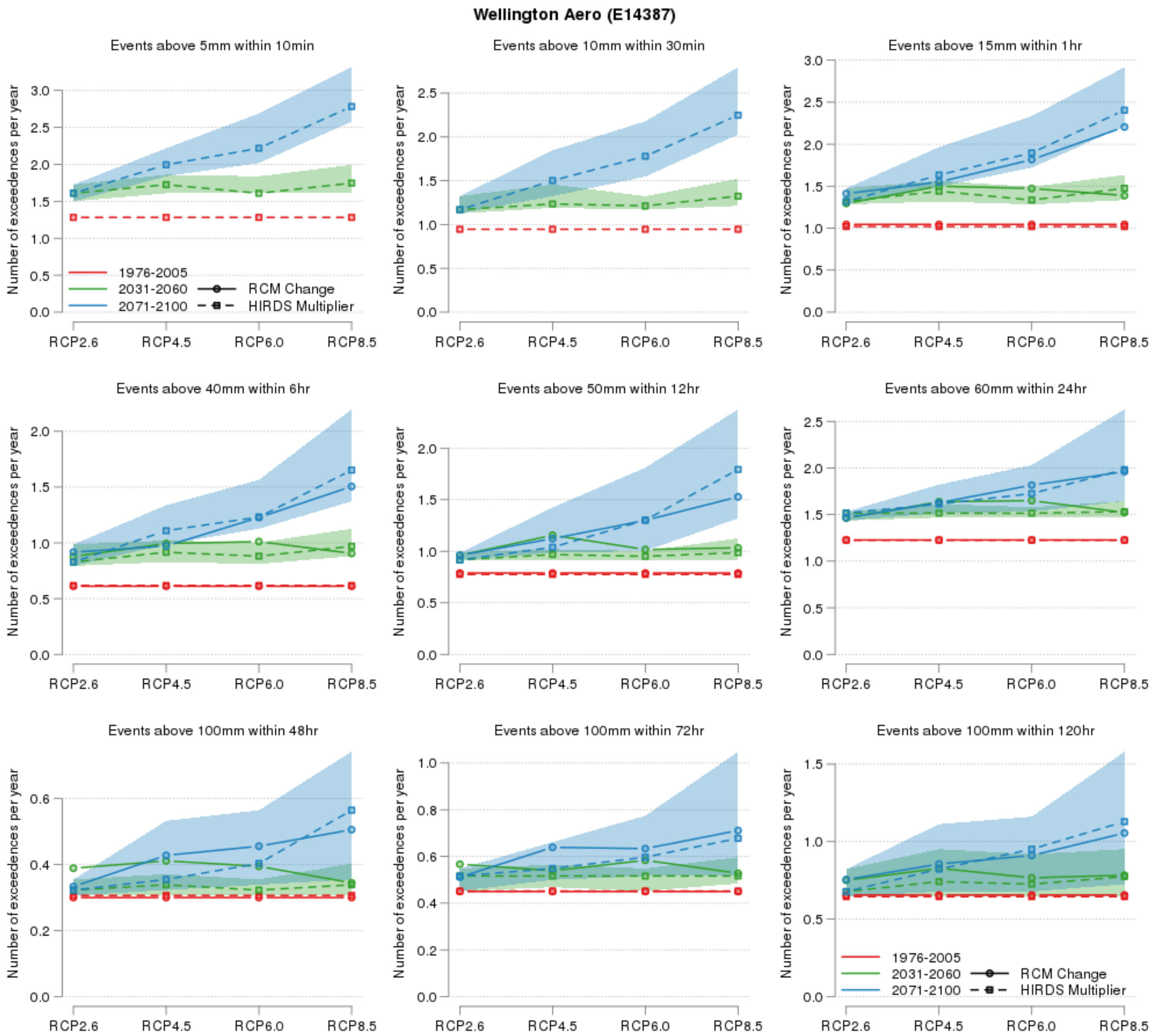

Figure 4-54: The change in rainfall exceedances with climate change for Wellington Aero. As Figure 4-53, but for Wellington Aero.

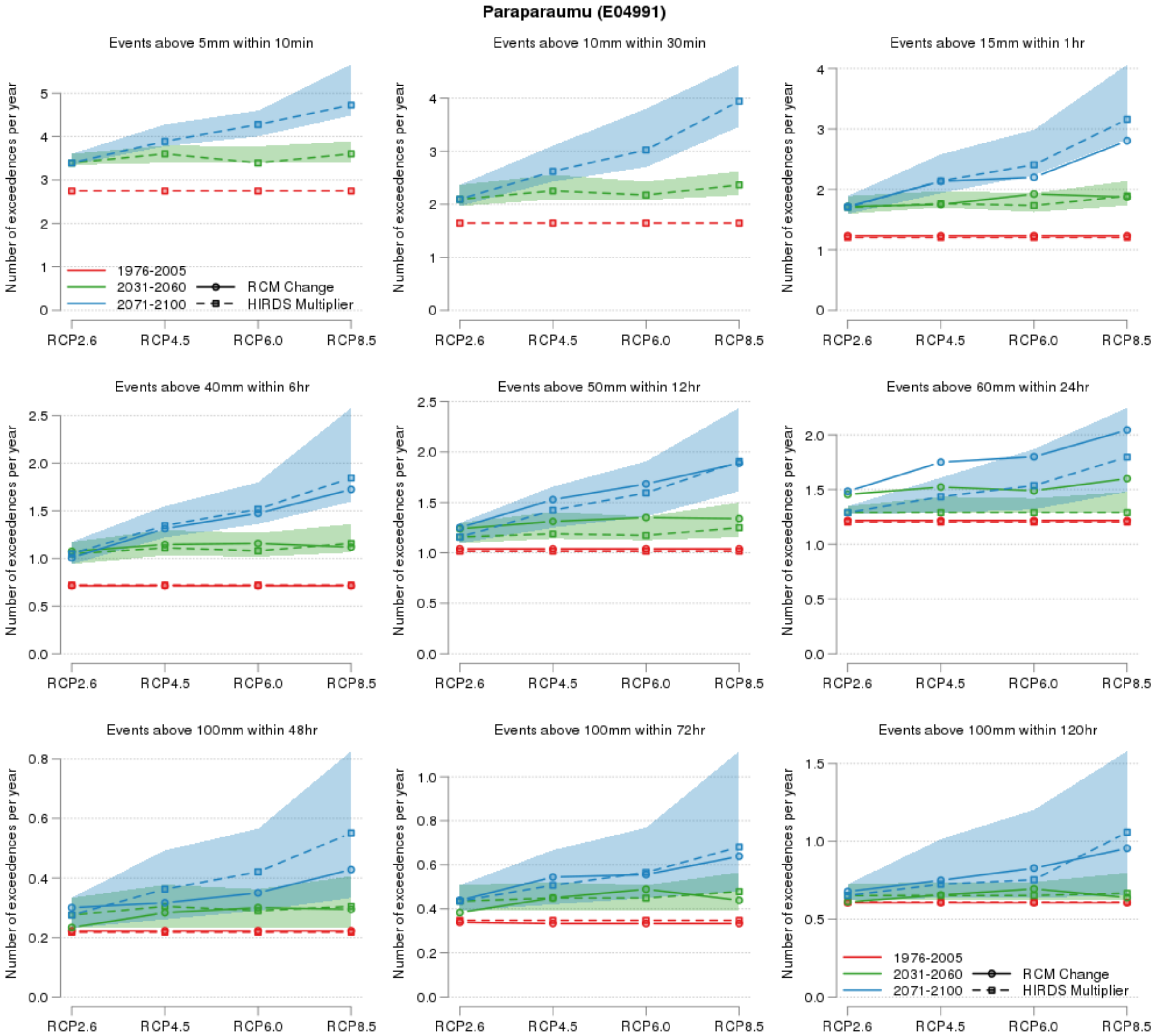

Figure 4-55: The change in rainfall exceedances with climate change for Paraparaumu. As Figure 4-53, but for Paraparaumu.

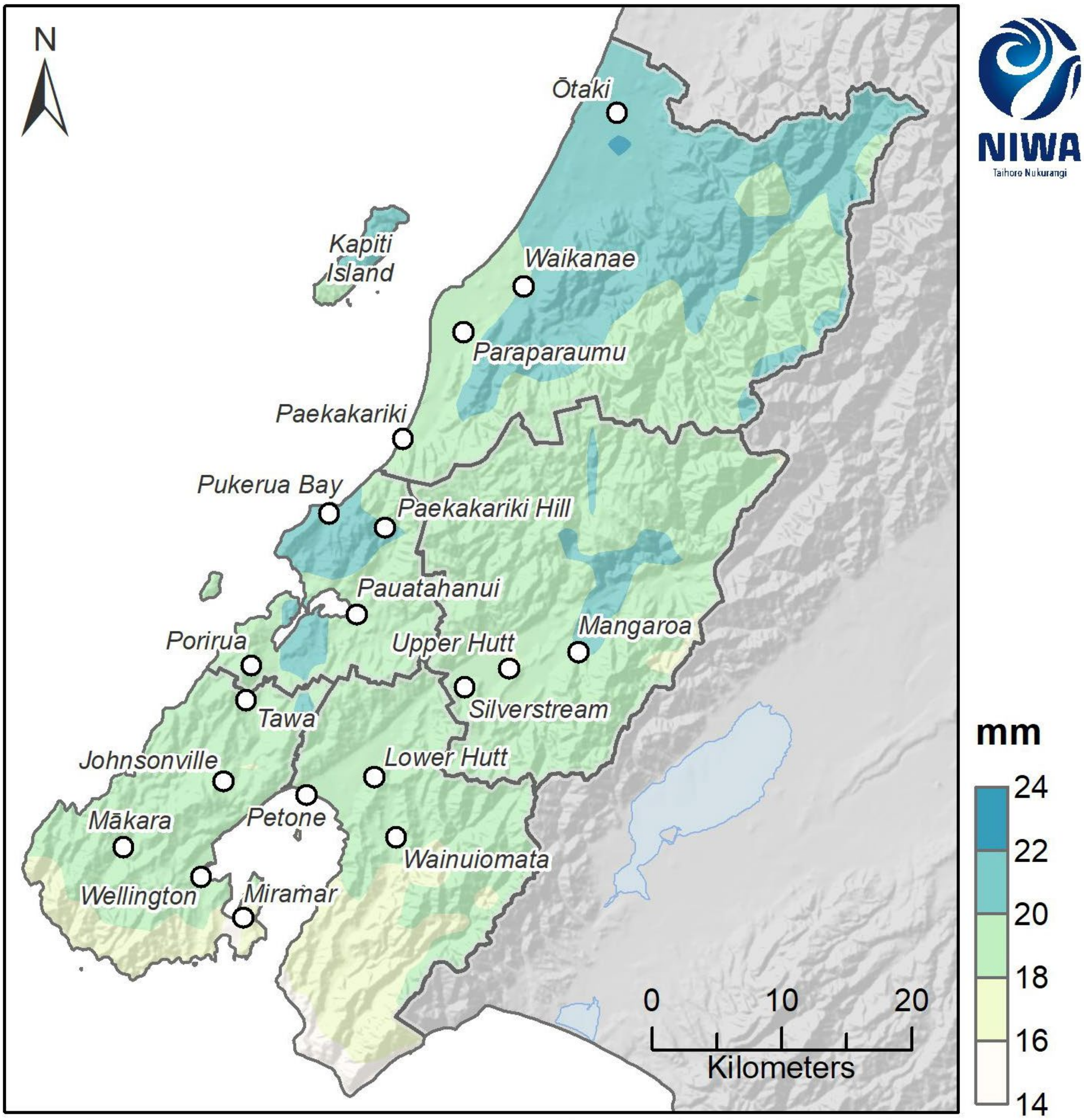

10-min duration, 100-yr recurrence interval rainfall depths

Historic rainfall depths (1853-2016)

Figure 4-56: Historic (1853-2016) 10-minute duration, 100-year magnitude rainfall depths for the area west of Wellington's ranges. Adapted from Pearce *et al.* (2019).

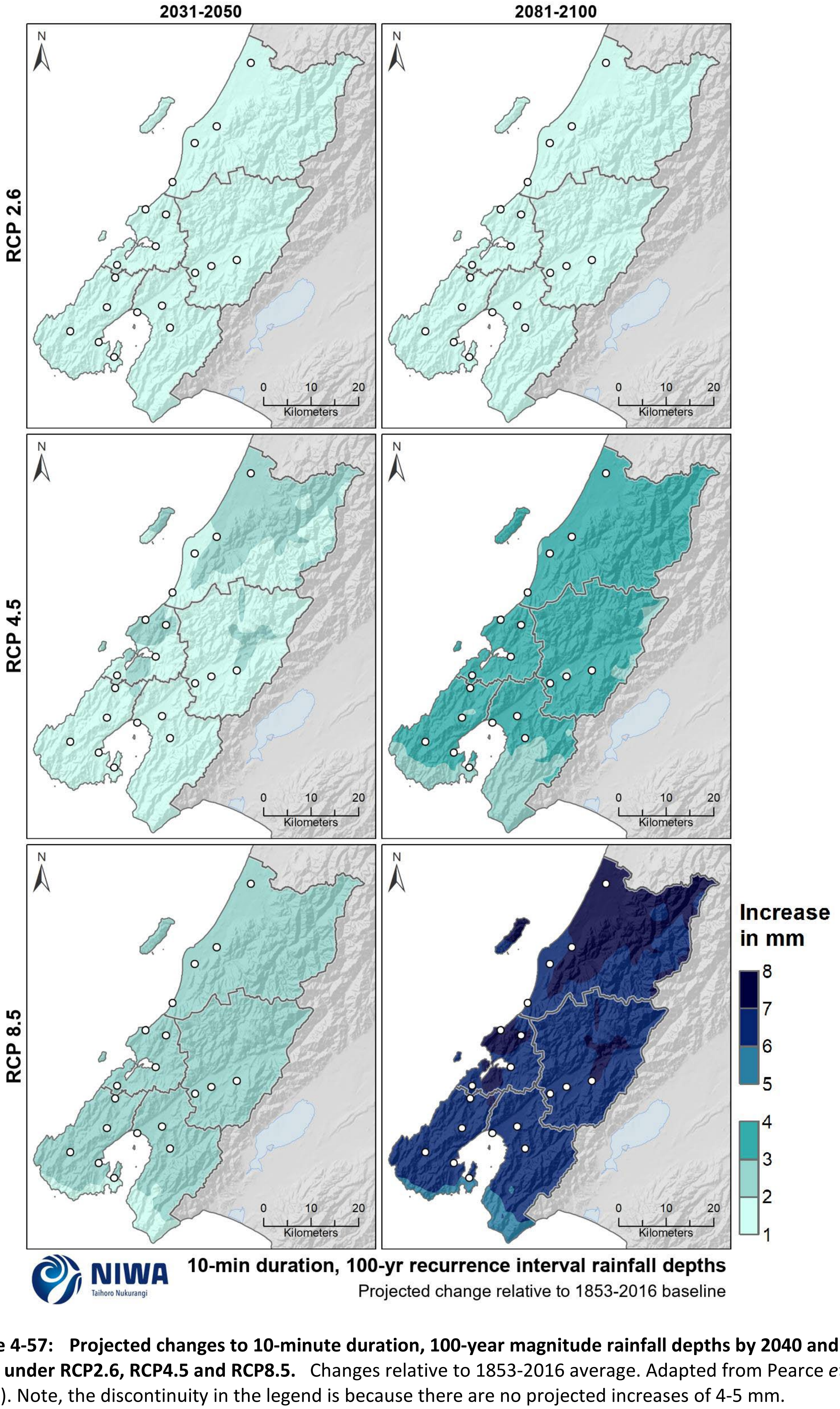

Figure 4-57: Projected changes to 10-minute duration, 100-year magnitude rainfall depths by 2040 and 2090, under RCP2.6, RCP4.5 and RCP8.5. Changes relative to 1853-2016 average. Adapted from Pearce *et al.* (2019). Note, the discontinuity in the legend is because there are no projected increases of 4-5 mm.

4.2.4 Dry spells

Projected dry spell day changes (relative to 1986-2005)

Annual:

Period	RCP2.6	RCP4.5	RCP8.5
2040	-2 to +6	+1-10	-2 to +8
2090	-2 to +8	-2 to +6	-1 to +13

The definition of a dry spell as considered here is a period of ten or more consecutive days where the daily rainfall is less than 1 mm on each day. This calculation is an aggregation of all days per year that are included in a dry spell (i.e., ≥ ten consecutive days with daily rainfall < 1 mm), no matter the length of the dry spell. Thus, a 10-day dry spell contributes 10 days, and a 13-day dry spell contributes 13 days, etc. The annual dry spell days are then averaged over the 20-year period of interest (e.g., 2031-2050), and across the six global models, to determine the ensemble-average annual dry spell day climatology (past) and future projections.

Historic (average over 1986-2005) and future (average over 2031-2050 and 2081-2100) maps for dry spell days are shown in this section. The historic maps show annual average numbers of dry spell days and the future projection maps show the change in the annual number of dry spell days compared with the historic period. Note that the historic maps are on a different colour scale to the future projection maps.

For the historic period, the annual number of dry spell days is highest for western and southwestern sections of the area about Paekakariki, Pukerua Bay and Mākara (Figure 4-58), with 30-45 dry spell days per year. For the remainder of the area, annual dry spell days range from 10-30 days in most populated areas of the area.

Representative concentration pathway (RCP) 2.6

By 2040 projected changes to dry spell days range from a decrease of up to 2 days through to an increase of up to 6 days (Figure 4-59).

By 2090, projected changes to dry spell days range from a decrease of up to 2 days through to an increase of up to 8 days (Figure 4-59). Projected increases of 2-6 days are common for the southwestern half of the area.

Representative concentration pathway (RCP) 4.5

By 2040, increases of 1-10 dry spell days are projected for the area (Figure 4-59), with highest increases of 6-10 dry spell days projected for limited areas near Wellington Harbour and Porirua.

By 2090, projected changes to dry spell days range from a decrease of 2 days to an increase of 6 days (Figure 4-59), with highest increases of 4-6 days for southern portions of the area.

Representative concentration pathway (RCP) 8.5

By 2040, projected changes to dry spell days range from a decrease of up to 2 days through to an increase of up to 8 days (Figure 4-59), with highest increases of 6-8 days about Mākara and Miramar.

By 2090, projected changes to dry spell days range from a decrease of up to 1 day through to an increase of up to 13 days (Figure 4-59). Largest increases of 8-13 dry spell days are projected for southwestern parts of the area.

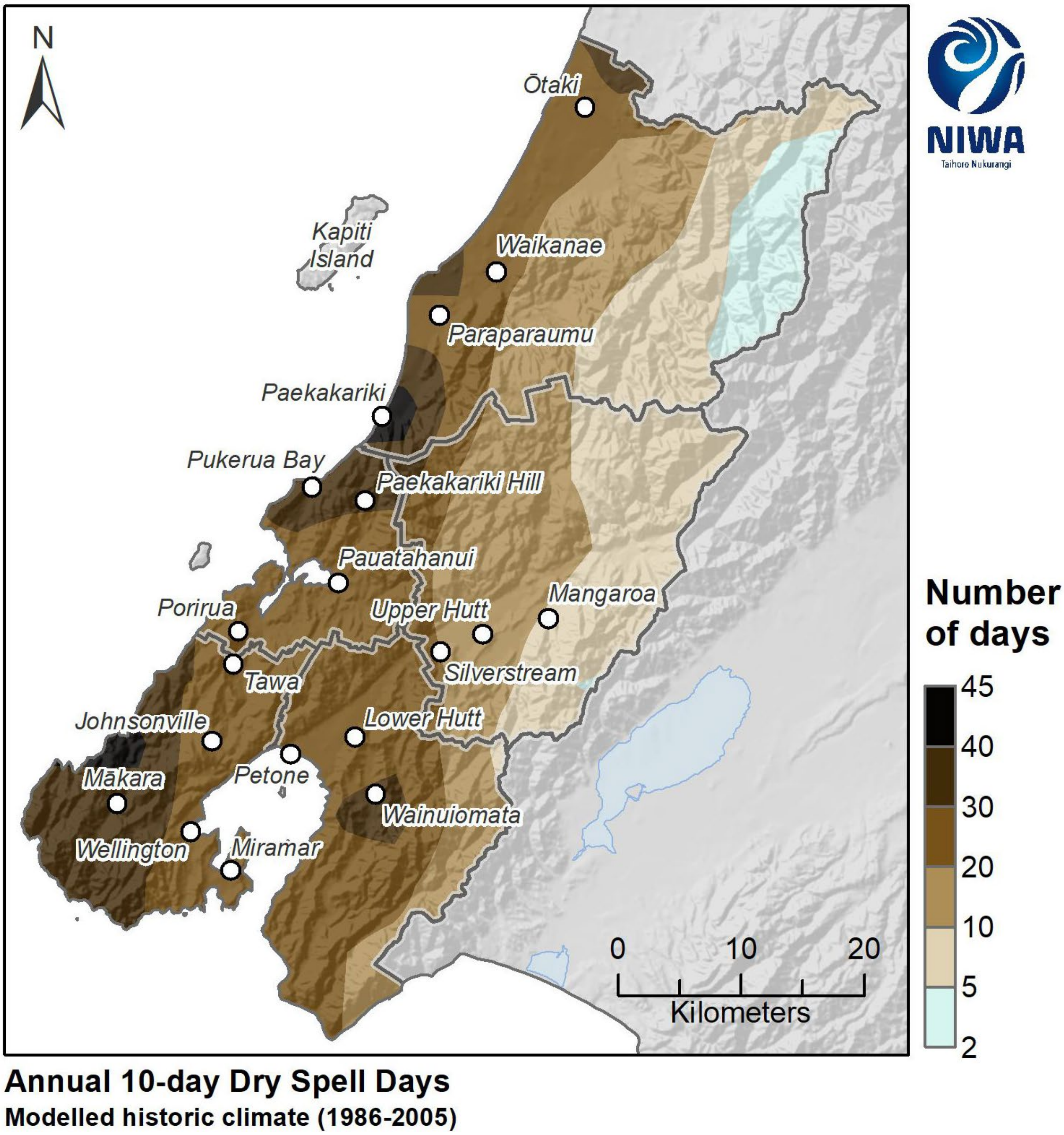

Figure 4-58: Modelled annual number of dry spell days (≥ ten consecutive days with daily rainfall < 1 mm), average over 1986-2005. Results are based on dynamical downscaled projections using NIWA's Regional Climate Model. Resolution of projection is 5km x 5km.

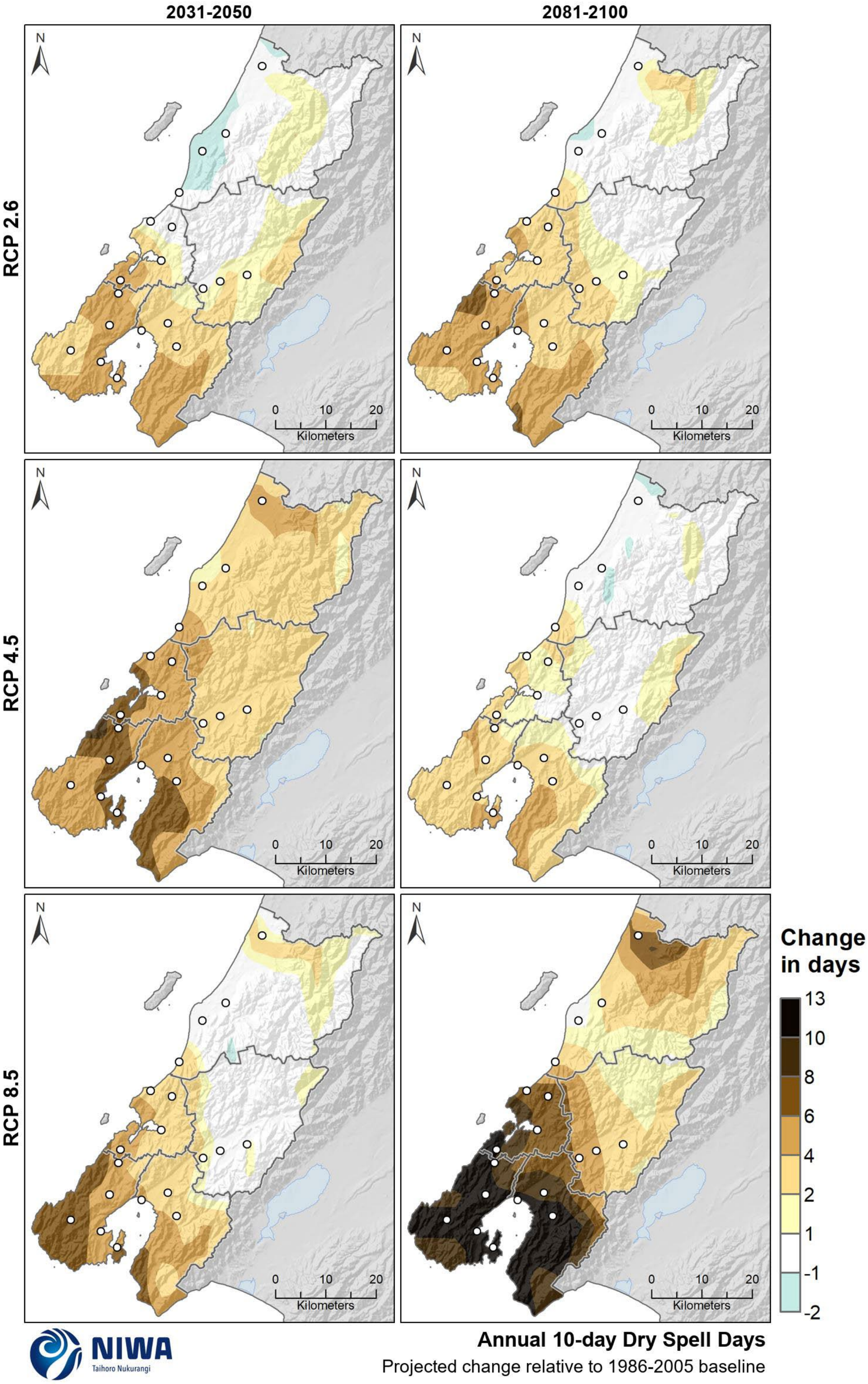

Figure 4-59: Projected annual dry spell day (≥ ten consecutive days with daily rainfall < 1 mm) changes by 2040 and 2090, under RCP2.6, RCP4.5 and RCP8.5. Changes relative to 1986-2005 average, based on the average of six global climate models. Results are based on dynamical downscaled projections using NIWA's Regional Climate Model. Resolution of projection is 5km x 5km.

4.3 Other climate variables

4.3.1 Potential evapotranspiration deficit

Projected potential evapotranspiration deficit accumulation changes (mm, relative to 1986-2005)

Annual:

Period	RCP2.6	RCP4.5	RCP8.5
2040	+10-80	+10-100	+10-120
2090	+10-80	+10-120	+10-135

One measure of meteorological drought[4] that is used in this section is 'potential evapotranspiration deficit' (PED). Evapotranspiration is the process where water held in the soil is gradually released to the atmosphere through a combination of direct evaporation and transpiration from plants. As the growing season advances, the amount of water lost from the soil through evapotranspiration typically exceeds rainfall, giving rise to an increase in soil moisture deficit. As soil moisture decreases, pasture production becomes moisture-constrained and evapotranspiration can no longer meet atmospheric demand[5].

The difference between this demand (evapotranspiration) and the actual evapotranspiration is defined as the 'potential evapotranspiration deficit' (PED). In practice, PED represents the total amount of water that needs to be replenished by irrigation, and/or rainfall, to maintain plant growth at levels unconstrained by water shortage. As such, PED estimates provide a robust measure of drought intensity and duration. Days when water demand is not met, and pasture growth is reduced, are often referred to as days of potential evapotranspiration deficit.

PED is calculated as the difference between potential evapotranspiration (PET) and rainfall, for days of soil moisture under half of available water capacity (AWC), where an AWC of 150mm for silty-loamy soils is consistent with estimates in previous studies (e.g. Mullan *et al*., 2005). PED, in units of mm, can be thought of as the amount of missing rainfall needed to keep pastures growing at optimum levels. Higher PED totals indicate drier soils. In New Zealand, an increase in PED of 30 mm or more corresponds to an extra week of reduced grass growth. Accumulations of PED greater than 300 mm indicate very dry conditions.

For the modelled historic period, the highest average PED accumulation is experienced in southwestern parts of the area from Porirua south to Miramar (150-215 mm per year). Other low elevation and western areas of the area generally experience 50-150 mm of PED per year. PED accumulation of 5-50 mm per year is modelled for the remainder of the area (Figure 4-60).

For all future scenarios, annual PED accumulation is projected to increase throughout the area (Figure 4-61). The increases are considerable relative to the historic period, even under RCP2.6. This is a similar feature of growing degree days (Section 4.1.3), highlighting the connection between both variables. The greatest increase is projected by 2090 under RCP8.5, with an increase of 100-135 mm

[4] Meteorological drought happens when dry weather patterns dominate an area and resulting rainfall is low. Hydrological drought occurs when low water supply becomes evident, especially in streams, reservoirs, and groundwater levels, usually after an extended period of meteorological drought.
[5] Atmospheric demand is the maximum evapotranspiration value, which depends on ambient atmospheric conditions, and assumes unlimited moisture availability.

PED accumulation in many southern portions of the area. For coastal areas north of Pauatahanui, an increase of 60-80 mm PED accumulation is projected by 2040 and 2090 under RCP4.5. For locations such as Wellington city, Johnsonville and Porirua, the projected increase in PED by 2090 under RCP8.5 would result in accumulated PED totals of approximately 250-335 mm per year. Such totals are equivalent to the historic annual average PED totals for the driest parts of the Wairarapa near Martinborough (Macara *et al.*, 2021).

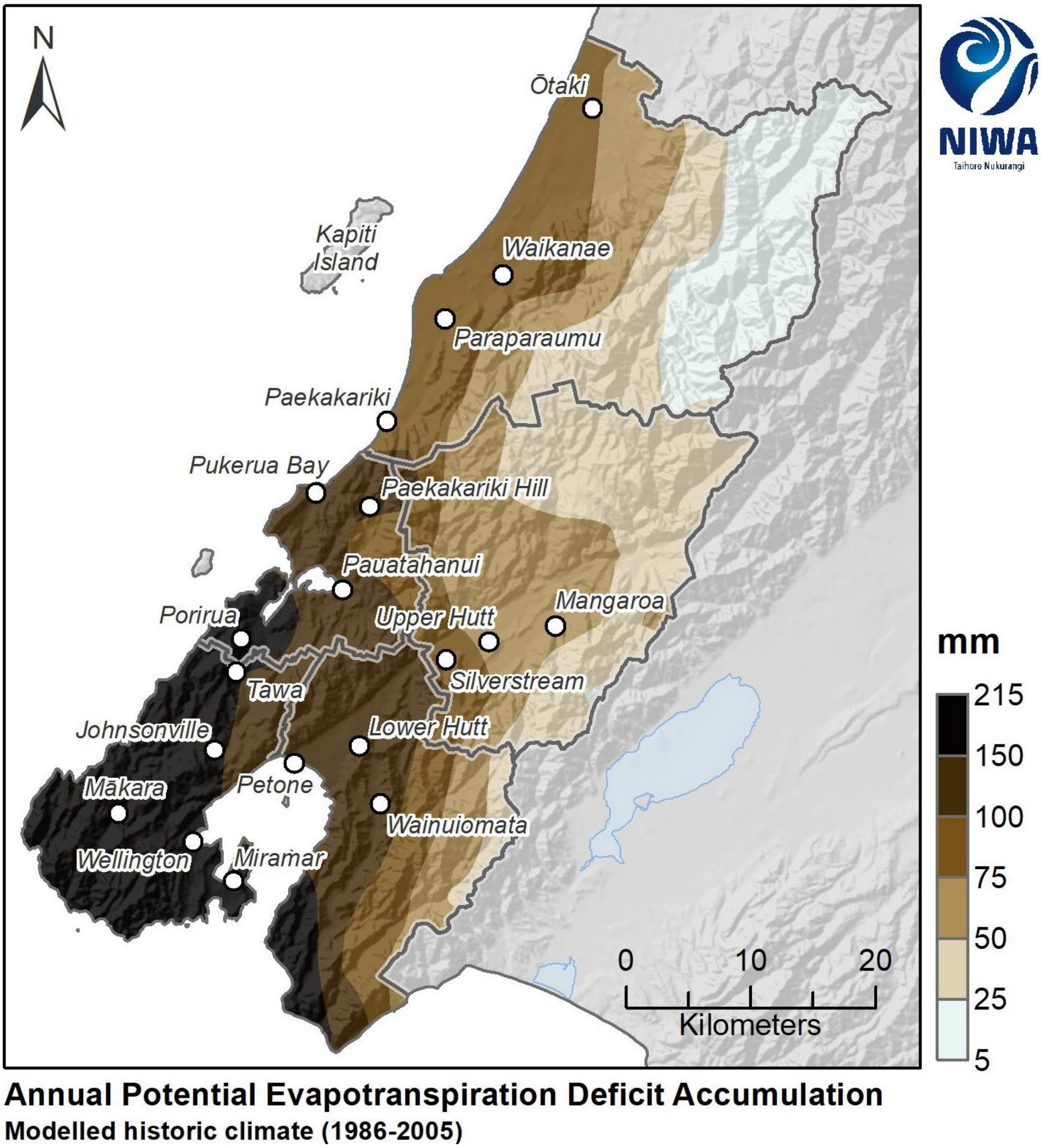

Figure 4-60: Modelled annual potential evapotranspiration deficit accumulation (mm), average over 1986-2005. Results are based on dynamical downscaled projections using NIWA's Regional Climate Model. Resolution of projection is 5km x 5km.

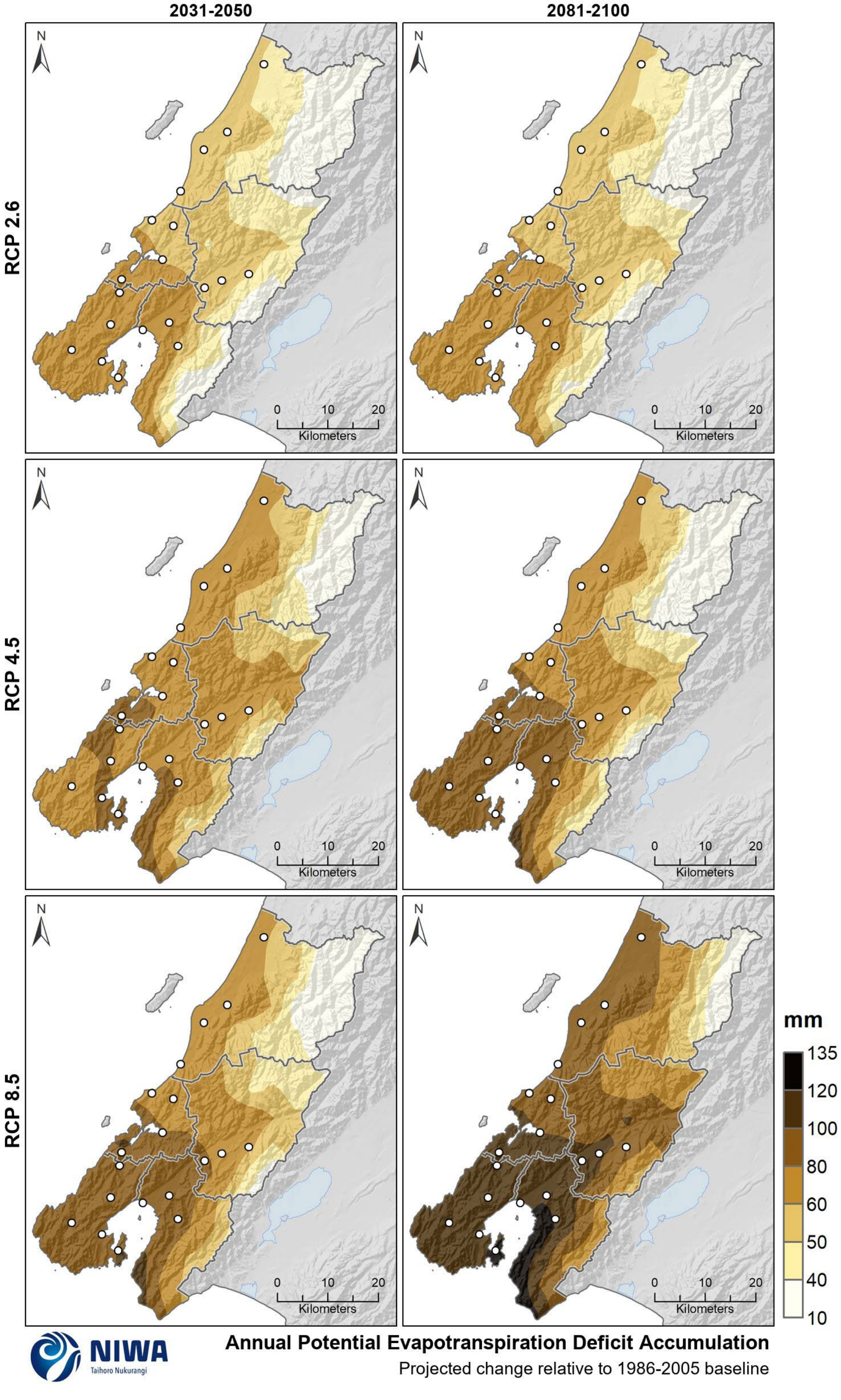

Figure 4-61: Projected annual potential evapotranspiration deficit accumulation (mm) changes by 2040 and 2090 under RCP2.6, RCP4.5 and RCP8.5. Relative to 1986-2005 average, based on the average of six global climate models. Results are based on dynamical downscaled projections using NIWA's Regional Climate Model. Resolution of projection is 5km x 5km.

4.3.2 Windy days

Projected windy day changes (relative to 1986-2005)

Annual:

Period	RCP2.6	RCP4.5	RCP8.5
2040	-1 to +4	-1 to +5	-1 to +5
2090	-1 to +4	-1 to +6	+2-11

A ‘windy day’ is considered here to have a daily mean wind speed of 10 m/s (36 km/h) or more. Future change (average over 2031-2050 and 2081-2100) maps for the annual number of windy days are shown in this section. Note that the historic map is not provided for mean wind speed as these data have not been bias-corrected, and therefore do not provide a reliable representation of the observed magnitude of this variable. In particular, the high wind speeds around the peaks in the mountain ranges are poorly captured in the low-resolution climate model. Because projected changes in windy days depend on exceedance of an absolute 10 m/s threshold, the projections should be considered indicative of future changes rather than as specific quantitative predictions.

Representative concentration pathway (RCP) 2.6

By 2040, projected changes to windy days range from a decrease of up to 1 day to an increase of up to 4 days (Figure 4-62). Projected decreases are limited to the northeast of the area, with greatest increases of 3-4 windy days projected for southern portions about Mākara east to Wainuiomata.

By 2090, projected changes to windy days range from a decrease of up to 1 day to an increase of up to 4 days (Figure 4-62). Greatest increases of 3-4 windy days are projected for southern portions near Wellington Harbour.

Representative concentration pathway (RCP) 4.5

By 2040, projected changes to windy days range from a decrease of up to 1 day to an increase of up to 5 days (Figure 4-62). Projected increases are progressively larger towards the south of the area. Increases of 3-4 windy days are projected for areas north of Wellington City, and south of Paekakariki.

By 2090, projected changes to windy days range from a decrease of up to 1 day to an increase of up to 6 days (Figure 4-62). Projected decreases are limited to the far northeast of the area. Increases of 5-6 windy days are projected for small portions about Wellington City and the Remutaka Range.

Representative concentration pathway (RCP) 8.5

By 2040, projected changes to windy days range from a decrease of up to 1 day to an increase of up to 5 days (Figure 4-62), with highest increases of 4-5 days for southern parts of the area.

By 2090, windy days are projected to increase by 2-11 days throughout the area (Figure 4-62). Highest increases of 8-11 days are projected for southern parts of the area, including the Hutt Valley. Increases of 6-8 days projected from Tawa north to Paekakariki, with projected increases of 3-4 days about Ōtaki.

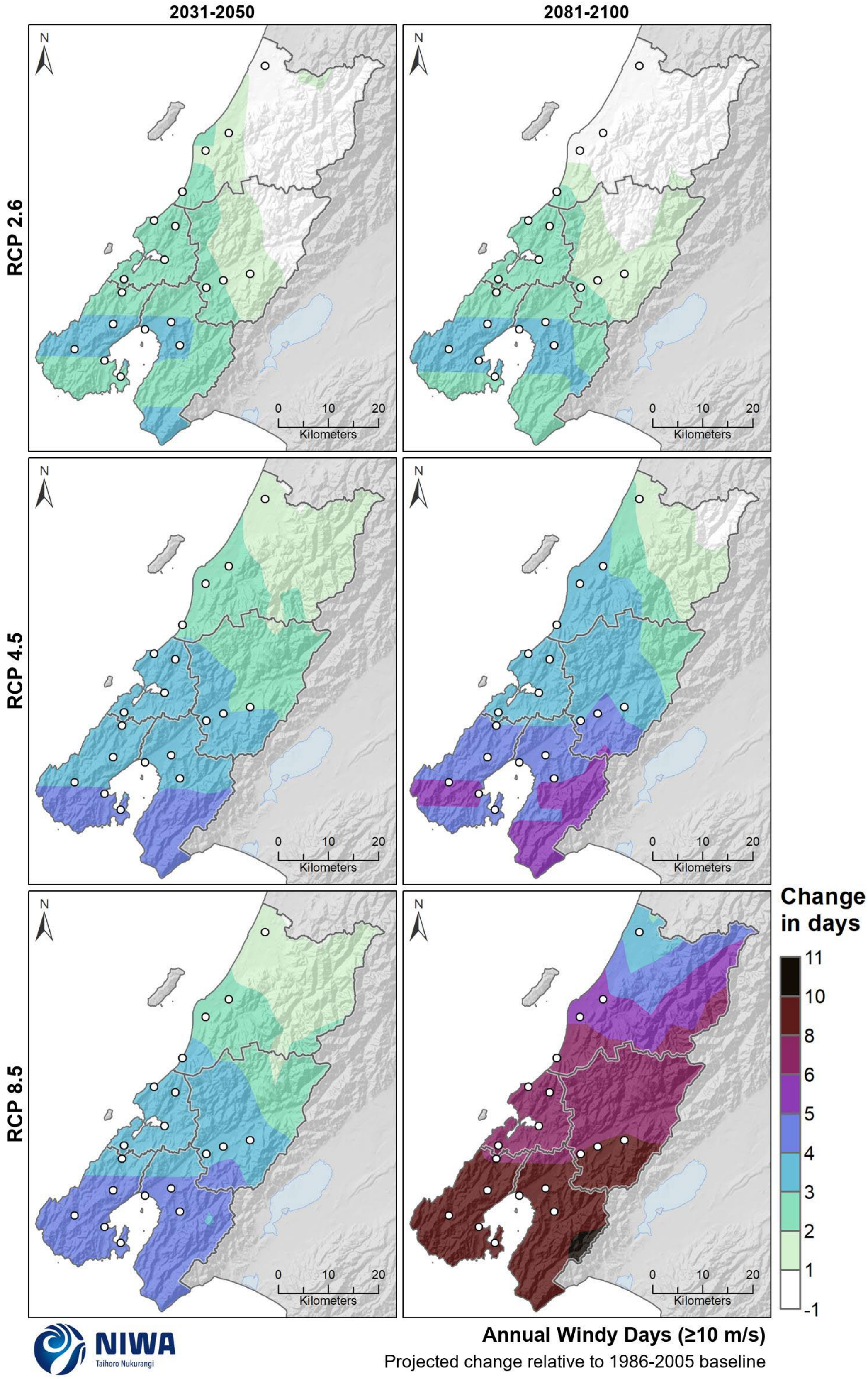

Figure 4-62: Projected change in the annual number of windy days (>10 m/s) by 2040 and 2090, under RCP2.6, RCP4.5 and RCP8.5. Relative to 1986-2005 average, based on the average of six global climate models. Results are based on dynamical downscaled projections using NIWA's Regional Climate Model. Resolution of projection is 5km x 5km.

5 Summary and conclusions

This report presents climate change projections for the area west of Wellington's Tararua and Remutaka Ranges. Historic climatic conditions are presented to provide a context for future changes. The future changes discussed in this report consider differences between the historical period 1986-2005 and two future time-slices, 2031-2050, "2040", and 2081-2100, "2090".

Changes to the future climate of the area are likely to be considerable, but typically less pronounced than the Wairarapa (Pearce *et al.*, 2017). The main projected changes comprise increases in heavy rainfall events, drought potential, dry spell days, hot days, and windy days, with considerable increases to GDD and PED due to higher temperatures. The following list summarises the projections of different climate variables in the area:

- Heavy rainfall events (as indicated by the 99th-percentile of daily rainfall totals) are generally projected to become more severe. By 2040, the magnitude of heavy rainfall events is projected to change by -1% to +12% (RCP8.5). By 2090, heavy rainfall event increases of 1-12% (RCP2.6) or 2-30% (RCP8.5) are projected.

- Rarer extreme rainfall events such as one-in-one-hundred year events are also expected to increase in both frequency (between two-fold and three fold increases for various durations) and magnitude (up to 40% increase), which may increase the chance of flooding.

- Drought potential is projected to increase across the area, with annual accumulated Potential Evapotranspiration Deficit (PED) totals increasing with time and greenhouse gas concentrations. By 2040, PED totals are projected to increase by 10-120 mm (RCP8.5). By 2090, PED totals are projected to increase by 10-80 mm (RCP2.6) or 10-135 mm (RCP8.5). These upper-range increases would see areas around Wellington city, Johnsonville and Porirua observing PED totals comparable to the contemporary climate of the driest parts of the Wairarapa.

- Projected changes in dry spell days (≥10 consecutive days of daily rainfall <1 mm) show variability across the area. By 2040, projected dry spell day changes for some areas range from -2 days (RCP2.6) to +10 days (RCP4.5). By 2090, projected annual dry spell day changes for parts of the area range from -2 days (RCP2.6 and RCP4.5) to +13 days (RCP8.5).

- The average number of windy days (daily mean wind speed ≥10 m/s) is typically expected to increase with time and greenhouse gas concentrations. The exception is northeastern parts of the area under RCP2.6, where little change (±1 day per year) is projected. Overall, up to 5 additional windy days are projected by 2040 (RCP8.5), with increases of up to 4 (RCP2.6) or 2-11 (RCP8.5) windy days by 2090.

- Annual average maximum temperatures are projected to increase by 0.75-1.25°C by 2040 under RCP8.5. By 2090, maximum temperatures are projected to increase by 0.50-1.00°C (RCP2.6) or 2.50-3.25°C (RCP8.5).

- Increasing maximum temperatures will result in more hot days (daily maximum air temperature ≥25°C), although extreme hot days (daily maximum air temperature >30°C) are expected to remain an uncommon occurrence for many parts of the area. By 2040, up to 10 more annual hot days are projected (RCP8.5), with up to 10 (RCP2.6) or 5-50 (RCP8.5) more annual hot days by 2090. By 2090, extreme hot days are projected to increase by up to 0.5 days (RCP2.6) or up to 5 days (RCP8.5).

- Projected increases to hot days result in additional heatwave days (≥3 days where daily maximum air temperature >25°C). By 2040, the number of annual heatwave days are projected to increase by up to 10 days (RCP8.5). By 2090, heatwave days are projected to increase by up to 5 days (RCP2.6) or up to 35 days (RCP8.5).
- Increasing maximum temperatures will result in fewer cold days (daily maximum air temperature <10°C). By 2040, the number of annual cold days are projected to decrease by 2-30 days (RCP8.5). By 2090, cold days are projected to decrease by 2-20 days (RCP2.6) or 5-85 days (RCP8.5).
- Annual average minimum temperatures are projected to increase by 0.50-0.75°C by 2040 under RCP8.5. By 2090, minimum temperatures are projected to increase by 0.25-0.75°C (RCP2.6) or 1.75-2.50°C (RCP8.5).
- Increasing minimum temperatures will result in fewer frost days (daily minimum air temperature ≤0°C). By 2040, up to 10 fewer annual frost days are projected (RCP8.5), with up to 10 (RCP2.6) or 30 (RCP8.5) fewer annual frost days by 2090.
- Increasing minimum temperatures will result in more warm nights (daily minimum air temperature >15°C). By 2040, up to 15 more annual warm nights are projected (RCP8.5), with up to 15 (RCP2.6) or 1-55 (RCP8.5) more annual warm nights by 2090.
- Annual average growing degree days (GDD) are projected to increase by 150-300 GDD by 2040 under RCP8.5. By 2090, growing degree days are projected to increase by 85-200 GDD (RCP2.6) or 500-850 GDD (RCP8.5). These upper-range increases would see some parts observing GDD totals comparable to those observed historically (1981-2010) in Auckland and low elevations of Northland.
- Projected changes in rainfall show variability across the area. By 2040, projected annual rainfall changes for some areas range from -2% (RCP4.5 and RCP8.5) to +8% (RCP2.6 and RCP4.5). By 2090, annual rainfall changes in parts of the area range from -8% to +12% (RCP8.5), with changes of up to +4% projected under RCP2.6. Larger and more extensive changes to rainfall are projected at the seasonal scale. By 2090, summer, autumn projected changes range from -8% to +12% (RCP8.5).
- Annual wet days (daily rainfall ≥1 mm) are mostly projected to decrease under all RCPs, with small increases projected for some parts of the area. By 2040, the number of annual wet days are projected to change by +1 to -8 days (RCP8.5). By 2090, wet day changes of +1 to -4 days (RCP2.6) or 2-21 fewer days (RCP8.5) are projected.

5.1 Recommendations for future work

This report provides the most comprehensive and up-to-date climate change projections for west of Wellington’s Tararua and Remutaka Ranges currently available. However, there are areas that were out of scope for this report, or where there is currently no New Zealand-specific information available, which may be considerations for future work. Some of these are indicated below:

- Projections of changes to large floods (magnitude and frequency) are not currently available, but investigations into how large floods may change in the future are the subject of a 5-year research programme led by NIWA. It is anticipated that data will likely become available for use by councils at the completion of this programme in 2025.
- A detailed analysis of wildfire risk in the context of projected climate change was beyond the scope of this report and there is much potential for future research on this front. One possibility for such work could be to analyse and map future areas of high fire risk by combining projected climate data such as temperature, precipitation, and wind with relevant fire risk factors such as vegetation type and flammability. Such work would likely require a collaborative research effort between NIWA and an institute specialised in wildfire research such as Scion.
- What are the potential changes to crop suitability with climate change and associated water needs, when the projected growing degree days and potential evapotranspiration deficit changes are taken into consideration. Modelling specific to west of Wellington's ranges could be carried out as this has been done for other parts of New Zealand for a range of crop types (e.g. Ausseil *et al*., 2019; Teixeira *et al*., 2020)[6].
- Prepare an update of the projections based on the IPCC AR6 climate models, which are expected to be available (downscaled for New Zealand) in 2024.

[6] For additional information about this work, refer to the "Climate change & its effect on our agricultural land" project at: https://deepsouthchallenge.co.nz/research-project/climate-change-its-effect-on-our-agricultural-land/

6 Acknowledgements

Olaf Morgenstern and Jonny Williams (both NIWA) are thanked for their contributions to the CMIP6 climate modelling section. Trevor Carey-Smith is thanked for his contribution to the section on changes already observed in extreme rainfall events. Tristan Meyers is thanked for providing an updated figure of rainfall anomalies observed during ENSO summers. Dr. Alex Pezza and other Greater Wellington Regional Council staff are thanked for their valuable reviews and feedback on draft versions of this report, and accompanying video material. Dr. Alex Pezza would like to acknowledge Gregor Macara and the NIWA team for their significant effort with this report and the spirit of collaboration in which this final version was possible after several rounds of revisions.

7 Glossary of abbreviations and terms

AR6	Sixth assessment report
avg	average
AWC	Available water capacity
CMIP5	Fifth Coupled Model Inter-comparison Project
CMIP6	Sixth Coupled Model Inter-comparison Project
ENSO	El Niño-Southern Oscillation
GCM	General circulation model
GDD	Growing degree days
GIS	Geographic Information System
GWRC	Greater Wellington Regional Council
IPCC	Intergovernmental Panel on Climate Change
IPO	Interdecadal Pacific Oscillation
km	kilometre
m/s	metres per second
mm	millimetres
NIWA	National Institute of Water and Atmospheric Research
PED	Potential Evapotranspiration Deficit
PET	Potential evapotranspiration
RCM	Regional climate modelling
RCP	Representative Concentration Pathway
SAM	Southern Annular Mode
SST	Sea surface temperature
VCSN	Virtual Climate Station Network

8 References

Arias, P.A., Bellouin, N., Coppola, E. , Jones, R.G., Krinner, G., Marotzke, J., Naik, V., Palmer, M.D., Plattner, G.-K., Rogelj, J., Rojas, M., Sillmann, J., Storelvmo, T., Thorne, P.W., Trewin, B., Achuta Rao, K., Adhikary, B., Allan, R.P., Armour, K., Bala, G., Barimalala, R., Berger, S., Canadell, J.G., Cassou, C., Cherchi, A., Collins, W., Collins, W.D., Connors, S.L., Corti, S., Cruz, F., Dentener, F.J., Dereczynski, C., Di Luca, A., Diongue Niang, A., Doblas-Reyes, F.J., Dosio, A., Douville, H., Engelbrecht, F., Eyring, V., Fischer, E., Forster, P., Fox-Kemper, B., Fuglestvedt, J.S., Fyfe, J.C., Gillett, N.P., Goldfarb, L., Gorodetskaya, I., Gutierrez, J.M., Hamdi, R., Hawkins, E., Hewitt, H.T., Hope, P., Islam, A.S., Jones, C. Kaufman, D.S., Kopp, R.E., Kosaka, Y., Kossin, J., Krakovska, S., Lee, J.-Y., Li, J., Mauritsen, T., Maycock, T.K., Meinshausen, M., Min, S.-K., Monteiro, P.M.S., Ngo-Duc, T., Otto, F., Pinto, I., Pirani, A., Raghavan, K., Ranasinghe, R., Ruane, A.C., Ruiz, L., Sallée, J.-B., Samset, B.H., Sathyendranath, S., Seneviratne, S.I., Sörensson, A.A., Szopa, S., Takayabu, I., Tréguier, A.-M., van den Hurk, B., Vautard, R., von Schuckmann, K., Zaehle, S., Zhang, X., Zickfeld, K. (2021) Technical Summary. In Climate Change 2021: The Physical Science Basis. Contribution of Working Group I to the Sixth Assessment Report of the Intergovernmental Panel on Climate Change [Masson-Delmotte, V., Zhai, P., Pirani, A., Connors, S.L., Péan, C., Berger, S., Caud, N., Chen, Y., Goldfarb, L., Gomis, M.I., Huang, M., Leitzell, K., Lonnoy, E., Matthews, J.B.R., Maycock, T.K., Waterfield, T., Yelekçi, O., Yu, R., Zhou, B. (eds.)]. Cambridge University Press, Cambridge, United Kingdom and New York, NY, USA, pp. 33−144. doi:10.1017/9781009157896.002.

Ausseil., A.G., Van Der Weerden, T., Beare, M., Teixeira, E., Baisden, T., Lieffering, M., Guo, J., Keller, L., Law, R., Noble, A. (2019) Climate change impacts on land use suitability. Prepared for the Deep South and Our Land and Water National Science Challenges. *Manaaki Whenua Contract Report*, LC3573. Lincoln, New Zealand: Manaaki Whenua.

Bjordal, J., Storelvmo, T., Alterskjær, K., Carlsen, T. (2020) Equilibrium climate sensitivity above 5°C plausible due to state-dependent cloud feedback. *Nature Geoscience*, 13: 718-721.

Bodeker, G., Cullen, N., Katurji, M., McDonald, A., Morgenstern, O., Noone, D., Renwick, J., Revell, L., Tait, A. (2022) Aotearoa New Zealand climate change projections guidance: Interpreting the latest IPCC WG1 report findings. Prepared for the Ministry for the Environment, Report number CR 501, 51p.

Carey-Smith, T., Henderson, R., Singh, S. (2018) High Intensity Rainfall Design System Version 4. *NIWA Client Report* 2018022CH.

Dean, S., Rosier, S., Carey-Smith, T., Stott, P.A. (2013) The role of climate change in the two-day extreme rainfall in Golden Bay, New Zealand, December 2011. *Bulletin of the American Meteorological Society,* 94: 561-563.

Eyring, V., Bony, S., Meehl, G.A., Senior, C.A., Stevens, B., Stouffer, R.J., Taylor, K.E. (2016) Overview of the Coupled Model Intercomparison Project Phase 6 (CMIP6) experimental design and organization. *Geoscientific Model Development,* 9: 1937-1958.

Fan, X., Miao, C., Duan, Q., Shen, C., Wu, Y. (2020) The Performance of CMIP6 Versus CMIP5 in Simulating Temperature Extremes Over the Global Land Surface. *Journal of Geophysical Research: Atmospheres*, 125. https://doi.org/10.1029/2020JD033031

Frame, D., Joshi, M., Hawkins, E., Harrington, L.J., de Roiste, M. (2017) Population-based emergence of unfamiliar climates. *Nature Climate Change*, 7:407-411.

Gusain, A., Ghosh, S., Karmakar, S. (2020) Added value of CMIP6 over CMIP5 models in simulating Indian summer monsoon rainfall. *Atmospheric Research*, 232. https://doi.org/10.1016/j.atmosres.2019.104680.

Hausfather, Z. (2019) CMIP6: the next generation of climate models explained. *CarbonBrief*. Accessed on 30/4/2021 from: https://www.carbonbrief.org/cmip6-the-next-generation-of-climate-models-explained

Hausfather, Z., Peters, G.P. (2020) Emissions – the 'business as usual' story is misleading. *Nature*, 577: 618-620.

Hawkins, E., Sutton, R. (2012) Time of emergence of climate signals. *Geophysical Research Letters*, 39. https://doi.org/10.1029/2011GL050087

Hawkins, E., Frame, D., Harrington, L., Joshi, M., King, A., Rojas, M., Sutton, R. (2020) Observed emergence of the climate change signal: From the familiar to the unknown. *Geophysical Research Letters*, 47, https://doi.org/10.1029/2019GL086259

IPCC (ed.) (2013) Climate Change 2013: The Physical Science Basis. *Contribution of Working Group I to the Fifth Assessment Report of the Intergovernmental Panel on Climate Change,* Cambridge, United Kingdom and New York, NY, USA: Cambridge University Press.

IPCC (ed.) (2014a) Climate Change 2014: Impacts, Adaptation, and Vulnerability. Part A: Global and Sectoral Aspects. *Contribution of Working Group II to the Fifth Assessment Report of the Intergovernmental Panel on Climate Change*, Cambridge, United Kingdom and New York, USA: Cambridge University Press.

IPCC (ed.) (2014b) Climate Change 2014: Impacts, Adaptation, and Vulnerability. Part B: Regional Aspects. *Contribution of Working Group II to the Fifth Assessment Report of the Intergovernmental Panel on Climate Change*, Cambridge, United Kingdom and New York, USA: Cambridge University Press.

IPCC (2014c) Climate change 2014: Mitigation of climate change. Contribution of Working Group III to the Fifth Assessment Report of the Intergovernmental Panel on Climate Change. In: Edenhofer, O., Pichs-Madruga, R., Sokona, Y., Farahani, E., Kadner, S., Seyboth, K., Adler, A., Baum, I., Brunner, S., Eickemeier, P., Kriemann, B., Savolainen, J., Schlömer, S., Von Stechow, C., Zwickel, T., Minx, J.C. (eds.). Cambridge University Press.

IPCC (2018) Global warming of 1.5C: An IPCC Special Report on the impacts of global warming of 1.5C above pre-industrial levels and related global greenhouse gas emission pathways, in the context of strengthening the global response to the threat of climate change, sustainable development, and efforts to eradicate poverty, Accessed on 8/10/2018 from http://ipcc.ch.

IPCC (2021) Summary for Policymakers. In: *Climate Change 2021: The Physical Science Basis. Contribution of Woking Group I to the Sixth Assessment Report of the Intergovernmental Panel on Climate Change* [Masson-Delmotte, V., Zhai, P., Pirani, A., Connors, S.L., Péan, C., Berger, S., Caud, N., Chen, Y., Goldfarb, L., Gomis, M.I., Huang, M., Leitzell, K., Lonnoy, E., Matthews, J.B.R., Maycock, T.K., Waterfield, T., Yelekçi, O., Yu, R., Zhou, B. (eds.)]. Cambridge University Press, Cambridge, United Kingdom and New York, NY, USA, pp. 3−32, doi:10.1017/9781009157896.001

IPCC (2022) AR6 Synthesis Report: Climate Change 2022. https://www.ipcc.ch/report/sixth-assessment-report-cycle/ Date accessed: 1 June 2022.

Kidson, J.W. (2000) An analysis of New Zealand synoptic types and their use in defining weather regimes. *International Journal of Climatology,* 20: 299-316.

Lawrence, J., Mackey, B., Chiew, F., Costello, M.J., Hennessy, K., Lansbury, N., Nidumolu, U.B., Pecl, G., Rickards, L., Tapper, N., Woodward, A., Wreford, A. (2022) *Australasia*. In: *Climate Change 2022: Impacts, Adaptation, and Vulnerability*. Contribution of Working Group II to the Sixth Assessment Report of the Intergovernmental Panel on Climate Change [Pörtner, H.-O., Roberts, D.C., Tignor, M., Poloczanska, E.S., Mintenbeck, K., Alegria, A., Craig, M., Langsdorf, S., Löschke, S., Möller, V., Okem, A., Rama, B. (eds)]. Cambridge University Press. In Press.

Macara, G.R. (2018) The climate and weather of New Zealand. NIWA Science and Technology Series, 74: 50.

Macara, G., Woolley, J.-M., Sood, A., Stuart, S. (2021) Climate change projections for the Wairarapa. Prepared for Greater Wellington Regional Council. *NIWA Client Report* 2021136WN, 124p.

McDonough, W. (2016) Carbon is not the enemy. *Nature*, 539: 349-351.

Meehl, G.A., Senior, C.A., Eyring, V., Flato, G., Lamarque, J.-F., Stouffer, R.J., Taylor, K.E., Schlund, M. (2020) Context for interpreting equilibrium climate sensitivity and transient climate response from the CMIP6 Earth system models. *Science Advances*, 6. DOI: 10.1126/sciadv.aba1981

Ministry for The Environment (2008) Climate Change Effects and Impacts Assessment. A Guidance Manual for Local Government in New Zealand. *In:* Mullan, B., Wratt, D., Dean, S., Hollis, M., Allan, S., Williams, T., Kenny, G., MFE (eds.) Wellington: Ministry for the Environment.

Ministry for the Environment (2017) Coastal hazards and climate change: Guidance for local government. Lead authors: Bell, R., Lawrence, J., Allan, S., Blackett, P., Stephens, S. Ministry for the Environment Publication ME-1292. Accessed at: http://www.mfe.govt.nz/publications/climate-change/preparing-coastal-change-summary-of-coastal-hazards-and-climate-change.

Ministry for the Environment (2018) Climate change projections for New Zealand: atmospheric projections based on simulations undertaken for the IPCC 5th Assessment, 2nd edition. Accessed at: https://www.mfe.govt.nz/node/21990.

Ministry for the Environment (2020) National Climate Change Risk Assessment for New Zealand – Arotakenga Tūraru mō te Huringa Āhuarangi o Āotearoa: Technical report – Pūrongo whaihanga. Wellington: Ministry for the Environment.

Ministry for the Environment & Stats NZ (2019) *New Zealand's Environmental Reporting Series: Our marine environment 2019.* Available from www.mfe.govt.nz and www.stats.govt.nz

Ministry for the Environment & Stats NZ (2020) *New Zealand's Environmental Reporting Series: Our atmosphere and climate 2020.* Available from www.mfe.govt.nz and www.stats.govt.nz

Mullan, A.B., Porteous, A., Wratt, D., Hollis, M. (2005) Changes in drought risk with climate change. *NIWA Client Report* WLG2005-23 for Ministry for the Environment and Ministry of Agriculture and Fisheries, Wellington.

Mullan, A.B., Stuart, S., Hadfield, M.G., Smith, M.J. (2010) Report on the Review of NIWA's 'Seven-Station' Temperature Series, NIWA Information Series No. 78: 175. Accessed at: https://www.niwa.co.nz/sites/niwa.co.nz/files/import/attachments/Report-on-the-Review-of-NIWAas-Seven-Station-Temperature-Series_v3.pdf.

NOAA (2022) Global Monitoring Laboratory. *Trends in Atmospheric Carbon Dioxide*. Accessed from https://gml.noaa.gov/ccgg/trends/global.html Date accessed: 23 March 2022.

Pearce, P., Fedaeff, N., Mullan, B., Sood, A., Bell, R., Tait, A., Collins, D., Zammit, C. (2017) Climate Change and variability – Wellington Region. Prepared by the National Institute of Water and Atmospheric Research, NIWA, for Greater Wellington Regional Council, *NIWA Client Report* 2017066AK.

Pearce, P., Fedaeff, N., Mullan, B., Rosier, S., Carey-Smith, T., Sood, A. (2019) Wellington Region climate change extremes and implications. Prepared by the National Institute of Water and Atmospheric Research, NIWA, for Greater Wellington Regional Council, *NIWA Client Report* 2019134AK.

Renwick, J.A., Thompson, D. (2006) The Southern Annular Mode and New Zealand climate. *Water & Atmosphere,* 14: 24-25.

Rosier, S., Dean, S., Stuart, S., Carey-Smith, T., Black, M.T., Massey, N. (2015) Extreme Rainfall in Early July 2014 in Northland, New Zealand – Was There an Anthropogenic Influence? In: Explaining Extremes of 2014 from a Climate Perspective, *Bulletin of the American Meteorological Society*, 96: S136-S140.

Royal Society of New Zealand (2016) Climate change implications for New Zealand: 72. Available from: http://www.royalsociety.org.nz/expert-advice/papers/yr2016/climate-change-implications-for-new-zealand/.

Salinger, M.J., Renwick, J.A., Mullan, A.B. (2001) Interdecadal Pacific oscillation and south Pacific climate. *International Journal of Climatology,* 21: 1705-1721.

Schwalm, C.R., Glendon, S., Duffy, P.B. (2020) RCP8.5 tracks cumulative CO_2 emissions. *Proceedings of the National Academy of Sciences of the United States of America*, 117: 19656-19657.

Simpkins, G. (2017) Progress in climate modelling. *Nature Climate Change*, 7: 684-685.

Sood, A. (2015) Improved bias corrected and downscaled regional climate model data for climate impact studies: Validation and assessment for New Zealand, submitted.

Tait, A., Henderson, R., Turner, R., Zheng, X.G. (2006) Thin plate smoothing spline interpolation of daily rainfall for New Zealand using a climatological rainfall surface. *International Journal of Climatology,* 26: 2097-2115.

Taylor, K.E., Stouffer, R.J., Meehl, G.A. (2012) An Overview of CMIP5 and the Experiment Design. *Bulletin of the American Meteorological Society,* 93: 485-498.

Teixeira, E., Ausseil, A.-G., Burgueño, E., Brown, H., Cichota, R., Davy, M., Ewert, F., Guo, J., Holmes, A., Holzworth, D., Hu, W., Ruiter, J.D., Hume, E., Jesson, L., Johnstone, P., Powell, J., Kersebaum, K.C., Kong, H., Liu, J., Lilburne, L., Meiyalaghan, S., Storey, R., Richards, K., Tait, A., Van Der Weerden, T. (2020) A Spatial Analysis Framework to Assess Responses of Agricultural Landscapes to Climates and Soils at Regional Scale. *Landscape Modelling and Decision Support.* Springer.

Tokarska, K.B., Stolpe, M.B., Sippel, S., Fischer, E.M., Smith, C.J., Lehner, F., Knutti, R. (2020) Past warming trend constrains future warming in CMIP6 models. *Science Advances*, 6. DOI: 10.1126/sciadv.aaz9549

Watt, M.S., Kirschbaum, M.U.F., Moore, J.R., Pearce, H.G., Bulman, L.S., Brockerhoff, E.G., Melia, N. (2019) Assessment of multiple climate change effects on plantation forests in New Zealand. *Forestry*, 92: 1-15. doi:10.1093/forestry/cpy024

Woolley, J.-M., Turner, R., Rampal, N., Carey-Smith, T., Yang, E., Pearce, P. (2020) Historic climate extremes analysis for the Wellington Region. Prepared by the National Institute of Water and Atmospheric Research, NIWA, for Greater Wellington Regional Council. *NIWA Client Report* 2020089AK.

World Climate Research Programme: WCRP (2021) WCRP-CMIP CMIP6_CVs version: 6.2.55.10. Accessed on 30/4/2021 from https://wcrp-cmip.github.io/CMIP6_CVs/docs/CMIP6_institution_id.html

Willeit, M., Ganopolski, A., Calov, R., Brovkin, V. (2019) Mid-Pleistocene transition in glacial cycles explained by declining CO^2 and regolith removal. *Science Advances,* 5: eaav7337.

Zelinka, M.D., Myers, T.A., McCoy, D.T., Po-Chedley, S., Caldwell, P.M., Ceppi, P., Klein, S.A., Taylor, K.E. (2020) Causes of Higher Climate Sensitivity in CMIP6 Models. *Geophysical Research Letters*, 47. https://doi.org/10.1029/2019GL085782

Zhu, J., Poulsen, C.J., Otto-Bliesner, B.L. (2020) High climate sensitivity in CMIP6 model not supported by paleoclimate. *Nature Climate Change*, 10: 378-379.

Appendix A Global and New Zealand climate change

Key messages

- The global climate system is warming and many of the recently observed climate changes are unprecedented.
- Global mean sea level increased by 0.20 m between 1901 and 2018. The average rate of sea level rise has increased from 1.3 mm per year between 1901 and 1971, to 3.7 mm per year between 2006 and 2018.
- Human activities (and associated greenhouse gas emissions) are estimated to have caused 1.07°C of global warming from 1850-1900 to 2010-2019.
- Continued increases in greenhouse gas emissions will cause further warming and impacts on all parts of the global climate system.

It is unequivocal that human influence has warmed the atmosphere, ocean and land (IPCC 2021). Widespread and rapid changes have occurred, including warming of the atmosphere and ocean, diminishing of ice and snow, sea-level rise, and increases in the concentration of greenhouse gases in the atmosphere. Human-induced climate change is already affecting the intensity and frequency of many extreme weather and climate events globally (IPCC, 2021). Increases in average temperatures will result in related increases in the occurrence of extreme temperatures. Global surface temperature was 1.09°C higher in 2011-2020 than 1850-1900 (IPCC, 2021). Global mean sea level has risen faster since 1900 than over any preceding century in at least the last 3000 years (IPCC, 2021). From the start of New Zealand's records (1901) to 2018, national mean coastal sea levels have risen 1.81 (±0.05) millimetres per year (Ministry for the Environment & Stats NZ, 2019).

Global atmospheric concentrations of carbon dioxide have increased to levels unprecedented in at least the last 3 million years (Willeit *et al.*, 2019). Carbon dioxide concentrations have increased by at least 40% since pre-industrial times, primarily from fossil fuel emissions and secondarily from net land use change emissions (IPCC, 2013). In December 2021, the global carbon dioxide concentration of the atmosphere was 416.9 parts per million (NOAA, 2022). The ocean has absorbed about 30% of the emitted anthropogenic carbon dioxide, causing ocean acidification. Due to the influence of greenhouse gases on the global climate system, it is extremely likely that human influence has been the dominant cause of the observed warming since the mid-20th century (IPCC, 2013; IPCC, 2018).

Published information about the expected impacts of climate change on New Zealand is summarised and assessed in the Australasia chapter of the IPCC Working Group II Sixth Assessment Report (Lawrence *et al.*, 2022), as well as a report published by the Royal Society of New Zealand (Royal Society of New Zealand, 2016). Key findings from these publications include:

The regional climate is changing. The Australasia region demonstrates long-term trends toward higher surface air and sea surface temperatures, more hot days and heatwaves, fewer cold extremes, and changed rainfall patterns. Increasing greenhouse gas concentrations have contributed to rising average temperatures in New Zealand. Changing precipitation patterns have resulted in increases in rainfall for the south and west of the South Island and decreases in the north of the North Island (Ministry for the Environment & Stats NZ, 2020). Some heavy rainfall events already carry the fingerprint of a changed climate, in that they have become more intense due to higher temperatures allowing the atmosphere to carry more moisture (Dean *et al.*, 2013). Frosts have become less common, while the number of warm days and heatwaves days is increasing (Ministry for the Environment & Stats NZ, 2020).

The region has exhibited warming to the present and is virtually certain to continue to do so. Based on observations, New Zealand's mean annual temperature has increased by an average of 1.07°C (± 0.24°C) per century since 1909 (Figure 8-1).

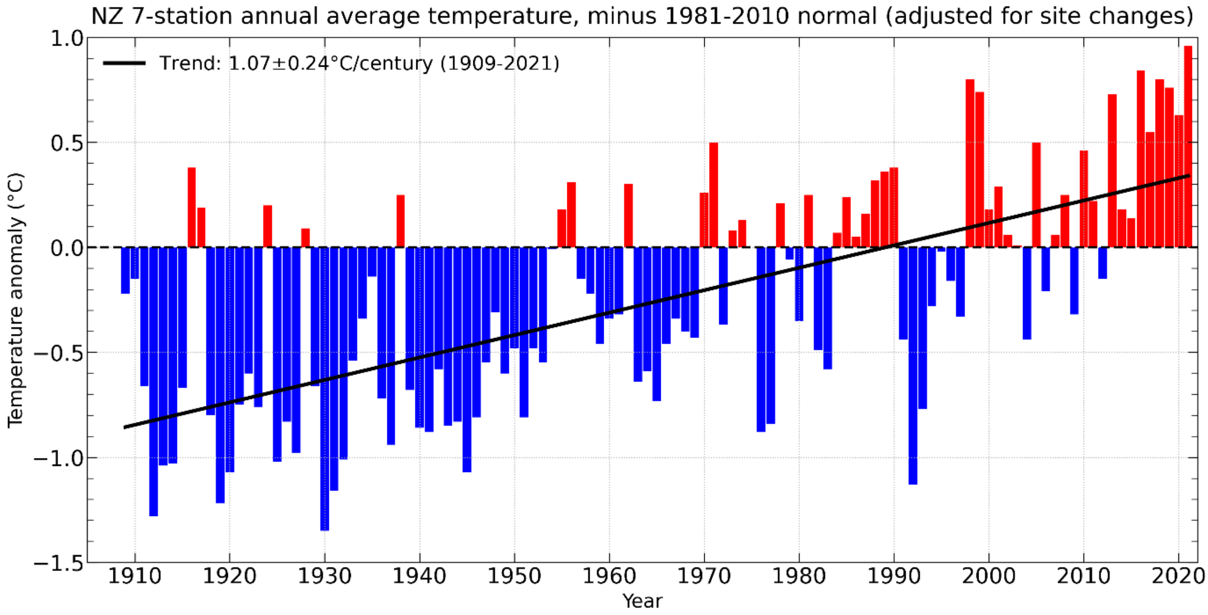

Figure 8-1: New Zealand national temperature series, 1909-2021. More information about the New Zealand seven-station temperature series can be found at https://niwa.co.nz/seven-stations

Warming is projected to continue through the 21st century along with other changes in climate. Warming is expected to be associated with ongoing significant glacier retreat, more frequent hot days, less frequent cold days, and increasing rainfall intensity. Annual average rainfall is projected to decrease in the north and east of the North Island, and to increase in southern and western parts of the South Island (Ministry for the Environment, 2018). Fire hazard is projected to increase in many parts of New Zealand, especially on the eastern coast in the southern half of both islands (Watt *et al.*, 2019). Regional sea level rise will very likely exceed the historical rate, consistent with global mean trends (Ministry for the Environment, 2017).

Impacts and vulnerability: Without adaptation, further climate-related changes are projected to have substantial impacts on water resources, coastal ecosystems, infrastructure, health, agriculture, and biodiversity. However, uncertainty in projected rainfall changes and other climate-related changes remains large for many parts of New Zealand, which creates significant challenges for adaptation.

Additional information about recent New Zealand climate change can be found through the Ministry for the Environment (2018), and the Ministry for the Environment & Stats NZ (2020).

Appendix B Year to year climate variability and climate change

Key messages

- Natural variability is an important consideration in addition to the underlying climate change signal. It will continue to affect the year-to-year climate of New Zealand into the future.
- El Niño-Southern Oscillation is the dominant mode of inter-annual climate variability and it impacts New Zealand primarily through changing wind, temperature and rainfall patterns.
- The Interdecadal Pacific Oscillation affects New Zealand through drier conditions in the east and wetter conditions in the west during the positive phase and the opposite in the negative phase.
- The Southern Annular Mode affects New Zealand through higher temperatures and settled weather during the positive phase and lower temperatures and unsettled weather during the negative phase.

Much of the material in this report focuses on the projected changes to the climate west of Wellington's ranges over the coming century due to increases in global anthropogenic greenhouse gas concentrations. However, natural variations will also continue to occur. Much of the variation in New Zealand's climate is random and lasts for only a short period, but longer term, quasi-cyclic variations in climate can be attributed to different factors. Three large-scale oscillations that influence climate in New Zealand are the El Niño-Southern Oscillation, the Interdecadal Pacific Oscillation, and the Southern Annular Mode (Ministry for the Environment, 2008). Those involved in (or planning for) climate-sensitive activities in the Wairarapa will need to cope with the combination of both anthropogenic change and natural variability.

The effect of El Niño and La Niña

El Niño-Southern Oscillation (ENSO) is a natural mode of climate variability that has wide-ranging impacts around the Pacific Basin (Ministry for the Environment, 2008). ENSO involves a movement of warm ocean water from one side of the equatorial Pacific to the other, changing atmospheric circulation patterns in the tropics and subtropics, with corresponding shifts for rainfall across the Pacific.

During El Niño, easterly trade winds weaken and relatively warm water moves eastward across the equatorial Pacific, accompanied by higher rainfall than normal in the central-east Pacific. La Niña produces opposite effects and is typified by an intensification of easterly trade winds, retention of warm ocean waters over the western Pacific. ENSO events occur on average 3 to 7 years apart, typically becoming established in April or May and persisting for about a year thereafter.

During El Niño events, the weakened trade winds usually cause New Zealand to experience a stronger than normal south-westerly airflow. This generally brings lower seasonal temperatures to the country, and wetter than normal summer conditions to the west of New Zealand (Salinger and Mullan, 1999; Figure 8-2). During La Niña conditions, the strengthened trade winds usually cause New Zealand to experience more north-easterly airflow than normal, higher-than-normal temperatures (especially during summer), and drier summer conditions in the south and west of the South Island, including areas west of Wellington's ranges (Figure 8-2).

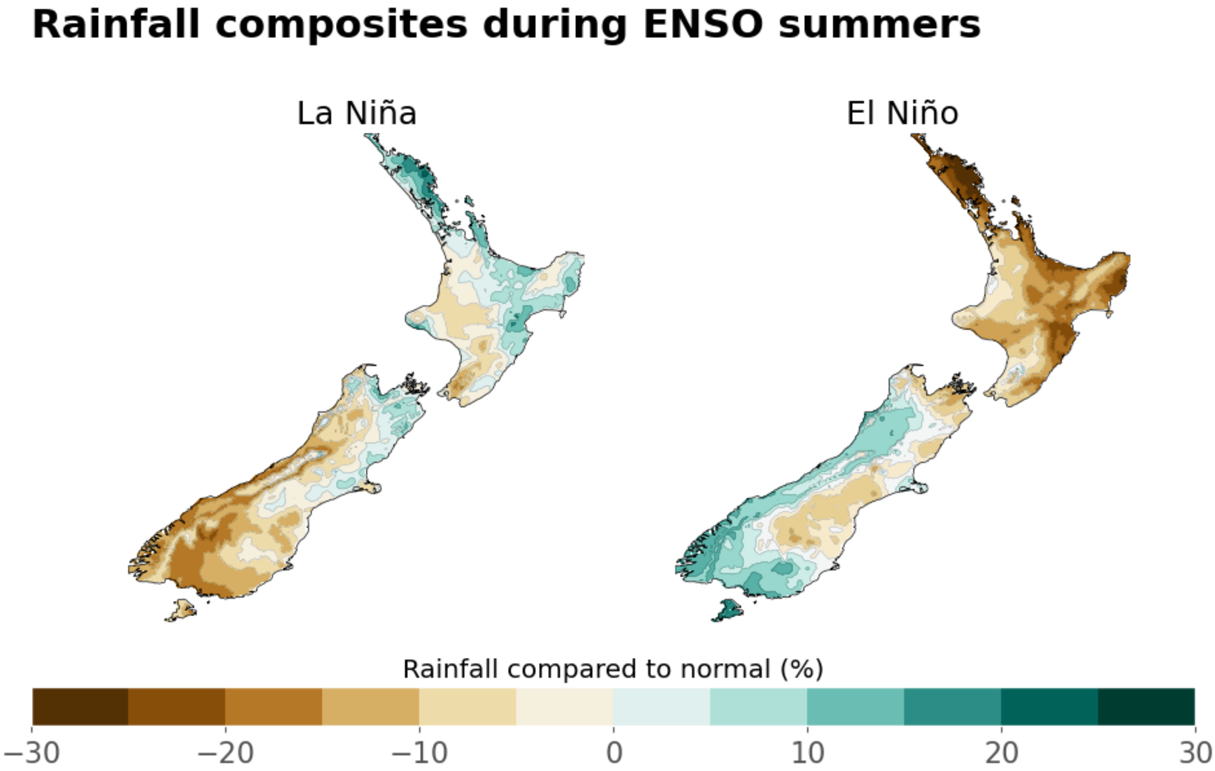

Figure 8-2: Average summer percentage of normal rainfall during La Niña (left) and El Niño (right). La Niña composite uses the following summers: 1973/74, 1974/75, 1975/76, 1988/89, 1998/99, 1999/2000, 2000/01, 2005/06, 2007/08, 2008/09. 2010/11, 2011/12, 2020/21, 2021/22. El Niño composite uses the following summers: 1972/73, 1977/78, 1982/83, 1986/87, 1990/91, 1991/92, 1992/93, 1993/94, 1994/95, 1997/98, 2004/05, 2009/10, 2015/16. Data: NIWA Virtual Climate Station Network. "Normal" refers to the 1991-2020 climatology. This figure was last updated in 2022. © NIWA.

According to IPCC (2013), ENSO is highly likely to remain the dominant mode of natural climate variability in the 21st century, and that rainfall variability relating to ENSO is likely to increase due to increased moisture availability. However, there is uncertainty about future changes to the amplitude and spatial pattern of ENSO.

The effect of the Interdecadal Pacific Oscillation

The Interdecadal Pacific Oscillation (IPO) is a large-scale, long-period oscillation that influences climate variability over the Pacific Basin including New Zealand (Salinger *et al.*, 2001). The IPO operates at a multi-decadal scale, with phases lasting around 20 to 30 years. During the positive phase of the IPO, sea surface temperatures around New Zealand tend to be lower, and westerly winds stronger, resulting in wetter conditions for western areas of both North and South Islands (including parts of the area west of Wellington's ranges). The opposite occurs in the negative phase. The IPO can modify New Zealand's connection to ENSO, and it also positively reinforces the impacts of El Niño (during IPO+ phases) and La Niña (during IPO- phases).

The effect of the Southern Annular Mode

The Southern Annular Mode (SAM) represents the variability of circumpolar atmospheric jets that encircle the Southern Hemisphere that extend out to the latitudes of New Zealand. The SAM is often coupled with ENSO, and both phenomena affect New Zealand's climate in terms of westerly wind strength and storm occurrence (Renwick & Thompson, 2006). In its positive phase, the SAM is associated with relatively light winds and more settled weather over New Zealand, with stronger westerly winds further south towards Antarctica. In contrast, the negative phase of the SAM is associated with unsettled weather and stronger westerly winds over New Zealand, whereas wind and storms decrease towards Antarctica.

The phase and strength of the SAM is influenced by the size of the ozone hole, giving rise to positive trends in the past during spring and summer. In the future other drivers are likely to have an impact on SAM behaviour, for example changing temperature gradients between the equator and the high southern latitudes would have an impact on westerly wind strength in the mid-high latitudes.

The influence of natural variability on climate change projections

It is important to consider human-induced climate change in the context of natural climate variability. An example of this for temperature is shown in Figure 8-3. The solid black line on the left-hand side represents the annual average temperature for New Zealand based on the average of a number of climate simulations forced by historic greenhouse gas concentrations. All the other line plots and shading refer to the modelled air temperature averaged over the New Zealand region from individual simulations. Post-2005, the coloured line plots show the annual temperature changes for the New Zealand region under four different scenarios of future greenhouse gas concentrations, with the heavier lines showing the six-model average temperature projections for each concentration scenario, and the lighter lines showing the results for each of the six downscaled climate models for both historical and future periods.

For the future 2006-2100 period, the models show very little warming trend after about 2030 under the low greenhouse gas concentration ("RCP2.6", blue shading) scenario, whereas temperature changes between +2.0°C and +3.5°C by 2100 are projected under the high concentration ("RCP8.5", red shading) scenario.

Figure 8-3 should not be interpreted as a set of specific predictions for individual years. However, it illustrates that although we expect a long term overall continuing upward trend in temperatures (other than for the RCP2.6 scenario), there will still be some relatively cool years. For this particular example, a year which is unusually warm under our present climate could become typical by about 2050, and an "unusually warm" year in 30-50 years' time (under the higher concentration scenarios) is likely to be warmer than anything we currently experience. The strength of future anthropogenic trends in other climate variables will be smaller in relation to their large year-to-year variability, with the notable exception of sea-level rise.

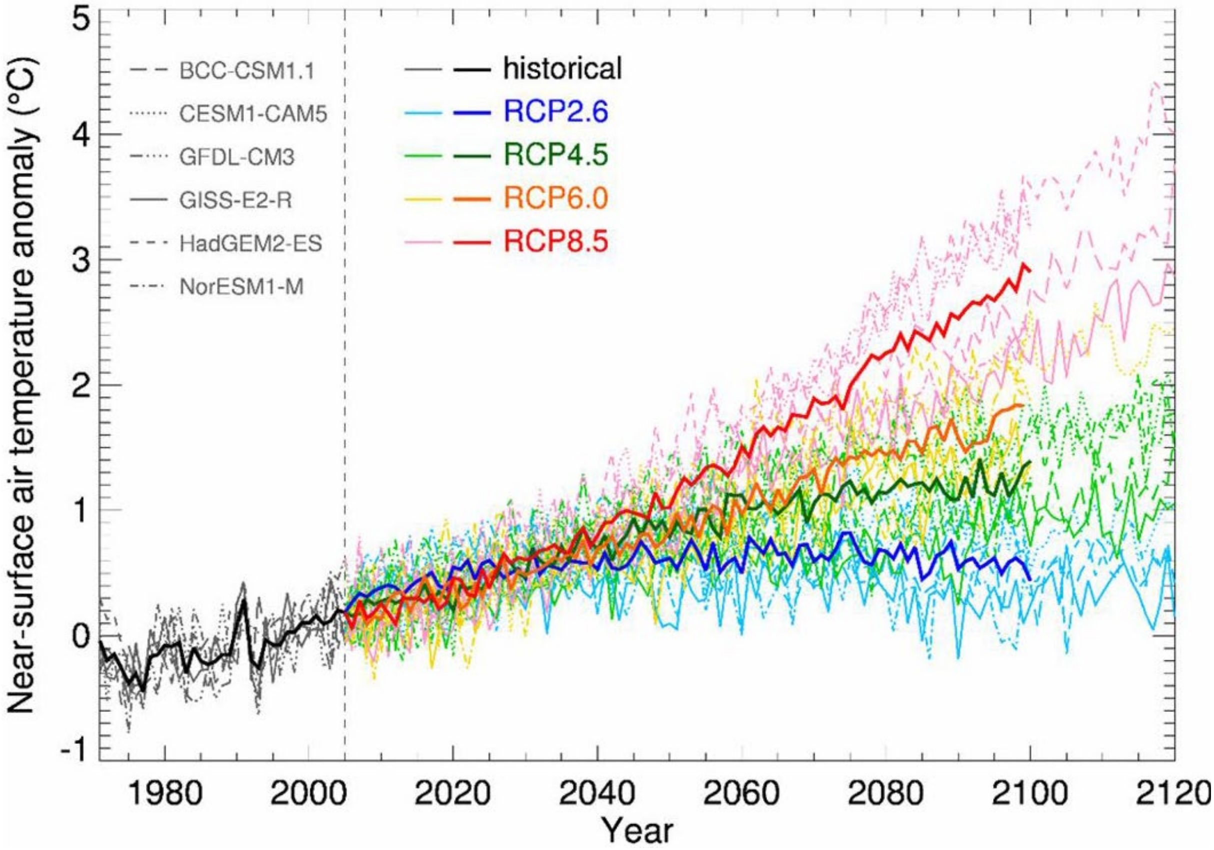

Figure 8-3: New Zealand air temperature - historical (black) and future projections for four RCPs and six downscaled climate models, illustrating future year-to-year variability. See text for full explanation. From Ministry for the Environment (2018).

Appendix C Methodology

Observed climate change west of Wellington's ranges

Several temperature and rainfall indices are presented in Section 3 which illustrate observed changes to climate west of Wellington's ranges. In some cases, the information has been obtained directly from previous GWRC-commissioned NIWA reports (Pearce *et al.*, 2017; 2019), and the reader is referred to those reports for further methodology details. Note that Wellington's mean temperature data have been updated to 2021 in the present report – an additional five years to what was presented in Pearce *et al.* (2017).

Wellington's observed temperature changes are compared with projected temperature changes in Section 3.1.1. Projected changes for this assessment were obtained from Ministry for the Environment (2018) and are reproduced in Table 8-1 below for clarity.

Table 8-1: Projected changes in seasonal and annual mean temperature (in °C) between 1986-2005 and 2031-2050, for the Wellington region, as derived from statistical downscaling. The changes are given for four RCPs (8.5, 6.0, 4.5 and 2.6), where the ensemble average is taken over (41, 18, 37, 23) models respectively. The values in each column represent the ensemble average, and in brackets the range (5th percentile to 95th percentile) over all models within that ensemble. Source: Ministry for the Environment (2018).

Region		Summer	Autumn	Winter	Spring	Annual
Wellington	RCP8.5	1.1 (0.5, 1.7)	1.1 (0.7, 1.5)	1.2 (0.7, 1.6)	0.9 (0.4, 1.3)	1.1 (0.6, 1.6)
	RCP6.0	0.8 (0.3, 1.4)	0.9 (0.2, 1.2)	0.8 (0.3, 1.3)	0.7 (0.2, 1.1)	0.8 (0.3, 1.2)
	RCP4.5	0.9 (0.4, 1.4)	0.9 (0.4, 1.4)	1.0 (0.6, 1.3)	0.8 (0.4, 1.1)	0.9 (0.5, 1.2)
	RCP2.6	0.7 (0.2, 1.2)	0.8 (0.3, 1.2)	0.7 (0.3, 1.1)	0.7 (0.3, 1.0)	0.7 (0.3, 1.1)

Climate modelling

NIWA has used global climate model simulations from the IPCC Fifth Assessment to generate climate change projections for New Zealand using both dynamical (regional climate modelling, RCM) and statistical downscaling procedures. These are described in more detail in a climate guidance manual prepared for the Ministry for the Environment (2018), but a short explanation for the dynamical procedure is provided below. All climate variables and indices presented in this report are based on the dynamical downscaling approach.

Coupled global atmosphere-ocean general circulation models (GCMs) are used to generate climate change projections for prescribed future greenhouse gas concentration scenarios, and results from these models are available through the Fifth Coupled Model Inter-comparison Project (CMIP5) archive (Taylor *et al*., 2012). Simulations from six GCMs were selected by NIWA for dynamical modelling, and the bias corrected sea surface temperatures (SSTs) from these six CMIP5 models were used to drive a global atmosphere-only GCM, which in turn drives a higher resolution regional climate model (RCM) for the New Zealand domain. These CMIP5 models were chosen because they produced the most consistent results when compared to historical climate and circulation patterns in the New Zealand and Southwest Pacific region. Additional selection criteria for the parent global models was that they were the least similar to each other such that they spanned the likely range of model differences. The dynamical downscaling procedure involves forcing a higher-resolution regional climate model (RCM) with data from a coarser global model (GCM) at the lateral boundaries to obtain finer scale detail over a limited area.

The six GCMs chosen for the sea surface temperatures were BCC-CSM1.1, CESM1-CAM5, GFDL-CM3, GISS-E2-R, HadGEM2-ES and NorESM1-M. The NIWA downscaling (RCM) produced simulations that contain daily climate variables, including precipitation and surface temperature, from 1971 through to 2100. The native resolution of the regional climate model is approximately 30 km (0.27 degrees). However, climate models are known to have considerable biases due to inadequate representation of some critical processes and features (e.g. clouds, precipitation). The daily precipitation projections, as well as daily maximum and minimum temperatures, were bias corrected so that the probability distributions from the RCM were aligned with those derived from the Virtual Climate Station Network (VCSN) data on the model resolution when the RCM is driven by the observed large scale circulation across New Zealand (known as 're-analysis' data, REAN; Sood, 2015). When the RCM is driven from the free-running GCMs, forced by CMIP5 sea surface temperatures (SSTs), additional biases occur due to biases in the large-scale circulation in the global model without data assimilation. Therefore, the climate variables from the RCM nested in the free running GCMs forced by historic greenhouse gas concentrations (RCPpast) are expected to have larger biases than where the lateral boundaries of the RCM are forced by reanalysis (REAN) data derived from observations.

The RCM output is then downscaled using interpolation and physically based models from ~30 km to a ~5 km grid at a daily time-step. The ~5 km grid corresponds to the VCSN grid[7]. Figure 8-4 shows a schematic for the dynamical downscaling method used in this report.

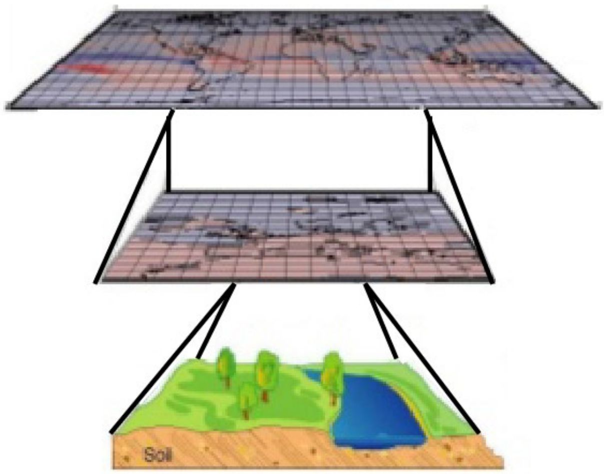

Figure 8-4: Schematic diagram showing the dynamical downscaling approach. This approach utilises outputs from global climate models (relatively low spatial resolution; ~140 km) to generate regional climate model projections of a relatively high spatial resolution (~5 km) that better accounts for New Zealand's complex topography.

The change in the mean climatologies of climate variables averaged from the six model simulations, the 6-model ensemble mean, is presented for the climate simulations rather than for any individual model. The model ensemble mean climatology of climate variables is a better representation of the corresponding climate change signal (i.e. projected change of climate variables compared to historic average; also termed signal), since the averaging process reduces the internal variability of the

[7] Virtual Climate Station Network, a set of New Zealand climate data based on a 5 km by 5 km grid across the country. Data have been interpolated from 'real' climate station records (Tait *et al*., 2006).

climate system (also termed noise). This is particularly relevant where the signal to noise ratio is small. Though only a small number of model simulations (six) were possible due to large computing resources required for running climate model simulations, they were very carefully selected to cover a wide range of the larger CMIP5 model ensemble.

Climate projections are presented as a 20-year average for two future periods: 2031-2050 (termed '2040') and 2081-2100 (termed '2090'). All maps show changes relative to the baseline climate of 1986-2005 (termed '1995'), as used by IPCC (2013). Hence the projected changes by 2040 and 2090 should be thought of as 45-year and 95-year projected trends. Note that the projected changes use 20-year averages, which will not entirely represent and smoothen the natural variability of the selected period. The baseline maps (1986-2005) show modelled historical climate conditions from the same six models as the future climate change projection maps.

Representative Concentration Pathways

Assessing possible changes for our future climate due to human activity is challenging because climate projections strongly depend on estimates for future greenhouse gas concentrations. In turn, those concentrations depend on global greenhouse gas emissions that are driven by factors such as economic activity, population changes, technological advances and policies for mitigation and sustainable resource use. This range of uncertainty has been dealt with by the IPCC through consideration of 'scenarios' that describe concentrations of greenhouse gases in the atmosphere. The wide range of scenarios are associated with possible economic, political, and social developments during the 21st century. In the 2013 IPCC Fifth Assessment Report, a selection of these scenarios were called Representative Concentrations Pathways (RCPs).

These representative pathways are abbreviated as RCP2.6, RCP4.5, RCP6.0, and RCP8.5, in the order of increasing radiative forcing in Watts/m^2 of area from increasing greenhouse gases (i.e. the change in net energy in the atmosphere due to greenhouse gas concentrations). RCP2.6 requires net global emissions to reduce to zero around the 3rd quarter of this century, leading to low anthropogenic greenhouse gas concentrations (also requiring removal of carbon dioxide from the atmosphere), and called the 'mitigation' pathway (and the scenario closest to the aspirational goal of the 2015 Paris Agreement of reducing global temperature rise below 2°C above pre-industrial times). RCP4.5 and RCP6.0 are two 'stabilisation' pathways (where greenhouse gas concentrations stabilise by 2100), and RCP8.5 represents continuing high global emissions without effective mitigation, which will lead to high greenhouse gas concentrations (a 'high end' pathway). Therefore, the RCPs represent the outcomes of a range of 21st-century climate policies.

Table 8-2 shows the projected global mean surface air temperature for each RCP. The full range of projected globally averaged temperature increases for all pathways for 2081-2100 (relative to 1986-2005) is 0.3 to 4.8°C (Figure 8-5). Warming will likely continue beyond 2100 under all RCPs except RCP2.6. Warming will continue to exhibit inter-annual-to-decadal variability and will not be regionally uniform.

Table 8-2: Projected change in global mean surface air temperature for the mid- and late- 21st century relative to the reference period of 1986-2005 for different RCPs. After IPCC (2013).

Scenario	Alternative name	2046-2065 (mid-century)		2081-2100 (end-century)	
		Mean (°C)	Likely range (°C)	Mean (°C)	Likely range (°C)
RCP2.6	Mitigation pathway	1.0	0.4 to 1.6	1.0	0.3 to 1.7
RCP4.5	Stabilisation pathway	1.4	0.9 to 2.0	1.8	1.1 to 2.6
RCP6.0	Stabilisation pathway	1.3	0.8 to 1.8	2.2	1.4 to 3.1
RCP8.5	High end pathway	2.0	1.4 to 2.6	3.7	2.6 to 4.8

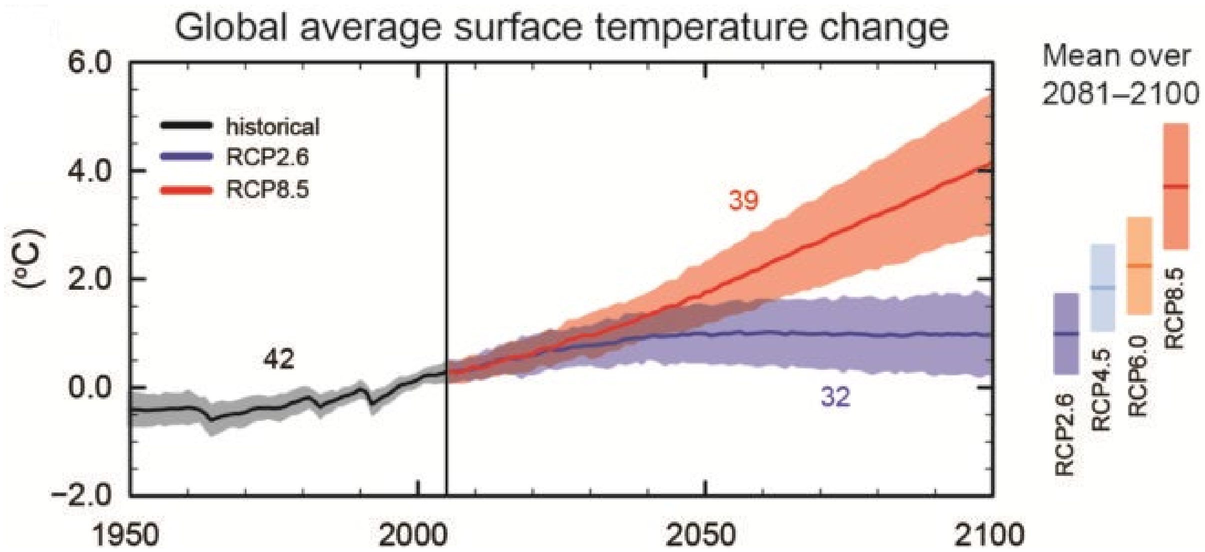

Figure 8-5: CMIP5 multi-model simulated time series from 1950-2100 for change in global annual mean surface temperature relative to 1986-2005. Time series of projections and a measure of uncertainty (shading) are shown for scenarios RCP2.6 (blue) and RCP8.5 (red). Black (grey shading) is the modelled historical evolution using historical reconstructed forcing. The mean and associated uncertainties averaged over 2081−2100 are given for all RCP scenarios as coloured vertical bars to the right of the graph (the mean projection is the solid line in the middle of the bars). The numbers of CMIP5 models used to calculate the multi-model mean is indicated on the graph. From IPCC (2013).

Cumulative greenhouse gas emissions will largely determine global mean surface warming by the late 21st century and beyond. Even if emissions are stopped, the inertia of many changes in global climate will continue for many centuries to come, with the longest lag effect being sea-level rise. This represents a substantial multi-century climate change commitment created by past, present and future emissions – particularly for coastal areas facing ongoing sea-level rise.

Appendix D CMIP6 climate modelling and latest IPCC Assessment

As described earlier in Appendix C, coupled global atmosphere-ocean general circulation models (GCMs) are used to generate climate change projections for prescribed future greenhouse gas concentration scenarios. The results from a selection of these models, presented is this report, were made available through the Fifth Coupled Model Inter-comparison Project (CMIP5). The sixth phase of the Coupled Model Inter-comparison Project (CMIP6; Eyring *et al.*, 2016) is underway, consisting of model results from approximately 100 distinct climate models produced across 53 different modelling groups including NIWA (Hausfather, 2019; WCRP, 2021). Some of the notable improvements to CMIP6 models include higher ocean resolution, and inclusion of new and more complex processes such as interactive chemistry, active land processes, ice sheets and permafrost (Simpkins, 2017).

CMIP6 model results are filtering through to the research community, enabling an assessment of the data available to-date, including:

- Improved simulation of Indian summer monsoon rainfall (Gusain *et al.*, 2020).
- CMIP6 ensemble means more skilful than CMIP5 ensemble means at simulating absolute and threshold indices of extreme temperature (Fan *et al.*, 2020).

Equilibrium climate sensitivity is the expected long-term warming after atmospheric CO2 concentrations are doubled (Hausfather, 2019). CMIP6 models available to-date have tended to show notably higher climate sensitivity than CMIP5 models (Hausfather, 2019), with values spanning 1.8-5.6°C, compared to a range of 2.1-4.7°C for CMIP5 (Meehl *et al.*, 2020; Zelinka *et al.*, 2020). This increase in sensitivity has been attributed to the differences in physical representation of clouds in models. Specifically, CMIP6 models demonstrate a decrease in extratropical low cloud coverage and albedo (Zelinka *et al.*, 2020).

An important factor contributing to climate sensitivity is the increase in liquid content relative to ice in clouds as the atmosphere warms. As the liquid content of a cloud increases, it generates an increasingly negative feedback which constrains warming, however this feedback ceases once the cloud is predominately liquid (Bjordal *et al.*, 2020). CMIP6 models have more supercooled-liquid clouds than CMIP5 models (Zelinka *et al.*, 2020), hence the phase transition from ice to liquid is weakened, which in turn reduces this negative feedback. This reduced negative feedback results in larger climate sensitivity in some CMIP6 models compared to CMIP5 models. Factors such as these demonstrate the complexity of physical processes which climate models must account for, and it is complexity like this that partly contributes to the range of climate projections produced by GCMs.

Studies assessing the plausibility of the models demonstrating higher sensitivity are ongoing (e.g. Zhu *et al.*, 2020), while projected warming by CMIP6 models may be constrained based on the model consistency with observed warming (Tokarska *et al.*, 2020). As part of its sixth assessment report (AR6), the Intergovernmental Panel on Climate Change (IPCC) have stated a likely equilibrium climate sensitivity range of 2.5-4.0°C, with a best estimate of 3°C (Arias *et al.*, 2021). The AR6 is underway, with the Synthesis Report (the final AR6 product) due for release in September 2022 (IPCC, 2022).

Climate models are evolving, and downscaled CMIP6 projections will provide additional insights of projected climate change in the area west of Wellington’s ranges. Bodeker *et al.* (2022) state that new knowledge from AR6 is unlikely to fundamentally change the existing projections. Therefore, findings in this report can continue to be used with reasonable confidence.

Appendix E Climate projection panels

Maximum temperature

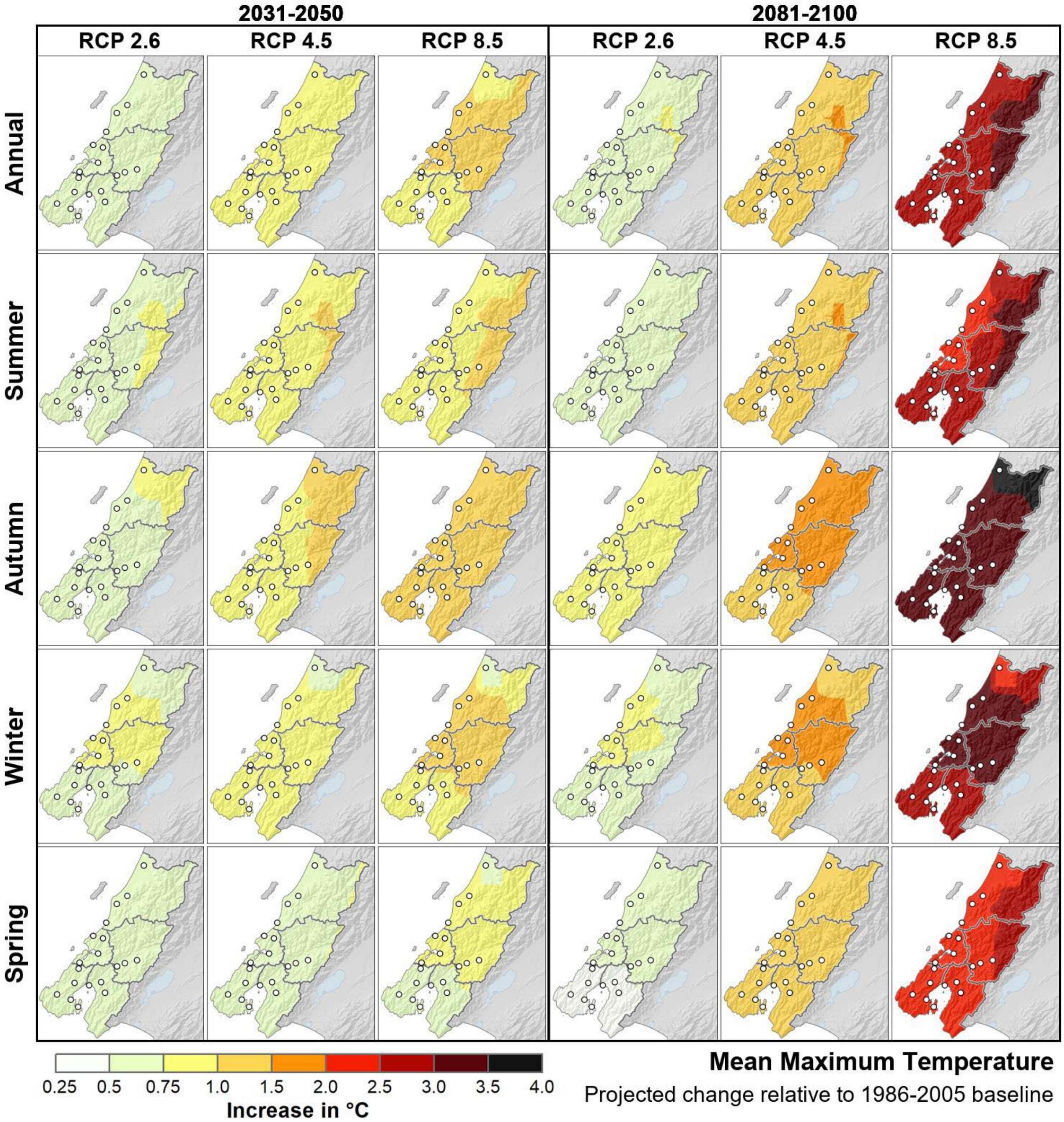

Minimum temperature

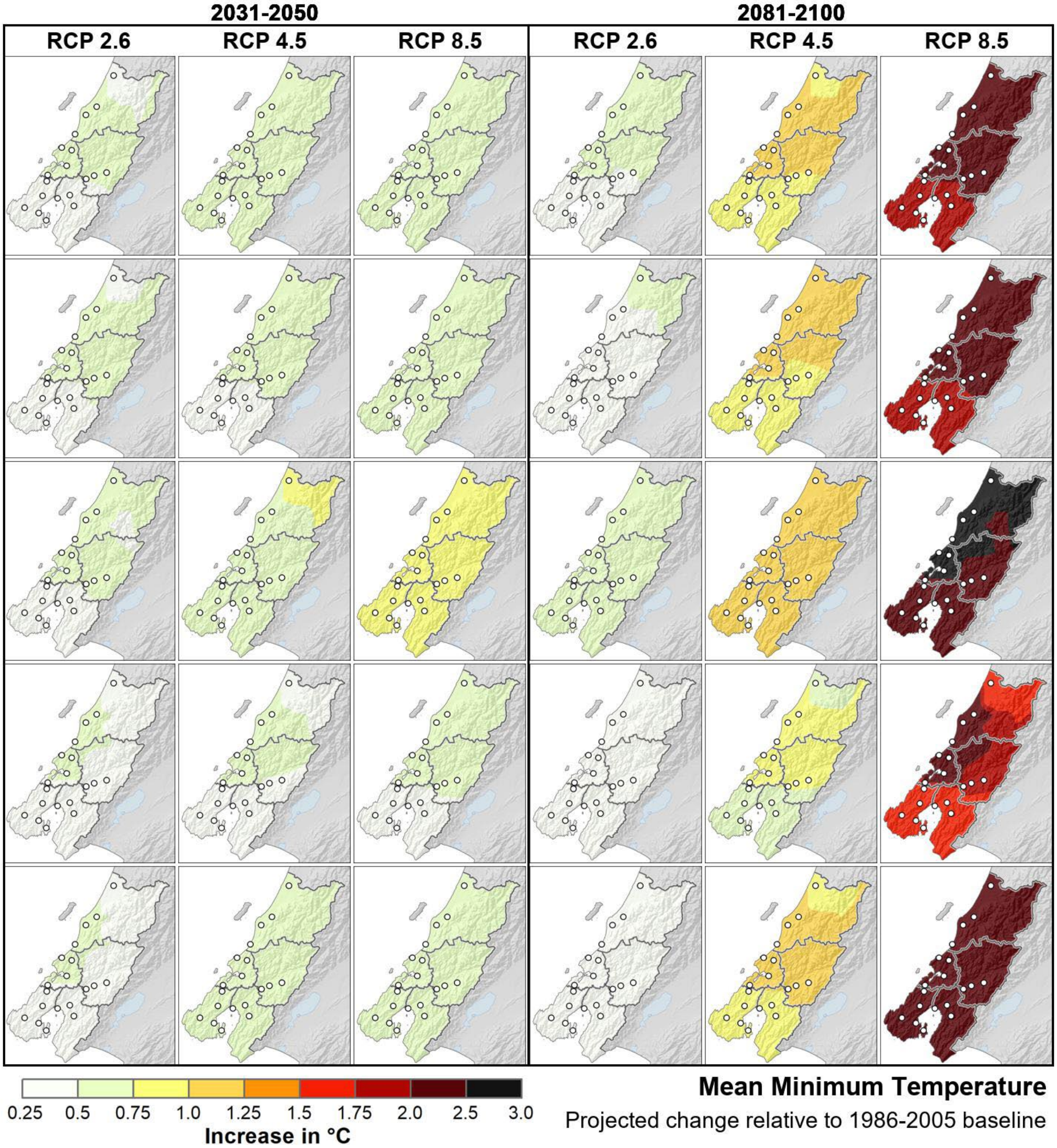

Rainfall totals

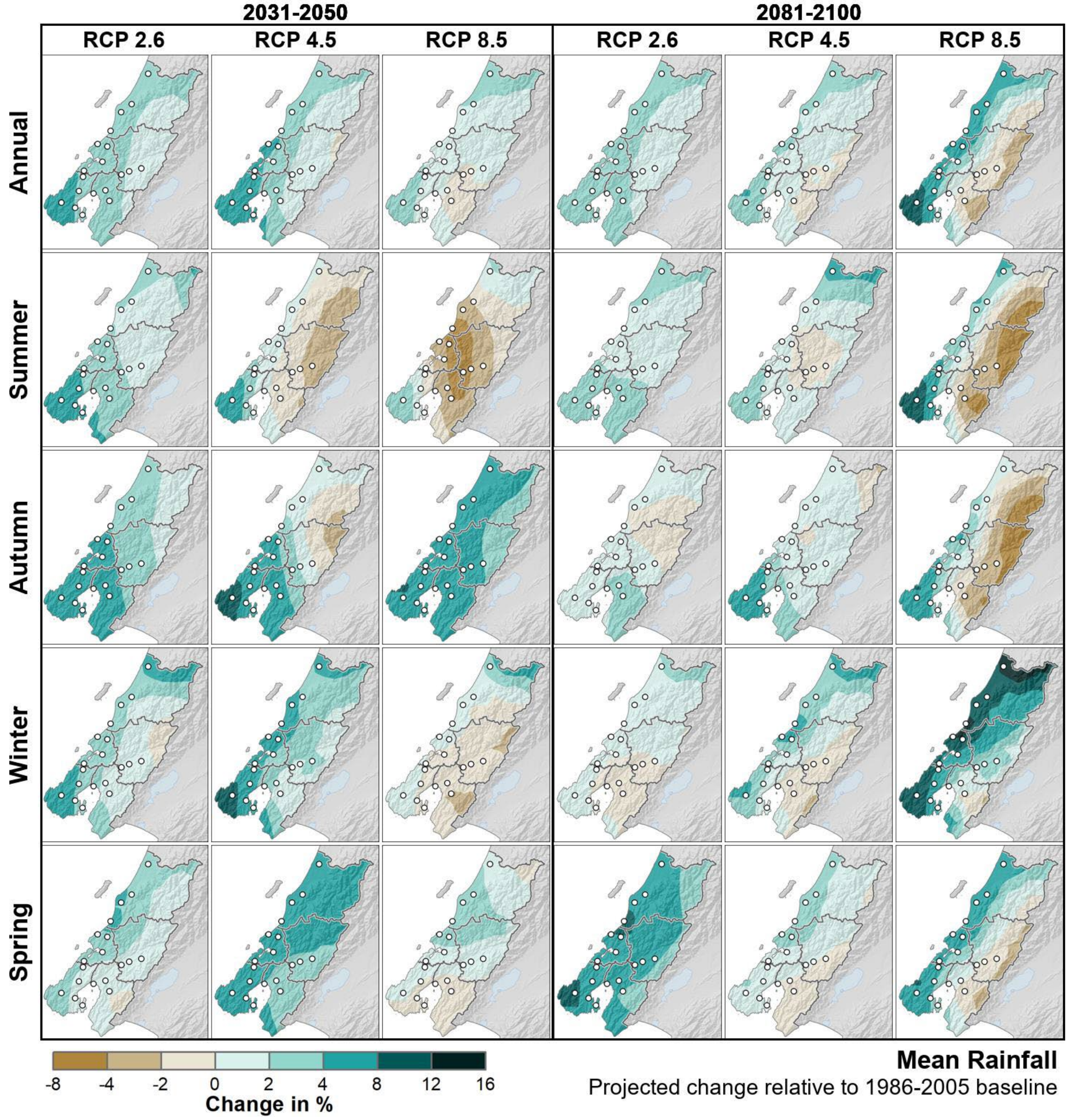

Wet days

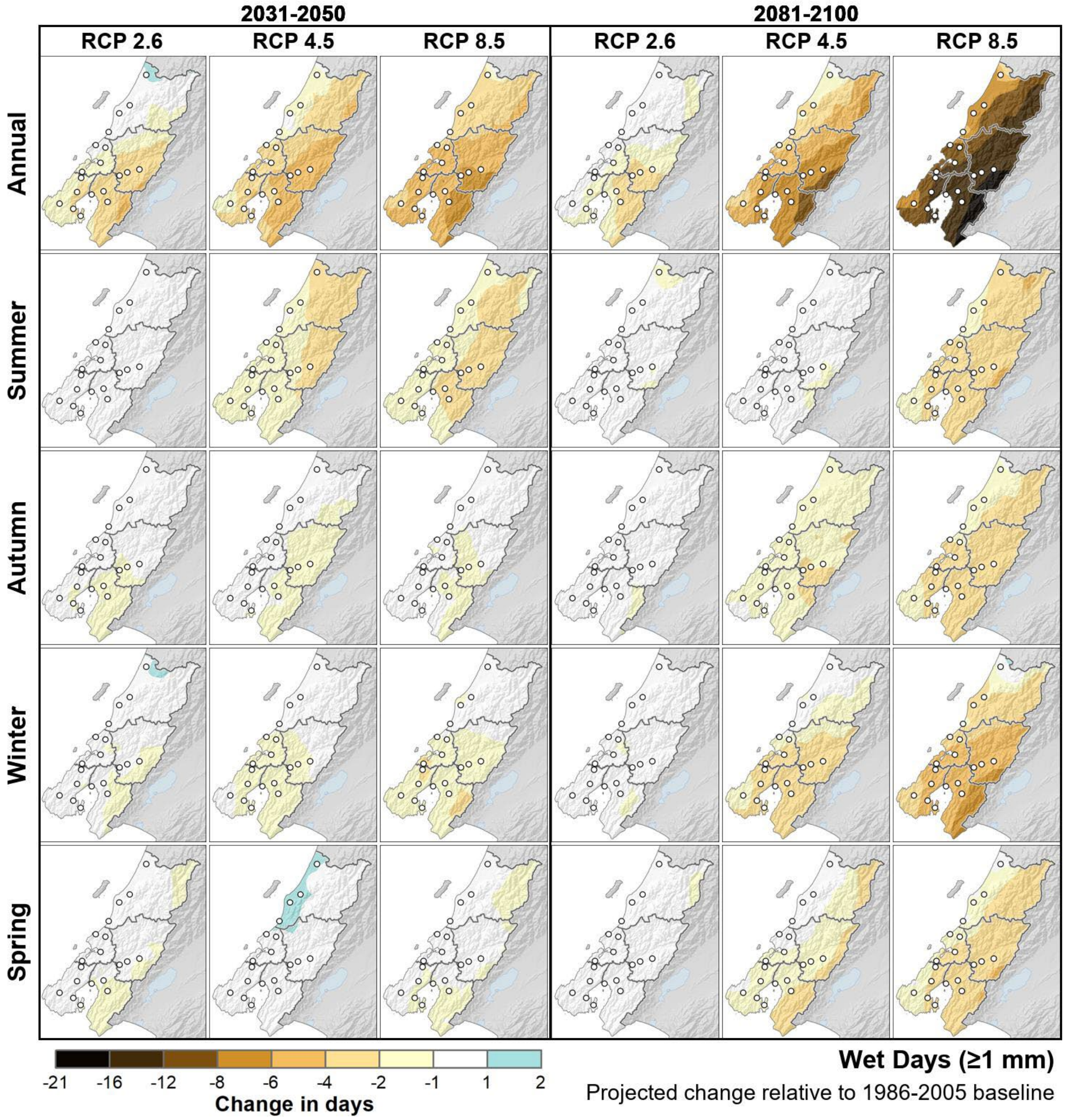
2031-2050
2081-2100
RCP 2.6
RCP 4.5
RCP 8.5
RCP 2.6
RCP 4.5
RCP 8.5
Annual
Summer
Autumn
Winter
Spring
-21
-16
-12
-8
-6
-4
-2
-1
1
2
Change in days
Wet Days (≥1 mm)
Projected change relative to 1986-2005 baseline